AD_____

Award Number: W81XWH-17-1-0456

TITLE: Novel Mechanisms Whereby p27 Drives Tumor Progression in PI3K-Activated Cancers

PRINCIPAL INVESTIGATOR: Joyce Slingerland, M.D., Ph.D.

CONTRACTING ORGANIZATION: University of Miami
Miami, FL 33136

REPORT DATE: October 2018

TYPE OF REPORT: Annual

PREPARED FOR: U.S. Army Medical Research and Materiel Command
Fort Detrick, Maryland 21702-5012

DISTRIBUTION STATEMENT:

☒ Approved for public release; distribution unlimited

The views, opinions and/or findings contained in this report are those of the author(s) and should not be construed as an official Department of the Army position, policy or decision unless so designated by other documentation.

REPORT DOCUMENTATION PAGE

Form Approved
OMB No. 0704-0188

1. REPORT DATE	2. REPORT TYPE	3. DATES COVERED
October 2018	Annual	15 Sep 2017 – 14 Sep 2018

4. TITLE AND SUBTITLE
Novel Mechanisms Whereby p27 Drives Tumor Progression in PI3K-Activated Cancers

5a. CONTRACT NUMBER

5b. GRANT NUMBER
W81XWH-17-1-0456

5c. PROGRAM ELEMENT NUMBER

6. AUTHOR(S)
Joyce Slingerland, M.D., Ph.D.

E-Mail: jslingerland@med.miami.edu

5d. PROJECT NUMBER

5e. TASK NUMBER

5f. WORK UNIT NUMBER

7. PERFORMING ORGANIZATION NAME(S) AND ADDRESS(ES)

University of Miami
1320 S. Dixie Hwy, Suite 650
Coral Gables, FL 33146

8. PERFORMING ORGANIZATION REPORT NUMBER

9. SPONSORING / MONITORING AGENCY NAME(S) AND ADDRESS(ES)

U.S. Army Medical Research and Materiel Command
Fort Detrick, Maryland 21702-5012

10. SPONSOR/MONITOR'S ACRONYM(S)

11. SPONSOR/MONITOR'S REPORT NUMBER(S)

12. DISTRIBUTION / AVAILABILITY STATEMENT

Approved for Public Release; Distribution Unlimited

13. SUPPLEMENTARY NOTES

14. ABSTRACT

p27 shifts from CDK inhibitor to oncogene when phosphorylated by PI3K effector kinases. We show p27 is a cJun co-regulator, whose assembly and chromatin association is governed by p27 phosphorylation. Cancer cells with high p27pT157pT198 or expressing a CDK-binding defective p27pT157pT198 phosphomimetic, p27CK-DD, cJun is activated, binds p27 and p27/cJun complexes localize to the nucleus. p27/cJun upregulates TGFB2 to drive metastasis in vivo. Global analysis shows p27/cJun recruitment to chromatin is increased by p27 phosphorylation and activates programs of EMT and metastasis. Human breast cancers with high p27pT157 differentially express p27-cJun regulated genes of prognostic relevance, supporting the biological significance of the work. p27/cJun also corepress pro-differentiation genes to increase cancer stem cells. In cancer cells with high p27pT157pT198 or phosphomimetic p27CK-DD, nearly half of p27/cJun co-targets are repressed and these govern differentiation. *PTPN12* was strongly downregulated though p27 and cJun recruitment of SIN3A, YY1, and HDAC1 to corepress this tumor suppressor gene, leading to increased sphere formation and tumor initiating cells. Upon PTPN12 loss, its substrate, PYK2, mediates STAT3 activation, increases spheres and ALDH1 activity and tumor initiating cells in vivo. Thus, p27-bound cJun represses differentiation genes and via PTPN12 repression, activates pathways that upregulate cancer initiating cells.

15. SUBJECT TERMS
Triple Negative Breast Cancer, PI3K pathway, cancer stem cells, p27Cterminal phosphorylation, Pyk2, STAT3, cJun:

16. SECURITY CLASSIFICATION OF:			17. LIMITATION OF ABSTRACT	18. NUMBER OF PAGES	19a. NAME OF RESPONSIBLE PERSON
U					USAMRMC
a. REPORT	b. ABSTRACT	c. THIS PAGE			19b. TELEPHONE NUMBER *(include area code)*
U	U	U	UU	17	

Table of Contents

Year 1 Annual Report W81XWH-17-1-0456
REVISED MAY 2019
Grant Title: Novel Mechanisms Whereby p27 Drives Tumor Progression in PI3K-Activated Cancers

200 word summary of most significant findings:
p27 shifts from CDK inhibitor to oncogene when phosphorylated by PI3K effector kinases. We show p27 is a cJun co-regulator, whose assembly and chromatin association is governed by p27 phosphorylation. Cancer cells with high p27pT157pT198 or expressing a CDK-binding defective p27pT157pT198 phosphomimetic, p27CK-DD, cJun is activated, binds p27 and p27/cJun complexes localize to the nucleus. p27/cJun upregulates TGFB2 to drive metastasis in vivo. Global analysis shows p27/cJun recruitment to chromatin is increased by p27 phosphorylation and activates programs of EMT and metastasis. Human breast cancers with high p27pT157 differentially express p27-cJun regulated genes of prognostic relevance, supporting the biological significance of the work. p27/cJun also corepress pro-differentiation genes to increase cancer stem cells. In cancer cells with high p27pT157pT198 or phosphomimetic p27CK-DD, nearly half of p27/cJun co-targets are repressed and these govern differentiation. *PTPN12* was strongly downregulated though p27 and cJun recruitment of SIN3A, YY1, and HDAC1 to corepress this tumor suppressor gene, leading to increased sphere formation and tumor initiating cells. Upon PTPN12 loss, its substrate, PYK2, mediates STAT3 activation, increases spheres and ALDH1 activity and tumor initiating cells in vivo. Thus, p27-bound cJun represses differentiation genes and via PTPN12 repression, activates pathways that upregulate cancer initiating cells.

INTRODUCTION:
p27 is a CDK inhibitor that is either degraded or deregulated in cancers. p27 gains pro-oncogenic effects to promote cancer invasion and metastasis when phosphorylated at threonine 157 (T157) and T198. We showed that PI3K-activated kinases phosphorylate p27 at T157 and T198 causing disruption of the cytoskeleton to increase cell motility. This grant investigates how 27pT157pT198 (p27pTpT) forms novel protein-protein complexes to activate epithelial to mesenchymal transition (EMT) and cancer stem cell (CSC) expansion.

Our recent work showed p27 is a critical mediator of metastasis. p27 knockdown decreased bone and lung metastasis in highly PI3K-activated cancer cell lines. C-terminal p27 phosphorylation drives EMT by upregulating EMT transcription factor expression. We showed p27pTpT promotes JAK2/STAT3 binding and activation, and STAT3 induction of TWIST1 to drive EMT. New data show p27pTpT also binds cJun-JNK to activate cJun, and nuclear cJun-p27 bind an enhancer to co-activate the *TGFB2* gene, further activating EMT.

p27pTpT may drive metastasis by upregulating both EMT and CSC expansion. p27 knockdown in lines with high p27pTpT decreased expression of embryonic stem cell transcription factors (ES-TFs) SOX2, NANOG and MYC, and decreased tumor spheres and CSC markers. Conversely, transduction of a phosphomimetic p27CK-DD increased CSC. Pyk2, STAT3, and cJun all bind to and are activated by p27pTpT and may alter transcription to activate EMT and CSC. Pyk2 knockdown partly reversed CSC upregulation by p27pTpT.

Our **hypothesis** is that p27 phosphorylation at T198 and T157 promotes binding to Pyk2, STAT3 and cJun to activate transcription programs governing EMT and cancer stem cell expansion. **AIM1** will test i) if p27pTpT drives CSC expansion by binding and activating signal transducers JNK-cJun and STAT3-Pyk2 to activate these transcription factors and will validate these pathways in human cancers and ii) if p27pTpT increases tumor initiating stem cells and metastasis from orthotopic xenograft tumors via Pyk2 in vivo.

AIM 2 will identify transcriptional targets of p27 that drive EMT and CSC programs. We will identify putative p27 target genes and test which may be co-regulated by cJun using

GOALS ACCOMPLISHED YEAR 1 of grant		ACCOMPLISHMENTS
AIM1 will test *i)* if p27pTpT increases sphere formation, CSC markers and ES-TF induction *in vitro* by activating STAT3, Pyk2, and/or cJun and *ii)* if p27pTpT mediates an increase in tumor initiating stem cells (T-ISC) in xenografts in vivo via Pyk2	**Revised Planned Time (mo)**	**Work completed (% completed)**
Aim 1 Major Task 1: Does p27pTpT activate CSC properties through STAT3, Pyk2, and/or cJun?	1-12	
Subtask 1 Are p27-dependent STAT3, PYK2, and/or JNK/cJun activation required for CSC effects Test if STAT3, JNK or Pyk2 drug inhibitors or shRNA knockdown reduce or abolish p27CK-DD driven sphere formation, CSC marker expression (ALDH1 by aldefluor assays and CD44 and CD24 by flow cytometry) and expression levels of ES-TFs, *SOX2, MYC* and *NANOG* as assayed by QPCR Test if transduction of $STAT3^{CA}$, Pyk2 or cJun can rescue the loss of CD44/CD24 markers, ALDH1, sphere formation and ES-TF expression observed after knockdown of p27 in 4175shp27 (upregulate)	1-12	100% completed We showed PI3K activated p27 C-terminal phosphorylation mediates cJun activation, p27-cJun binding and nuclear translocation in MDA-MB231 breast and bladder cancer lines to induce oncogenic gene expression including *TGFB2*. **Manuscript 1 Figures 1-3 below (also Appendix 1 PNAS reprint Figure 1-3)** We showed activated p27 (p27CK-DD and p27pTpT) downregulated PTPN12 which activated Pyk2 and in turn activates STAT3. All 3 are needed to increase in embryonic stem cell transcription factors and increase spheres in vitro. We showed STAT3shRNA and Pyk2 siRNA, ShRNA and PYK2 inhibitors, knockdown of cJun and of TGFB2 reduce or abolish p27CK-DD driven sphere formation, CSC marker expression (ALDH1 by aldefluor assays and CD44 and CD24 by flow cytometry) and expression levels of ES-TFs, *SOX2, MYC* and *NANOG* as assayed by QPCR) **See manuscript #2 Figs 3-5 in the report body (see also Appendix 2 Fig 3-5)**
Milestone(s) Achieved: 1. Identify other lines in which p27pTpT drives JNK-Jun, Pyk2 or STAT3 2. Show if activation of these kinase by p27 is required for p27pTpT dependent unpregulation of CSC		All data were completed also in the UMUC3 cell lines See Appendix 2 Supplemental Figs 4-5)

features in vitro. 3. Show loss of CSC properties upon p27 knockdown is rescued by JNK-Jun or Pyk2		
Local IRB/IACUC Approval for work of AIM 3	3	submitted
Milestone Achieved: IACUC Approval	6	obtained
AIM 1 Major Task 2 Test if T-ISC abundance is higher in cells with high p27pTpT or after p27CK-DD transfection and if this depends on p27-activated Pyk2 in vivo	6-36	
Subtask 1 Assay T-ISC abundance in 4175, 4175shp27 and 4175-shp27transfected with Pyk2 using limiting dilution assays injecting 100,000, 10,000, 1,000 and 100 cells with matrigel into the mammary fat pad of NODSCID IL2R□-/- mice	1-12	We showed that T-ISC abundance is greater in 1833 vs parental 231 and that p27 knockdown abolishes the gain in CSC abundance. We showed 231p27CK-DD expressing phosphomimetic p27 has increased CSC in vitro and in vivo in T-ISC limiting dilution T-ISC assays. And that p27chRNA, cJun ShRNA and PYK2shRNA each abolish this gain in T-ISC using limiting dilution assays injecting 100,000, 10,000, 1,000 and 100 cells with matrigel into the mammary fat pad of NODSCID IL2Rγ-/- mice. **This data is presented in the second manuscript Figure 5 below (see also Appendix 2 manuscript Fig 5 and Supplemental Fig 4 and 6)**
Subtask 2 Compare T-ISC frequency in vivo in assays as described above using MFC-7, MCF-7p27CK-DD and MCF7p27CK-DD with Pyk2 knockdown	1-12	We have not repeated these assays in MCF-7 as they appear to be redundant to the data above. We consider this aim complete
Milestone(s) Achieved: will test if p27pTpT increases tumor initiating cells and drives metastasis *in vivo* via Pyk2 activation		We have shown that p27pTpT increases tumor initiating cells in vivo via cJun mediated PTPN12 repression and Pyk2 activation (manuscript #2

		below) and drives metastasis *in vivo* via cJun mediated *TGFB2* **(See manuscript #1 below and Appendix1 PNAS reprint)**
AIM1 Major Task 3 Test p27pTpT effects on growth and formation of metastasis	1-12	Completed in year 1
When tumors from 100,000 cell group from each of the experiments above reach 1 cm diameter, they will be surgically removed and animals followed for metastasis by weekly IVIS	1-14	Tumors from 100,000 cell group from each of the experiments were surgically removed and animals followed for metastasis by weekly IVIS. We showed p27CK-DD drives metastasis and this is abrogated by cJun, TGFB2 or PYK2 knockdown. 1833 showed an excess metastasis vs parental 231 line and this was abolished with shp27 **(see Manuscript #2 Figures 6 Appendix #2 Fig 6 and Supplemental Fig6)**
Test primary tumors removed for formation of spheres, ALDH1 activity and CD44/CD24 status Characterize removed tumors for pAKT, pSTAT3, p27, ALDH1 and Ki67 by IHC	1-14	Showed increased TGFB2 which decreased with ShcJun and Shp27 and no change in Ki67 but greater CSC features
	1-14	
Milestone(s) Achieved: Will have shown if lines that have higher CSC also have increased metastatic ability and if this depends on p27-driven kinase activation		We showed in 1833 vs 231 and UMUC3-Lul2 vs UMUC3- both pairs of cell lines with PI3K activation and high p27pT157pT198 vs parental controls, have higher CSC in vitro. In the 231 model, we showed the p27-driven gain in CSC associated with increased metastatic ability that requires cJun, TGFB2 & Pyk2 See Manuscript 2 Figure 4-6 below and Appendix 2 Figure 4-6 and Supplemental Data Fig 4-6)

AIM 2 Investigates putative gene targets of p27 and if p27 activates EMT and CSC transcription programs.	1-24	
Aim 2 Major Task 1 Identify putative p27 target genes by combined ChIP-Seq/RNA Seq, focusing on targets implicated in EMT and CSC		
Subtask 1 ChIP assays for p27 and cJun are already developed. We will next use ChIP-Seq to assess p27 gene occupancy in 4175 +/- PI3K inhibitors and in MCF-12A vs MCF12Ap27CK-DD	1-24	We have completed ChIP-Seq of p27 and of cJun and found that p27 co-occupies over half of cJun binding sites at chromatin to up or down regulate cJun action. Comparison with RNA Sequencing shows p27-cJun drive oncogenic programs of gene expression. This was done 231, 1833, 231p27CK-DD and 1833shp27 lines. 1833 is a high metastatic sister cell line of 231 and 4175. 1833 was assayed +/- PI3K inhibitors. (See Manuscript #1 Figures 1-4 and Appendix 1 Figs 1, 6,7 and SFigs 1, 6,7). See also ChIP Seq RNA Seq data in Manuscript 2 below Figs 1,2 detailed also in Appendix 2, Figs 1,2 and S Figs 1,2) We are carrying out a STAT3 ChIP Seq in these lines since p27, cJun appear to annotate many target genes that have STAT3 consensus motifs and at which STAT3 is bound in other lines on ENCODE data. This work will be completed in year 2 Planned work with MCF-12A is no longer required since it appears redundant to the findings above in MCF12A, the 231 sister cell lines and the UMUC3 cell liens with low and high p27 activation.

Subtask 2 test if a subset of p27-bound genes are also bound by cJun in 4175 +/- PI3K inhibitors and in MCF-12A vs MCF12Ap27CK-DD	12-24	We have identified p27 and cJun annotated genes that are differentially expressed in p27 activated lines vs controls and shown that these targeted genes are downregulated by PI3K inhibition. See data in Manuscript #1 Figures 1-4 and Appendix 1 Figs 1,2, 6, 7 and SFigs 1, 2, 6, 7). See also ChIP Seq RNA Seq data in Manuscript 2 below Figs 1,2 detailed also in Appendix 2, Figs 1-3 and S Figs 1-3)
Subtask 3 Total RNA will be isolated and rRNA-depleted fractions subjected to high throughput sequencing (RNA-Seq)	12-18	RNA Seq completed in 231, 1833, 231p27CK-DD and 1833shp27 lines. See data in Manuscript #1 Figures 1,2,6,7 and Appendix 1 Figs 1, 2 6,7 and SFigs 1, 2, 6,7). See also ChIP Seq/RNA Seq data in Manuscript 2 below Figs 1-3 detailed also in Appendix 2, Figs 1-3 and S Figs 1-3)
Subtask 4 Data analysis of ChIP-Seq/RNA-Seq Will look for p27 regulated genes that are also regulated by cJun or STAT3	24-36	P27-cJun regulated genes have been identified. We are completing STAT3 ChIP to identify cJun-p27 regulated targets that are also co-regulated by STAT3
Milestone(s) Achieved: will have identified genomic sites bound by p27 and or cJun and if these genes are expressed or repressed.		We have identified genomic sites bound by p27 and cJun that are either activated or repressed. Gene ontogeny analysis reveals these to govern oncogenic and stem cell related processes

combined ChIP-Seq/ RNA-Seq, focusing on genes implicated in EMT and CSC. We will further assay how p27 modulates selected target genes and if C-terminal phosphorylation shifts p27 from a co-repressor to co-activator of drivers of CSC self-renewal.

AIM 3 will compare action of induced transgenic p27CK-DD vs p27CK- to expand tissue stem cell compartments, alter development and give rise to cancer in mice. This grant may reveal novel pro-oncogenic effects of p27 that extend beyond cytoskeleton disruption and identify a novel, broader function of p27 as a phosphorylation-dependent transcriptional regulator of EMT and stem cells with implications for cancer and differentiation. This work may also illuminate why

PI3K/mTOR inhibitor drugs have had limited efficacy as monotherapies in humans and identify complimentary nodes including Pyk2, STAT3, and JNK for targeted intervention.

KEYWORDS:
Triple Negative Breast Cancer, PI3K pathway, cancer stem cells, p27Cterminal phosphorylation, Pyk2, STAT3, cJun

ACCOMPLISHMENTS:

1. What were the major goals of the project?

The major goals of the project remain as stated in the approved SOW. Study goals are listed Table 1 below. To date we have completed AIM1 and over half of AIM2 and will complete AIM2 and 3 in the remainder of the grant period.

The Table below summarizes the goals and work completed in the first year.

The data for the first of two manuscripts coming from this work has now been published in PNAS April 2, 2019 | vol. 116 | no. 14 | 7005–7014. The abstract and results section with main figures referred to in the SOW above are presented below. Please note that the complete reprint containing all of the main figures, the six Supplemental Sfigs and Supplemental Tables 1-6 is appended to this report. For review of supplemental data, please see the appended reprint (Appendix 1).

p27 transcriptionally co-regulates cJun to drive programs of tumor progression

Hyunho Yoon, Minsoon Kim, Kibeom Jang, Miyoung Shin, Alexandra Besser, Xue Xiao, Dekuang Zhao, Seth Wander, Karoline Briegel, Lluis Morey, Andy Minn, and Joyce Slingerland

ABSTRACT p27 shifts from CDK inhibitor to oncogene when phosphorylated by PI3K effector kinases. Here, we show p27 is a cJun co-regulator, whose assembly and chromatin association is governed by p27 phosphorylation. In breast and bladder cancer cells with high p27pT157pT198 or expressing a CDK-binding defective p27pT157pT198 phosphomimetic, p27CK-DD, cJun is activated, binds p27 and p27/cJun complexes localize to the nucleus. p27/cJun upregulates TGFB2 to drive metastasis in vivo. Global analysis of p27/cJun chromatin binding and gene expression shows cJun recruitment to many target genes is p27-dependent, increased by p27 phosphorylation and activates programs of EMT and metastasis. Finally, human breast cancers with high p27pT157 differentially express p27-cJun regulated genes of prognostic relevance, supporting the biological significance of the work.

PI3K is activated in over 60% of human cancers, mediating C-terminal p27 phosphorylation. Present work reveals cooperation between PI3K and cJun pathways: p27 phosphorylation by PI3K-activated kinases stimulates p27-cJun co-recruitment to chromatin and activation of transcription programs of cell adhesion, motility, TGFB2 and EMT to drive tumor progression. Prior analysis showed high p27pT157 strongly associates with activated AKTpS273 and p90RSKpT359 in human breast cancers. These cancers also differentially express p27/cJun target genes and identify a poor prognostic group. In cancers, the cell cycle restraining effects of p27 are lost though increased proteolysis and decreased translation. Present work reveals a previously unknown oncogenic action of p27, in which p27 acts as a novel cJun co-activator to drive oncogenic gene expression programs. This manuscript has been published by PNAS (see Appendix). For ease of review of the grant funded data, all figures and the results section are included in this report below. For the supplemental figures, please see the appended reprint (Appendix 1). After each section below, we indicate which part of the SOW the figures pertain to.

p27 drives an EMT gene expression program. Prior work showed that C-terminal p27 phosphorylation mediates activation of TWIST1 to drive a morphologic EMT (*1*). To investigate effects of p27 on metastatic gene programs more broadly, global gene expression assayed by RNA sequencing (RNA-seq) was compared in MDA-MB-231 (hereafter 231), a breast cancer line with low metastatic ability, MDA-MB-231-1833 a bone-tropic highly metastatic derivative line (*2*) (hereafter 1833), and 1833shp27, in which p27 was stably depleted (*3*). To test effects of phosphorylated p27pT157pT198, we used MDA-MB-231 transduced with p27 bearing phosphomimetic threonine to aspartic acid mutations at T157 and T198) (*1*). Since as little as 2-3 fold p27 overexpression arrests the cell cycle and would not permit study of phosphomimetic p27, p27 was also mutated to abolish cyclin and CDK binding (*4*), yielding p27CK-DD (*1*). Notably, upon transduction of p27CK- and p27CK-DD, only the phosphomimetic p27 induces a morphologic EMT, and confers excess metastasis, indicating that these phosphorylations are critical to p27-driven EMT (*1*).

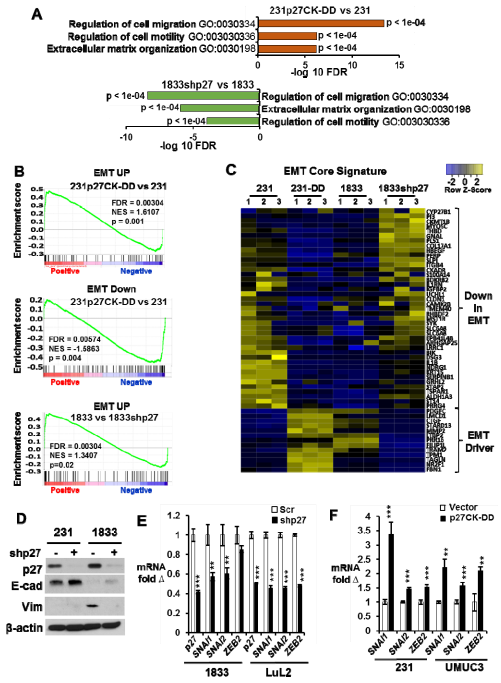

Fig 1. p27 activates an EMT gene expression program. (A) GO analysis of genes governing cell migration, motility and extracellular matrix in 231 vs 231p27CK-DD and in 1833 vs 1833shp27 (FDR, fold discovery rate). (B) GSEA shows differential expression of EMT core signature genes (27) upregulated (EMT UP) and downregulated (EMT down) in the indicated lines. NES; normalized enrichment score, FDR and p values shown. (C) Heat map of mean fold changes in differentially expressed EMT core signature genes in parental 231, 231p27CK-DD, 1833, and 1833shp27. Genes altered by p27 knockdown revert away from the Taube EMT core signature (27). Genes listed in SI appendix, Table S1. (D) Effects of stable p27 depletion in 1833 on p27 and EMT markers (E-cadherin and Vimentin) by Western (β-actin as loading control, data representative from >3 repeat assays). (E) Effects of stable p27 depletion (shp27) on qPCR expression of EMT transcription factors (SNAI1, SNAI2, and ZEB2) in PI3K-activated lines (1833 and LuL2) vs. scramble shRNA controls (Scr). (F) Effects of stable p27CK-DD expression on expression of EMT transcription factors in 231 and UMUC3 vs. vector only control lines. In E and F, means graphed +/- SEM from >3 replicates of >3 biologic assays (**p < 0.01, ***p < 0.001). (See also SI Appendix, Fig. S1 A, B).

Gene ontogeny analysis (GO) revealed activation of programs associated with cell motility, migration and extracellular matrix organization in 231p27CK-DD compared to 231, and in 1833 versus 1833shp27 (Fig. 1*A*). Differentially expressed genes in these lines were

compared with an established "EMT core signature" derived by over-expression of master EMT regulators in human mammary epithelial cells (*5*). Gene set enrichment analysis (GSEA) showed genes upregulated in this signature (EMT UP) were increased in 231p27CK-DD compared to 231 and in highly metastatic 1833 versus 1833shp27, while genes downregulated in the EMT signature were also decreased in the highly metastatic lines (Fig. 1*B* and SI Appendix, Fig. S1*A*). EMT core signature genes differentially expressed in both 231p27CK-DD versus 231 and in 1833 versus 1833shp27 are shown in Fig. 1*C*. Genes downregulated during EMT were decreased in 231p27CK-DD and 1833 compared to both 231 and 1833shp27, while genes activated in the EMT signature were increased in both highly metastatic lines (Fig. 1*C*, see gene list, SI Appendix, Table S1). Thus, p27 knockdown reverses the expression of an EMT gene profile, supporting the notion that p27 drives metastasis, in part, by activating an EMT transcription program.

Comparison of EMT markers and drivers showed 1833 expressed negligible E-CADHERIN and higher N-CADHERIN and VIMENTIN than 231 (Fig. 1*D*). p27-mediated EMT activation was validated by qPCR of major EMT-driving transcription factors in two different breast and bladder cancer models with sister lines of low and high metastatic ability. MDA-MB-231-4175 (hereafter 4175) is a highly metastatic 231 variant with tropism to lung (*6*), while 1833, as noted above, has bone metastatic tropism (*2*). UMUC3-LuL2 (hereafter LuL2) is a lung metastatic derivative of the bladder carcinoma line, UMUC3 (*7*). Both metastatic variants have higher PI3K activation and higher p27pT157 and p27pT198 than parental cells (*1, 3*). p27 depletion decreased expression of master EMT transcription factors (EMT-TF) *SNAI1*, *SNAI2*, and *ZEB2* in highly metastatic 1833 and LuL2 (Fig. 1*E*), confirming findings on RNA-seq (see SI Appendix, Fig. S1*B*) while p27CK-DD transduction upregulated EMT-TFs in both breast (231) and bladder (UMUC3) lines (Fig. 1*F*).

p27pT157pT198 activates TGF-β signaling by inducing *TGB2* expression. To further identify p27-regulated gene programs, we focused on genes both stringently upregulated by p27CDKDD transduction in 231 and also downregulated in 1833 by p27 depletion. 489 genes were increased by over two fold ($p < 0.005$, $q < 0.1$) in 231p27CK-DD versus 231, while 229 genes were downregulated by at least one half (fold-change

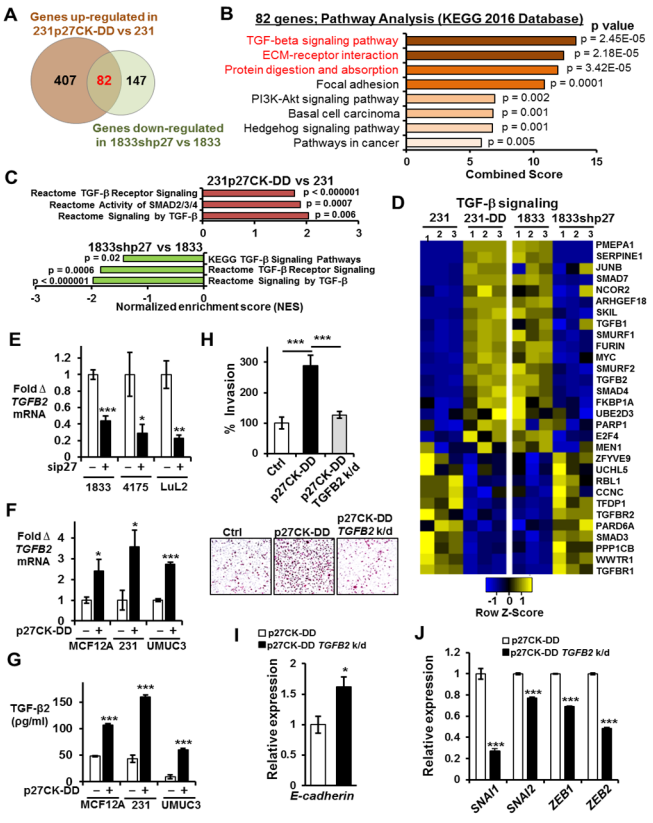

Fig. 2. TGF-β signaling is regulated by p27. *(A)* Venn diagram depicts genes upregulated in 231p27CK-DD vs. 231 (fold change > 2.0, p value < 0.005, q value < 0.1) and downregulated in 1833shp27 vs. 1833 (fold-change < 0.5, p value < 0.005, q value < 0.1). Gene numbers are indicated. See also SI Appendix, Table S2. *(B)* GO analysis shows the top signaling pathways in the KEGG 2016 database related to the 82 genes upregulated in 231p27CK-DD vs 231 and decreased with p27 loss in 1833. See also SI Appendix, Fig. S1C. *(C)* Pathway analysis of these 82 differentially expressed genes. NES; normalized enrichment score. See also SI Appendix, Fig. S1D. *(D)* Heatmaps show differential expression of 30 TGF-β signaling pathway genes from 3 independent RNA seq experiments. See also SI Appendix, Fig. S1D, E and Table S3. *(E)* Effects of short term siRNA-mediated p27 depletion (sip27) on *TGFB2* mRNA by qPCR at 48 hrs in PI3K-activated, metastatic lines (1833, 4175, and LuL2) vs. scramble siRNA controls. *(F & G)* Effects of stable p27CK-DD expression on *TGFB2* mRNA (F) and on secreted TGF-β2 (pg/ml) over 48 hours (G) in indicated lines. *(H)* Quantitative data (top) and representative images (bottom) of matrigel invasion in 231, 231p27CK-DD, and *TGFB2*-depleted 231p27CK-DD (*TGFB2* k/d- for depletion see SI Appendix, Fig. S4A). *(I and J)* Effects of *TGFB2* depletion on *CDH1* expression (I) and EMT drivers (*SNAI1*, *SNAI2, ZEB1*, and *ZEB2*; J). Means +/- SEM graphed from ≥3 replicates of ≥3 different biologic assays (*p < 0.05, **p < 0.01, ***p < 0.001). See also SI Appendix, Fig. S1F-H.

> 0.5, p < 0.005, q < 0.1) by p27 depletion in 1833. Of these, 82 genes were both upregulated in 231p27CK-DD versus 231 and also downregulated in 1833shp27 versus. 1833 (Fig. 2*A* and SI Appendix, Table S2). GO analysis showed that the 82 genes that are both upregulated by p27CK-DD in 231 and downregulated in 1833 upon p27 loss, are associated with important oncogenic pathways including TGF-β, focal adhesion, extracellular matrix receptor interaction and PI3K-AKT signaling pathways (Fig. 2*B* and SI Appendix, Fig. S1*C*). GSEA also showed TGF-β signaling activation in 231p27CK-DD compared to 231, while p27 knockdown impaired TGF-β pathway activation in 1833 (Fig. 2*C* and *D*, and SI Appendix, Fig. S1*D* and Table S3). Similarly, treatment with PI3K/mTOR inhibitor, PF04691502 (hereafter PF1502) at a dose known to inhibit PI3K in these lines and to decrease both p27pT157 and p27pT198 (*3*), downregulated genes associated with TGF-β pathway

activation (SI Appendix, Fig. S2*E*). Thus TGF-β signaling is activated by p27CK-DD transduction in 231, and inhibited by p27 knockdown and by PI3K inhibition in 1833.

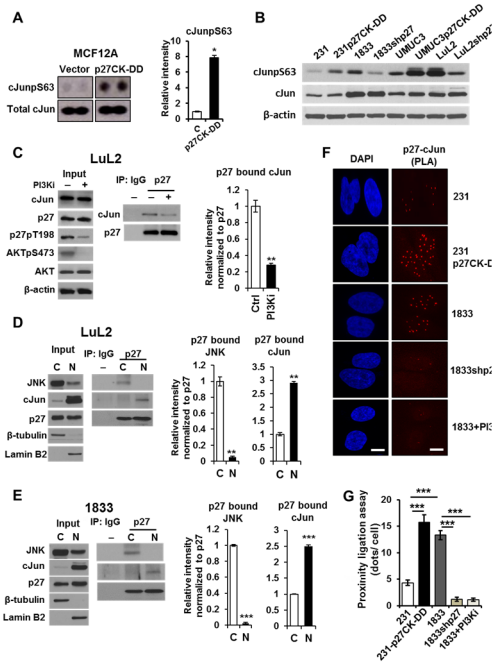

Fig. 3. Association of cJun with p27 is increased by p27 phosphorylation. *(A)* Activated cJun (cJunpS63) in MCF12A controls (Vector) and MCF12Ap27CK-DD (p27CK-DD) by dot blot (mean densitometry +/-SEM graphed on right). *(B)* Westerns of cJun, JunpS63, and β-actin in the indicated lines. *(C)* Lul2 were treated for 48 hours with PI3K inhibitor, PF1502 (PI3Ki). Westerns show input (left) for p27 immunoprecipitation (IP)-blotting to detect p27-associated cJun (middle). Densitometric quantitation of p27 bound cJun (right). See also SI Appendix, Fig. S2A and B. *(D and E)* Nuclear (N) and cytoplasmic (C) fractions of LuL2 (D) and 1833 (E) were immunoblotted (left) and p27-associated cJun and JNK detected by IP-blot (middle), with densitometry on right. *(F) In situ* proximity ligation assay (PLA) shows p27-Jun associated complexes in indicated lines and in 1833 treated with PF1502 (PI3Ki) indicated by red fluorescent dots. *(G)* Mean dots graphed ± SEM from triplicate PLA; ANOVA with post hoc comparisons (***p < 0.001). Scale bar, 10 µm. See also EMSA data, SI appendix, Fig. S2C.

Upregulation of *TGFB2* by p27 was confirmed by qPCR in three highly metastatic lines, 1833, 4175 and LuL2. In all 3 lines, p27 depletion decreased *TGFB2* (Fig. 2*E*). Furthermore, p27CK-DD transduction increased *TGFB2* expression and TGF-β2 secretion in the immortal, non-transformed mammary epithelial line, MCF12A, and in low-metastatic 231 and UMUC3 lines (Fig. 2*F* and *G*). In MCF12A, TGF-β2 induced a morphological change from an epithelial to a more mesenchymal phenotype (SI Appendix, Fig. S1*F*). TGF-β2 upregulated *SNAI1* and *SNAI2* expression in MCF12A, 231, and UMUC3 (SI Appendix, Fig. S1*G*) and increased matrigel invasion by 231 and UMUC3 (Fig. 2*G* and SI Appendix, Fig. S1*H*) confirming its importance to EMT in these models. In 231, EMT activation by p27CK-DD, as shown by increased matrigel invasion, decreased E-cadherin and higher N-cadherin and EMT-TF expression, were all reversed by *TGFB2* depletion (Fig. 2*H-J*), indicating that TGF-β2 is a key driver of EMT activation by p27. Thus, C-terminally phosphorylated p27 appears to activate an EMT program, in part by inducing *TGFB2* expression.

p27/cJun complex formation and nuclear localization are regulated by p27 phosphorylation. To investigate how p27 upregulates *TGFB2* expression, a phosphoprotein array was compared in MCF12A

and MCF12Ap27CK-DD. Notably, p27CK-DD-expression significantly increased serine 63-phosphorylated, activated cJun (hereafter cJunpS63) in MCF12A (Fig. 3*A*). p27CK-DD-transduced 231 and UMUC3 also had more cJunpS63 than parental lines, while p27 depletion in metastatic 1833 and LuL2 lines decreased cJunpS63 (Fig. 3*B*). cJun forms heterodimeric AP-1 transcription factor complexes that contributes to transformation (*8*). An *in silico* search revealed AP-1 consensus binding sites upstream of the *TGFB2* coding sequence.

To test if p27 might interact with cJun to regulate *TFGB2* expression, we next assayed if cellular p27 binds cJun. Treatment of LuL2 with PF1502, over 48 hours decreased AKTpS473 and reduced p27 phosphorylation at T198 (Fig. 3*C*, left), without affecting p27 or cJun levels. cJun was detected in cellular p27 immunoprecipitates in Lul2. PI3K inhibition decreased both p27pT198 and p27-bound cJun (Fig. 3*C*). Furthermore, more p27-associated cJun was detected in p27CK-DD-transduced 231 and UMUC3 than in vector control cells as assayed by densitometry (SI Appendix, Fig. S2*A* and *B*). Both observations suggest that the interaction of p27 with cJun is increased by p27 phosphorylation.

Levels of p27 associated cJun and JNK were assessed in nuclear and cytoplasmic fractions. In both LuL2 and 1833, JNK was largely cytoplasmic, while cJun was predominantly nuclear (Fig. 3*D* and *E*, left). p27-associated cJun was 2-3 fold higher in nuclear than in cytoplasmic fractions, while p27- associated JNK was detected only in the cytoplasm. (Fig. 3*D* and *E*, right). Proximity ligation assays (PLA) confirmed the interaction between nuclear p27 and cJun, and that this is greater in 231p27CK-DD than in control 231 cells (Fig. 3*F* and *G*). EMSA revealed that p27 can bind an AP1 consensus motif (SI Appendix, Fig. S2*C*).

cJun and p27 are co-recruited to a site upstream of *TGFB2*. Since p27 could associated with both cJun and with AP1 motifs, we next assayed if nuclear p27/cJun complexes might mediate the *TGFB2* gene induction observed in p27-activated cells. Publicly available cJun ChIP-seq ENCODE data revealed that cJun binds a 5'-TGAG/CTCA-3' AP1 consensus site upstream of the *TGFB2* transcriptional start site (TSS) in human cells (Fig. 4*A*). ChIP-qPCR showed cJun and p27 are co-recruited to this AP1 site. More p27 and cJun were associated with this AP1 motif in 231p27CK-DD and 1833 than in 231 vector controls. Notably, chromatin

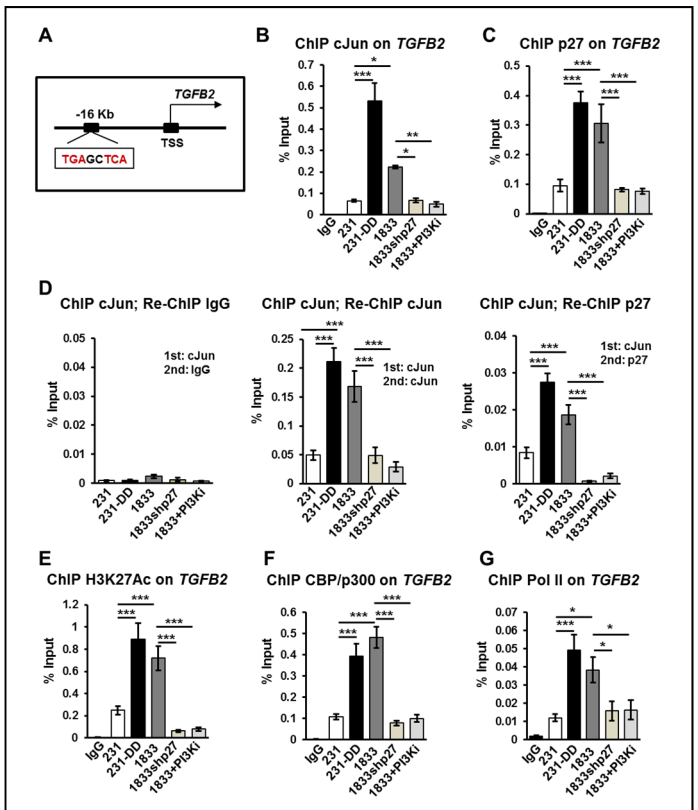

Fig. 4. cJun and p27 are co-recruited to a *TGFB2* AP1 site. *(A)* cJun/AP1 consensus motif upstream of *TGFB2* transcriptional start site (TSS). *(B and C)* ChIP-PCR with cJun (B) and p27 (C) antibodies, respectively, show binding to an AP1 site upstream of *TGFB2* in indicated lines and in 1833 treated for 48 hrs with PF1502 (PI3Ki). *(D)* ChIP-Re-ChIP assay of p27 association with cJun bound *TGFB2* AP1 site in the indicated lines. *(E-G)* ChIP assays show H3K27Ac (E), CBP/p300 (F), and Pol II (G) binding to the *TGFB2* AP1 site in the indicated lines. Means +/- SEM graphed from ≥3 replicates of ≥3 biologic assays, and post-hoc p-values from ANOVA (*p < 0.05, **p < 0.01, ***p < 0.001). See also SI appendix, Fig. S3.

association of both p27 and cJun decreased with p27 depletion and with loss of p27 phosphorylation following PI3K/mTOR inhibition with PF1502 (Fig. 4*B* and *C*). Neither p27 nor cJun bound to irrelevant sites (SI Appendix, Fig. S3*A*). Sequential ChIP assays with cJun followed by re-ChIP with p27 antibodies indicated that cJun and p27 co-occupy this *TGFB2* site, with greater recruitment in p27CK-DD-expressing and in PI3K-activated cells, and loss of both p27 and cJun upon p27 knockdown and PI3K inhibition (Fig. 4*D*). Thus, C-terminal p27 phosphorylation appears to increase cJun/p27 co-recruitment to this AP1 motif upstream of *TGFB2*. The bladder cancer models showed similar patterns of p27 and cJun recruitment to this *TGFB2* AP1 site (SI Appendix, Fig. S3*B*). H3K27Ac, coactivator CBP/p300, and RNA polymerase II (Pol II) were more abundant at this *TGFB2* site in p27pT157pT198 or p27CK-DD expressing cells than in 231 controls, and decreased significantly with p27 depletion and PI3K inhibition (Fig. 4*E-G*). Since p27 knockdown decreases *TGFB2* expression and p27CK-DD transduction induces *TGFB2* to increase TGF-β2 secretion, these data suggest a model in which C-terminal p27 phosphorylation promotes p27 and cJun recruitment, and interaction with CBP/p300 and Pol II at this enhancer to induce *TGFB2* expression (SI Appendix, Fig. S3*C*).

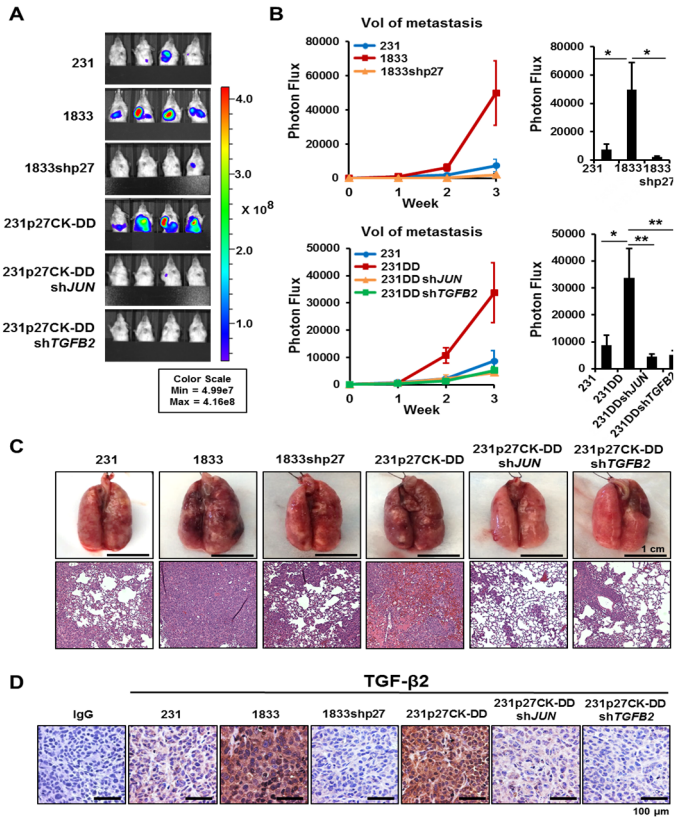

Fig. 5. cJun and TGF-β2 are required for p27 driven metastasis *in vivo*. *(A)* Primary orthotopic tumors were removed and animals followed by IVIS for metastasis. Representative bioluminescence images of tumor bearing mice 3 weeks after primary tumor removal. Color scale depicts photon flux (photons/second) from tumor bearing mice. *(B)* Mean bioluminescence (normalized photon flux)/second from tumor metastases (excluding regrowth of primary tumor at inguinal fat pad) is graphed for each group. Means +/- SEM graphed, p-values from ANOVA (*p < 0.05, **p < 0.01, ***p < 0.001). *(C)* Representative whole lung images (scale bar, 1 cm) and photomicrographs of metastatic lung tumors (scale bar, 100 µm) from indicated groups. *(D)* Representative TGF-β2 IHC in primary tumors from indicated lines. Scale bar, 100 µm. See also SI Appendix, Fig. S4.

cJun and TGF-β2 mediate p27-driven metastasis from primary tumors *in vivo*. Since p27 appears to drive a TGF-β2 dependent EMT, we assayed the functional contribution of C-terminally phosphorylated p27, cJun and TGF-β2 to metastasis *in vivo*. NOD-SCID mice were injected orthotopically with 231, 1833, 1833shp27, 231p27CK-DD, and with 231p27CK-DD depleted of either *JUN* or *TGFB2* (depletion shown in SI Appendix, Fig. S4*A*). After removal of primary tumors at 300 mm^3, mice were monitored for metastasis from the primary site. 1833 and 231p27CK-DD yielded significantly more metastases in liver, lymph nodes, and lung than vector control 231 cells (Fig. 5*A*-*C*). p27 depletion in 1833 and loss of cJun or TGF-β2 expression in 231p27CK-DD significantly decreased p27-driven metastasis *in vivo* (Fig. 5*A*-*C*). While 1833 and 231p27CK-DD formed more metastasis than 231, primary tumor growth and Ki67 staining did not differ significantly between groups (SI Appendix, Fig. S4*B* and *C*). TGFβ-2 levels, assayed by IHC, were elevated in primary tumors from 1833 and 231p27CK-DD compared to 231, and decreased in 1833shp27 tumors and in both *JUN* and *TGFB2*-depleted 231p27CK-DD-derived tumors (Fig. 5*D* and SI

Appendix, Fig. S4*D*). Thus, cJun activation and *TGFB2* induction appear to be required for p27 driven metastasis in this breast cancer model.

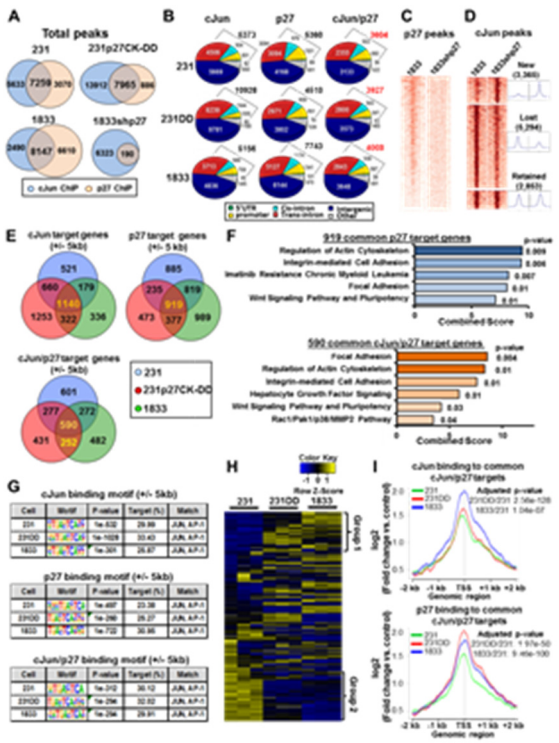

Fig. 6. Genome-wide DNA binding of p27 and cJun. *(A)* Venn diagrams show mean p27- and cJun- DNA binding peaks in 231, 231p27CK-DD, 1833 and 1833shp27 from two independent ChIP-Seq assays, each with two biologic replicates. *(B)* Genomic distribution of DNA binding peaks for p27, cJun and for peaks occupied by both p27 and cJun in the indicated lines. *(C and D)* DNA binding heatmaps of p27 (C) and cJun ChIP (D) in 1833 and 1833shp27, respectively. See also SI Appendix, Fig. S5A, and see Fig S5B for cJun-regulated pathways affected by loss of p27. *(E)* Venn diagrams show mean numbers of target genes (+/-5 kb of TSS) bound by cJun only, p27 only, and both cJun/p27 in 231, 231p27CK-DD (231DD) and 1833. *(F)* GO analysis (WikiPathway 2016) showing major signaling pathways related to 919 p27 target genes and 590 cJun/p27 co-target genes bound in all 3 lines (from E, above). See also SI Appendix, Fig. S5C. *(G)* Binding motif search shows top transcription motif bound by cJun only, p27 only, and cJun/p27 for binding motifs +/- 5 kb from TSS for each line. See also SI Appendix, Fig. S5D (binding at all sites). *(H)* Heatmaps show expression profile from RNA-seq of genes bound by both cJun and p27 in ChIP-Seq in all 3 lines. *(I)* Signal intensities of p27 and cJun were quantitated at target genes bound by both cJun and p27 in all 3 cell lines. Significant differences calculated with paired t-test, and p values adjusted by Bonferroni Hochberg. See also SI Appendix, Fig. S5E and F for signal intensities of cJun and p27 binding to group 1 and group 2 genes, respectively.

Identification of cJun/p27-regulated target genes. To test if p27 binds more broadly to chromatin and to identify phosphorylation dependent patterns of chromatin occupancy by p27 and cJun, ChIPseq was performed in 231, 231p27CK-DD and 1833. As a control, we also performed p27 ChIPseq in 1833shp27. This revealed that p27 is broadly recruited to chromatin and that a significant proportion of cJun ChIPseq peaks also contain p27 (Fig. 6*A*), suggesting that cJun and p27 may function together at common sites. Notably, 231p27CK-DD showed greater recruitment not only of p27, but also of cJun to chromatin, even at sites not shared by p27. This may result from p27-mediated cJun activation (Fig. 3*B*). Genomic distribution analysis showed that a little over half of the sites bound by cJun, p27, and both cJun/p27 were located at promoters or intronic sites, while remaining sites occupy intergenic regions (Fig. 6*B*). Importantly, ChIPseq heat maps showed that the p27 signal was abrogated in p27-depeleted 1833shp27 cells (Fig. 6*C*). Interestingly, the chromatin occupancy of cJun was modulated by p27 depletion: among a little over 10,000 cJun bound peaks detected in 1833, 5,294 sites were shared by p27 and

lost or decreased upon p27 knockdown, while 2853 cJun bound peaks were unaffected. In addition, 3365 new, exclusively cJun bound peaks were acquired (Fig. 6*D* and SI Appendix, Fig. S5*A*). GO analysis of 1,364 genes annotated by the 5,294 cJun-bound peaks that are lost with p27 depletion in 1833, showed that these p27-regulated cJun targets are associated with Notch, apoptosis and cytoskeleton signaling (SI Appendix, Fig. S5*B*). Thus, p27 may be required for cJun recruitment to an important fraction of cJun regulated genes.

Evaluation of binding at target genes (+/-5 kb of the TSS) revealed that p27 is recruited to over 2000 target genes in each of the 3 lines (Fig. 6*E*, right Venn diagram). Notably, GO of the 919 p27 targets common to all 3 lines, reveals that p27 binds genes involved in focal adhesion, actin cytoskeleton, integrin signaling, and Wnt pathways (Fig. 6*F*, top). GO of cJun targets common to all 3 lines identifies genes governing cell surface adhesion, integrin and growth factor pathways (SI Appendix, Fig. S5*C*). There were 590 cJun/p27 target genes commonly bound in all 3 lines (Fig. 6*E*, bottom; SI Appendix, Table S*4*). These are associated with pathways similar to those for each factor alone and also include hepatocyte growth factor (HGF) and Rac1/Pak1 signaling (Fig. 6*F*, bottom). p27 and cJun were also co-recruited to 252 novel target genes in both 231p27CK-DD and 1833 that were not bound in 231 (Fig. 6*E*, bottom).

DNA binding motif analysis revealed that AP1 binding consensus motifs including JunB, Fra1, and BATF were the top-enriched DNA motif for p27 and cJun individually and account for nearly one third of the sites bound by both cJun and p27 (binding motifs+/-5 kb of TSS, Fig. 6*G*; genome wide binding motifs in SI Appendix, Fig. S5*D*). Thus, p27 and cJun are commonly recruited to genes bearing cJun consensus motifs.

Differential expression of cJun/p27 target genes in lines with different metastatic potential. To evaluate the potential for p27 and cJun to co-regulate gene expression, patterns of chromatin annotation were compared with RNAseq gene expression data. Of the 919 genes annotated by p27 in all 3 lines, over half were differentially expressed in each of 231p27CK-DD (492/919) and 1833 (456/919) compared to 231 (any fold change vs 231, q >0.1). cJun/p27 target genes bound in all 3 lines showed two differential

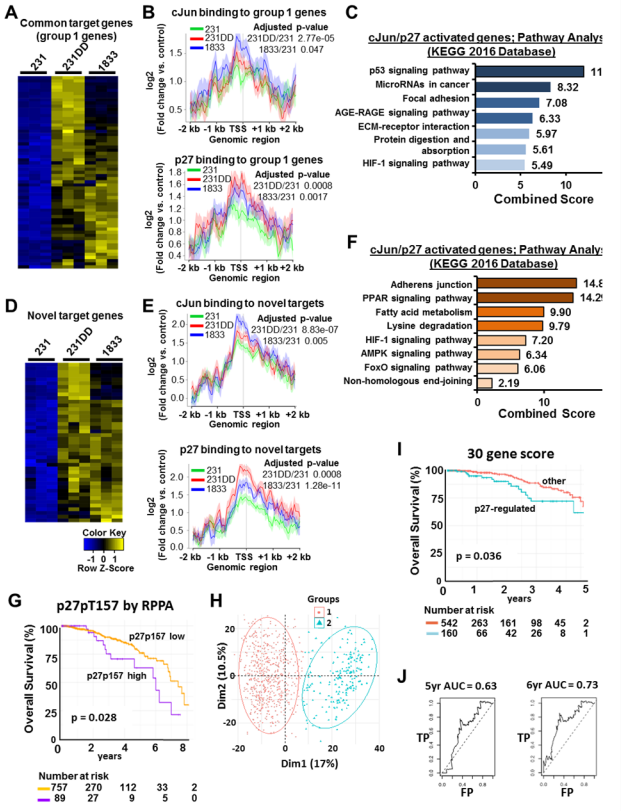

Fig. 7. cJun/p27 regulated target genes govern cancer programs of tumor progression. *(A)* Heat map of expression of 61 p27/cJun target genes common to all 3 lines whose expression is upregulated in 231p27CK-DD (231DD) and 1833 lines vs 231. See also SI Appendix, Table S4. *(B)* Mean amplitudes of target gene binding by cJun and by p27 are shown for the differentially expressed genes in (A) in the indicated cell lines. *(C)* GO analysis shows the top signaling pathways related to the differentially expressed genes identified in (A) above. *(D)* Heat map of expression of 43 novel p27/cJun novel target genes bound in 231DD and 1833 but not 231 that are differentially expressed in the indicated cell lines. See also SI Appendix, Table S5. *(E)* Mean amplitude of target gene binding by cJun and by p27 are shown for the differentially expressed genes in (D) in the indicated cell lines. *(F)* GO analysis shows the main signaling pathways related to the genes identified in (D) above. See also SI Appendix, Fig. S6 for validation of cJun/p27 co-target genes. *(G)* KM graph showing differential overall survival among women whose breast cancers have high versus low p27pT157 on RPPA from n=846 cases in the TCGA/TCPA dataset. *(H)* Principle component analysis of 30 p27 regulated genes expressed among n=703 breast cancers. *(I)* KM graph shows overall breast cancer survival according to differential expression of the p27-regulated 30 gene profile among the training set (n=703 cases). *(J)* The prognostic value of this p27-regulated 30 gene signature for OS was validated using Region of Curve (ROC) analysis in an independent breast cancer validation cohort.

expression patterns: group 1 genes were upregulated in 231p27CK-DD and 1833 compared to 231 controls, while group 2 were downregulated. p27/cJun target genes activated in both highly metastatic lines identify putative oncogenes (group 1, Fig. 6*H*) while those downregulated in metastatic derivatives compared to control 231 may encode tumor suppressors (group 2, Fig. 6*H*).

Lines with p27 activation showed greater recruitment of both cJun and p27 to target genes: recruitment of both p27 and cJun to all 590 common target genes (Fig. 6*H*) and to differentially expressed cJun/p27-targets from both groups 1 and 2 (SI Appendix, Fig. S5*E* and *F*) was significantly greater in 231p27CK-DD and 1833 than in 231, similar to the pattern detected at the *TGFB2* AP1 site (Fig. 4). Differential expression of cJun/p27-activated group 1 genes and p27 and cJun binding intensities are shown in (Fig.7*A* and *B* and SI Appendix, Table S4). These cJun/p27-activated genes associated strongly with cancer signaling pathways, including pro-oncogenic p53, cancer-related miRNAs, focal adhesion, RAGE and HIF1 signaling (Fig. 7*C*).

p27-cJun targets bound exclusively in 1833 and 231p27CK-DD and not in 231 might include novel pro-oncogenes whose binding is only acquired when highly phosphorylated p27pT157T198 binds cJun. A subset of these novel p27-cJun target genes was upregulated in the

highly metastatic lines (Fig. 7*D* and *E* and SI Appendix, Table S5). This gene set also directs pathways associated with tumor progression and metastasis (Fig. 7*F*). We validated p27 and cJun binding to 3 target genes (*MYO10, PAI1*, and *KLF8*) by ChIP-qPCR and verified their differential expression by RT-qPCR. *MYO10* is a gene implicated in cell invasion and metastasis (*9*). Both binding of cJun and p27 to an AP1 site +2 kb of *MYO10*, and *MYO10* expression were greater in 231p27CK-DD and 1833 than in 231, and were downregulated in 1833shp27 (SI Appendix, Fig. S6*A-D*). Differential cJun/p27 binding to, and expression of two other target genes, *PAI1/SERPINE1* (a known prognostic factor for breast cancer (*10*)) and *KLF8,* an EMT mediator (*11*), were also verified (SI Appendix, Fig. S6 *E-L*). Taken together, p27 appears to bind cJun and promote recruitment to and transactivation of gene programs that contribute to tumor progression and metastasis.

p27/cJun target genes are differentially expressed in breast cancers with high p27pT157. We next assayed if primary human breast cancers with C-terminally phosphorylated p27 would show differential expression of p27/cJun regulated genes identified herein. Among primary breast cancers in the TCGA database, 846 had gene expression, p27pT157 levels on Reverse Phase Protein Array, and outcome data available. Of these, cancers in the top decile of p27pT157 expression showed significantly worse overall survival (OS, Fig. 7G, p=0.028). A subset of 392 genes, differentially expressed in the "high p27pT157" breast cancers versus all others, were also coordinately differentially expressed in p27-activated 231p27CK-DD and 1833 compared to 231 and 1833shp27. Of these 392 differentially expressed genes, 25% (97/392) were Jun-bound, and 16% (63/392) were showed both p27 and cJun binding on ChIPseq and include the validated target, PAI1. Univariate and multivariate analysis of each of these genes in a training data set of 702 breast cancers identified the 30 "p27-regulated genes", differentially expressed in both p27-activated cell lines and in "high p27pT157" cancers that contribute most importantly to patient outcome. Principle component analysis showed that these 30 genes cluster patients into two groups (Fig. 7H) that have significantly different OS on Kaplan Meyer analysis (Fig. 7I, p=0.036). The prognostic value of this p27-regulated gene signature for OS was validated using Region of Curve (ROC) analysis in an independent breast cancer validation cohort and yielded an ROC of 0.63 at 5 years and of 0.73 at 6 years of follow up

(Fig. 7J). The coordinate expression of p27-regulated gene drivers of poor patient outcome in both p27-activated cancer lines and in primary breast cancers with high C-terminal p27 phosphorylation supports the biologic relevance of p27-driven gene regulation to metastatic tumor progression.

1. D. Zhao *et al.*, Cytoplasmic p27 promotes epithelial-mesenchymal transition and tumor metastasis via STAT3-mediated Twist1 upregulation *Oncogene* **34**, 5447-5459 (2015).
2. Y. Kang *et al.*, A multigenic program mediating breast cancer metastasis to bone. *Cancer Cell* **3**, 537-549 (2003).
3. S. Wander *et al.*, PI3K/mTOR inhibition can impair tumor invasion and metastasis in vivo despite a lack of antiproliferative action in vitro: implications for targeted therapy. *Breast Cancer Res Treat* **138**, 369-381 (2013).
4. J. Vlach, S. Hennecke, B. Amati, Phosphorylation-dependent degradation of the cyclin-dependent kinase inhibitor p27. *EMBO J* **16**, 5334-5344 (1997).
5. J. H. Taube *et al.*, Core epithelial-to-mesenchymal transition interactome gene-expression signature is associated with claudin-low and metaplastic breast cancer subtypes. *Proc.Natl.Acad.Sci.U.S.A* **107**, 15449-15454 (2010).
6. A. J. Minn *et al.*, Genes that mediate breast cancer metastasis to lung. *Nature* **436**, 518-524 (2005).
7. J. B. Overdevest *et al.*, CD24 Offers a Therapeutic Target for Control of Bladder Cancer Metastasis Based on a Requirement for Lung Colonization. *Cancer Res.* **71**, 3802-3811 (2011).
8. J. Hess, P. Angel, M. Schorpp-Kistner, AP-1 subunits: quarrel and harmony among siblings. *J.Cell Sci.* **117**, 5965-5973 (2004).
9. R. Cao *et al.*, Elevated expression of myosin X in tumours contributes to breast cancer aggressiveness and metastasis. *Br.J.Cancer* **111**, 539-550 (2014).
10. M. D. Sternlicht *et al.*, Prognostic value of PAI1 in invasive breast cancer: evidence that tumor-specific factors are more important than genetic variation in regulating PAI1 expression. *Cancer Epidemiol.Biomarkers Prev.* **15**, 2107-2114 (2006).
11. X. Wang *et al.*, Kruppel-like factor 8 induces epithelial to mesenchymal transition and epithelial cell invasion. *Cancer Res.* **67**, 7184-7193 (2007).

The data for a second manuscript (Manuscript #2) is planned to be submitted within the next year. The results to date, including abstract and results section with figures are presented below. The part of the SOW completed above indicates which Figures and S Figures of Manuscript #2 pertain to which parts of the SOW. Please note that the entire manuscript# 2 with the Supplemental Sfigs and tables is appended to this report as Appendix 2. For review of Supplemental data referred to below, please see the appended preprint Appendix #2

p27 binds cJun, YY1 and HDAC1 to co-repress PTPN12 and increase tumor-initiating stem cells

Hyunho Yoon, Kibeom Jang, Miyoung Shin, Minsoon Kim, Dekuang Zhao, Xue Xiao, Lluis Morey, and Joyce M. Slingerland

ABSTRACT: The CDK inhibitor, p27, acquires pro-oncogenic actions in cancer. We showed p27pT157pT198 is broadly recruited to chromatin with cJun to activate gene drivers of EMT and metastasis. Here, we show p27 also interacts with cJun to corepress pro-differentiation genes and increase cancer-initiating stem cells. In breast and bladder cancer cells expressing high endogenous p27pT157pT198 or phosphomimetic cyclin- and CDK-binding-defective p27CK-DD, nearly half of p27/cJun co-targets are repressed and these govern adipogenesis, cardiac and hematopoietic differentiation. The gene encoding phosphatase PTPN12 was strongly

downregulated in p27-activated cells. p27 and cJun recruit SIN3A, YY1, and HDAC1 to corepress this tumor suppressor gene, leading to increased sphere formation and tumor initiating cells. Upon PTPN12 loss, its substrate, PYK2, mediates STAT3 activation, increases spheres and ALDH1 activity in vitro and tumor initiating cells in vivo. Thus, p27-bound cJun represses differentiation genes and via PTPN12 repression, activates pathways that upregulate cancer initiating cells.

C-terminally phosphorylated p27 downregulates genes associated with differentiation

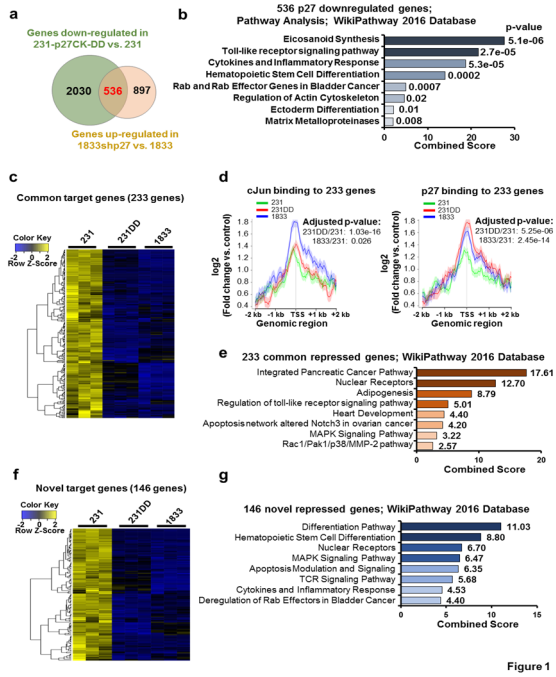

Figure 1 **Fig. 1. C-terminally phosphorylated 27/cJun target tumor suppressor genes**. **a**, Venn diagram comparing genes downregulated in 231p27CK-DD vs. 231 (fold-change < 0.75, p value < 0.005, q value < 0.1) and upregulated in 1833shp27 vs. 1833 (fold change > 1.5, p value < 0.005, q value < 0.1). Gene numbers are indicated. See also Supplementary Table 1a. **b**, ENRICHR analysis from the WikiPathway 2016 database using the 536 p27-downregulated genes from (**a**). See also Supplementary Fig. 1a. **c**, Heat map showing differential expression of 233 cJun/p27 target genes that are commonly bound in all of 231, 231p27CK-DD (231DD), and 1833. See also Supplementary Table 1b. **d**, Graphs shows differential binding of cJun (left) and p27 (right) to 233 target genes commonly bound in 231, 231p27CK-DD (231DD), and 1833. **e**, Pathway analysis (WikiPathway 2016) of 233 cJun/p27 target genes common to all 3 lines whose expression is downregulated in p27 activated lines compared to control 231. See also Supplementary Fig. 1b. **f**, Heat map showing differential expression profile of 233 cJun/p27 target genes that are novel targets bound in, 231p27CK-DD (231DD), and 1833 but not in 231. See also Supplementary Table 1c. WikiPathway database showing the main signaling pathways associated with these 146 unique targets downregulated in p27 activated lines compared to 231. See also Supplementary Fig. 1c

Despite its identification over a decade ago as a mediator of cell motility and metastasis, the mechanisms governing the broad pro-oncogenic p27 actions in cancers have not been fully characterized. We recently identified p27 as a cJun co-regulator and showed that p27-bound cJun activates target genes implicated in tumor progression (see PNAS paper results above) Here, we investigated the potential for p27/cJun to repress target genes. We evaluated p27-regulated genes whose expression is decreased in highly metastatic breast cancer cells with high endogenous p27pT157pT198 or in cells transduced with Cyclin-CDK binding defective, phosphomimetic p27 (p27CK-DD). RNA sequencing analysis (RNA-Seq) was performed in the parental MDA-MB-231 (hereafter 231) breast cancer line, p27CK-DD transfected 231, in MDA-MB-231-1833 (hereafter 1833) and in 1833shp27 with stable depletion of p27 1833

is a highly metastatic derivative isolated from xenografted 231 bone metastases that expresses high levels of p27pT157pT198 due to PI3K activation. To identify putative tumor suppressors repressed by p27, we looked for genes downregulated in 231p27CK-DD cells versus parental. p27CK-DD expression in 231 downregulated 2,566 genes (fold-change < 0.75, $p < 0.005$, $q < 0.1$). We then asked which of these were also upregulated upon p27 depletion in 1833. Expression of 1,433 genes increased (fold-change > 1.5, $p < 0.005$, $q < 0.1$) in 1833shp27compared to 1833. Of these, 536 genes upregulated upon p27 knockdown in 1833 were also downregulated by p27CK-DD (Fig. 1a; Supplementary Table 1a). Gene set enrichment analysis showed these 536 p27-downregulated genes are associated with hematopoietic stem cell and ectoderm differentiation, and cancer pathways (Fig. 1b and Supplementary Fig. 1a). Thus, C-terminal phosphorylation of p27 mediates downregulation of gene profiles associated with differentiation.

We next looked for genes directly repressed by p27-bound cJun. C-terminally phosphorylation of p27 promotes its binding to cJun, and cJun/p27 complexes localize to the nucleus to transcriptionally co-regulate target genes (see PNAS paper above) ChIP sequencing analysis (ChIP-Seq) revealed 590 target genes were bound by both p27 and cJun within +/-5Kb of their transcriptional start sites in 231, 231p27CK-DD and 1833. While nearly half of these cJun/p27 target genes were upregulated in highly metastatic lines and may serve as oncogenes, many were repressed. Of 590 p27/cJun target genes, the expression of 233 of these genes was significantly repressed in 231p27CK-DD and 1833 compared to 231 (fold-change > 1.5, $p < 0.005$, $q < 0.1$; Fig. 1c; Supplementary Table 1b). Notably, more cJun and p27 bound to these 233 repressed target genes in 231p27CK-DD and 1833 than in 231 (Fig. 1d). Gene ontology (GO) showed these commonly repressed genes are associated with developmental and cancer related signaling including the Notch3 and MAPK pathways, but notably also with differentiation of cardiac and fat tissue (Fig. 1e and Supplementary Fig. 1b).

Genomic analysis also identified a discrete set of cJun/p27 target genes bound in 231p27CK-DD and 1833, but not in parental 231. cJun/p27 targets genes bound and downregulated uniquely in 1833 and 231p27CK-DD cells but not in 231 might represent novel targets whose stable binding and repression requires a higher threshold of p27 phosphorylation. Of the 252 cJun/p27 target genes bound only in the p27

activated lines, 146 genes were strongly downregulated in the p27-activated lines compared to 231 (Fig. 1F and Supplementary Fig. 1c; Supplementary Table 1c). GO analysis revealed that these cJun/p27-repressed genes also associated strongly with differentiation including hematopoietic stem cell differentiation, and with cancer pathways (Fig. 1g). Thus, in cells with activated, C-terminally phosphorylated p27, cJun and p27 corepress genes strongly associated with cancer pathways and with cardiac, myogenic and hematopoietic stem cell differentiation.

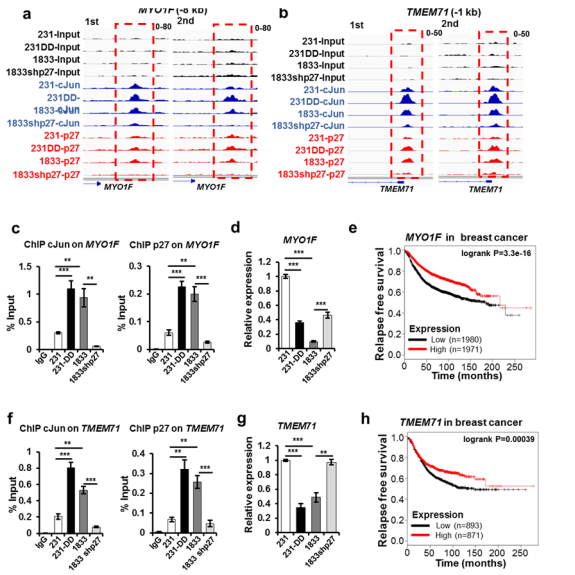

Fig. 2. Validation of novel cJun/p27 repressed tumor suppressors, *MYO1F* and *TMEM71*. **a**, ChIP-Seq tracks show cJun and p27 binding at site -8 kb of the *MYO1F* transcription start site (TSS). **b**, ChIP-Seq tracks of cJun and p27 bindings at a site -1 kb of the *TMEM71* TSS. **c**, **d**, **e**, Validation of binding to and expression of *MYO1F*, a cJun/p27 repressed target gene bound in all 3 lines. (**c**) ChIP-qPCR with anti-cJun (left) and anti-p27 (right) antibodies at the -8 kb site of *MYO1F*. (**d**) qPCR expression of *MYO1F* by qPCR in the indicated lines. (**e**) Kaplan-Meier plotter^{TM} data showing relapse free survival curves according to *MYO1F* mRNA expression above or below the median in 3951 primary breast cancers (red line: high, n = 1971; black line: low, n = 1980). **f**, **g**, **h**, Validation of p27/cJun binding to and expression of *TMEM71*, a cJun/p27 repressed target gene unique to 231p27CK-DD (231DD) and 1833, but not bound in 231. (**f**) ChIP-qPCR with anti-cJun (left) and -p27 (right) antibodies at the site -1kb of the *TMEM71* TSS. (**g**) qPCR expression of *TMEM71* in the indicated lines. (**h**) Kaplan-Meier plotter^{TM} data showing relapse free survival curves according to *TMEM71* expression above or below the median in 1764 primary breast cancers (red line: high, n = 871; black line: low, n = 893). All non-KM graphs show mean ± SEM from at least 3 replicate assays, and p-values were represented by ANOVA analysis (**p < 0.01, ***p < 0.001). See also Supplementary Fig. 2.

C-terminally phosphorylated p27 downregulates tumor suppressor genes

A series of transcriptionally repressed cJun/p27 co-target genes were selected for validation. *MYO1F* is a cJun and p27 target identified in all of 231, 231p27CK-DD and 1833 (Fig. 2a). p27 and cJun recruitment to *TMEM71* may require higher p27 phosphorylation since binding to this target was detected only in 1833 and 231CK-DD but not in 231(Fig. 2b). The cJun/p27 binding sites on *MYO1F* (-8 kb) and *TMEM71* (-1 kb) both contain AP1 consensus motifs. cJun and p27 binding observed by ChIP-Seq at these targets was confirmed by ChIP-qPCR, with greater binding in 231p27CK-DD and 1833 cells than in 231. p27 depletion decreased not only p27 recruitment (as expected) but also significantly attenuated cJun recruitment to these promoters (Fig. 2c, f), suggesting p27 facilitates cJun binding or

enhances complex stability. Furthermore, expression of both *MYO1F* and *TMEM71* was lower in 231-p27CK-DD and 1833 cells than in 231, and increased in 1833shp27 (Fig. 2d, g). *MYO1F* encodes a form of myosin expressed mainly in mammalian immune cells. MYO1F depletion increased thyroid cancer cell motility, and mutational inactivation of *MYO1F* induced tumor proliferation, suggesting a tumor suppressor role for MYO1F. The biological function of transmembrane protein, TMEM71, has not been characterized. Of note, both of these novel cJun/p27-repressed target genes appear to play tumor suppressor roles in human breast cancer, since high expression of each is associated with improved relapse-free survival on Kaplan Meier (KM) analysis of breast cancer patient data from KM-Plotter™ (Fig. 2e, h).

Two other cJun/p27 co-target genes were validated and may play tumor suppressor roles. cJun and p27 binding to *SH3TC1* (-1 kb) and *RCSD1* (-2 kb) was greater in p27-activated lines and both decreased upon p27 knockdown in ChIP Seq tracks. This pattern was validated by ChIP-qPCR (Supplementary Fig. 2a, b, e, f, respectively). Both *SH3TC1* and *RCSD1* were significantly repressed in 231p27CK-DD and 1833 compared to 231, while p27 knockdown in 1833 increased expression of both (Supplementary Fig. 2c, g, respectively). The biological function of SH3TC1 is not known. RCSD1 (RCSD Domain Containing 1) is involved in actin filament binding. An *RCSD1-ABL1* translocation is associated with acute lymphoblastic leukemia, suggesting that RCSD1 disruption is oncogenic. Interestingly, RCSD1 promotes cardiomyogenic differentiation. KM Plotter data analysis revealed that loss of each of each of *SH3TC1* and *RCSD1* correlates with poor breast cancer patient outcome (Supplementary Fig. 2d, h, i), suggesting the both may be breast cancer tumor suppressors. Thus, cJun and p27 can corepress genes that mediate differentiation and that appear to act as tumor suppressors in breast cancer.

A novel complex of p27, cJun, YY1 and HDAC1 transcriptionally represses *PTPN12*

PTPN12 was one of the most strongly downregulated genes in p27CK-DD compared to 231 (log2 fold change = -2.82, p = 7.05e-293, q = 1.15e-289; Fig. 3a). Loss of PTPN12 was confirmed in p27CK-DD expressing MCF12A and 231, and in two highly metastatic derivatives, 1833 and 4175, compared to 231 (Fig. 3b, c).

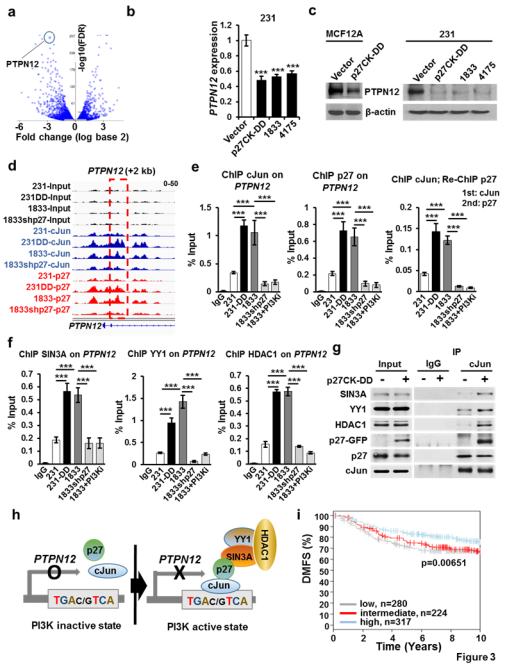

Fig. 3. cJun/p27 represses *PTPN12* transcription in complex with YY1, SIN3A and HDAC1. a, A volcano plot of genes differentially expressed in 231-p27CK-DD vs. 231-vector by RNA-Seq. *PTPN12* expression was strongly decreased by p27CK-DD transduction (FDR < 0.01, log2 Fold change = -2.81, $p < 0.0001$). **b**, qPCR expression of *PTPN12* in MCF12A-vector and MCF12A-p27CK-DD (left); and in 231, 231-p27CK-DD, 1833, and 4175 cells (right). **c**, Lysates from the indicated lines from (**b**) above were analyzed by Western for PTPN12 with β-actin as a loading control. **d**, ChIP-Seq analysis with anti-cJun and -p27 antibodies. Schematic representation for cJun and p27 bindings at the +2 kb site of *PTPN12* TSS. See also Supplementary Fig. 3a. **e**, ChIP-qPCR analysis for cJun and p27 binding and for ChIP cJun; Re-ChIP p27 at the +2 kb site of *PTPN12* TSS in 231, 231p27CK-DD (231-DD), 1833, 1833shp27, and 1833 treated with PI3K inhibitor (1833+PI3Ki). IgG; negative control (see also controls for ChIP Re-ChIP Supplementary Fig. 3b, c). **f**, ChIP analysis using anti-SIN3A, anti-YY1, and anti-HDAC1 antibodies show binding at the +2 kb site of *PTPN12* TSS. See also Supplementary Fig. 3d. **g**, ChIP-Western blot. After ChIP with cJun antibody, cJun-bound chromatin immunoprecipitates (IP cJun) were resolved and associated p27, SIN3A, YY1, and HDAC1 detected by Western in 231 and 231p27CK-DD (right). Input protein levels are shown (left). **h**, Proposed model of cJun/p27 complex in the transcriptional regulation of *PTPN12*. **i**, Kaplan-Meier analysis using distant metastasis free survival (DMFS) from Gene Expression-Based Outcome for Breast Cancer Online (GOBO; www.co.bmc.lu.se/gobo). n = 821 patients, p = 0.00651. All non-KM graphs show mean ± SEM, and p-values were represented by Student's T Test or ANOVA analysis (**$p < 0.01$, ***$p < 0.001$).

Our ChIPSeq identified cJun and p27 binding sites at -1 and at +2 kb on *PTPN12*. Recruitment of each of cJun and p27 to both sites was greater in p27-activated lines than in 231, and both decreased upon p27 depletion in 1833 (Fig. 3d). The +2 kb site bears a cJun consensus motif and publicly available ENCODE ChIPSeq tracks showed cJun bound this site in K562 cells (Supplementary Fig. 3a). ChIP-qPCR confirmed that cJun and p27 are co-recruited the +2 kb *PTPN12* promoter proximal site, with greater binding in 231p27CK-DD and 1833 than 231. Notably, in 1833, both p27 depletion and treatment with a PI3K inhibitor that abolishes p27 T157 and T198 phosphorylation, attenuated p27 and cJun recruitment to this site. These data are consistent with the notion that cJun co-recruitment with p27 to chromatin is regulated by p27 phosphorylation (Fig. 3e). ChIP/ re-ChIP assays confirmed that cJun and p27 co-occupy the site +2 kb of *PTPN12*, and that C-terminally phosphorylated p27 regulates this (Fig. 3e and Supplementary Fig. 3b, c). To support the validity of our findings in more than one model system and in a different cancer type, we next evaluated cJun and p27 binding to this *PTPN12* site in a human bladder cancer model of sister cell lines, including the parental UMUC3 low

metastatic line and the highly lung metastatic UMUC3-LuL2 (hereafter LuL2) line derived by serial passage in vivo of UMUC3. We also compared UMUC3 overexpressing p27CK-DD and LuL2 with p27 depletion (LuL2shp27). A for the breast cancer models, cJun and p27 were recruited to the +2 kb *PTPN12* site in a p27-dependent manner in this series of bladder cancer models (Supplementary Fig. 3d, e).

To further investigate cJun/p27-mediated gene repression, we assayed for the presence of YY1 and SIN3A, which are known to recruit HDAC1 to other developmentally important transcription factors. Analysis of publicly available ENCODE tracks showed these repressive elements can bind this *PTPN12* site (Supplementary Fig. 3a). SIN3A, YY1 and HDAC1 were detected at this +2 kb *PTPN12* site in our breast cancer lines. Their recruitment was enhanced in p27CK-DD expressing 231, and reduced by p27 depletion and by PI3K inhibition in 1833 (Fig. 3f). Moreover, cJun ChIP-Western also showed SIN3A, YY1, and HDAC1 binding was p27-regulated (Fig. 3g). p27 can form a transcriptional repressive complex with E2F4 . However, ChIP-qPCR with anti-E2F4 showed no E2F4 recruitment to the cJun/p27 binding site at +2 kb on *PTPN12* (Supplementary Fig. 3f). These data suggest a model in which p27 and cJun recruit SIN3A, YY1, and HDAC1 to this AP1 motif to repress *PTPN12* expression (Fig. 3h). PTPN12 is frequently lost in aggressive triple negative breast cancers. The biologic importance of *PTPN12* loss is supported by Kaplan-Meier analysis that shows poor outcome in breast cancer patients whose tumors have reduced *PTPN12* expression ($p = 0.00651$, Fig. 3i).

p27 increases stem-like cells *in vitro* through loss of PTPN12 and activation of PYK2

Since cJun/p27 complexes repress genes associated with differentiation (present data) and activate drivers of EMT and metastasis (see summary of PNAS paper above) both of which are linked to cancer stem cells, we assayed effects of p27 on tumor initiating ability. Sphere formation is a stem cell property assayed in vitro. The MCF12A normal human mammary epithelial line is immortal but non-tumorigenic and formed spheres slowly over 4-6 weeks. Transduction of p27CK-DD, but not p27CK- alone, significantly increased mammosphere formation compared to vector control in MCF12A (Fig. 4a). p27CK-DD expression caused a shift from predominantly surface $CD44^+/CD24^+$ to a population expressing stem cell markers

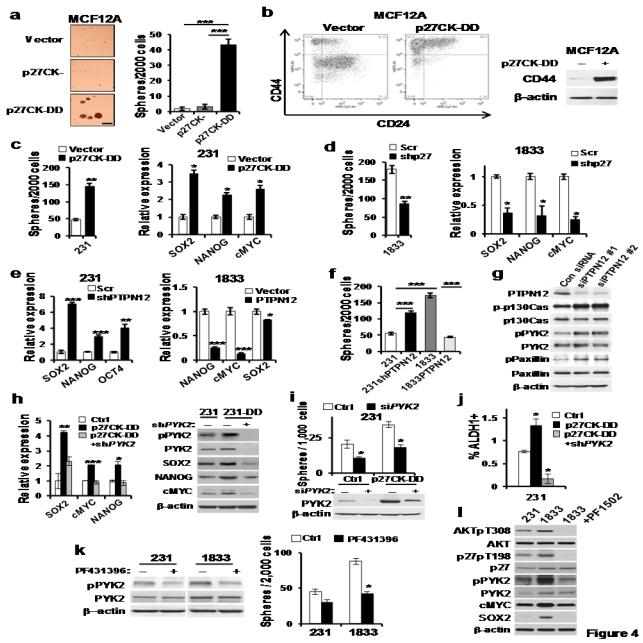

Fig. 4. Activated p27 increases CSC properties *in vitro* via loss of PTPN12 and activation of pPYK2. a, Sphere forming assays in MCF12A-vector, MCF12A-p27CK-, and MCF12A-p27CK-DD lines. Left: representative images in vector only (top), p27CK- (middle), and p27CK-DD (bottom) of MCF12A. Scale bars, 100 μm. Right: Mean spheres/2000 cells plated graphed +/-SEM. **b**, Surface expression of CD44 and CD24 in MCF12A-vector and MCF12A-p27CK-DD assayed by Flow cytometry (left). Western shows CD44 with β-actin controls in the same cells. **c**, Sphere forming assays and qPCR for *SOX2, MYC* and *NANOG* expression in 231-vector and 231-p27CK-DD. See also Supplementary Fig. 4a. **d**, Effects of stable *p27* knockdown (shp27) on sphere formation and *SOX2, MYC* and *NANOG* expression in 1833-scramble (Scr), and 1833shp27. See also Supplementary Fig. 4b-d. **e**, Effects of stable PTPN12 knockdown on qPCR expression CSC-TFs in 231 cells. The cells were infected with shPTPN12 lentiviruses. The expression and CSC-TFs (SOX2, NANOG and OCT4) was analyzed by qPCR (left). Overexpression of PTPN12 in 1833 on qPCR expression (NANOG, cMYC, and SOX2; right). See also Supplementary Fig. 4e, f. **f**, Sphere forming assay in 231, 231shPTPN12, 1833, and 1833PTPN12. See also Supplementary Fig. 4g-j. **g**, Effects of transient PTPN12 knockdown on protein tyrosine activation. 231 cells were transfected with control siRNA, PTPN12 siRNA #1 and #2, and subjected to Western blot for protein kinases. **h**, Effects of stable PYK2 knockdown on qPCR expression (left) and Western blot (right) of CSC-TFs in 231-p27CK-DD. **i**, Sphere forming assay in 231 and 231-p27CK-DD with transient PYK2 knockdown (top) confirmed by Western blot (bottom). **j**, Effects of stable PYK2 knockdown on ALDH1+ expression analyzed by flow cytometry. **k**, Sphere forming assay in 231 and 231 with PYK2 kinase inhibitor (PF431396) treatment (right). The cells were subjected to Western blot for PYK2 phosphorylation (left). **l**, PI3K inhibition reverses p27-mediated SOX2 and cMYC expression. 231, 1833, and 1833+PF1502 (PI3Ki) cells were subjected to Western blot for the indicated proteins. All graphs show mean ± SEM from at least 3 replicate assays, and p-values were represented by Student's T Test or ANOVA analysis (*p < 0.05, **p < 0.01, ***p < 0.001)

$CD44^{+}CD24^{low/-}$ (Fig. 4b, left), a hall mark of breast cancer initiating cells. CD44 was markedly increased (Fig. 4b, right) and MCF12Ap27CK-DD cells acquired the ability to form soft agar colonies (Supplementary Fig. 4a). p27CK-DD increased sphere formation and expression of embryonic stem cell transcription factors (ES-TFs) *SOX2*, *NANOG*, and *cMYC* in 231 (Fig. 4c) and increased spheres in MCF7 breast cancer cells and in the UMUC3 bladder cancer line (Supplementary Fig. 4b)

Conversely, p27 depletion in highly metastatic breast cancer (1833) and bladder cancer models (UMUC3-LuL2) (Supplementary Fig. 4c) significantly reduced not only mammospheres, but also ES-TF expression (Fig. 4d and Supplementary Fig. 4d). Soft agar colony formation increased in 231p27CK-DD and decreased with p27 depletion in 1833 (Supplementary Fig. 4e).

To address the role of PTPN12 in p27-regulated tumor initiation, PTPN12 was depleted in 231 and UMUC3, and overexpressed in 1833 (Supplementary Fig.

4f-h). PTPN12 depletion (sh*PTPN12*) in the weakly metastatic breast (231) and bladder cancer lines (UMUC3) increased ES-TF expression (Fig. 4e, left and Supplementary Fig. 4h) and *PTPN12* transduction in 1833 decreased *NANOG, cMYC*, and *SOX2* expression (Fig. 4e, right). *PTPN12* depleted 231 and UMUC3 formed more spheres (Fig. 4f and Supplementary Fig. 4i) and *PTPN12* overexpressing 1833 formed fewer (Fig. 4f). Effects on soft agar colony formation were similar: *PTPN12* depletion increased and *PTPN12* overexpression decreased colony formation (Supplementary Fig. 4j).

PTPN12 dephosphorylates mediators of focal adhesion signaling Paxillin, PYK2, and $p130^{Cas}$. Transient PTPN12 knockdown activated these substrates in 231 (Fig. 4g). Stable PTPN12 depletion activated pPYK2 in 231, while PTPN12 overexpression decreased pPYK2 in 1833 (Supplementary Fig. 4g). Notably, in 231p27CK-DD, PYK2 depletion reversed the stem cell effects of phosphomimetic p27 expression, decreasing ES-TF expression (Fig. 4h), sphere formation (Fig. 4i) and ALDH1 activity (Fig. 4j). Treatment with PYK2 inhibitor, PF431396, also attenuated sphere formation in 231p27CK-DD cells (Fig. 4k). Notably, PI3K inhibition over 48 hrs decreased AKTpT308, led to loss of p27pT198, and pPYK2, and reduced MYC and SOX2, consistent with the notion that PI3K drives p27 phosphorylation leading to *PTPN12* repression, PYK2 activation and cancer stem cell (CSC) expansion (Fig. 4l).

p27 increases phospho-PYK2 to activate STAT3 and upregulate a STAT3 gene expression signature

Although FAK is known to regulate CSC, the role of PYK2 (also known as FAK2) is less well studied. STAT3 is. PYK2 inhibition by 48 hrs of treatment with PYK2 inhibitor, PF431396, not only decreased activated pPYK2 but significantly downregulated activated STAT3pS63 (pSTAT3), a known regulator of breast CSC expansion (Fig. 5a). Both acute and stable PYK2 depletion also reduced pSTAT3, indicating that PYK2 is required for STAT3 activation in these cells (Fig. 5b, c).

Since phosphorylated p27 represses *PTPN12* and activates PYK2 to drive STAT3 activation, p27 activated lines would have activation of STAT3-dependent genes. We used The Cancer Genome Atlas (TCGA)/The Cancer Proteome Atlas (TCPA) data to identify genes differentially expressed between primary human breast cancers in the top quartiles of pSTAT3 and p27pT157 expression and all others. This

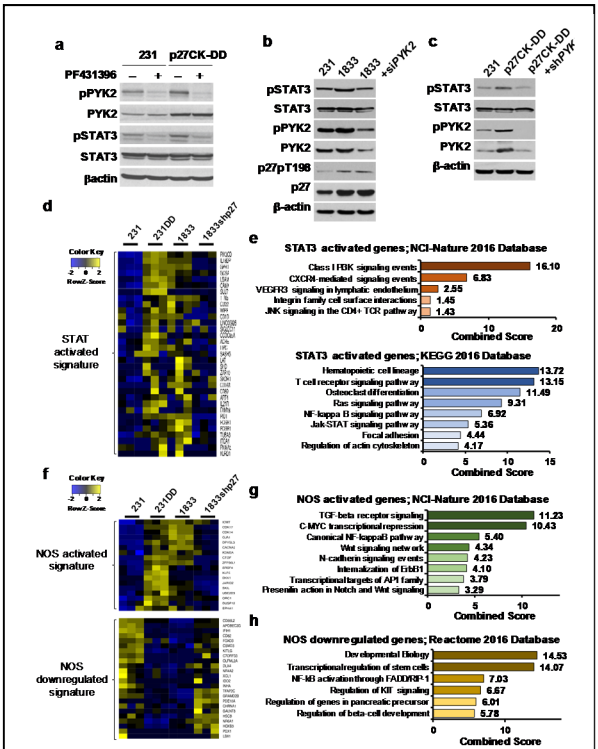

Fig. 5. p27 activated lines show PYK2-dependent STAT3 activation and show preferential downregulation of genes repressed in ESC, NOS and STAT3 gene signatures. a, Western blots show total and phosphorylated PYK2 and STAT3 levels in the indicated lines and effects of 48 hrs of PF431396. **b**, Effects of transient siPYK2-mediated PYK2 loss on total and phosphorylated PYK2 and STAT3. Levels of p27 and p27pT198 are shown. **c**, Effects of stable shPYK2 expression on total and phosphorylated PYK2 and STAT3. **d,** Gene expression heatmaps show changes in expression of STAT3 target signatures in 231, 231p27CK-DD, 1833 and 1833shp27. **e**, Gene ontogeny in NCI-Nature and KEGG 2016 database of STAT3 activated target genes. See also Supplementary Fig. 5a. **f**, Gene expression heatmaps of NOS target gene signatures genes in the indicated cell lines. **g**, **h**, Gene ontogeny of NOS target genes that are regulated by p27. See also Supplementary Fig. 5b.

pSTAT3/p27pT157 (STAT-3) activated gene expression profile was then compared to the genes differentially expressed in 231, 231p27CK-DD, 1833 versus 1833shp27. p27-activate lines express a subset of STAT3-activated genes identified in human ER negative breast cancers (heatmaps in Fig. 5d). GO analysis of genes upregulated in both p27-activated breast cancer lines and the STAT-3 activation signature from primary cancers identifies signaling pathways strongly associated with cancer and cancer stem cells (Fig. 5e and Supplementary Fig. 5a).

Since p27 activated lines appear to be enriched for tumor initiating stem cells, we assayed for preferential expression of target genes up and downregulated by NANOG, OCT4 and SOX2 (NOS) in ESC. A subset of NOS signature genes were also coordinately expressed in p27 activated 231p27CK-DD and 1833 compared to 231 and 1833shp27 (Fig. 5f). GO of these shared NOS target signature genes expressed in our p27-activated lines identifies important stem cell and developmental pathways (Fig. 5g, h and Supplementary Fig. 5b).

p27 mediates tumor-initiating stem cell expansion through loss of PTPN12 and activation of PYK2

Tumor-initiating stem cells (T-ISC) abundance was assayed *in vivo* by injecting limiting dilutions of 231, 231-p27CK-DD, 1833, and 1833shp27 (10, 100, or 1000 cells/mouse) orthotopically into Balb/c nude mice.

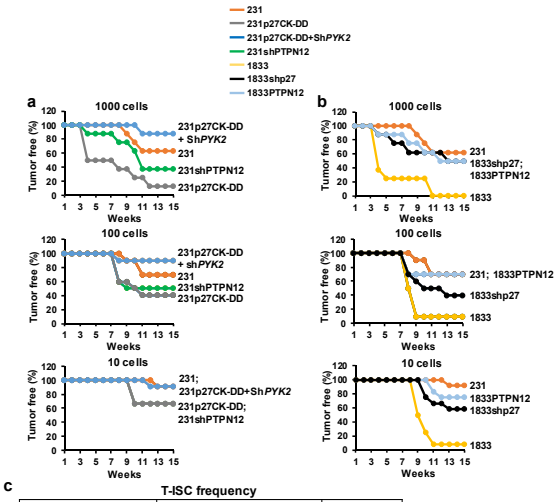

c

T-ISC frequency

Group	Limiting dilution (Tumors/Implantation)			Frequency
	1000 cell	100 cell	10 cell	
231	3/8	3/10	1/12	1/1,032
231p27CK-DD	7/8	6/10	4/12	1/175
231p27CK-DDsh*PYK2*	1/8	1/10	1/12	1/2,845
231sh*PTPN12*	6/8	6/10	5/12	1/402
1833	8/8	9/10	11/12	1/14
1833shp27	4/8	6/10	5/12	1/402
1833-PTPN12	4/8	3/10	3/12	1/645

Pairwise Differences		p-value
231	231p27CK-DD↑	0.0028
231	1833↑	<0.0001
231	231sh*PTPN12*↑	0.0437
231p27CK-DD	231p27CK-DD + sh*PYK2*↓	0.0002
1833	1833shp*27*↓	<0.0001
1833	1833-PTPN12↓	<0.0001

Figure 6

Fig. 6. p27 is required for tumor-initiating ability *in vivo* via loss of PTPN12 and activation of pPYK2. a, **b**, Graphs showing tumor free mice (%). The cells were injected in the mammary fat pads of Balb/c nude mice at limiting dilution (n = 8, 10, 12 mice per group) of 231 vector controls, 231p27CK-DD, 231p27CK-DD + shPYK2 and 231shPTPN12 (**a**); 1833, 1833PTPN12 and 1833shp27 (**b**). **c**, Tumor-initiating stem cell (T-ISC) frequencies (top) were calculated by L-Calc Limiting Dilution Software in the indicated cell lines. Pairwise comparisons of T-ISC frequencies are shown (bottom). See also Supplementary Fig. 6

T-ISC frequency was considerably higher and tumor latency shorter for 1833 cells and for 231p27CK-DD and compared to 231, and T-ISC frequency was decreased significantly by p27 depletion in 1833 (Fig. 6a, b) and by cJun depletion in 231p27CK-DD (Supplementary Fig. 6a, b). Thus, C-terminally phosphorylated p27 appears to increase tumor-initiating cell abundance in a cJun-dependent manner *in vivo* in this model.

PTPN12 depletion in 231 significantly increased T-ISC abundance (Fig. 6a), while PTPN12 overexpression in 1833decreased T-ISC (Fig. 6b). PYK2 knockdown in 231p27CK-DD abrogated the gain in T-ISC abundance conferred by phosphomimetic p27CK-DD and prolonged tumor latency (Fig. 6a). T-ISC frequency is calculated in Fig. 6c. Taken together, these data support a model of PI3K-activated cancers, in which p27 appears to activate T-ISC expansion or maintenance though p27/cJun-dependent PTPN12 loss and the resulting activation of PYK2.

We are currently completing the STAT3 ChIP Seq and will combined this analysis in the next year with the prior RNA seq of to determine the overlap between p27, cJun and STAT2 bound genes and which of the p27cJun regulated genes might also be bound and regulated by STAT3. This data will be submitted in the upcoming grant year if all goes well. A draft manuscript of this work with the supplemental figures is appended for DOD review.

2. What opportunities for training and professional development has the project provided?

This project supported the work our technician, two graduate Students who completed their PhDs and left the lab last year (Kibeom Jang and Minsoon Kim), and a current PhD student, Setayamah Razavipour, and one post-doctoral fellow, Hyunho Yoon. Trainees meet weekly or bi-weekly for one on one mentoring sessions with the PI and we meet as a project team all together every 2-3 weeks. These trainees participate in lab meeting weekly where we present our research progress and get critiques in a supportive friendly environment for improvement of research plans and presentation skills. Trainees also have numerous opportunities to attend seminars from UM researchers and invited speakers from each of 4 different molecular biology graduate program seminar series and the Cancer Center's Distinguished lecture series. Individuals with advanced professional skills and experience assist others in attaining greater proficiency. I also encourage all of my grant funded participants to attend scientific conferences particularly the Miami Winter symposium, a local high quality international meeting, and to attend the Cancer Center's international Epigenetics Symposia.

3. How were the results disseminated to communities of interest?

The following invited talks were presented at academic institutions and conferences:
Academic Seminars:
Slingerland, JM. p27: a c-Jun coregulator that activates transcription programs driving CSC and metastasis, Loyola University Medical Center, Cardinal Bernardin Cancer Center, Chicago, IL, April 25, 2018

Plenary Speaker at International Meetings

1.Slingerland JM. p27: a cJun coregulator that activates transcription programs driving cancer stem cells and metastasis, Miami Winter Symposium: STEM CELLS: today's research tomorrow's therapies. January 28-31, 2018.

2.Slingerland, JM. The Dr Jekyll and Mr Hyde of p27: Cytoplasmic p27 promotes EMT and metastasis and increases CSCThink Tank 28 - Breast Cancer Symposium, Porta Blancu, Nieuwpoort, Curaçao, January 21 -28, 2018

4. What do you plan to do during the next reporting period to accomplish the goals?

The goals remaining to be accomplished are summarized in the table below

GOALS TO BE ACCOMPLISHED		
Aim 2 Major Task 2 Test if p27 modulates target gene transcription and if C-terminal phosphorylation shifts p27 from a co-repressor to co-activator of key drivers of stem cell self-renewal	12-36	
Subtask 1 Establish conditions for Co-IP of p27 with p130, E2F4 and HDAC1 and SIN3A	12-18	We have established the techniques for these IPs but have not yet completed the comparisons of these complexes in lines that show low and high PI3K activation and p27 activating C-terminal phosphorylation.

Subtask 2 test if PI3K activity shifts p27 from a p130/E2F4/SIN3A co-repressor to a co-activator at target genes that govern CSC and EMT-TFs: *SNAI1, SNAI2, TWIST1, TGF-□□□□*	12-36	Planned for next year
Milestone(s) Achieved: identify that p27pTpT recruits JNK/cJun to activate cJun driven target sites, or recruits Pyk2 to activate STAT3 or cJun dependent transcription programs governing EMT and CSC		The combined analysis of p27, cJun and STAT3 ChIP Sequencing will be analyzed in 231, 231p27CK-DD, 1833 and 1833shp27, together with differential gene expression in these lines from RNA Sequencing. This analysis is expected to yield another manuscript within the next year.
AIM 3 compares the effects of inducible transgenic p27CK-DD vs p27CK- to expand tissue stem cells and alter global and mammary development and tumor formation in mice	1-12	We have established mouse strains with Cre inducible p27CK- (2 mouse lines) or p27CK-DD (one mouse line) and have begun to cross these with the following Cre inducible strains: 1. ROSA26Cre; 2. MMTVA-Cre 3. Lgr5Cre The expression pf p27CK- or p27CK-DD in induced target organs and phenotypes will be characterized over the next 2 years.
Subtask 1Comparison of global transgenic p27CK-DD and p27CK- expression on organ development and tumor formation	12-24	Data will emerge on this in years 2 and 3 from the studies on p27 in the mammary gland (MMTV-Cre), gut (Lgr5Cre), and whole animal multi-organ development (Rosa 26-Cre).
Analysis of tumors	12-24	Planned if they emerge

Subtask 2 Effects of transgenic p27CK- and p27CK-DD on mammary tumor formation	24-36	This will be done with the bi-genic animals (MMTV-Cre X p27CK-DD) that are just beginning to be born.
Milestone(s) Achieved: Will have shown effects of p27CK- and p27CK-DD on organ and tumor development and on mammary gland development and tumor formation		This work will take at least the next 2 years to complete and may extend beyond the grant funding period

IMPACT:

What was the impact on the development of the principal discipline(s) of the project?

Our work provides novel evidence that p27 acts as a co-regulator of the transcriptional activity of cJun, and this is enhanced by C-terminal phosphorylation of p27 which is brought about by oncogenic PI3K activation. PI3K is activated in over 60% of human cancers, mediating C-terminal p27 phosphorylation. Present work reveals cooperation between PI3K and cJun pathways: p27 phosphorylation by PI3K-activated kinases stimulates p27-cJun co-recruitment to chromatin and activation of transcription programs of cell adhesion, motility, TGFB2 and EMT to drive tumor progression. In human breast cancers, high p27pT157 is strongly associated with activated AKTpS273 and p90RSKpT359. Cancers with high p27pT157 differentially express p27/cJun target genes, and a subset of these have been identified that have strong prognostic value in breast cancer. In cancers, the cell cycle restraining effects of p27 are lost though increased proteolysis and decreased translation. Present work reveals a previously unknown oncogenic action of p27, in which p27 acts as a novel cJun co-activator to drive oncogenic gene expression programs.

What was the impact on other disciplines?

Nothing to report. This work may impact the field of developmental biology since the p27 may play critical roles to regulate transcriptional programs during development.

What was the impact on technology transfer?

Nothing to report yet. Our work has provided a novel rationale for combine therapeutic targeting of PI3K activated breast cancers using PI3K/mTOR kinase inhibitors together with Pyk2 inhibitors. If preclinical testing supports this therapeutic strategy, it could be brought forward to the clinic. In addition, evaluation of JAK2/PI3K inhibitor combinations are supported by our work.

What was the impact on society beyond science and technology?

Nothing to report yet.

CHANGES/PROBLEMS:

Changes in approach and reasons for change

Nothing to report -- No changes to plan.

Actual or anticipated problems or delays and actions or plans to resolve them

None to report

Personnel Issues:

A senior post doc involved in the project Dr Hyunho Yoon left the lab in Sept 2018. We are currently recruiting a new PDF to replace him

Changes that had a significant impact on expenditures

Significant changes in use or care of human subjects, vertebrate animals, biohazards, and/or select agents
Nothing to report

Significant changes in use or care of human subjects
Nothing to report

Significant changes in use or care of vertebrate animals
Nothing to report

Significant changes in use of biohazards and/or select agents
Nothing to report

PRODUCTS:

Publications, conference papers, and presentations

Journal publications
p27 transcriptionally co-regulates cJun to drive programs of tumor progression
Hyunho Yoon , Minsoon Kim, Kibeom Jang, Miyoung Shin, Alexandra Besser, Xue Xiao, Dekuang Zhao, Seth Wander, Karoline Briegel, Lluis Morey, Andy Minn, and Joyce Slingerland
PNAS | April 2, 2019 | vol. 116 | no. 14 | 7005–7014 (Reprint in Appendix 1)

p27 binds cJun, YY1 and HDAC1 to co-repress PTPN12 and increase tumor-initiating stem cells
Hyunho Yoon, Kibeom Jang, Miyoung Shin, Minsoon Kim, Dekuang Zhao, Xue Xiao, Lluis Morey, and Joyce M. Slingerland manuscript will be submitted when we complete the STAT3 ChIP seq and combine its analysis with the p27 and cJun ChiPSeq and RNA seq in the p27 activated and parental cell liens described above. (draft Manuscript Appendix 2)

Books or other non-periodical, one-time publications
Nothing to report

Other publications, conference papers, and presentations
Academic Seminar:
Slingerland, JM. p27: a c-Jun coregulator that activates transcription programs driving CSC and metastasis, Loyola University Medical Center, Cardinal Bernardin Cancer Center, Chicago, IL, April 25, 2018

Poster presentation at International Meetings:
Yoon H, Shin M, Jang K, Kim M, Besser A, Zhao D, Slingerland JM. Phosphorylated p27 promotes tumor-initiating ability and tumor metastasis by repressing PTPN12 transcription. Miami Winter Symposium: STEM CELLS: today's research tomorrow's therapies. January 28-31, 2018.

Plenary Speaker at International Meetings
1.Slingerland JM. p27: a cJun coregulator that activates transcription programs driving cancer stem cells and metastasis, Miami Winter Symposium: STEM CELLS: today's research tomorrow's therapies. January 28-31, 2018.

2. Slingerland, JM. The Dr Jekyll and Mr Hyde of p27: Cytoplasmic p27 promotes EMT and metastasis and increases CSC presented at Think Tank 28 - Breast Cancer Symposium, Porta Blancu, Nieuwpoort, Curaçao, January 21 -28, 2018

Website(s) or other Internet site(s)
Nothing to report

Technologies or techniques
New techniques will be reported at publication- no publications yet.

Inventions, patent applications, and/or licenses
Nothing to report

Other Products
Nothing to report

PARTICIPANTS & OTHER COLLABORATING ORGANIZATIONS:
Dr Karoline Briegel has been a major co-investigator working with us on AIM 3. to develop the p27CK-DD inducible transgenic mice.

What individuals have worked on the project?

Name:	Joyce M. Slingerland, MD, PhD
Project Role:	PI
Researcher Identifier (e.g. ORCID ID):	0000-0003-1487-8554
Nearest person month worked:	2.25
Contribution to Project:	Dr. Slingerland coordinated and supervised all experiments.
Funding Support:	Other funding source includes BCRF, FBCF, NIH-NCI
Name:	Karoline Briegel, PhD
Project Role:	Co-Investigator
Researcher Identifier (e.g. ORCID ID):	N/A
Nearest person month worked:	1.2 mo

Contribution to Project:	Assist in the development of p27CK- and p27CK-DD inducible transgenic mice and in their characterization
Funding Support:	Other funding support from NIH-NCI
Name:	Hyunho Yoon
Project Role:	Post doctoral Associate
Researcher Identifier (e.g. ORCID ID):	N/A
Nearest person month worked:	12 mo- left the lab in Sept 2018
Contribution to Project:	Planned and executed experiments. Gather and analyze data.
Funding Support:	100% from this grant
Name:	Alan Burgess
Project Role:	Research Associate
Researcher Identifier (e.g. ORCID ID):	N/A
Nearest person month worked:	Started in Sept 2018 (will be 12 mo on next year's report)
Contribution to Project:	Plan and execute experiments. Gather and analyze data.
Funding Support:	100% from this grant
Name:	Seyefatemeh Razavipour, MS
Project Role:	Grad student
Researcher Identifier (e.g. ORCID ID):	N/A

Nearest person month worked:	9 mo
Contribution to Project:	Plan and execute experiments. Gather and analyze data.
Funding Support:	100% from this grant

Has there been a change in the active other support of the PD/PI(s) or senior/key personnel since the last reporting period?

Joyce Slingerland (PI):

New grant

K12 CA226330-01 2018-2023
UM Calabresi Clinical Oncology Research Career Development Award
Slingerland (PI)

What other organizations were involved as partners?
None

p27 transcriptionally coregulates cJun to drive programs of tumor progression

Hyunho Yoon[a,1], Minsoon Kim[a,b,1], Kibeom Jang[a,b], Miyoung Shin[a], Alexandra Besser[a,c], Xue Xiao[d], Dekuang Zhao[a], Seth A. Wander[a], Karoline Briegel[a,e], Lluis Morey[a,f,g], Andy Minn[h,i], and Joyce M. Slingerland[a,b,c,f,j,2]

[a]Braman Family Breast Cancer Institute, Sylvester Comprehensive Cancer Center, University of Miami Miller School of Medicine, Miami, FL 33136; [b]Department of Biochemistry and Molecular Biology, University of Miami Miller School of Medicine, Miami, FL 33136; [c]Sheila and David Fuente Graduate Program in Cancer Biology, University of Miami Miller School of Medicine, Miami, FL 33136; [d]Bioinformatics Core, Sylvester Comprehensive Cancer Center, University of Miami Miller School of Medicine, Miami, FL 33136; [e]Department of Surgery, University of Miami Miller School of Medicine, Miami, FL 33136; [f]Cancer Epigenetics Program, Sylvester Comprehensive Cancer Center, University of Miami Miller School of Medicine, Miami, FL 33136; [g]Department of Human Genetics, University of Miami Miller School of Medicine, Miami, FL 33136; [h]Department of Radiation Oncology, Perelman School of Medicine, University of Pennsylvania, Philadelphia, PA 19104; [i]Abramson Family Cancer Research Institute, Perelman School of Medicine, University of Pennsylvania, Philadelphia, PA 19104; and [j]Department of Medicine, University of Miami Miller School of Medicine, Miami, FL 33136

Edited by Joan S. Brugge, Harvard Medical School, Boston, MA, and approved February 13, 2019 (received for review October 10, 2018)

p27 shifts from CDK inhibitor to oncogene when phosphorylated by PI3K effector kinases. Here, we show that p27 is a cJun coregulator, whose assembly and chromatin association is governed by p27 phosphorylation. In breast and bladder cancer cells with high p27pT157pT198 or expressing a CDK-binding defective p27pT157pT198 phosphomimetic (p27CK−DD), cJun is activated and interacts with p27, and p27/cJun complexes localize to the nucleus. p27/cJun up-regulates *TGFB2* to drive metastasis in vivo. Global analysis of p27 and cJun chromatin binding and gene expression shows that cJun recruitment to many target genes is p27 dependent, increased by p27 phosphorylation, and activates programs of epithelial–mesenchymal transformation and metastasis. Finally, human breast cancers with high p27pT157 differentially express p27/cJun-regulated genes of prognostic relevance, supporting the biological significance of the work.

p27 | cJun | EMT | TGF-β2 | transcriptional regulation

The CDK inhibitor, p27, was discovered as a mediator of growth arrest by transforming growth factor type β (TGF-β) that impedes cell cycle progression by inhibiting cyclin-dependent kinases (CDKs) (1–3). p27 is invariably deregulated in human cancers, but unlike typical tumor suppressors, mutations or deletions of the *CDKN1B* gene encoding p27 are rare. p27 can be functionally disrupted in cancers by excess proteolysis, by decreased translation, or by C-terminal phosphorylation (4, 5).

The phosphatidylinositol 3′-kinase (PI3K) pathway is activated in most human cancers (6) by genetic changes activating receptor tyrosine kinases, PI3K components, or effector kinases (7) or by loss of its negative regulator, phosphatase and tensin homolog (8). PI3K-activated kinases phosphorylate p27 at two sites, T157 and T198. Phosphorylation at T157 in the p27 nuclear localization signal delays nuclear import (9), and T198 phosphorylation stabilizes the protein (10, 11), leading to accumulation of p27 in the cytoplasm. Notably, up to 60% of newly diagnosed breast cancers express activated pAKT, and this correlates with detection of both nuclear and cytoplasmic p27 (9) and with detection of p27pT198 (12) by immunohistochemical analysis. Despite strong cytoplasmic p27 expression, nuclear p27 remains present in all AKT-activated cancers, and cancers with both nuclear and cytoplasmic p27 have a worse prognosis than those with exclusively nuclear p27 (9, 13). Proteomic analysis showed that levels of activated AKTpS473, $p70^{S6K}$pT389, and $p90^{RSK}$pT359 are all strongly correlated with phosphorylated p27pT157 in over 700 primary human breast cancers from The Cancer Genome Atlas (TCGA) and The Cancer Proteome Atlas (TCPA) (14), supporting that PI3K activates p27 phosphorylation in human cancer. It is increasingly clear that p27pT157pT198 drives tumor metastasis via multiple mechanisms. Phosphorylation of p27 at T157 and T198 (9, 15–19) impairs its CDK inhibitory action (20, 21) and promotes binding to RhoA/ROCK1 to disrupt the actin skeleton and enhance cell motility and invasion (18, 22). Increased p27pT157pT198 also facilitates metastases in PI3K-activated cancer models (13, 14) and contributes to epithelial–mesenchymal transformation (EMT) by activating STAT3-dependent TWIST1 induction (14).

p27 is regulated by both the PI3K and TGF-β pathways. Members of the TGF-β family of cytokines bind heterotetrameric TGF-β receptors to activate SMADs, which homo- and heterodimerize and translocate to the nucleus to activate gene expression programs (23, 24). The TGF-β pathway regulates tissue differentiation and morphogenesis in development and activates cytostatic and apoptotic processes to maintain tissue homeostasis (24). Although TGF-β mediates cell cycle arrest via p27 in normal epithelial cells (1, 2), these cytostatic effects are disrupted in cancers, and aberrant TGF-β signaling stimulates EMT, invasion, and metastasis (23, 24). The PI3K and TGF-β pathways have been shown to cooperate to mediate EMT (7), but mechanisms underlying this are not fully known.

The present work reveals a previously unknown mechanism whereby oncogenic activation of the PI3K and TGF-β pathways cooperates to drive EMT and metastasis. We identify a role for

Significance

PI3K is activated in over 60% of human cancers, mediating C-terminal p27 phosphorylation. This work reveals cooperation between PI3K and cJun pathways: p27 phosphorylation by PI3K-activated kinases stimulates p27/cJun corecruitment to chromatin and activation of transcription programs of cell adhesion, motility, *TGFB2*, and epithelial–mesenchymal transformation to drive tumor progression. Prior analysis showed that high p27pT157 strongly associates with activated AKTpS273 and $p90^{RSK}$pT359 in human breast cancers. These cancers also differentially express p27/cJun target genes and identify a poor prognostic group. In cancers, the cell cycle-restraining effects of p27 are lost through increased proteolysis and decreased translation. We reveal a previously unknown oncogenic action of p27, in which p27 acts as a cJun coactivator to drive oncogenic gene expression programs.

Author contributions: H.Y., M.K., K.J., A.B., S.A.W., K.B., L.M., and J.M.S. designed research; J.M.S. obtained grant funding; H.Y., M.K., K.J., A.B., S.A.W., and K.B. performed research; K.J., M.S., and D.Z. contributed new reagents/analytic tools; H.Y., M.K., K.J., M.S., A.B., X.X., S.A.W., L.M., A.M., and J.M.S. analyzed data; and H.Y., M.K., and J.M.S. wrote the paper.

The authors declare no conflict of interest.

This article is a PNAS Direct Submission.

Data deposition: The data reported in this paper have been deposited in the National Center for Biotechnology Information Gene Expression Omnibus database, https://www.ncbi.nlm.nih.gov/geo (accession no. GSE112446).

[1]H.Y. and M.K. contributed equally to this work.

[2]To whom correspondence should be addressed. Email: jslingerland@med.miami.edu.

This article contains supporting information online at www.pnas.org/lookup/suppl/doi:10.1073/pnas.1817415116/-/DCSupplemental.

p27 in which it functionally interacts with cJun as a transcriptional coregulator. p27 and cJun interaction, nuclear localization, and the distribution and extent of p27 and cJun recruitment to chromatin are increased by C-terminal p27 phosphorylation. At a large subset of target genes, cJun binding is p27 dependent, suggesting that p27 may be an obligate cJun coactivator at these sites. *TGFB2* is identified as a p27/cJun target gene required for p27-driven metastasis in vivo. p27/cJun complexes activate oncogenic target gene programs associated with EMT and cancer metastasis, and these target genes are preferentially expressed in primary human breast cancers with high levels of activated p27pT157.

Results

p27 Drives an EMT Gene Expression Program. Prior work showed that C-terminal p27 phosphorylation mediates activation of TWIST1 to drive a morphologic EMT (14). To investigate effects of p27 on metastatic gene programs more broadly, global gene expression assayed by RNA sequencing (RNA-seq) was compared in MDA-MB-231 (hereafter 231), a breast cancer line with low metastatic ability; in MDA-MB-231-1833, a bone-tropic highly metastatic derivative line (25) (hereafter 1833); and in 1833shp27, in which p27 was stably depleted (13). To test the effects of phosphorylated p27pT157pT198, we used 231 transduced with p27 bearing phosphomimetic threonine-to-aspartic acid mutations at T157 and T198 (14). Since as little as two- to threefold p27 overexpression arrests the cell cycle and would not permit study of phosphomimetic p27, p27 was also mutated to p27CK− to abolish cyclin-CDK binding (26), yielding p27CK−DD (14). Notably, comparison of 231 transduced with either p27CK− or p27CK−DD showed only the phosphomimetic p27CK−DD induces a morphologic EMT and confers excess metastasis, indicating that these phosphorylations are critical to p27-driven EMT (14).

Gene ontogeny (GO) analysis revealed activation of programs associated with cell motility, migration, and extracellular matrix (ECM) organization in 231p27CK−DD compared with 231, and in 1833 vs. 1833shp27 (Fig. 1*A*). Differentially expressed genes in these lines were compared with an established "EMT core signature" derived by overexpression of master EMT regulators in human mammary epithelial cells (27). Gene set enrichment analysis (GSEA) showed that genes up-regulated in this signature were increased in 231p27CK−DD compared with 231 and in highly metastatic 1833 vs. 1833shp27, while genes down-regulated in the EMT signature were also decreased in the highly metastatic lines (Fig. 1*B* and *SI Appendix*, Fig. S1*A*). EMT core signature genes differentially expressed in both 231p27CK−DD vs. 231 and 1833 vs. 1833shp27 are shown in Fig. 1*C*. Genes down-regulated during EMT were decreased in 231p27CK−DD and in 1833 compared with both 231 and 1833shp27, while genes activated in the EMT signature were increased in both highly metastatic lines (Fig. 1*C*; see gene list in *SI Appendix*, Table S1). Thus, p27 knockdown reverses the expression of an EMT gene profile, supporting the notion that p27 drives metastasis, in part, by activating an EMT transcription program.

Comparison of EMT markers and drivers showed that 1833 expressed negligible E-Cadherin and Vimentin compared to 231 (Fig. 1*D*). p27-mediated EMT activation was validated by qPCR of major EMT-driving transcription factors in two different breast and bladder cancer models with sister lines of low and high metastatic ability. MDA-MB-231-4175 (hereafter 4175) is a highly metastatic 231 variant with tropism to lung (28), while 1833, as noted above, has bone metastatic tropism (25). UMUC3-LuL2 (hereafter LuL2) is a lung metastatic derivative of the bladder carcinoma line UMUC3 (29). Both metastatic variants have higher PI3K activation and higher p27pT157 and p27pT198 than parental cells (13, 14). p27 depletion decreased expression of the master EMT transcription factors (EMT-TFs) *SNAI1*, *SNAI2*, and *ZEB2* in highly metastatic 1833 and LuL2 (Fig. 1*E*), confirming findings on RNA-seq (*SI Appendix*, Fig. S1*B*), while p27CK−DD transduction up-regulated EMT-TFs in both breast (231) and bladder (UMUC3) lines (Fig. 1*F*).

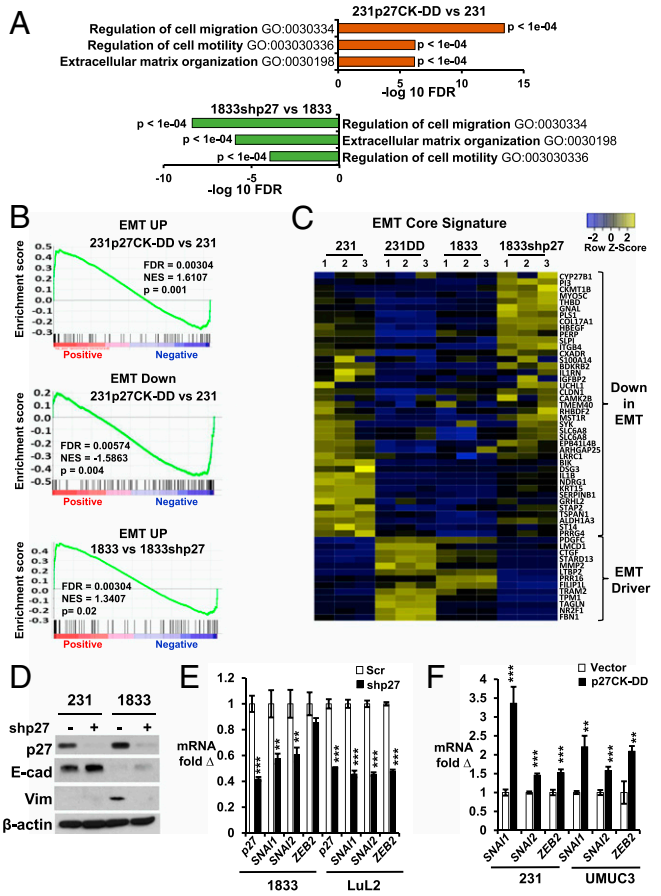

Fig. 1. p27 activates an EMT gene expression program. (*A*) GO analysis of genes governing cell migration, motility, and ECM in 231 vs. 231p27CK−DD and in 1833 vs. 1833shp27. FDR, fold discovery rate. (*B*) GSEA shows differential expression of EMT core signature genes (27) up-regulated (EMT UP) and down-regulated (EMT Down) in the indicated lines. Normalized enrichment score (NES), FDR, and *P* values are shown. (*C*) Heatmap of mean fold changes in differentially expressed EMT core signature genes in parental 231, 231p27CK−DD, 1833, and 1833shp27. Genes altered by p27 knockdown revert away from the Taube et al. (27) EMT core signature. Genes are listed in *SI Appendix*, Table S1. (*D*) Effects of stable p27 depletion in 1833 on p27 and the EMT markers E-cadherin (E-cad) and Vimentin (Vim) by Western blot (β-actin as loading control; data representative of more than three repeat assays). (*E*) Effects of stable p27 depletion (shp27) on qPCR expression of EMT-TFs (*SNAI1*, *SNAI2*, and *ZEB2*) in PI3K-activated lines (1833 and LuL2) vs. scramble shRNA controls (Scr). (*F*) Effects of stable p27CK−DD expression on expression of EMT-TFs in 231 and UMUC3 vs. vector-only control lines. In *E* and *F*, means ± SEM graphed from three or more replicates of three or more biologic assays (***P* < 0.01, ****P* < 0.001). 231DD, 231p27CK−DD. See also *SI Appendix*, Fig. S1 *A* and *B*.

p27pT157pT198 Activates TGF-β Signaling by Inducing *TGB2* Expression. To further identify p27-regulated gene programs, we focused on genes both stringently up-regulated by p27CK−DD transduction in 231 and down-regulated in 1833 by p27 depletion. A total of 489 genes were increased by over twofold ($P < 0.005$, $q < 0.1$) in 231p27CK−DD vs. 231, while 229 genes were down-regulated by at least one half (fold change > 0.5, $P < 0.005$, $q < 0.1$) by p27 depletion in 1833. Of these, 82 genes were both up-regulated in 231p27CK−DD vs. 231 and also down-regulated in 1833shp27 vs. 1833 (Fig. 2*A* and *SI Appendix*, Table S2). GO analysis showed that the 82 genes that are both up-regulated by p27CK−DD in 231 and down-regulated in 1833 upon p27 loss are associated with important oncogenic pathways, including TGF-β, focal adhesion, ECM receptor interaction, and PI3K-AKT signaling pathways (Fig. 2*B* and *SI Appendix*, Fig. S1*C*). GSEA also showed TGF-β signaling

activation in 231p27CK–DD compared with 231, while p27 knockdown impaired TGF-β pathway activation in 1833 (Fig. 2 *C* and *D* and *SI Appendix*, Fig. S1*D* and Table S3). Similarly, treatment with the PI3K/mammalian target of rapamycin (mTOR) inhibitor, PF04691502 (hereafter PF1502), at a dose known to inhibit PI3K in these lines and to decrease both p27pT157 and p27pT198 (13), down-regulated genes associated with TGF-β pathway activation (*SI Appendix*, Fig. S1 *D* and *E*). Thus, TGF-β signaling is activated by p27CK–DD transduction in 231 and inhibited by p27 knockdown and by PI3K inhibition in 1833.

Up-regulation of *TGFB2* by p27 was confirmed by qPCR in three highly metastatic lines: 1833, 4175, and LuL2. In all three lines, p27 depletion decreased *TGFB2* expression (Fig. 2*E*). Furthermore, p27CK–DD transduction increased *TGFB2* expression and TGF-β2 secretion in the immortal, nontransformed mammary epithelial line MCF12A and in the low-metastatic 231 and UMUC3 lines (Fig. 2 *F* and *G*). In MCF12A, TGF-β2 induced a morphological change from an epithelial to a more mesenchymal phenotype (*SI Appendix*, Fig. S1*F*). TGF-β2 up-regulated *SNAI1* and *SNAI2* expression in MCF12A, 231, and UMUC3 (*SI Appendix*, Fig. S1*G*) and increased Matrigel invasion by 231 and UMUC3 (Fig. 2*G* and *SI Appendix*, Fig. S1*H*), confirming its importance to EMT in these models. In 231, EMT activation by p27CK–DD was shown by increased Matrigel invasion, decreased E-cadherin, and higher EMT-TF expression. All of these were reversed by *TGFB2* depletion (Fig. 2 *H–J*), indicating that TGF-β2 is a key driver of EMT activation by p27. Thus, C-terminally phosphorylated p27 appears to activate an EMT program, in part, by inducing *TGFB2* expression.

p27/cJun Complex Formation and Nuclear Localization Are Regulated by p27 Phosphorylation. To investigate how p27 up-regulates *TGFB2* expression, a phosphoprotein array was compared in MCF12A and MCF12Ap27CK–DD. Notably, p27CK–DD expression significantly increased serine 63-phosphorylated, activated cJun (hereafter cJunpS63) in MCF12A (Fig. 3*A*). p27CK–DD–transduced 231 and UMUC3 also had more cJunpS63 than parental lines, while p27 depletion in metastatic 1833 and LuL2 lines decreased cJunpS63 (Fig. 3*B*). cJun forms heterodimeric AP-1 transcription factor complexes that contribute to transformation (30). An in silico search revealed AP-1 consensus binding sites upstream of the *TGFB2* coding sequence.

To test whether p27 might interact with cJun to regulate *TGFB2* expression, we next assayed if cellular p27 binds cJun. Treatment of LuL2 with PF1502 over 48 h decreased AKTpS473 and reduced p27 phosphorylation at T198 (Fig. 3*C*, *Left*) without affecting p27 or cJun levels. cJun was detected in cellular p27 immunoprecipitates in LuL2. PI3K inhibition decreased both p27pT198 and p27-bound cJun (Fig. 3*C*). Furthermore, more p27-associated

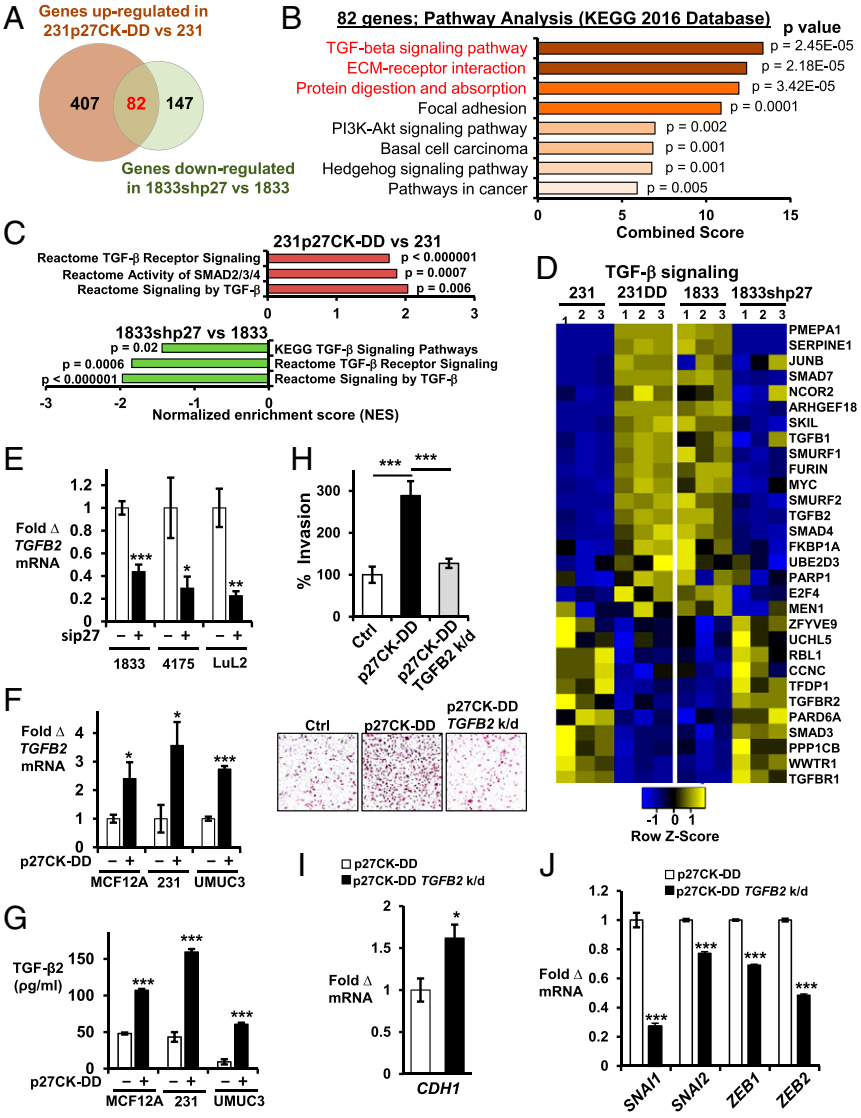

Fig. 2. TGF-β signaling is regulated by p27. (*A*) Venn diagram depicts genes up-regulated in 231p27CK–DD vs. 231 (fold change >2.0, $P < 0.005$, $q < 0.1$) and down-regulated in 1833shp27 vs. 1833 (fold change <0.5, $P < 0.005$, $q < 0.1$). Numbers of genes are indicated. See also *SI Appendix*, Table S2. (*B*) GO analysis shows the top signaling pathways in the Kyoto Encyclopedia of Genes and Genomes (KEGG) 2016 database related to the 82 genes up-regulated in 231p27CK–DD vs. 231 and that decreased with p27 loss in 1833. See also *SI Appendix*, Fig. S1*C*. (*C*) Pathway analysis of these 82 differentially expressed genes. NES, normalized enrichment score. See also *SI Appendix*, Fig. S1*D*. (*D*) Heatmaps show differential expression of 30 TGF-β signaling pathway genes from three independent RNA-seq experiments. See also *SI Appendix*, Fig. S1 *D* and *E* and Table S3. (*E*) Effects of short-term siRNA-mediated p27 depletion (sip27) on *TGFB2* mRNA by qPCR at 48 h in PI3K-activated, metastatic lines (1833, 4175, and LuL2) vs. scramble siRNA controls. (*F* and *G*) Effects of stable p27CK–DD expression on *TGFB2* mRNA (*F*) and on secreted TGF-β2 (pg/mL) over 48 h (*G*) in the indicated lines. (*H*) Quantitative data (*Top*) and representative images (*Bottom*) of Matrigel invasion in 231, 231p27CK–DD, and *TGFB2*-depleted (*TGFB2* k/d) 231p27CK–DD (for *TGFB2* depletion, see *SI Appendix*, Fig. S4*A*). (*I* and *J*) Effects of *TGFB2* depletion on *CDH1* expression (*I*) and on EMT drivers (*SNAI1*, *SNAI2*, *ZEB1*, and *ZEB2*) (*J*). Means ± SEM graphed from three or more replicates of three or more different biologic assays (*$P < 0.05$, **$P < 0.01$, ***$P < 0.001$). 231DD, 231p27CK–DD. See also *SI Appendix*, Fig. S1 *F–H*.

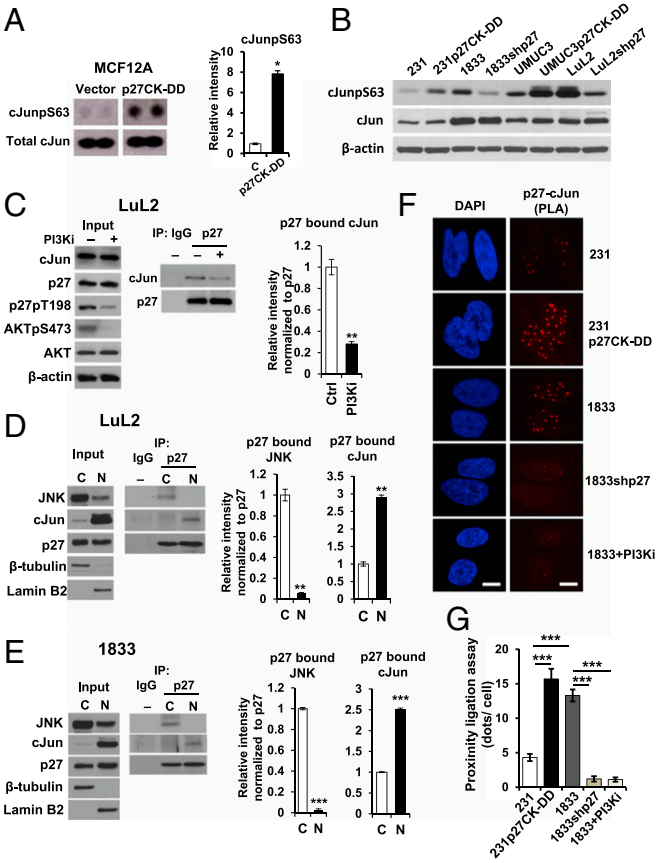

Fig. 3. Association of cJun with p27 is increased by p27 phosphorylation. (*A*) Activated cJun (cJunpS63) in MCF12A controls (Vector) and MCF12Ap27CK−DD (p27CK−DD) by dot blot (*Left*) and densitometry values graphed as mean ± SEM (*Right*, $*P < 0.05$). (*B*) Western blots of cJun, cJunpS63, and β-actin in the indicated lines. (*C*) LuL2 treated for 48 h with the PI3K inhibitor PF1502 (PI3Ki). Western blots show input (*Left*) for p27 immunoprecipitation (IP) blotting to detect p27-associated cJun (*Middle*). Densitometric quantitation of p27-bound cJun (*Right*, $**P < 0.01$). See also *SI Appendix*, Fig. S2 *A* and *B*. (*D* and *E*) Nuclear (N) and cytoplasmic (C) fractions of LuL2 (*D*) and 1833 (*E*) were immunoblotted (*Left*), and p27-associated cJun and JNK were detected by IP blot (*Middle*) with densitometry (*Right*, $**P < 0.01$, $***P < 0.001$). (*F*) In situ PLA shows p27/cJun complexes in the indicated lines and in 1833 treated with PF1502 (PI3Ki), indicated by red fluorescent dots. (*G*) Dots (mean ± SEM) graphed from triplicate PLAs; ANOVA with post hoc comparisons ($***P < 0.001$). (Scale bar: 10 μm.) See also EMSA data in *SI Appendix*, Fig. S2C.

cJun was detected in p27CK−DD–transduced 231 and UMUC3 than in vector control cells, as assayed by densitometry (*SI Appendix*, Fig. S2 *A* and *B*). These observations suggest that the interaction of p27 with cJun is increased by p27 phosphorylation.

Levels of p27-associated cJun and Jun N-terminal kinase (JNK) were assessed in nuclear and cytoplasmic fractions. In both LuL2 and 1833, JNK was largely cytoplasmic, while cJun was predominantly nuclear (Fig. 3 *D* and *E*, *Left*). p27-associated cJun was two- to threefold higher in nuclear vs. cytoplasmic fractions, while p27-associated JNK was detected only in the cytoplasm (Fig. 3 *D* and *E*, *Right*). Proximity ligation assays (PLAs) confirmed the interaction between nuclear p27 and cJun and that this interaction is greater in 231p27CK−DD than in control 231 cells (Fig. 3 *F* and *G*). Electrophoretic mobility shift assay (EMSA) revealed that p27 can bind an AP-1 consensus motif (*SI Appendix*, Fig. S2C).

cJun and p27 Are Corecruited to a Site Upstream of *TGFB2*. Since p27 could associate with cJun and bind to AP-1 motifs, we next assayed if nuclear p27/cJun complexes might mediate the *TGFB2* gene induction observed in p27-activated cells. Publicly available cJun ChIP sequencing (ChIP-seq) ENCODE data revealed that cJun binds a 5′-TGAG/CTCA-3′ AP-1 consensus site upstream of the *TGFB2* transcriptional start site (TSS) in human cells (Fig. 4*A*). ChIP-qPCR showed that cJun and p27 are corecruited to this AP-1 site. More p27 and cJun were associated with this AP-1 motif in 231p27CK−DD and 1833 than in 231 vector controls. Notably, chromatin association of both p27 and cJun decreased with p27 depletion and with loss of p27 phosphorylation following PI3K/mTOR inhibition with PF1502 (Fig. 4 *B* and *C*). Neither p27 nor cJun bound to irrelevant sites (*SI Appendix*, Fig. S3*A*). Sequential ChIP assays with cJun followed by re-ChIP with p27 antibodies indicated that cJun and p27 co-occupy this *TGFB2* site, with greater recruitment in p27CK−DD–expressing and PI3K-activated cells, and with loss of both p27 and cJun from this site upon p27 knockdown and PI3K inhibition (Fig. 4*D*). Thus, C-terminal p27 phosphorylation appears to increase cJun/p27 corecruitment to this AP-1 motif upstream of *TGFB2*. The bladder cancer models showed similar patterns of p27 and cJun recruitment to this *TGFB2* AP-1 site (*SI Appendix*, Fig. S3*B*). H3K27Ac, coactivator CBP/p300, and RNA polymerase II (Pol II) were more abundant at this *TGFB2* site in p27pT157pT198 or p27CK−DD–expressing cells than in 231 controls and decreased significantly with p27 depletion and PI3K inhibition in 1833 (Fig. 4 *E*–*G*). Because p27 knockdown decreases *TGFB2* expression and because p27CK−DD transduction induces *TGFB2*

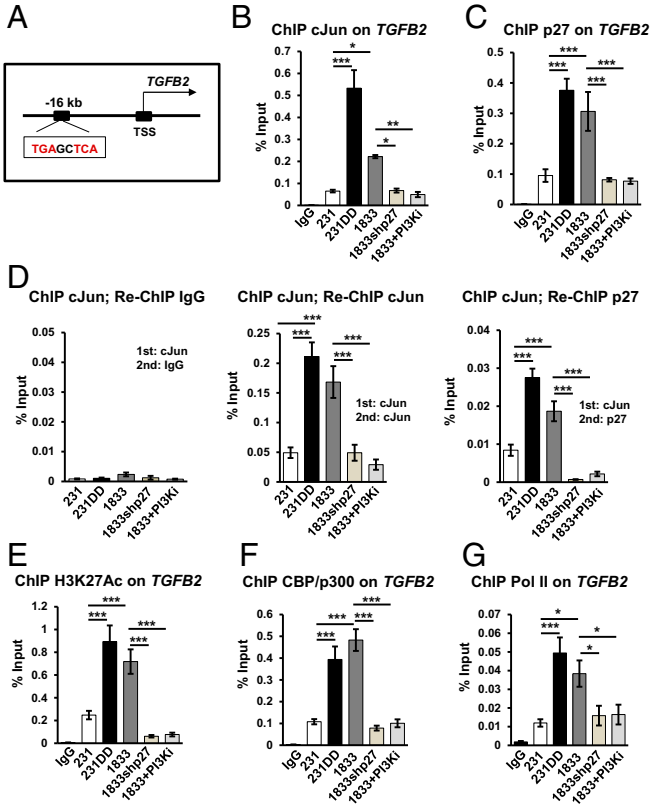

Fig. 4. cJun and p27 are corecruited to a *TGFB2* AP-1 site. (*A*) cJun/AP-1 consensus motif upstream of *TGFB2* TSS. (*B* and *C*) ChIP-qPCR with cJun (*B*) and p27 (*C*) antibodies show binding to an AP-1 site upstream of *TGFB2* in the indicated lines and in 1833 treated for 48 h with PF1502 (PI3Ki). (*D*) ChIP-re-ChIP assay of p27 association with cJun-bound *TGFB2* AP-1 site in the indicated lines. (*E*–*G*) ChIP assays show H3K27Ac (*E*), CBP/p300 (*F*), and Pol II (*G*) binding to the *TGFB2* AP-1 site in the indicated lines. Means ± SEM graphed from three or more replicates of three or more biologic assays; post hoc *P* values from ANOVA ($*P < 0.05$, $**P < 0.01$, $***P < 0.001$). See also *SI Appendix*, Fig. S3. 231DD, 231p27CK−DD.

to increase TGF-β2 secretion, these data suggest a model in which C-terminal p27 phosphorylation promotes p27 and cJun recruitment as well as interaction with CBP/p300 and Pol II at this enhancer to induce *TGFB2* expression (*SI Appendix*, Fig. S3*C*).

cJun and TGF-β2 Mediate p27-Driven Metastasis from Primary Tumors in Vivo. Since p27 appears to drive a TGF-β2–dependent EMT, we assayed the functional contribution of C-terminally phosphorylated p27, cJun, and TGF-β2 to metastasis in vivo. NOD-SCID mice were injected orthotopically with 231, 1833, 1833shp27, and 231p27CK−DD, and with 231p27CK−DD depleted of either *JUN* or *TGFB2* (depletion shown in *SI Appendix*, Fig. S4*A*). After removal of primary tumors at 300 mm^3, mice were monitored for metastasis from the primary site. Orthotopic injection of each of 1833 and 231p27CK−DD yielded significantly more metastases in liver, lymph nodes, and lung than vector control 231 cells (Fig. 5 *A*–*C*). p27 depletion in 1833 and loss of cJun or TGF-β2 expression in 231p27CK−DD significantly decreased p27-driven metastasis in vivo (Fig. 5 *A*–*C*). While 1833 and 231p27CK−DD formed more metastasis than 231, primary tumor growth and Ki67 staining did not differ significantly between groups (*SI Appendix*, Fig. S4 *B* and *C*). TGF-β2 levels, assayed by immunohistochemistry, were elevated in primary tumors from 1833 and 231p27CK−DD compared with 231 and were decreased in 1833shp27 tumors and in both *JUN*- and *TGFB2*-depleted 231p27CK−DD–derived tumors (Fig. 5*D* and *SI Appendix*, Fig. S4*D*). Thus, cJun activation and *TGFB2* induction appear to be required for p27-driven metastasis in this breast cancer model.

Identification of cJun/p27-Regulated Target Genes. To test if p27 binds more broadly to chromatin and to identify phosphorylation-dependent patterns of chromatin occupancy by p27 and cJun, ChIP-seq was performed in 231, 231p27CK−DD, and 1833. As a control, we also performed p27 ChIP-seq in 1833shp27. This revealed that p27 is broadly recruited to chromatin and that a significant proportion of cJun ChIP-seq peaks also contain p27 (Fig. 6*A*), suggesting that cJun and p27 may function together at common sites. Notably, 231p27CK−DD showed greater recruitment not only of p27 but also of cJun to chromatin, even at sites not shared by p27. The latter may result from p27-mediated cJun activation (Fig. 3*B*). Genomic distribution analysis showed that a little over half of the sites bound by cJun, p27, and both cJun/p27 are located at promoters or intronic sites, whereas the remaining sites occupy intergenic regions (Fig. 6*B*). Importantly, ChIP-seq heatmaps showed that the p27 signal was abrogated in p27-depleted 1833shp27 cells (Fig. 6*C*). Interestingly, the chromatin occupancy of cJun was also modulated by p27 depletion: among a

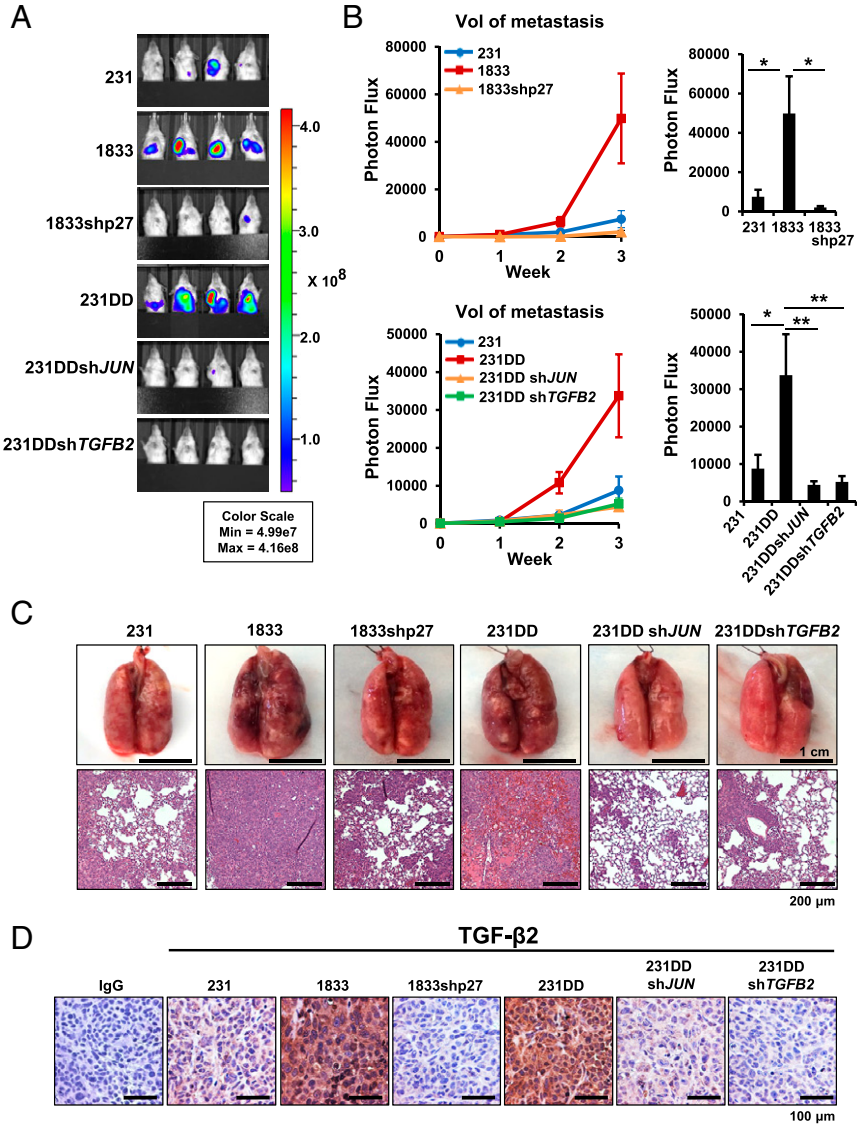

Fig. 5. cJun and TGF-β2 are required for p27-driven metastasis in vivo. (*A*) Primary orthotopic tumors were removed and animals were followed for metastasis using the bioluminescence in vivo imaging system (IVIS). Representative bioluminescence images of tumor-bearing mice 3 wk after primary tumor removal. Color scale depicts photon flux (photons per second) from tumor-bearing mice. (*B*) Mean (±SEM) bioluminescence (normalized photon flux) per second from tumor metastases (excluding regrowth of primary tumor at inguinal fat pad) is graphed for each group. *P* values from ANOVA (*$P < 0.05$, **$P < 0.01$, ***$P < 0.001$). (*C*) Representative whole-lung images (scale bar: 1 cm) and photomicrographs (scale bar: 200 μm) of metastatic lung tumors from the indicated groups. (*D*) Representative TGF-β2 immunohistochemistry images in primary tumors from the indicated lines. (Scale bar: 100 μm.) 231DD, 231p27CK−DD. See also *SI Appendix*, Fig. S4.

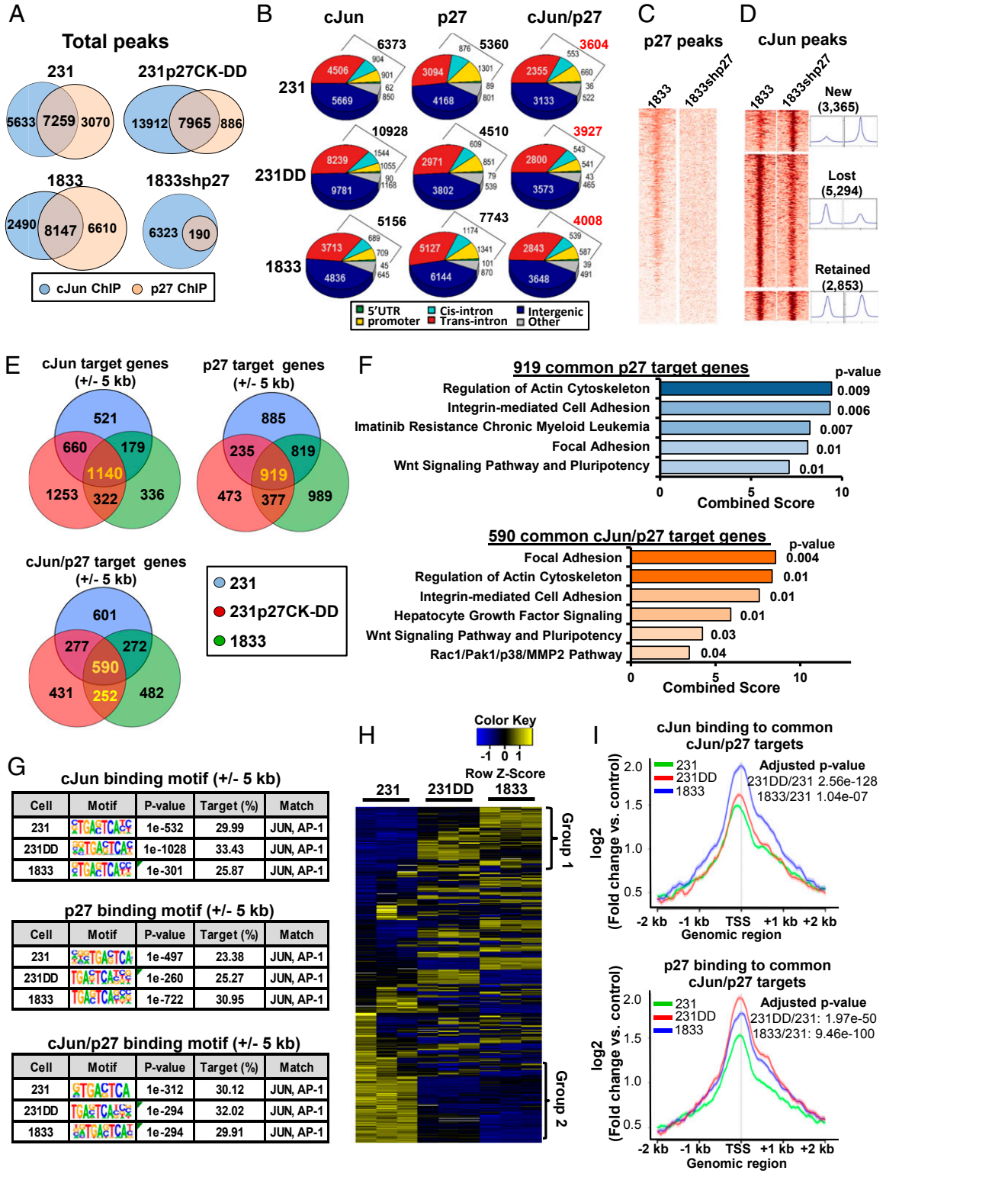

Cell	Motif	P-value	Target (%)	Match
231		1e-532	29.99	JUN, AP-1
231DD		1e-1028	33.43	JUN, AP-1
1833		1e-301	25.87	JUN, AP-1

Cell	Motif	P-value	Target (%)	Match
231		1e-497	23.38	JUN, AP-1
231DD		1e-260	25.27	JUN, AP-1
1833		1e-722	30.95	JUN, AP-1

Cell	Motif	P-value	Target (%)	Match
231		1e-312	30.12	JUN, AP-1
231DD		1e-294	32.02	JUN, AP-1
1833		1e-294	29.91	JUN, AP-1

Fig. 6. Genome-wide DNA binding of p27 and cJun. (*A*) Venn diagrams show mean p27- and cJun-DNA binding peaks in 231, 231p27CK–DD, 1833, and 1833shp27 from two independent ChIP-seq assays, each with two biologic replicates. (*B*) Genomic distribution of DNA binding peaks for p27, cJun, and for peaks occupied by both p27 and cJun in the indicated lines. (*C* and *D*) DNA binding heatmaps of p27 (*C*) and cJun ChIP (*D*) in 1833 and 1833shp27. See also *SI Appendix*, Fig. S5*A* and see *SI Appendix*, Fig. S5*B* for cJun-regulated pathways affected by loss of p27. (*E*) Venn diagrams show mean numbers of target genes (±5 kb from the TSS) bound by cJun only, p27 only, and both cJun and p27 in 231, 231p27CK–DD, and 1833. (*F*) GO analysis (WikiPathway 2016) showing major signaling pathways related to 919 p27 target genes and 590 cJun/p27 cotarget genes bound in all three lines from *E*. See also *SI Appendix*, Fig. S5*C*. (*G*) Binding motif search shows top transcription motif bound by cJun only, p27 only, and cJun/p27 for binding motifs ±5 kb from the TSS for each line. See *SI Appendix*, Fig. S5*D* for binding at all sites. (*H*) Heatmaps show expression profile from RNA-seq of genes bound by both cJun and p27 in ChIP-seq in all three lines. (*I*) Signal intensities of p27 and cJun were quantitated at target genes bound by both cJun and p27 in all three cell lines. Significant differences calculated with paired *t* test, and *P* values adjusted by Bonferroni–Hochberg. See also *SI Appendix*, Fig. S5 *E* and *F* and Table S4 for signal intensities of cJun and p27 binding to group 1 and group 2 genes, respectively. 231DD, 231p27CK–DD.

little over 10,000 cJun-bound peaks detected in 1833, 5,294 sites were shared by p27 and were lost or decreased upon p27 knockdown, while 2,853 cJun-bound peaks were unaffected. In addition, 3,365 new, exclusively cJun-bound peaks were acquired (Fig. 6*D* and *SI Appendix*, Fig. S5*A*). GO analysis of 1,364 genes annotated by the 5,294 cJun-bound peaks that are lost with p27 depletion in 1833 showed that these p27-regulated cJun targets are associated with Notch, apoptosis, and cytoskeleton signaling (*SI Appendix*, Fig. S5*B*). Thus, p27 may be required for cJun recruitment to an important fraction of cJun-regulated genes.

Evaluation of binding at target genes (±5 kb from the TSS) revealed that p27 is recruited to over 2,000 target genes in each of the three lines (Fig. 6*E*, *Top Right* Venn diagram). Notably, GO analysis of the 919 p27 targets common to all three lines reveals that p27 binds genes involved in focal adhesion, actin cytoskeleton, integrin signaling, and Wnt pathways (Fig. 6*F*, *Top*). GO analysis of cJun targets common to all three lines identifies genes governing cell surface adhesion, integrin and growth factor pathways (*SI Appendix*, Fig. S5*C*). There were 590 cJun/p27 target genes commonly bound in all three lines (Fig. 6*E*, *Bottom* and *SI Appendix*, Table S4). These are associated with pathways similar to those for each factor alone and also include hepatocyte growth factor and Rac1/Pak1 signaling (Fig. 6*F*, *Bottom*). p27 and cJun were also corecruited to 252 novel target genes in both 231p27CK−DD and 1833 that were not bound in 231 (Fig. 6*E*, *Bottom*).

DNA binding motif analysis revealed that AP-1 binding consensus motifs, including JunB, Fra1, and BATF, were the top-enriched DNA motifs for p27 and cJun individually and account for nearly one-third of the sites bound by both cJun and p27 (binding motifs ±5 kb from the TSS, Fig. 6*G*; genome-wide binding motifs in *SI Appendix*, Fig. S5*D*). Thus, p27 and cJun are commonly recruited to genes bearing cJun consensus motifs.

Differential Expression of cJun/p27 Target Genes in Lines with Different Metastatic Potential. To evaluate the potential for p27 and cJun to coregulate gene expression, patterns of chromatin annotation were compared with RNA-seq gene expression data. Of the 919 genes annotated by p27 in all three lines, over half were differentially expressed in 231p27CK−DD (492/919) and in 1833 (456/919) compared with 231 (any fold change vs. 231, q > 0.1). cJun/p27 target genes bound in all three lines showed two differential expression patterns. Group 1 genes were up-regulated in 231p27CK−DD and in 1833 compared with 231 controls, while group 2 genes were down-regulated. cJun/p27 target genes activated in both highly metastatic lines identify putative oncogenes (group 1, Fig. 6*H*), while those down-regulated in metastatic derivatives compared with control 231 may encode tumor suppressors (group 2, Fig. 6*H*).

Lines with p27 activation showed greater recruitment of both cJun and p27 to target genes: recruitment of both p27 and cJun to all 590 common target genes (Fig. 6*I*) and to differentially expressed cJun/p27 targets from both groups 1 and 2 (*SI Appendix*, Fig. S5 *E* and *F*) was significantly greater in 231p27CK−DD and 1833 than in 231, similar to the pattern detected at the *TGFB2* AP-1 site (Fig. 4). Differential expression of cJun/p27-activated group 1 genes and p27 and cJun binding intensities are shown in Fig. 7 *A* and *B* and *SI Appendix*, Table S4. These cJun/p27-activated genes associated strongly with cancer signaling pathways, including prooncogenic p53, cancer-related miRNAs, focal adhesion, the receptor for advanced glycation end- products (RAGE), and hypoxia inducible factor-1 (HIF-1) (Fig. 7*C*).

cJun/p27 targets that were bound exclusively in 1833 and 231p27CK−DD, but not in 231, might include novel prooncogenes whose binding is only acquired when highly phosphorylated p27pT157pT198 binds cJun. A subset of these novel cJun/p27 target genes was up-regulated in the highly metastatic lines (Fig. 7 *D* and *E* and *SI Appendix*, Table S5). This gene set also directs pathways associated with tumor progression and metastasis (Fig. 7*F*). We validated p27 and cJun binding to three target genes (*MYO10*, *PAI1*, and *KLF8*) by ChIP-qPCR and verified their differential expression by RT-qPCR. *MYO10* is a gene implicated in cell invasion and metastasis (31). Both the binding of cJun and p27 to an AP-1 site +2 kb from *MYO10* and *MYO10* expression were greater in 231p27CK−DD and 1833 than in 231 and were down-regulated in 1833shp27 (*SI Appendix*, Fig. S6 *A–D*). Differential cJun/p27 binding to, and induction of, two other target genes, *PAI1*/*SERPINE1* [a known prognostic factor for breast cancer (32)] and *KLF8* [an EMT mediator (33)], were also verified (*SI Appendix*, Fig. S6 *E–L*). Together, p27 appears to bind cJun and promote recruitment to, and transactivation of, gene programs that contribute to tumor progression and metastasis.

p27/cJun Target Genes Are Differentially Expressed in Breast Cancers with High p27pT157. We next assayed if primary human breast cancers with C-terminally phosphorylated p27 would show differential expression of cJun/p27-regulated genes identified herein. Among primary breast cancers in the TCGA database, 846 had gene expression, p27pT157 levels on reverse phase protein array, and outcome data available. Of these, cancers in the top decile of p27pT157 expression showed significantly worse overall survival (OS) (Fig. 7*G*, $P = 0.028$). A subset of 392 genes, differentially expressed in the "p27pT157 high" breast cancers vs. all others, was also coordinately differentially expressed in p27-activated 231p27CK−DD and 1833 compared with 231 and 1833shp27. Of these 392 differentially expressed genes, 25% (97/392) were Jun-bound and 16% (63/392) showed both p27 and cJun binding on ChIP-seq and included the validated target, *PAI1*. Univariate and multivariate analysis of each of these genes in a training dataset of 702 breast cancers identified the 30 p27-regulated genes differentially expressed both in p27-activated cell lines and in the cancers with high p27pT157 that contribute most importantly to patient outcome. Principle component analysis showed that these 30 genes cluster patients into two groups (Fig. 7*H*) that have significantly different OS on Kaplan–Meier analysis (Fig. 7*I*, $P = 0.036$). The prognostic value of this p27-regulated gene signature for OS was validated using receiver operating characteristic (ROC) curve analysis in an independent breast cancer validation cohort and yielded an area under the ROC curve (AUC) of 0.63 at 5 y and of 0.73 at 6 y of follow-up (Fig. 7*J*). The coordinate expression of p27-regulated gene drivers of poor patient outcome both in p27-activated cancer lines and in primary breast cancers with high C-terminal p27 phosphorylation supports the biologic relevance of p27-driven gene regulation to metastatic tumor progression.

Discussion

The cyclin-CDK inhibitor p27 is a ubiquitously expressed, critical negative regulator of the G1 to S phase cell cycle transition (4). p27 inhibits cyclin-CDK complexes in the nucleus of quiescent cells but accumulates in the cytoplasm in early G1 (34). Transient C-terminal p27 phosphorylation by pAKT in early G1 delays nuclear p27 import (9) and promotes cyclin D-CDK4/6 assembly and activation (21, 35, 36) as Src and cyclin E-Cdk2 phosphorylate p27 to mediate its proteolysis and promote G1 transit (37, 38). The coordinate phosphorylation of p27 at T157 and T198 also promotes its binding to RhoA/ROCK1 (18) to alter the actin cytoskeleton in normal cells, mediating changes in cell shape required for execution of later cell cycle phases (39, 40).

In the last two decades, p27 has been found to act as both tumor suppressor and oncogene and as a critical regulator of development. The present work opens the possibility that these roles might be modulated by a transcriptional regulatory action of p27. p27 deregulation is a hallmark of human cancers. The tumor-suppressor, CDK-inhibitory function of p27 is impaired through miRNA-mediated decreases in p27 translation and by accelerated p27 proteolysis in Src-activated cells (4). p27 also acquires prooncogenic functions through its C-terminal phosphorylation by PI3K-activated kinases (41). C-terminal p27 phosphorylation at T157 and T198 attenuates CDK inhibitory action and increases cyclin D-CDK activation (21, 35) and disrupts the actin cytoskeleton through RhoA/ROCK1 inactivation (18, 22) to promote cancer metastasis (42). Enforced expression of p27 in the cytoplasm of malignant

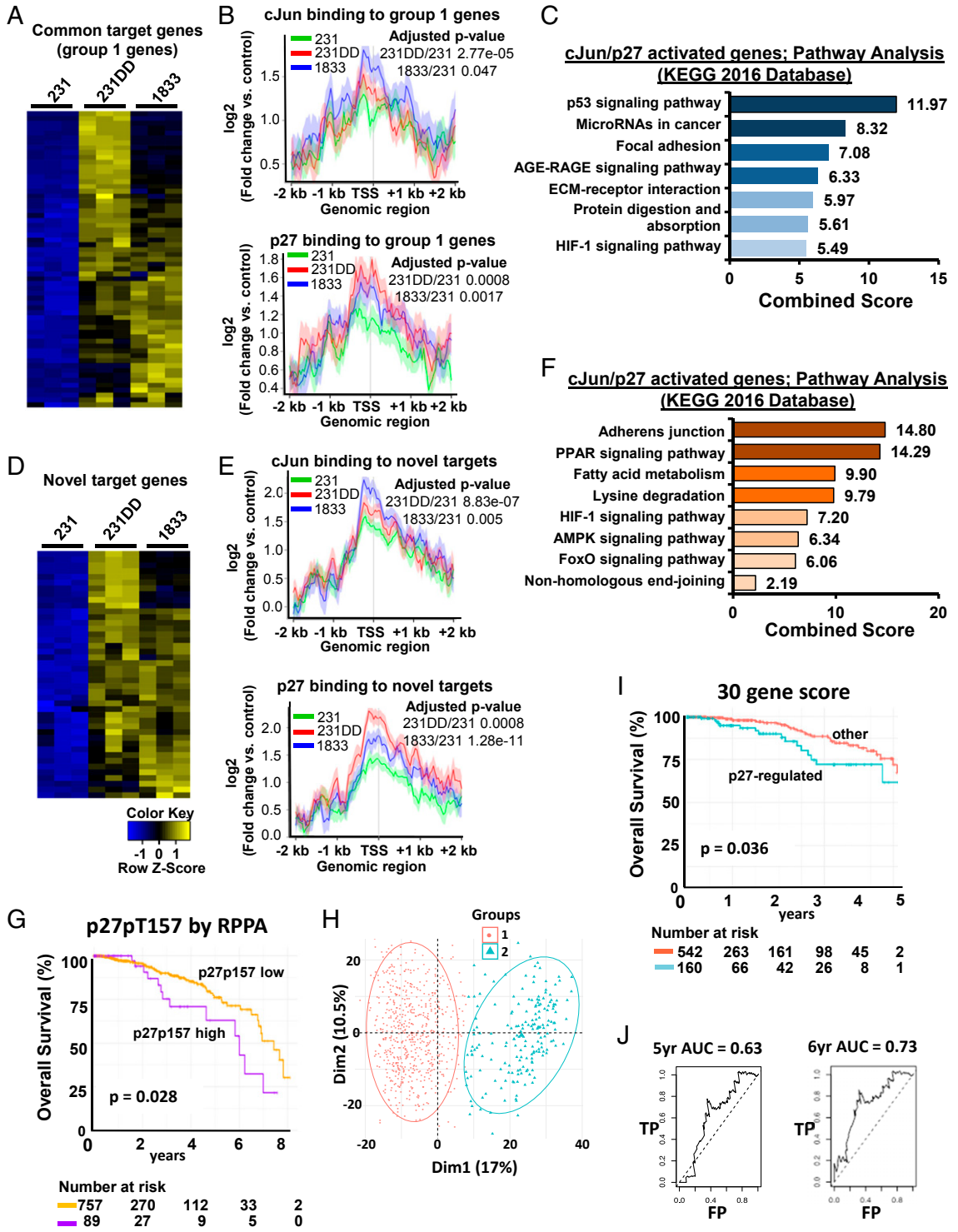

Fig. 7. cJun/p27-regulated target genes govern cancer programs of tumor progression. (*A*) Heatmap of expression of 61 p27/cJun target genes common to all three lines whose expression is up-regulated in 231p27CK–DD (231DD) and 1833 lines vs. 231. See also *SI Appendix*, Table S4. (*B*) Mean amplitudes of target gene binding by cJun (*Top*) and p27 (*Bottom*) are shown for the differentially expressed genes in *A* in the indicated cell lines. (*C*) GO analysis shows the top signaling pathways related to the differentially expressed genes identified in *A*. (*D*) Heatmap of expression of 43 newly acquired cJun/p27 target genes bound in 231DD and 1833, but not in 231, that are differentially expressed in the indicated cell lines. See also *SI Appendix*, Table S5. (*E*) Mean amplitude of target gene binding by cJun (*Top*) and p27 (*Bottom*) are shown for the differentially expressed genes in *D* in the indicated cell lines. (*F*) GO analysis shows the main signaling pathways related to the genes identified in *D*. See *SI Appendix*, Fig. S6 for validation of cJun/p27 cotarget genes. (*G*) Kaplan–Meier (KM) graph showing differential OS among women whose breast cancers have high vs. low p27pT157 on reverse phase protein array (RPPA) from $n = 846$ cases in the TCGA/TCPA dataset. (*H*) Principle component analysis of 30 p27-regulated genes expressed among $n = 703$ breast cancers. (*I*) KM graph shows overall breast cancer survival according to differential expression of the p27-regulated 30 gene profile among the training set ($n = 703$ cases). (*J*) The prognostic value of this p27-regulated 30 gene signature for OS was validated using ROC analysis in an independent breast cancer validation cohort. AGE-RAGE, advanced glycation end products-receptor for advanced glycation end products; AMPK, 5′ AMP-activated protein kinase; FP, false positive; KEGG, Kyoto Encyclopedia of Genes and Genomes; PPAR, peroxisome proliferator-activated receptor; TP, true positive.

cells with high endogenous PI3K activation is sufficient to increase cell invasion and metastasis (43, 44). Although aberrantly detected in cytoplasm, p27 is never exclusively cytoplasmic, nor is nuclear p27 limited in PI3K-activated cancers (9, 15, 16). Delayed nuclear import and increased stability of C-terminally phosphorylated p27 permit novel protein interactions in both cytoplasm and nucleus that drive oncogenesis. Our prior work showed that p27CK−DD, but not p27CK−, interacts with and activates STAT3 to induce *TWIST1* expression and a morphologic EMT and showed that C-terminal p27 phosphorylation critically mediates metastasis (14). Here, we identify a mechanism of oncogene cooperation between the PI3K pathway and cJun and reveal a previously unknown p27/cJun partnership that provides new insight into the profound effects of p27 on tumor metastasis. It is not clear that any of the p27 phenotypes resulting from these phosphorylations has primacy over any other. Rather, we posit that they would act together to promote transformation in the context of constitutive oncogenic PI3K activation. We show that p27 is broadly recruited to chromatin and cooperates with cJun to activate gene programs that govern focal adhesion, cytoskeleton, and signaling regulators of cell motility and metastasis.

Several lines of evidence have suggested a role for p27 in transcriptional regulation during embryogenesis. As CDK inhibitor, p27 acts to coordinate cell cycle exit with terminal differentiation (40, 41). p27 also plays CDK-independent developmental roles in collaboration with tissue-specific transcription factors, including MYOD and neurogenin 2. In mice, p27 interacts functionally with the proneural factor neurogenin 2 in neuronal differentiation (45), and in *Xenopus laevis*, the p27 homolog Xic1 cooperates with the myogenic factor MYOD to mediate myogenesis (46, 47). These effects are cell cycle independent, since a *cdknx* mutant encoding a *xic1* devoid of cyclin-CDK binding restored differentiation defects in *cdknx*-null frogs (46, 47). Tissue differentiation defects in p27-null mice (48–50) are also rescued by p27CK−-knockin (51). These developmental actions may reflect transcriptional roles of p27, whose potential regulation by periodic AKT activation and p27 phosphorylation have yet to be explored. Further evidence for an interaction in transcription came from a ChIP-on-chip survey in NIH 3T3 cells that showed that p27 binds gene promoters in complex with p130, E2F4, HDAC1, and SIN3A (52). This complex appears to mediate *SOX2* repression during ES cell differentiation and in quiescent mouse embryonic fibroblasts (MEFs) (53). A recent genomic survey confirmed broad chromatin association of p27 in quiescent MEFs (54), but biologic targets and function were not characterized.

The present work provides a comprehensive comparison of p27–chromatin binding in human cancer cells with different metastatic potential and reveals the unexpected finding that p27 functionally cooperates with cJun to regulate transcription programs associated with cell adhesion and metastasis. cJun participates in homo- and heterodimeric AP-1 transcription factor complexes to activate drivers of transformation, proliferation, apoptosis, and metastasis in human cancers (30). JNKs phosphorylate and activate cJun (55). cJun regulates EMT during differentiation (55) and drives cancer cell motility and invasion (56), and its levels correlate with poor breast cancer patient outcome (57). Here, we show that cJun interacts with p27 and that its transcriptional activity is importantly regulated by p27. p27 phosphorylation increases its coprecipitation with cJun and cJun activation and increases the magnitude of, and changes the distribution of, cJun/p27 corecruitment to chromatin. A significant proportion of cJun-annotated sites are shared by p27, and cJun recruitment to these sites decreased dramatically with p27 depletion. Thus, p27 phosphorylation may not only promote its interaction with cJun complexes, but also facilitate their stable chromatin association.

Approximately half of p27 binding sites are promoter proximal, and cJun/AP-1 consensus motifs were the most common DNA binding motif. p27 targets in our PI3K-activated lines were nearly twice as abundant as reported in quiescent MEFs (54). The inactivation of PI3K/AKT and the loss of p27pT157pT198 in quiescence (21) may account for these differences. AKT activation is required for G1 to S phase progression, and, in normal mammary epithelial cells, AKT activation and p27 phosphorylation at T157 and T198 peak in mid-G1 (21). Cyclic changes in p27pT157pT198 abundance may modulate p27-regulated transcription across the cell cycle. In cancers with oncogenic PI3K activation, the increased C-terminal p27 phosphorylation may abrogate the corepressive functions of p27 observed in quiescent cells and alter both coregulator and transcriptional target gene selection, directing constitutive p27/cJun association to drive prooncogenic changes in gene expression.

p27 is a central node, integrating PI3K and TGF-β signaling pathways to maintain expression of a profile of EMT genes. Both TGF-β2 and TGF-β2-induced gene profiles are up-regulated in p27-activated models. TGF-β2 is a known EMT driver (58) that promotes metastasis in a variety of malignancies, including gliomas (59) and pancreatic (60, 61) and breast cancers (62). cJun/p27 complexes are corecruited to *TGFB2* to drive its expression as well as associate with chromatin more broadly to modulate transcription of genes critical for cell adhesion, cytoskeletal regulation, and signaling. Metastasis from primary orthotopic tumors was reduced by p27 depletion in 1833 and by *JUN* or *TGFB2* depletion in 231p27CK−DD, supporting the functional importance of these pathways in metastasis.

A large number of cJun/p27 target genes were differentially expressed in p27-activated lines compared with control 231. These cJun/p27 target genes associate with prooncogenic signaling, including p53, cancer-related miRNAs, HIF-1, focal adhesion, and ECM pathways. In addition, in the highly metastatic lines, a new set of target genes were acquired that govern metabolic and HIF-1/hypoxia-regulated pathways. cJun/p27 target genes identified in 231p27CK−DD and 1833, but not activated in 231, may require a threshold of p27 phosphorylation for binding and gene induction. The binding and expression of the validated cJun/p27 targets—*PAI1*/*SERPINE1*, *MYO10*, and *KLF8*—were p27 dependent and increased in metastatic lines. All play roles in EMT or in cancer cell motility and metastasis and are associated with early breast cancer metastasis (31–33).

While cyclin-CDKs have long been known to govern transcription via pRb-family phosphorylation and activation of E2Fs, the present work identifies a novel prooncogenic function for p27 as a transcriptional coregulator of cJun. In over 60% of human cancers, PI3K/AKT constitutively activates effectors AKT, SGK1, and $p90^{RSK1}$, all of which phosphorylate p27 (4, 42). AKT activation is associated with both cytoplasmic p27 (9, 15, 16) and detection of C-terminally phosphorylated p27 in primary human breast cancers (12, 14). That genes differentially regulated by p27 in our cell line models were also differentially expressed in primary breast cancers with high p27pT157 supports the biologic relevance of this mechanism of p27 action in vivo. Moreover, this p27-regulated gene profile is associated with poor cancer survival, indicating its relevance to disease progression. Together, our findings support a model in which C-terminal phosphorylation promotes p27 interaction with cJun, leading to p27/cJun corecruitment to, and activation of, oncogenic genes that drive programs of EMT and cancer metastasis.

Materials and Methods

All materials and methods, including the source of p27 phosphomimetic mutant-expressing cells, lentivirus production and infection, siRNA-mediated knockdown of p27, real-time qPCR, Western blotting, immunoprecipitation, nuclear and cytoplasmic fractionation, transwell invasion assay, ChIP assay, orthotopic xenograft assay, immunohistochemistry, PLA, EMSA, RNA-seq, RNA-seq bioinformatic analysis, ChIP-seq and bioinformatic analysis thereof, analysis of p27-regulated gene expression in primary human breast cancers from TCGA/TCPA, and statistical analysis and references pertaining to these methods are detailed in *SI Appendix, Supplemental Materials and Methods*. Reagents and resources are listed in *SI Appendix*, Table S6. Animal work was compliant with University of Miami Institutional Animal Care and Use Committee.

Data Availability

Data have been deposited in the National Center for Biotechnology Information Gene Expression Omnibus repository under accession no. GSE112446.

ACKNOWLEDGMENTS. This work was supported by the NIH Grant 2R01CA105118-05A1 (to J.M.S.) and by the Department of Defense Breast Cancer Research Program Grant W81XWH-17-1-0456 (to J.M.S. and K.B.). J.M.S., S.A.W., and A.B. were supported by the Doris Duke Charitable Foundation, and K.B. was supported by NIH Grant R01GM113256A1.

1. Koff A, Ohtsuki M, Polyak K, Roberts JM, Massagué J (1993) Negative regulation of G1 in mammalian cells: Inhibition of cyclin E-dependent kinase by TGF-beta. *Science* 260:536–539.
2. Slingerland JM, et al. (1994) A novel inhibitor of cyclin-Cdk activity detected in transforming growth factor beta-arrested epithelial cells. *Mol Cell Biol* 14:3683–3694.
3. Polyak K, et al. (1994) p27Kip1, a cyclin-Cdk inhibitor, links transforming growth factor-beta and contact inhibition to cell cycle arrest. *Genes Dev* 8:9–22.
4. Chu IM, Hengst L, Slingerland JM (2008) The Cdk inhibitor p27 in human cancer: Prognostic potential and relevance to anticancer therapy. *Nat Rev Cancer* 8:253–267.
5. Larrea MD, Wander SA, Slingerland JM (2009) p27 as Jekyll and Hyde: Regulation of cell cycle and cell motility. *Cell Cycle* 8:3455–3461.
6. Mayer IA, Arteaga CL (2016) The PI3K/AKT pathway as a target for cancer treatment. *Annu Rev Med* 67:11–28.
7. Engelman JA (2009) Targeting PI3K signalling in cancer: Opportunities, challenges and limitations. *Nat Rev Cancer* 9:550–562.
8. Chiang GG, Abraham RT (2007) Targeting the mTOR signaling network in cancer. *Trends Mol Med* 13:433–442.
9. Liang J, et al. (2002) PKB/Akt phosphorylates p27, impairs nuclear import of p27 and opposes p27-mediated G1 arrest. *Nat Med* 8:1153–1160.
10. Liang J, et al. (2007) The energy sensing LKB1-AMPK pathway regulates p27(kip1) phosphorylation mediating the decision to enter autophagy or apoptosis. *Nat Cell Biol* 9:218–224.
11. Kossatz U, et al. (2006) C-terminal phosphorylation controls the stability and function of p27kip1. *EMBO J* 25:5159–5170.
12. Motti ML, De Marco C, Califano D, Fusco A, Viglietto G (2004) Akt-dependent T198 phosphorylation of cyclin-dependent kinase inhibitor p27kip1 in breast cancer. *Cell Cycle* 3:1074–1080.
13. Wander SA, et al. (2013) PI3K/mTOR inhibition can impair tumor invasion and metastasis in vivo despite a lack of antiproliferative action in vitro: Implications for targeted therapy. *Breast Cancer Res Treat* 138:369–381.
14. Zhao D, et al. (2015) Cytoplasmic p27 promotes epithelial-mesenchymal transition and tumor metastasis via STAT3-mediated Twist1 upregulation. *Oncogene* 34: 5447–5459.
15. Viglietto G, et al. (2002) Cytoplasmic relocalization and inhibition of the cyclin-dependent kinase inhibitor p27(Kip1) by PKB/Akt-mediated phosphorylation in breast cancer. *Nat Med* 8:1136–1144.
16. Shin I, et al. (2002) PKB/Akt mediates cell-cycle progression by phosphorylation of p27 (Kip1) at threonine 157 and modulation of its cellular localization. *Nat Med* 8: 1145–1152.
17. Hong F, et al. (2008) mTOR-raptor binds and activates SGK1 to regulate p27 phosphorylation. *Mol Cell* 30:701–711.
18. Larrea MD, et al. (2009) RSK1 drives p27Kip1 phosphorylation at T198 to promote RhoA inhibition and increase cell motility. *Proc Natl Acad Sci USA* 106:9268–9273.
19. Fujita N, Sato S, Tsuruo T (2003) Phosphorylation of p27Kip1 at threonine 198 by p90 ribosomal protein S6 kinases promotes its binding to 14-3-3 and cytoplasmic localization. *J Biol Chem* 278:49254–49260.
20. Ciarallo S, et al. (2002) Altered p27(Kip1) phosphorylation, localization, and function in human epithelial cells resistant to transforming growth factor beta-mediated G(1) arrest. *Mol Cell Biol* 22:2993–3002.
21. Larrea MD, et al. (2008) Phosphorylation of p27Kip1 regulates assembly and activation of cyclin D1-Cdk4. *Mol Cell Biol* 28:6462–6472.
22. Besson A, Gurian-West M, Schmidt A, Hall A, Roberts JM (2004) p27Kip1 modulates cell migration through the regulation of RhoA activation. *Genes Dev* 18:862–876.
23. Massagué J (2008) TGFbeta in cancer. *Cell* 134:215–230.
24. Massagué J (2012) TGFβ signalling in context. *Nat Rev Mol Cell Biol* 13:616–630.
25. Kang Y, et al. (2003) A multigenic program mediating breast cancer metastasis to bone. *Cancer Cell* 3:537–549.
26. Vlach J, Hennecke S, Amati B (1997) Phosphorylation-dependent degradation of the cyclin-dependent kinase inhibitor p27. *EMBO J* 16:5334–5344.
27. Taube JH, et al. (2010) Core epithelial-to-mesenchymal transition interactome gene-expression signature is associated with claudin-low and metaplastic breast cancer subtypes. *Proc Natl Acad Sci USA* 107:15449–15454.
28. Minn AJ, et al. (2005) Genes that mediate breast cancer metastasis to lung. *Nature* 436:518–524.
29. Overdevest JB, et al. (2011) CD24 offers a therapeutic target for control of bladder cancer metastasis based on a requirement for lung colonization. *Cancer Res* 71: 3802–3811.
30. Hess J, Angel P, Schorpp-Kistner M (2004) AP-1 subunits: Quarrel and harmony among siblings. *J Cell Sci* 117:5965–5973.
31. Cao R, et al. (2014) Elevated expression of myosin X in tumours contributes to breast cancer aggressiveness and metastasis. *Br J Cancer* 111:539–550.
32. Sternlicht MD, et al. (2006) Prognostic value of PAI1 in invasive breast cancer: Evidence that tumor-specific factors are more important than genetic variation in regulating PAI1 expression. *Cancer Epidemiol Biomarkers Prev* 15:2107–2114.
33. Wang X, et al. (2007) Krüppel-like factor 8 induces epithelial to mesenchymal transition and epithelial cell invasion. *Cancer Res* 67:7184–7193.
34. Connor MK, et al. (2003) CRM1/Ran-mediated nuclear export of p27(Kip1) involves a nuclear export signal and links p27 export and proteolysis. *Mol Biol Cell* 14:201–213.
35. James MK, Ray A, Leznova D, Blain SW (2008) Differential modification of p27Kip1 controls its cyclin D-cdk4 inhibitory activity. *Mol Cell Biol* 28:498–510.
36. LaBaer J, et al. (1997) New functional activities for the p21 family of CDK inhibitors. *Genes Dev* 11:847–862.
37. Grimmler M, et al. (2007) Cdk-inhibitory activity and stability of p27Kip1 are directly regulated by oncogenic tyrosine kinases. *Cell* 128:269–280.
38. Chu I, et al. (2007) p27 phosphorylation by Src regulates inhibition of cyclin E-Cdk2. *Cell* 128:281–294.
39. Besson A, Assoian RK, Roberts JM (2004) Regulation of the cytoskeleton: An oncogenic function for CDK inhibitors? *Nat Rev Cancer* 4:948–955.
40. Besson A, Dowdy SF, Roberts JM (2008) CDK inhibitors: Cell cycle regulators and beyond. *Dev Cell* 14:159–169.
41. Sicinski P, Zacharek S, Kim C (2007) Duality of p27Kip1 function in tumorigenesis. *Genes Dev* 21:1703–1706.
42. Wander SA, Zhao D, Slingerland JM (2011) p27: A barometer of signaling deregulation and potential predictor of response to targeted therapies. *Clin Cancer Res* 17:12–18.
43. Denicourt C, Saenz CC, Datnow B, Cui XS, Dowdy SF (2007) Relocalized p27Kip1 tumor suppressor functions as a cytoplasmic metastatic oncogene in melanoma. *Cancer Res* 67:9238–9243.
44. Wu FY, et al. (2006) Reduction of cytosolic p27(Kip1) inhibits cancer cell motility, survival, and tumorigenicity. *Cancer Res* 66:2162–2172.
45. Nguyen L, et al. (2006) p27kip1 independently promotes neuronal differentiation and migration in the cerebral cortex. *Genes Dev* 20:1511–1524.
46. Vernon AE, Philpott A (2003) A single cdk inhibitor, p27Xic1, functions beyond cell cycle regulation to promote muscle differentiation in Xenopus. *Development* 130: 71–83.
47. Messina G, et al. (2005) p27Kip1 acts downstream of N-cadherin-mediated cell adhesion to promote myogenesis beyond cell cycle regulation. *Mol Biol Cell* 16: 1469–1480.
48. Kiyokawa H, et al. (1996) Enhanced growth of mice lacking the cyclin-dependent kinase inhibitor function of p27(Kip1). *Cell* 85:721–732.
49. Nakayama K, et al. (1996) Mice lacking p27(Kip1) display increased body size, multiple organ hyperplasia, retinal dysplasia, and pituitary tumors. *Cell* 85:707–720.
50. Fero ML, et al. (1996) A syndrome of multiorgan hyperplasia with features of gigantism, tumorigenesis, and female sterility in p27(Kip1)-deficient mice. *Cell* 85: 733–744.
51. Besson A, et al. (2007) Discovery of an oncogenic activity in p27Kip1 that causes stem cell expansion and a multiple tumor phenotype. *Genes Dev* 21:1731–1746.
52. Pippa R, et al. (2012) p27Kip1 represses transcription by direct interaction with p130/E2F4 at the promoters of target genes. *Oncogene* 31:4207–4220.
53. Li H, et al. (2012) p27(Kip1) directly represses Sox2 during embryonic stem cell differentiation. *Cell Stem Cell* 11:845–852.
54. Biçer A, et al. (2017) ChIP-Seq analysis identifies p27(Kip1)-target genes involved in cell adhesion and cell signalling in mouse embryonic fibroblasts. *PLoS One* 12: e0187891.
55. Jochum W, Passegué E, Wagner EF (2001) AP-1 in mouse development and tumorigenesis. *Oncogene* 20:2401–2412.
56. Smith LM, et al. (1999) cJun overexpression in MCF-7 breast cancer cells produces a tumorigenic, invasive and hormone resistant phenotype. *Oncogene* 18:6063–6070.
57. Gee JM, Barroso AF, Ellis IO, Robertson JF, Nicholson RI (2000) Biological and clinical associations of c-jun activation in human breast cancer. *Int J Cancer* 89:177–186.
58. Heldin CH, Vanlandewijck M, Moustakas A (2012) Regulation of EMT by TGFβ in cancer. *FEBS Lett* 586:1959–1970.
59. Kingsley-Kallesen M, Luster TA, Rizzino A (2001) Transcriptional regulation of the transforming growth factor-beta2 gene in glioblastoma cells. *In Vitro Cell Dev Biol Anim* 37:684–690.
60. Schlingensiepen KH, et al. (2011) Transforming growth factor-beta 2 gene silencing with trabedersen (AP 12009) in pancreatic cancer. *Cancer Sci* 102:1193–1200.
61. Cui XP, et al. (2014) HOXA10 promotes cell invasion and MMP-3 expression via TGFβ2-mediated activation of the p38 MAPK pathway in pancreatic cancer cells. *Dig Dis Sci* 59:1442–1451.
62. Beisner J, et al. (2006) A novel functional polymorphism in the transforming growth factor-beta2 gene promoter and tumor progression in breast cancer. *Cancer Res* 66: 7554–7561.

A

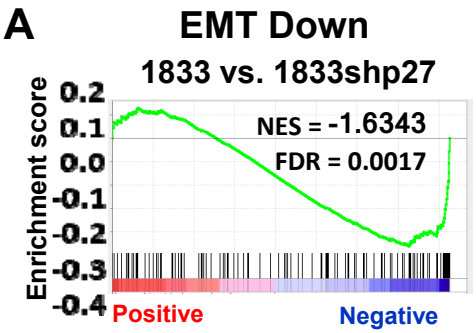

B

	1833 vs. 231			1833shp27 vs. 1833		
Gene ID	Fold Change	p value	q value	Fold Change	p value	q value
TGFB2	**1.40**	5.01.E-58	3.48.E-56	**0.68**	9.41.E-09	1.21.E-07
SNAI1	**1.63**	2.59.E-02	5.49.E-02	**0.85**	3.78.E-01	5.69.E-01
SNAI2	**1.16**	4.82.E-02	9.38.E-02	**0.31**	6.65.E-47	1.33.E-44
ZEB2	**1.20**	6.88.E-03	1.71.E-02	**0.73**	2.20.E-05	1.54.E-04
CDH1	**0.17**	3.12.E-09	2.02.E-08	**1.82**	1.00.E-03	4.57.E-03

C

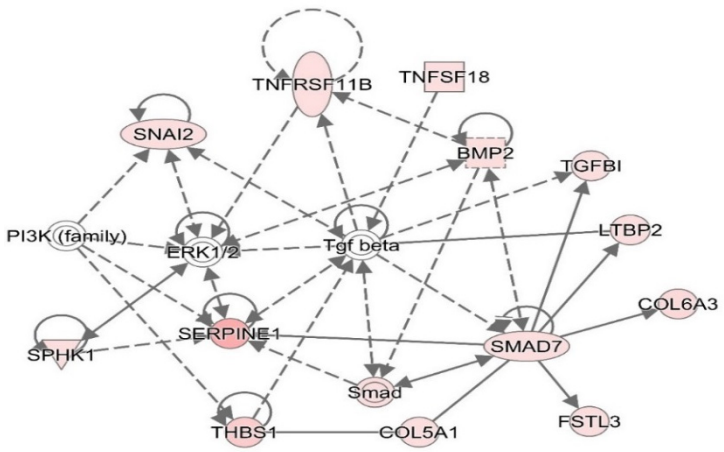

D

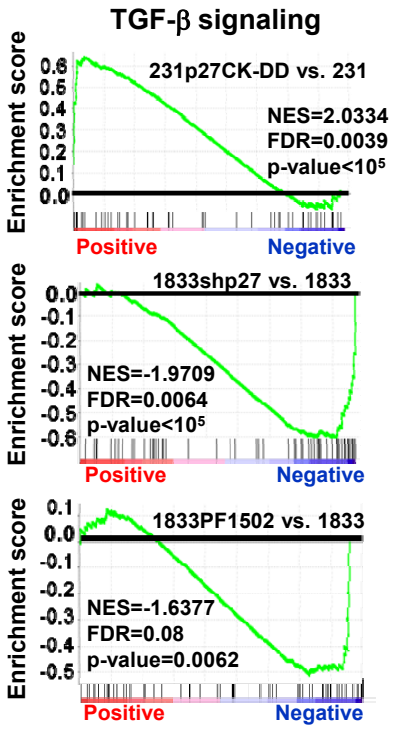

E

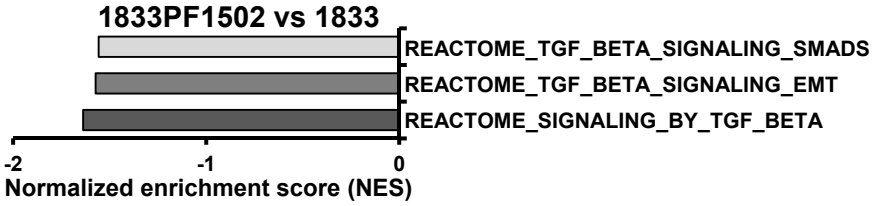

F

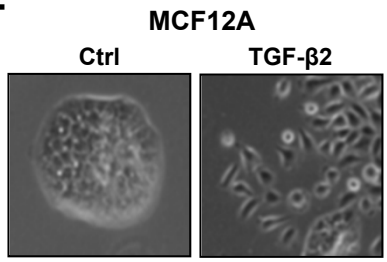

G

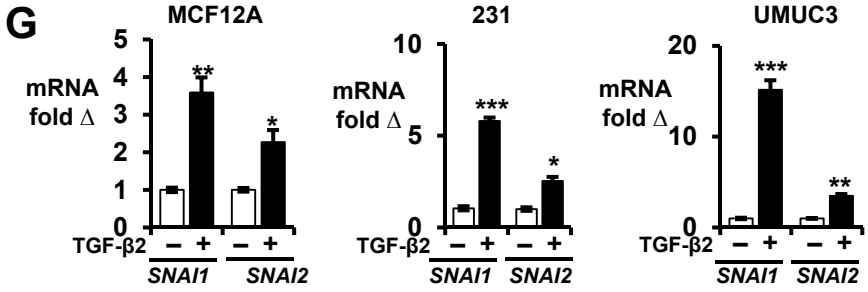

H

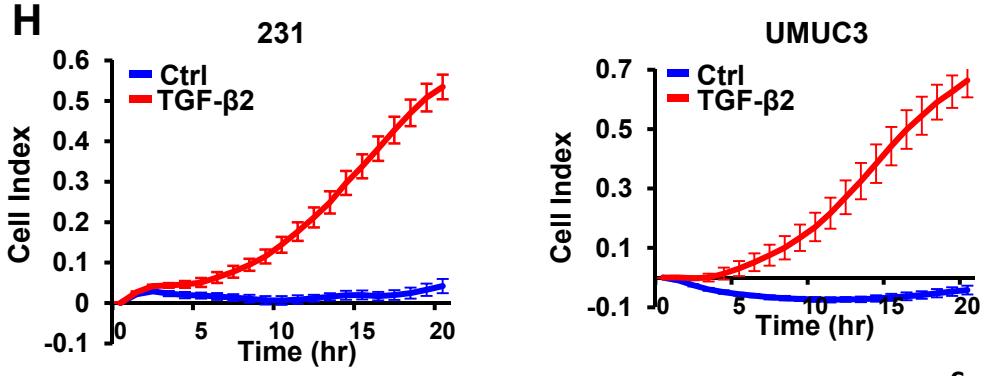

Supplemental Figure S1

www.pnas.org/cgi/doi/10.1073/pnas.1817415116

Supplemental Figure S1. EMT and TGF-β2 pathways are activated in 231p27CK-DD and 2833 (reference Figures 1 and 2).

(A) Enrichment plots of genes involved in EMT in 1833 vs. 1833shp27.

(B) Expression of EMT and *TGFB2* genes in RNA sequencing data.

(C) p27-dependent gene network. Ingenuity Pathway Analysis (IPA) showing the top signaling pathways in 82 genes upregulated by p27CK-DD expression in 231 and downregulated by p27 knockdown in 1833.

(D) Enrichment plots of genes involved in TGF-β signaling pathway in the indicated cell lines.

(E) Pathway analysis of TGF-β pathway genes differentially expressed in 1833 treated with PF1502 for 48 hours (1833PF1502) vs. 1833. NES; normalized enrichment score.

(F) TGF-β2 (10 ng/ml) for 16 hours induces a switch from epithelial to mesenchymal morphology, indicative of EMT.

(G) Effects of TGF-β2 (10 ng/ml) on EMT transcription factors (*SNAI1* and *SNAI2*) in MCF12A, 231 and UMUC3.

(H) Cell invasion assay after TGF-β2 treatment in 231 and UMUC3, analyzed by the Real-Time Cell Analysis Excelligence system. All graphs show mean +/- SEM from at least 3 biologic repeat and triplicate replicate assays, and p-values are from Student's T Test and ANOVA (*$p < 0.05$, **$p < 0.01$, ***$p < 0.001$).

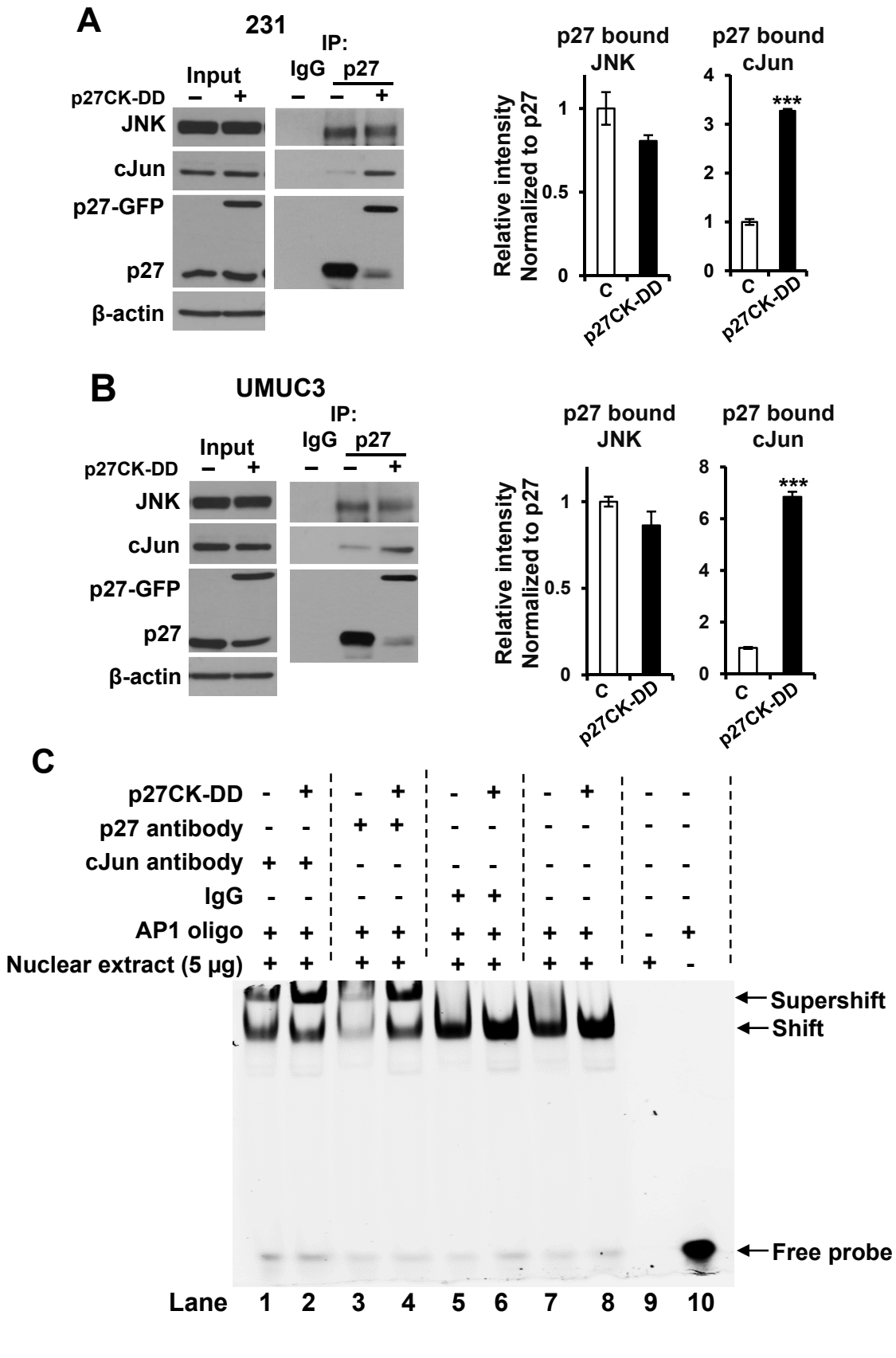

Supplemental Figure S2

Supplemental Figure S2. cJun binding to p27 is greater in p27CK-DD expressing cells (reference Figure 3).

(A and B) p27 immunoprecipitation/ Western (IP) shows associated cJun and JNK in 231, 231p27CK-DD (A), UMUC3, and UMUC3p27CK-DD (B). Graphs show quantitation of cJun associated p27 normalized to total precipitated p27 (endogenous and p27CK-DD) on right. All graphs show mean +/- SEM, Student's T Test (***$p < 0.001$).

(C) Electrophoretic mobility shift assay (EMSA) shows complex formation (shift) of AP1 oligo upon addition of 231 and 231p27CK-DD nuclear extract (lanes 1-8). Supershift reflects complex formation with cJun and p27 antibodies (lanes 1-4). IgG serves as nonspecific antibody control.

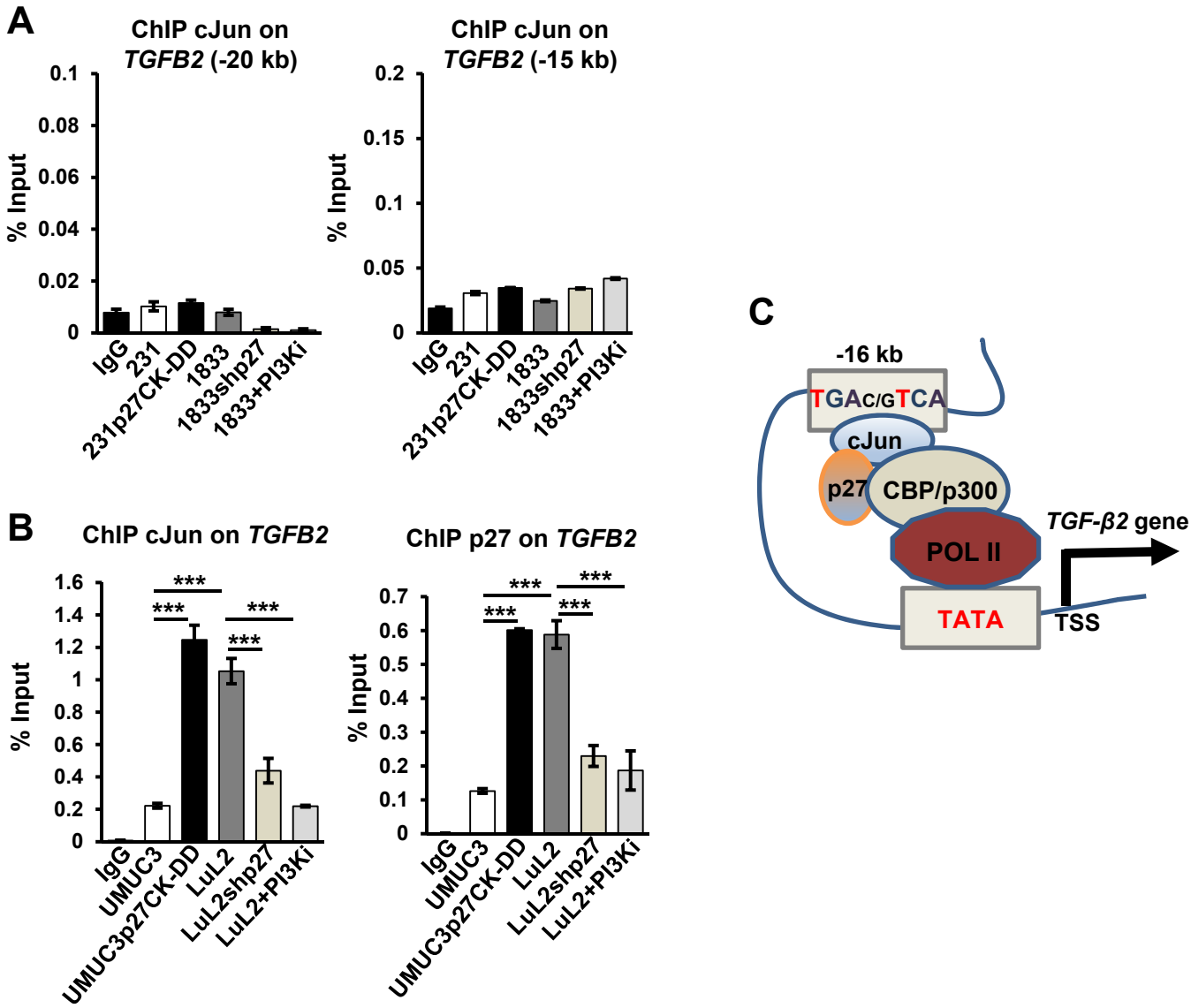

Supplemental Figure S3

Supplemental Figure S3. cJun and p27 bind the *TGFB2* gene (reference Figure 4).

(A) ChIP-qPCR assays using cJun and p27 antibodies, respectively, show lack of binding to -20 kb and -15 kb negative control sites upstream of *TGFB2* in the indicated cell lines.

(B) ChIP-qPCR assays show binding to a site -16 kb upstream of *TGFB2* in parental UMUC3 and metastatic UMUC3-LuL2 bladder cancer cell lines. PI3Ki indicates PI3K inhibitor (PF1502 at 250 nM for 48 hrs). All graphs show mean +/- SEM; p-values by ANOVA with post hoc comparisons (***$p < 0.001$).

(C) Schematic diagram showing the transcription complex of p27/cJun on *TGFB2*.

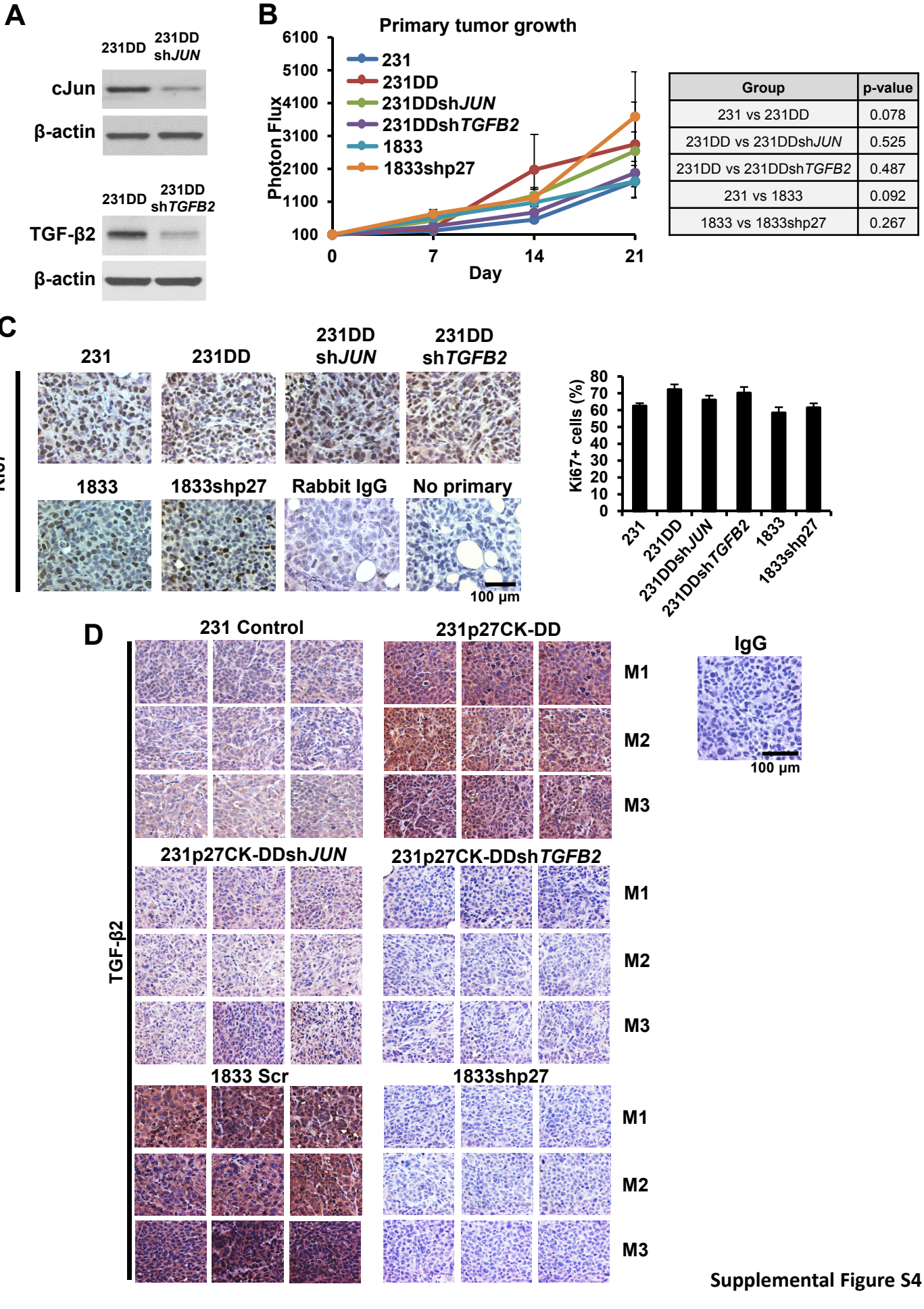

Group	p-value
231 vs 231DD	0.078
231DD vs 231DDsh*JUN*	0.525
231DD vs 231DDsh*TGFB2*	0.487
231 vs 1833	0.092
1833 vs 1833shp27	0.267

Supplemental Figure S4

Supplemental Figure S4. cJun and TGF-β2 are required for p27 dependent metastasis *in vivo* (reference Figure 5).

(A) Western blots for cJun and TGF-β2 in lines with or without shRNA depletion.

(B) Primary tumor growth measured as photon flux/time by IVIS did not differ significantly between groups. Mean tumor growth/time was compared using "compareGrowthCurves" function of the statmod software (http://bioinf.wehi.edu.au/software/compareCurves).

(C) Ki67 IHC staining is similar in different tumor groups. The mean % cells positive for Ki67 (+/- SEM) is graphed from >3 high power fields from at least 3 different primary tumors for each group.

(D) TGF-β2 IHC shows increased TGF-β2 in tumors formed from 1833 and 231p27CK-DD cells compared to 231 controls. Depletion of p27 depletion in 1833 and of cJun or TGF-β2 in 231p27CK-DD reduces TGF-β2 protein expression in metastatic tumors. Scale bar, 100 μm.

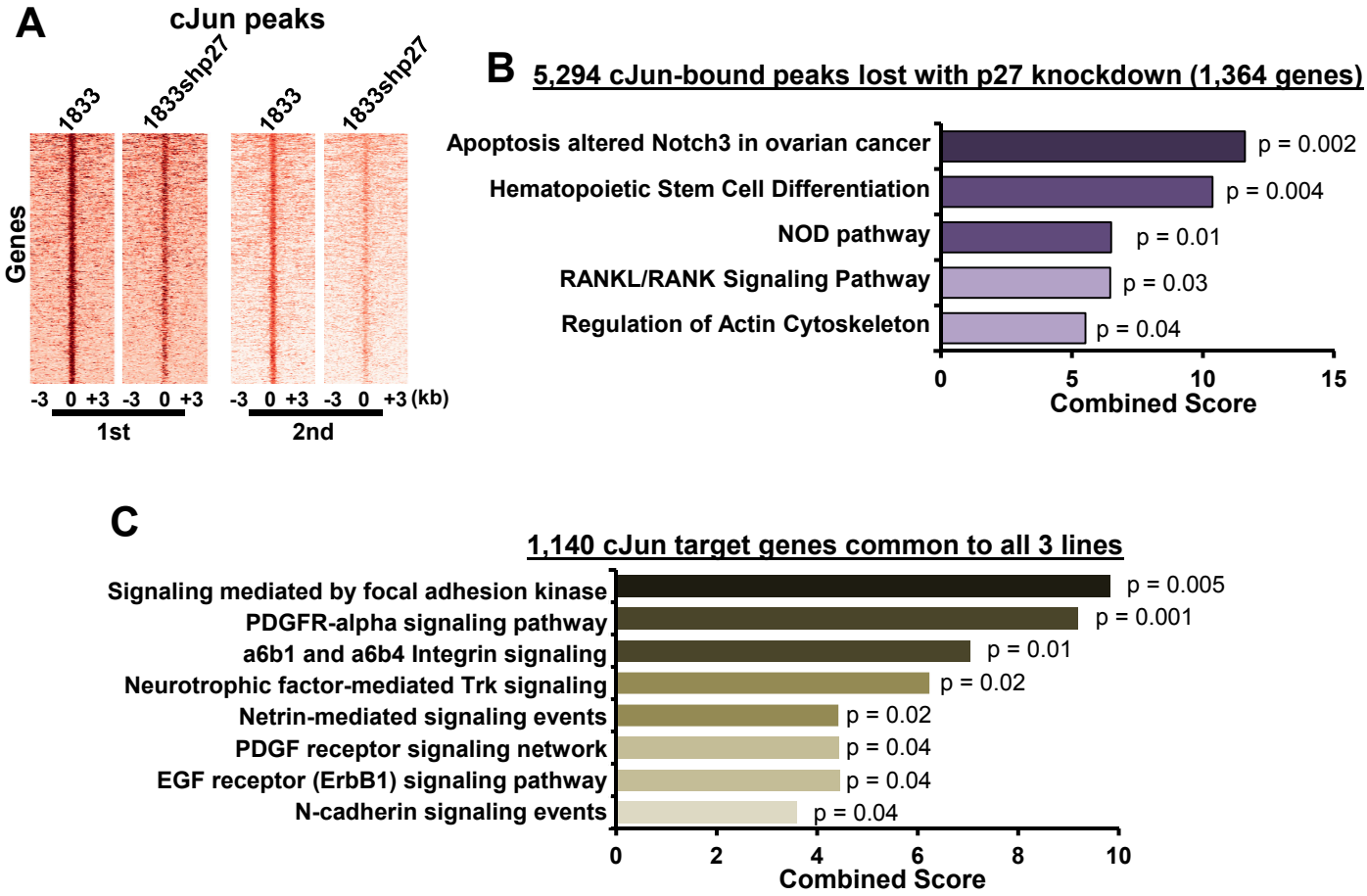

D

cJun binding motif

Cell	Motif	P-value	Target (%)	Match
231		1e-3133	32.79	JUN, AP-1
231DD		1e-6489	42.78	JUN, AP-1
1833		1e-1054	28.89	JUN, AP-1

p27 binding motif

Cell	Motif	P-value	Target (%)	Match
231		1e-2123	28.46	JUN, AP-1
231DD		1e-1965	35.88	JUN, AP-1
1833		1e-1822	37.55	JUN, AP-1

cJun/p27 binding motif

Cell	Motif	P-value	Target (%)	Match
231		1e-1841	33.5	JUN, AP-1
231DD		1e-2026	36.12	JUN, AP-1
1833		1e-961	35.72	JUN, AP-1

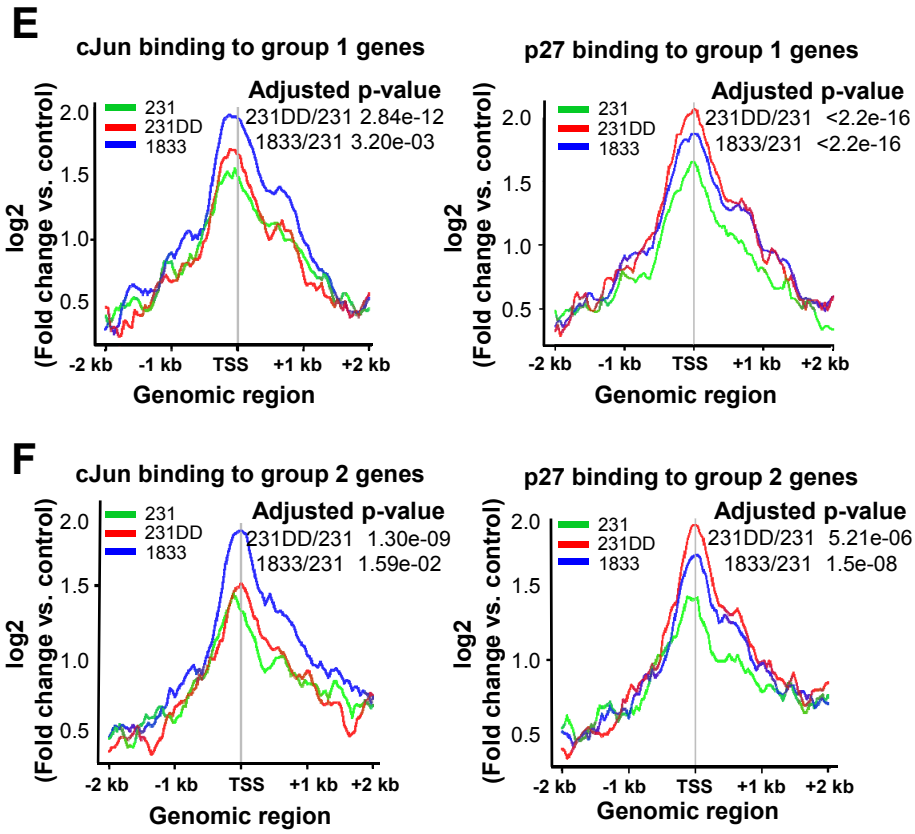

Supplemental Figure S5

Supplemental Figure S5. Genome-wide DNA binding of p27 and cJun (reference Figure 6).

(A) Binding heatmaps of cJun ChIP in 1833 and 1833shp27 from 2 independent ChIP-Seq assays.

(B) ENRICHR pathway analysis (WikiPathway 2016 database) of 1,364 cJun target genes from 5,294 cJun and p27 bound peaks that are lost upon p27 depletion in 1833 cells.

(C) Pathway analysis of 1,140 cJun target genes common to all of 231, 231DD, and 1833.

(D) Binding motif search (all binding sites) shows the cJun/AP-1 consensus motif is the top transcription motif bound by cJun only, p27 only, and cJun/p27 for each line.

(E and F) Graphs shows mean p27 and cJun binding to DNA in Group 1 (E) and Group 2 (F) genes (depicted in Figure 6H) in each of 231, 231p27CK-DD and 1833.

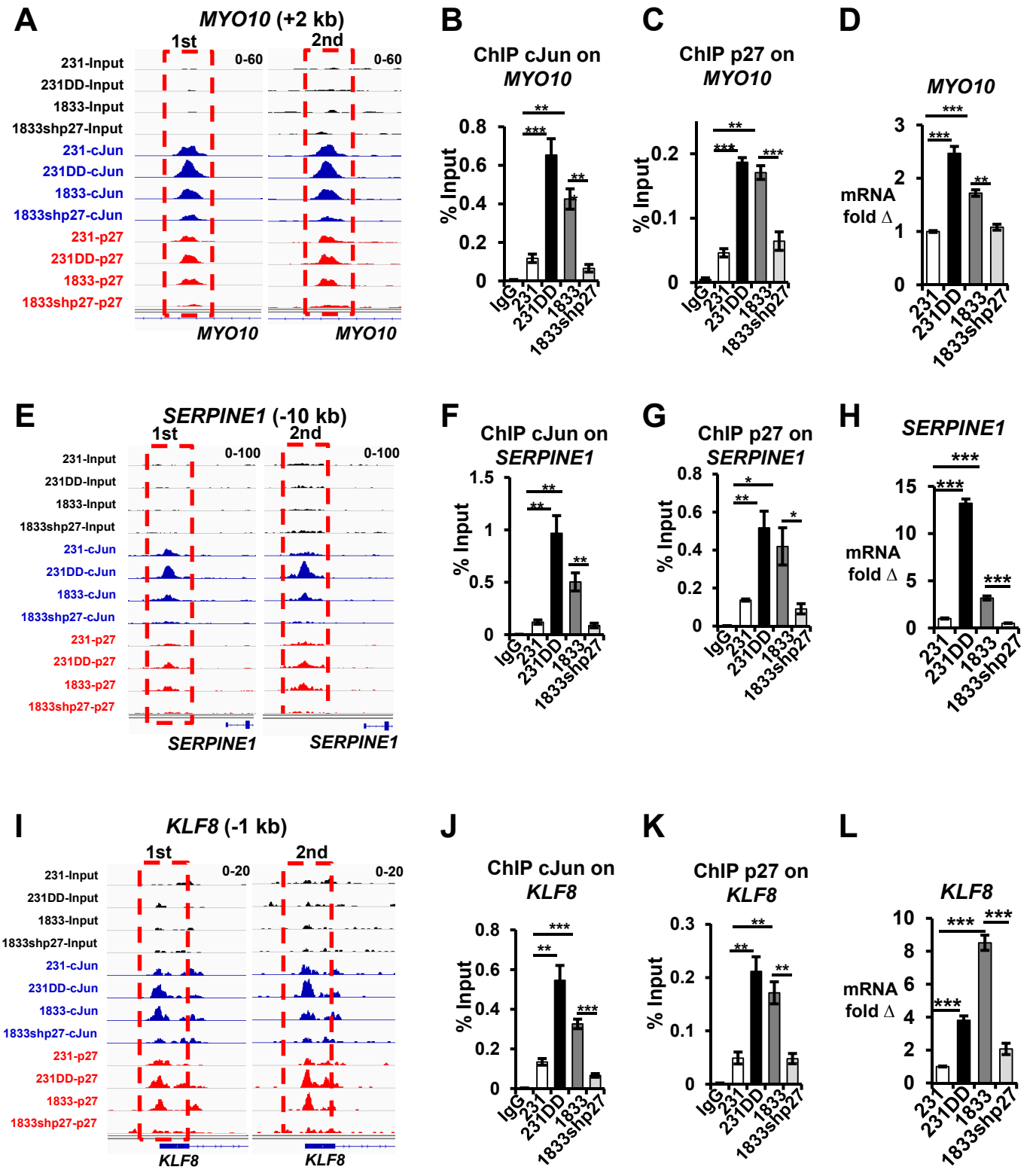

Supplemental Figure S6

Supplemental Figure S6. Validation of 3 cJun/p27 target genes identified by ChIP Seq (reference Figure 7).

(A, E and I) p27 and cJun binding to target genes, *MYO10* (A), *SERPINE1* (E) and *KLF8* (I), shown as IGV genome browser tracks.

(B-D) Validation of cJun/p27 binding to and expression of *MYO10*. ChIP-qPCR with cJun (B) and p27 antibodies (C) at +2 kb from the *MYO10* transcription start site. (D) The expression level of *MYO10* by qPCR in the indicated cell lines.

(F-H) Validation of cJun/p27 binding to and expression of *SERPINE1*. ChIP-qPCR with cJun (F) and p27 (G) antibodies and qPCR validation (H) in the indicated cell lines.

(J-L) ChIP-qPCR with cJun (J) and p27 (K) antibodies at -1 kb upstream of the *KLF8* TSS and pPCR of *KLF8* expression (L) in the indicated cell lines. All bar graphs show mean +/- SEM from at least 3 biologic repeat assays, and p-values were represented by ANOVA with post hoc comparisons (*$p < 0.05$, **$p < 0.01$, ***$p < 0.001$).

SUPPLEMENTAL TABLES

Supplemental Table S1. EMT core signature genes differentially regulated in p27 activated lines vs 231 and 1833shp2 (See Figure 1C).

	231DD vs. 231	231DD vs. 231	231DD vs. 231	1833 vs. 231	1833 vs. 231	1833 vs. 231	1833shp27 vs. 1833	1833shp27 vs. 1833	1833shp27 vs. 1833
Gene ID	**Fold Change**	**p value**	**q value**	**Fold Change**	**p value**	**q value**	**Fold Change**	**p value**	**q value**
CYP27B1	**0.98**	9.42.E-01	9.67.E-01	**1.04**	8.75.E-01	9.27.E-01	**1.17**	3.80.E-01	5.70.E-01
PI3	**0.84**	3.95.E-01	5.47.E-01	**2.13**	8.51.E-03	2.50.E-02	**3.84**	1.39.E-15	4.13.E-14
CKMT1B	**0.98**	7.93.E-01	NA	**1.03**	9.89.E-01	9.94.E-01	**1.17**	2.05.E-01	NA
MYO5C	**0.71**	3.12.E-02	7.46.E-02	**1.24**	4.11.E-02	9.87.E-02	**2.31**	8.69.E-33	8.80.E-31
THBD	**0.46**	3.81.E-26	1.15.E-24	**1.43**	2.25.E-06	1.25.E-05	**1.83**	1.93.E-13	4.64.E-12
GNAL	**0.76**	9.09.E-02	1.79.E-01	**1.18**	3.80.E-01	5.87.E-01	**2.21**	1.03.E-08	1.33.E-07
PLS1	**0.60**	4.43.E-19	8.83.E-18	**1.12**	5.27.E-02	1.22.E-01	**1.33**	2.13.E-05	1.50.E-04
COL17A1	**0.28**	5.21.E-70	5.65.E-68	**2.25**	2.53.E-29	8.38.E-28	**3.07**	2.40.E-62	6.81.E-60
HBEGF	**0.76**	2.90.E-08	2.35.E-07	**1.18**	1.04.E-03	3.71.E-03	**1.22**	1.07.E-04	6.26.E-04
PERP	**0.53**	1.47.E-35	6.02.E-34	**1.06**	3.10.E-01	5.07.E-01	**1.04**	5.41.E-01	7.13.E-01
SLPI	**0.47**	1.58.E-03	5.64.E-03	**1.96**	6.46.E-02	1.45.E-01	**1.85**	1.84.E-03	7.79.E-03
ITGB4	**0.77**	8.03.E-04	3.09.E-03	**4.71**	9.81.E-59	9.25.E-57	**6.94**	4.38.E-98	2.57.E-95
CXADR	**0.24**	9.13.E-29	3.01.E-27	**1.38**	4.25.E-03	1.34.E-02	**1.29**	2.50.E-02	7.14.E-02
S100A14	**0.86**	5.33.E-01	6.73.E-01	**1.26**	7.41.E-01	8.91.E-01	**1.03**	8.86.E-01	9.43.E-01
BDKRB2	**0.32**	1.80.E-05	9.66.E-05	**7.79**	9.05.E-05	3.94.E-04	**2.47**	8.51.E-06	6.52.E-05
IL1RN	**0.67**	4.67.E-02	NA	**8.48**	8.17.E-02	1.76.E-01	**1.06**	5.34.E-01	NA
IGFBP2	**0.82**	2.80.E-01	NA	**2.53**	4.60.E-01	6.67.E-01	**1.02**	8.71.E-01	NA
UCHL1	**0.98**	7.93.E-01	NA	**2.02**	8.04.E-01	8.91.E-01	**1.03**	6.50.E-01	NA
CLDN1	**0.37**	5.82.E-24	1.58.E-22	**1.10**	2.84.E-01	4.75.E-01	**1.09**	3.50.E-01	5.39.E-01
CAMK2B	**0.85**	5.24.E-01	6.65.E-01	**1.20**	7.59.E-01	8.91.E-01	**1.13**	5.25.E-01	7.02.E-01
TMEM40	**0.73**	2.33.E-01	3.73.E-01	**1.31**	6.30.E-01	8.09.E-01	**1.11**	5.88.E-01	7.50.E-01
RHBDF2	**0.78**	2.84.E-03	9.51.E-03	**1.25**	2.44.E-02	6.29.E-02	**1.19**	9.53.E-02	2.09.E-01
MST1R	**0.47**	4.54.E-14	6.56.E-13	**2.75**	3.27.E-19	5.96.E-18	**2.93**	2.28.E-23	1.33.E-21
SYK	**0.93**	5.39.E-01	NA	**1.88**	7.39.E-01	8.91.E-01	**1.02**	8.24.E-01	NA
SLC6A8	**0.90**	4.02.E-01	5.54.E-01	**1.39**	3.28.E-02	8.14.E-02	**1.25**	1.03.E-01	2.21.E-01
SLC6A8	**0.90**	4.02.E-01	5.54.E-01	**1.39**	3.28.E-02	8.14.E-02	**1.25**	1.03.E-01	2.21.E-01
EPB41L4B	**0.59**	2.97.E-19	6.04.E-18	**1.47**	3.94.E-11	3.77.E-10	**1.30**	1.68.E-04	9.42.E-04
ARHGAP25	**0.41**	2.78.E-05	1.45.E-04	**1.20**	4.41.E-01	6.46.E-01	**0.99**	9.61.E-01	9.83.E-01
LRRC1	**0.93**	3.14.E-01	4.63.E-01	**1.14**	6.46.E-02	1.45.E-01	**1.03**	7.15.E-01	8.39.E-01
BIK	**0.16**	2.36.E-24	6.55.E-23	**5.20**	1.82.E-17	2.93.E-16	**1.38**	8.26.E-02	1.87.E-01
DSG3	**0.78**	1.38.E-01	NA	**9.61**	1.40.E-01	2.75.E-01	**1.01**	8.55.E-01	NA
IL1B	**0.11**	1.04.E-185	5.99.E-183	**4.74**	1.31.E-100	2.78.E-98	**2.12**	2.46.E-22	1.33.E-20
NDRG1	**0.31**	1.06.E-124	2.84.E-122	**3.07**	8.39.E-90	1.46.E-87	**1.44**	5.25.E-11	9.57.E-10
KRT15	**0.48**	1.12.E-12	1.45.E-11	**2.31**	1.26.E-14	1.64.E-13	**1.43**	2.48.E-03	1.00.E-02
SERPINB1	**0.43**	5.82.E-65	5.18.E-63	**2.66**	3.69.E-76	4.90.E-74	**1.25**	4.54.E-04	2.29.E-03
GRHL2	**0.74**	1.95.E-01	3.27.E-01	**9.54**	5.45.E-02	1.25.E-01	**1.08**	4.64.E-01	NA
STAP2	**0.57**	1.36.E-11	1.59.E-10	**1.46**	1.46.E-05	7.20.E-05	**1.07**	4.45.E-01	6.31.E-01
TSPAN1	**0.52**	2.77.E-14	4.08.E-13	**3.31**	7.10.E-29	2.31.E-27	**1.87**	5.34.E-09	7.22.E-08
ALDH1A3	**0.35**	7.55.E-36	3.13.E-34	**3.91**	2.60.E-48	1.85.E-46	**2.80**	3.15.E-26	2.22.E-24
ST14	**0.44**	2.50.E-04	1.08.E-03	**3.58**	6.09.E-05	2.74.E-04	**1.24**	2.98.E-01	4.82.E-01
PRRG4	**0.77**	2.18.E-02	5.49.E-02	**2.03**	2.15.E-07	1.36.E-06	**1.44**	4.25.E-03	1.61.E-02
LMCD1	**2.42**	1.72.E-26	5.31.E-25	**0.74**	3.20.E-03	1.03.E-02	**0.88**	1.42.E-01	2.85.E-01
CTGF	**4.41**	2.25.E-153	7.89.E-151	**0.30**	2.09.E-76	2.79.E-74	**0.39**	1.21.E-62	3.48.E-60
STARD13	**2.54**	6.76.E-61	5.63.E-59	**0.52**	6.64.E-23	1.54.E-21	**0.57**	1.85.E-20	8.45.E-19

MMP2	**9.72**	4.64.E-20	9.86.E-19	**0.07**	2.24.E-03	7.49.E-03	**0.52**	3.65.E-04	1.89.E-03
LTBP2	**2.59**	1.28.E-69	1.36.E-67	**0.41**	5.50.E-55	4.68.E-53	**0.37**	1.98.E-46	3.88.E-44
PRR16	**1.17**	3.16.E-02	7.54.E-02	**0.57**	3.58.E-15	4.87.E-14	**0.38**	1.41.E-36	1.84.E-34
FILIP1L	**1.26**	1.86.E-03	6.52.E-03	**0.71**	2.26.E-06	1.25.E-05	**0.54**	1.41.E-15	4.19.E-14
TRAM2	**1.67**	7.16.E-24	1.94.E-22	**0.74**	1.65.E-06	9.31.E-06	**0.64**	8.89.E-16	2.71.E-14
TPM1	**2.42**	3.45.E-87	5.33.E-85	**0.79**	5.37.E-06	2.82.E-05	**0.36**	1.99.E-73	6.73.E-71
TAGLN	**9.97**	5.62.E-272	7.74.E-269	**0.99**	9.31.E-01	9.70.E-01	**0.59**	1.15.E-07	1.25.E-06
NR2F1	**2.69**	7.42.E-36	3.09.E-34	**0.93**	4.87.E-01	6.94.E-01	**0.52**	3.22.E-10	5.24.E-09
FBN1	**2.10**	5.28.E-28	1.70.E-26	**0.92**	2.79.E-01	4.69.E-01	**0.64**	9.05.E-19	3.63.E-17

Supplemental Table S2. 82 genes upregulated in 231p27CK-DD vs 231 and decreased by p27 depletion in 1833 by RNA sequencing data (See Figure 2A).						
	231DD vs. 231	231DD vs. 231	231DD vs. 231	1833shp27 vs. 1833	1833shp27 vs. 1833	1833shp27 vs. 1833
Gene ID	Fold Change	p value	q value	Fold Change	p value	q value
PDGFB	**25.18**	2.09E-116	5.12E-114	**0.07**	5.73E-63	1.68E-60
AMTN	**22.35**	3.47E-72	3.93E-70	**0.36**	3.96E-07	3.86E-06
CGB8	**13.25**	3.57E-42	1.78E-40	**0.24**	1.58E-12	3.38E-11
AMOT	**12.59**	2.68E-45	1.49E-43	**0.27**	1.81E-31	1.70E-29
LINC01583	**12.46**	1.95E-34	7.65E-33	**0.44**	9.53E-06	7.22E-05
PMEPA1	**10.91**	1.95E-34	7.65E-33	**0.10**	3.73E-192	1.10E-188
SERPINE1	**9.84**	5.62E-272	7.74E-269	**0.14**	2.18E-212	9.60E-209
COL1A1	**9.10**	4.34E-68	4.34E-66	**0.31**	1.84E-18	7.21E-17
LOC100507431	**8.57**	2.99E-36	1.26E-34	**0.50**	5.35E-04	2.65E-03
C4orf26	**7.70**	8.42E-78	1.07E-75	**0.31**	1.08E-10	1.91E-09
NKILA	**6.56**	2.14E-53	1.49E-51	**0.39**	9.48E-07	8.58E-06
FLRT2	**6.50**	4.72E-143	1.51E-140	**0.36**	5.80E-61	1.60E-58
AMIGO2	**6.36**	4.72E-143	1.51E-140	**0.20**	1.82E-197	6.41E-194
ANGPTL4	**6.22**	4.04E-142	1.27E-139	**0.22**	4.84E-43	8.45E-41
GPR132	**6.20**	3.33E-33	1.26E-31	**0.29**	2.51E-23	1.45E-21
THBS1	**5.87**	8.35E-259	9.34E-256	**0.17**	3.96E-160	5.81E-157
MYO7B	**5.86**	3.11E-93	5.45E-91	**0.43**	3.28E-20	1.45E-18
EDN1	**5.56**	1.99E-231	1.70E-228	**0.21**	5.21E-154	7.06E-151
FERMT1	**5.18**	7.14E-191	4.41E-188	**0.48**	8.24E-29	6.82E-27
MIR181A2HG	**5.05**	5.31E-22	1.27E-20	**0.46**	1.47E-05	1.07E-04
LBH	**4.85**	5.61E-161	2.14E-158	**0.33**	4.46E-20	1.96E-18
ABAT	**4.60**	4.85E-16	8.02E-15	**0.39**	2.91E-06	2.42E-05
COL4A1	**4.60**	1.40E-182	7.35E-180	**0.23**	4.58E-161	7.34E-158
HHIP	**4.59**	2.94E-12	3.66E-11	**0.26**	6.78E-49	1.41E-46
VGLL3	**4.53**	1.25E-74	1.48E-72	**0.49**	2.06E-09	2.96E-08
HHIP-AS1	**4.46**	1.51E-32	5.60E-31	**0.30**	7.29E-29	6.06E-27
COL6A3	**4.42**	1.10E-67	1.07E-65	**0.39**	9.65E-36	1.18E-33
CTGF	**4.41**	2.25E-153	7.89E-151	**0.39**	1.21E-62	3.48E-60
AGMO	**4.25**	1.45E-14	2.19E-13	**0.39**	4.27E-06	3.45E-05
LOC79160	**4.22**	1.19E-14	1.81E-13	**0.24**	3.32E-31	3.05E-29
MYH16	**4.05**	3.14E-27	9.89E-26	**0.18**	4.61E-32	4.47E-30
MARCH4	**4.05**	8.77E-55	6.21E-53	**0.46**	1.58E-15	4.66E-14
PIK3IP1	**4.04**	4.31E-52	2.90E-50	**0.46**	1.96E-10	3.31E-09
ADTRP	**4.01**	9.89E-48	5.82E-46	**0.14**	3.71E-104	2.73E-101
LINC00452	**3.97**	3.87E-44	2.06E-42	**0.30**	2.15E-29	1.81E-27
MYCT1	**3.88**	8.81E-28	2.80E-26	**0.24**	2.14E-17	7.62E-16
CDS1	**3.84**	2.79E-23	7.36E-22	**0.50**	2.09E-04	1.14E-03

KCNJ15	**3.79**	1.41E-10	1.49E-09	**0.38**	4.93E-09	6.70E-08
SMAD7	**3.68**	4.03E-81	5.59E-79	**0.38**	6.05E-29	5.06E-27
FSTL3	**3.58**	1.55E-76	1.93E-74	**0.35**	3.34E-30	2.91E-28
TUBA4A	**3.49**	3.96E-173	1.82E-170	**0.38**	1.55E-63	4.64E-61
TNFSF18	**3.46**	3.00E-09	2.75E-08	**0.31**	4.54E-19	1.87E-17
WNT5B	**3.39**	1.63E-101	3.24E-99	**0.50**	9.90E-22	5.06E-20
LSAMP	**3.38**	1.37E-15	2.20E-14	**0.39**	6.90E-09	9.14E-08
HTR2C	**3.37**	1.75E-06	1.12E-05	**0.25**	1.14E-20	5.35E-19
NRXN3	**3.35**	1.26E-10	1.34E-09	**0.35**	3.12E-14	8.17E-13
EPHA4	**3.19**	1.40E-91	2.39E-89	**0.46**	1.99E-25	1.32E-23
LOC101059948	**3.16**	2.23E-07	1.62E-06	**0.50**	3.42E-04	1.79E-03
ADAM19	**3.14**	6.22E-64	5.46E-62	**0.33**	9.14E-65	2.93E-62
SAP30L-AS1	**3.08**	8.84E-38	3.89E-36	**0.41**	3.27E-19	1.36E-17
TNFRSF11B	**3.05**	5.71E-51	3.68E-49	**0.39**	8.55E-15	2.38E-13
DNAJB2	**3.03**	1.51E-97	2.88E-95	**0.48**	7.39E-25	4.79E-23
MUM1L1	**3.00**	1.23E-05	6.81E-05	**0.46**	8.81E-08	9.78E-07
NUAK1	**2.98**	3.38E-135	9.60E-133	**0.30**	4.42E-117	4.58E-114
COL5A1	**2.92**	2.06E-62	1.75E-60	**0.37**	1.79E-40	2.77E-38
FST	**2.91**	3.31E-95	6.05E-93	**0.35**	9.94E-80	3.81E-77
NOG	**2.84**	3.88E-54	2.74E-52	**0.41**	1.64E-27	1.25E-25
GALNT10	**2.82**	8.42E-125	2.28E-122	**0.40**	1.17E-67	3.81E-65
JAG1	**2.73**	1.49E-75	1.79E-73	**0.46**	2.14E-59	5.80E-57
ADAMTS6	**2.71**	3.27E-57	2.40E-55	**0.31**	3.59E-62	1.01E-59
CYP7B1	**2.71**	1.61E-04	7.23E-04	**0.44**	1.39E-05	1.02E-04
TUFT1	**2.69**	1.07E-87	1.69E-85	**0.37**	8.83E-45	1.61E-42
NRP2	**2.67**	7.20E-44	3.79E-42	**0.30**	4.98E-75	1.72E-72
LTBP2	**2.59**	1.28E-69	1.36E-67	**0.37**	1.98E-46	3.88E-44
LINC01111	**2.58**	5.06E-07	3.50E-06	**0.33**	2.15E-09	3.07E-08
COL4A2	**2.58**	2.31E-53	1.60E-51	**0.44**	1.34E-26	9.63E-25
GPNMB	**2.56**	5.15E-07	3.55E-06	**0.40**	4.07E-06	3.30E-05
SNAI2	**2.53**	1.09E-66	1.02E-64	**0.31**	6.65E-47	1.33E-44
NNMT	**2.48**	1.44E-42	7.27E-41	**0.24**	8.79E-50	1.87E-47
LPCAT2	**2.46**	1.03E-42	5.20E-41	**0.32**	7.71E-28	6.02E-26
GALNT16	**2.45**	2.27E-09	2.11E-08	**0.40**	7.80E-10	1.19E-08
SPHK1	**2.45**	1.53E-49	9.63E-48	**0.44**	1.22E-23	7.30E-22
IGFBP7	**2.44**	1.76E-78	2.28E-76	**0.48**	6.07E-38	8.63E-36
TPM1	**2.42**	3.45E-87	5.33E-85	**0.36**	1.99E-73	6.73E-71
ARHGEF18	**2.41**	9.41E-105	1.96E-102	**0.45**	1.05E-33	1.14E-31
RND1	**2.38**	1.84E-06	1.17E-05	**0.45**	5.85E-05	3.68E-04
LOC101927497	**2.29**	3.53E-08	2.84E-07	**0.40**	2.88E-09	4.05E-08
HIC1	**2.19**	1.33E-05	7.32E-05	**0.48**	3.07E-05	2.06E-04

BMP2	**2.17**	8.03E-04	3.09E-03	**0.29**	1.04E-26	7.56E-25
STK32A	**2.14**	3.56E-03	1.16E-02	**0.46**	1.06E-04	6.25E-04
LINC01179	**2.08**	2.04E-04	8.96E-04	**0.25**	5.43E-15	1.53E-13
TGFBI	**2.05**	3.38E-43	1.73E-41	**0.34**	1.37E-50	3.03E-48

Supplemental Table S3. TGF-β signaling signature genes regulated by p27 in RNA sequencing data (See Figure 2D).						
	231DD vs. 231	231DD vs. 231	231DD vs. 231	1833shp27 vs. 1833	1833shp27 vs. 1833	1833shp27 vs. 1833
TGF-β signature	Fold Change	p value	q value	Fold Change	p value	q value
PMEPA1	**10.91**	1.95.E-34	7.65.E-33	**0.10**	3.73.E-192	1.10.E-188
SERPINE1	**9.84**	5.62.E-272	7.74.E-269	**0.14**	2.18.E-212	9.60.E-209
JUNB	**7.17**	1.14.E-113	2.66.E-111	**0.92**	6.71.E-01	8.10.E-01
SMAD7	**3.68**	4.03.E-81	5.59.E-79	**0.38**	6.05.E-29	5.06.E-27
NCOR2	**2.43**	5.13.E-22	1.23.E-20	**0.82**	2.10.E-01	3.79.E-01
ARHGEF18	**2.41**	9.41.E-105	1.96.E-102	**0.45**	1.05.E-33	1.14.E-31
SKIL	**2.01**	2.62.E-33	9.97.E-32	**0.55**	2.05.E-16	6.61.E-15
TGFB1	**1.91**	1.59.E-20	3.46.E-19	**0.84**	5.41.E-02	1.34.E-01
SMURF1	**1.81**	4.58.E-31	1.62.E-29	**0.75**	2.75.E-07	2.77.E-06
FURIN	**1.60**	3.25.E-23	8.49.E-22	**0.53**	3.75.E-18	1.42.E-16
MYC	**1.59**	1.50.E-24	4.20.E-23	**0.75**	5.16.E-06	4.12.E-05
SMURF2	**1.53**	6.65.E-26	1.99.E-24	**0.72**	7.21.E-10	1.11.E-08
TGFB2	**1.46**	8.99.E-16	1.46.E-14	**0.68**	9.41.E-09	1.21.E-07
SMAD4	**1.31**	4.81.E-08	3.82.E-07	**0.68**	1.43.E-11	2.78.E-10
FKBP1A	**1.21**	2.68.E-04	1.15.E-03	**0.81**	1.63.E-04	9.13.E-04
UBE2D3	**1.20**	2.01.E-03	6.97.E-03	**0.87**	1.55.E-02	4.80.E-02
PARP1	**1.16**	3.44.E-03	1.12.E-02	**0.92**	7.20.E-02	1.68.E-01
E2F4	**1.09**	9.00.E-02	1.78.E-01	**0.78**	7.66.E-06	5.91.E-05
MEN1	**1.04**	5.66.E-01	7.00.E-01	**0.79**	9.74.E-04	4.47.E-03
ZFYVE9	**0.91**	8.36.E-02	1.67.E-01	**1.08**	2.06.E-01	3.74.E-01
UCHL5	**0.86**	5.16.E-02	1.13.E-01	**1.08**	2.86.E-01	4.68.E-01
RBL1	**0.85**	1.71.E-03	6.08.E-03	**1.13**	3.31.E-02	9.01.E-02
CCNC	**0.83**	3.65.E-03	1.18.E-02	**1.07**	3.41.E-01	5.30.E-01
TFDP1	**0.82**	3.61.E-05	1.84.E-04	**1.09**	9.56.E-02	2.09.E-01
TGFBR2	**0.80**	2.23.E-04	9.70.E-04	**1.44**	4.14.E-14	1.07.E-12
PARD6A	**0.76**	1.17.E-02	3.25.E-02	**1.32**	1.76.E-02	5.34.E-02
SMAD3	**0.69**	1.62.E-10	1.71.E-09	**1.16**	4.21.E-03	1.60.E-02
PPP1CB	**0.66**	1.16.E-10	1.24.E-09	**1.17**	1.06.E-02	3.51.E-02
WWTR1	**0.64**	1.53.E-11	1.76.E-10	**1.30**	6.51.E-06	5.07.E-05
TGFBR1	**0.61**	8.62.E-27	2.67.E-25	**1.29**	1.23.E-05	9.11.E-05

Supplemental Table S4. Differential expression of 590 genes commonly bound by cJun/p27 in all lines (See Figure 6H and 7A).

	231DD vs. 231	231DD vs. 231	231DD vs. 231	1833 vs. 231	1833 vs. 231	1833 vs. 231	1833shp27 vs. 1833	1833shp27 vs. 1833	1833shp27 vs. 1833
Gene ID	**Fold Change**	**p value**	**q value**	**Fold Change**	**p value**	**q value**	**Fold Change**	**p value**	**q value**
AMTN	**22.35**	3.47.E-72	3.93.E-70	**2.03**	8.51.E-03	2.06.E-02	**0.36**	3.96.E-07	3.86.E-06
LINC02551	**8.57**	2.99.E-36	1.26.E-34	**1.42**	1.64.E-01	2.62.E-01	**0.50**	5.35.E-04	2.65.E-03
LOC100507487	**7.83**	8.56.E-61	7.03.E-59	**2.86**	1.16.E-10	8.52.E-10	**1.58**	4.89.E-05	3.14.E-04
THBS1	**5.87**	8.35.E-259	9.34.E-256	**1.80**	2.49.E-16	2.97.E-15	**0.17**	3.96.E-160	5.81.E-157
KCNA7	**4.04**	7.47.E-08	5.80.E-07	**2.39**	4.26.E-03	1.11.E-02	**0.53**	1.05.E-03	4.79.E-03
LINC00452	**3.97**	3.87.E-44	2.06.E-42	**3.49**	8.34.E-31	2.34.E-29	**0.30**	2.15.E-29	1.81.E-27
MXRA8	**3.40**	1.24.E-47	7.25.E-46	**1.73**	2.23.E-07	1.15.E-06	**1.10**	3.51.E-01	5.41.E-01
NFATC4	**2.92**	7.92.E-13	1.04.E-11	**0.87**	5.02.E-01	6.21.E-01	**4.26**	2.99.E-27	2.23.E-25
MYO10	**2.72**	1.44.E-32	5.34.E-31	**2.07**	1.52.E-17	1.97.E-16	**0.69**	2.57.E-11	4.80.E-10
PDGFC	**2.59**	2.45.E-97	4.61.E-95	**2.47**	1.26.E-78	1.36.E-76	**0.56**	2.29.E-28	1.86.E-26
PLEK2	**2.51**	1.04.E-57	7.77.E-56	**3.24**	5.39.E-108	9.95.E-106	**0.55**	3.01.E-22	1.61.E-20
ZFP69B	**2.43**	7.26.E-20	1.52.E-18	**1.86**	6.50.E-09	4.04.E-08	**0.79**	1.52.E-02	4.74.E-02
SOX4	**2.39**	1.80.E-42	9.06.E-41	**0.92**	2.85.E-01	4.06.E-01	**0.63**	1.51.E-07	1.60.E-06
LTBP4	**2.31**	9.06.E-35	3.60.E-33	**1.52**	5.68.E-04	1.76.E-03	**1.08**	6.87.E-01	8.20.E-01
SH3BP5L	**2.27**	6.58.E-59	5.19.E-57	**1.06**	3.29.E-01	4.52.E-01	**0.68**	6.14.E-09	8.20.E-08
PXDC1	**2.25**	4.79.E-65	4.31.E-63	**1.04**	4.29.E-01	5.53.E-01	**0.58**	6.78.E-17	2.31.E-15
MYOM3	**2.22**	5.54.E-05	2.72.E-04	**2.01**	7.99.E-04	2.41.E-03	**0.88**	4.25.E-01	6.13.E-01
TRPC3	**2.20**	1.77.E-06	1.13.E-05	**1.18**	4.02.E-01	5.27.E-01	**1.03**	8.64.E-01	9.31.E-01
TINAGL1	**2.20**	1.54.E-57	1.14.E-55	**0.46**	2.09.E-32	6.25.E-31	**0.92**	2.55.E-01	4.35.E-01
LOC101928279	**2.03**	6.77.E-04	2.65.E-03	**5.04**	3.86.E-18	5.25.E-17	**1.11**	4.30.E-01	6.17.E-01
LY6G5C	**2.03**	2.26.E-03	7.76.E-03	**2.78**	1.39.E-05	5.66.E-05	**1.06**	7.20.E-01	8.42.E-01
PLAU	**2.00**	2.88.E-66	2.65.E-64	**1.02**	6.66.E-01	7.63.E-01	**0.68**	1.17.E-13	2.88.E-12
FOXO6	**1.99**	5.32.E-03	1.64.E-02	**1.06**	8.44.E-01	8.95.E-01	**1.02**	9.10.E-01	9.54.E-01
ZFP36L1	**1.98**	8.95.E-23	2.27.E-21	**2.07**	8.64.E-26	1.87.E-24	**0.55**	1.12.E-20	5.23.E-19
EGFR-AS1	**1.88**	2.49.E-06	1.55.E-05	**2.63**	1.64.E-13	1.60.E-12	**0.78**	3.02.E-02	8.36.E-02
EPHB3	**1.85**	4.77.E-04	1.93.E-03	**0.28**	1.64.E-06	7.60.E-06	**1.57**	2.56.E-02	7.28.E-02
MICALCL	**1.85**	4.48.E-04	1.82.E-03	**1.59**	1.47.E-02	3.35.E-02	**0.54**	3.85.E-04	1.98.E-03
LINC00513	**1.84**	8.92.E-05	4.20.E-04	**3.12**	1.18.E-14	1.25.E-13	**0.79**	4.30.E-02	1.11.E-01
LINC01561	**1.82**	6.41.E-04	2.52.E-03	**0.72**	1.42.E-01	2.32.E-01	**0.62**	1.82.E-02	5.50.E-02
DNLZ	**1.77**	3.87.E-09	3.50.E-08	**0.92**	5.52.E-01	6.66.E-01	**1.03**	7.93.E-01	8.88.E-01
LINC01137	**1.75**	1.84.E-07	1.36.E-06	**1.38**	8.91.E-03	2.15.E-02	**0.45**	1.72.E-10	2.93.E-09
BEND7	**1.68**	1.33.E-13	1.86.E-12	**1.12**	1.46.E-01	2.38.E-01	**0.95**	5.02.E-01	6.83.E-01
SEMA7A	**1.68**	4.09.E-21	9.21.E-20	**0.86**	1.11.E-02	2.61.E-02	**0.92**	2.03.E-01	3.71.E-01
CCDC80	**1.67**	2.28.E-13	3.11.E-12	**1.10**	2.00.E-01	3.06.E-01	**0.42**	1.45.E-44	2.61.E-42
RUNX1	**1.66**	1.29.E-10	1.37.E-09	**1.37**	3.68.E-04	1.18.E-03	**0.88**	5.55.E-02	1.37.E-01
CCDC124	**1.65**	3.34.E-17	5.89.E-16	**1.18**	4.10.E-02	8.15.E-02	**0.81**	1.88.E-01	3.49.E-01
OLFM2	**1.64**	4.77.E-02	1.06.E-01	**1.74**	4.09.E-02	8.14.E-02	**0.65**	3.29.E-02	8.97.E-02
CAP2	**1.63**	2.72.E-20	5.87.E-19	**1.06**	3.39.E-01	4.63.E-01	**0.75**	2.68.E-06	2.25.E-05
F13A1	**1.61**	5.17.E-04	2.08.E-03	**1.38**	3.69.E-02	7.45.E-02	**0.60**	4.95.E-04	2.47.E-03
LOC101929705	**1.59**	1.50.E-03	5.38.E-03	**0.69**	4.09.E-02	8.15.E-02	**1.26**	1.78.E-01	3.36.E-01
ELK3	**1.58**	2.89.E-17	5.11.E-16	**1.79**	7.96.E-28	1.92.E-26	**0.86**	1.65.E-03	7.08.E-03
SFT2D3	**1.58**	1.58.E-06	1.01.E-05	**1.39**	1.61.E-03	4.59.E-03	**1.00**	9.87.E-01	9.94.E-01
SFN	**1.57**	2.07.E-18	3.94.E-17	**0.93**	2.88.E-01	4.09.E-01	**1.01**	8.82.E-01	9.41.E-01
MICAL3	**1.57**	2.64.E-11	2.98.E-10	**1.10**	2.02.E-01	3.08.E-01	**1.07**	3.49.E-01	5.39.E-01
COL7A1	**1.57**	3.39.E-12	4.19.E-11	**0.56**	3.25.E-13	3.08.E-12	**0.28**	3.37.E-58	8.87.E-56
KLHL21	**1.56**	7.45.E-17	1.29.E-15	**1.74**	2.06.E-19	3.06.E-18	**1.13**	7.15.E-02	1.67.E-01

INHBE	**1.55**	8.45.E-02	1.69.E-01	**3.66**	2.19.E-07	1.13.E-06	**0.41**	3.29.E-06	2.72.E-05
SYNPO	**1.55**	1.64.E-06	1.05.E-05	**0.99**	9.02.E-01	9.35.E-01	**0.68**	2.53.E-05	1.74.E-04
BEST3	**1.55**	2.64.E-02	6.46.E-02	**1.76**	5.47.E-03	1.39.E-02	**0.80**	1.75.E-01	3.31.E-01
MIR392S	**1.54**	6.64.E-02	1.39.E-01	**1.62**	8.57.E-02	1.53.E-01	**0.90**	5.40.E-01	7.12.E-01
NBL1	**1.53**	1.08.E-01	2.05.E-01	**1.35**	3.23.E-01	4.46.E-01	**0.95**	7.95.E-01	8.89.E-01
LOC440028	**1.51**	8.34.E-03	2.43.E-02	**2.53**	8.04.E-10	5.50.E-09	**1.27**	3.68.E-02	9.78.E-02
SMG7-AS1	**1.51**	3.99.E-02	9.14.E-02	**1.43**	1.00.E-01	1.74.E-01	**1.16**	4.04.E-01	5.93.E-01
LOC100505658	**1.51**	1.03.E-01	1.97.E-01	**1.83**	2.62.E-02	5.56.E-02	**1.11**	5.85.E-01	7.47.E-01
HRH1	**1.51**	2.74.E-17	4.87.E-16	**1.11**	5.00.E-02	9.70.E-02	**0.99**	8.39.E-01	9.17.E-01
NDUFA4L2	**1.49**	1.18.E-01	2.19.E-01	**1.55**	1.31.E-01	2.18.E-01	**0.92**	6.78.E-01	8.15.E-01
IGFBP3	**1.49**	3.06.E-19	6.20.E-18	**0.85**	2.44.E-02	5.21.E-02	**0.40**	3.43.E-36	4.28.E-34
TMC7	**1.49**	1.79.E-04	7.96.E-04	**1.88**	3.98.E-09	2.55.E-08	**0.92**	3.71.E-01	5.61.E-01
DISC1	**1.48**	1.17.E-01	2.18.E-01	**1.63**	7.69.E-02	1.39.E-01	**1.41**	7.07.E-02	1.66.E-01
SLC7A7	**1.48**	4.51.E-04	1.83.E-03	**0.50**	2.87.E-06	1.28.E-05	**0.98**	9.24.E-01	9.62.E-01
GSTO2	**1.47**	5.33.E-02	1.16.E-01	**2.77**	1.27.E-07	6.74.E-07	**0.82**	1.97.E-01	3.61.E-01
MIR199A1	**1.47**	9.97.E-02	1.92.E-01	**1.82**	3.92.E-02	7.86.E-02	**0.99**	9.51.E-01	9.77.E-01
LOC101927972	**1.45**	1.60.E-01	2.81.E-01	**1.58**	1.22.E-01	2.06.E-01	**0.91**	6.34.E-01	7.84.E-01
OSBPL10-AS1	**1.44**	1.68.E-01	2.91.E-01	**1.72**	7.36.E-02	1.34.E-01	**1.09**	6.77.E-01	8.14.E-01
MAP7D1	**1.43**	4.23.E-16	7.01.E-15	**0.89**	4.33.E-02	8.56.E-02	**0.82**	7.68.E-03	2.68.E-02
RFX7	**1.42**	4.04.E-06	2.43.E-05	**1.66**	9.84.E-12	8.04.E-11	**0.96**	5.29.E-01	7.04.E-01
POGZ	**1.42**	4.02.E-07	2.84.E-06	**1.17**	2.99.E-02	6.23.E-02	**1.00**	9.88.E-01	9.94.E-01
ZNF778	**1.42**	4.73.E-06	2.80.E-05	**1.56**	3.83.E-09	2.45.E-08	**0.87**	5.96.E-02	1.45.E-01
PINK1	**1.41**	1.79.E-09	1.69.E-08	**1.10**	1.67.E-01	2.65.E-01	**0.80**	1.80.E-03	7.65.E-03
PCDHGB1	**1.41**	3.53.E-03	1.15.E-02	**1.24**	6.29.E-02	1.18.E-01	**1.26**	2.32.E-02	6.71.E-02
VARS	**1.41**	1.88.E-11	2.15.E-10	**1.30**	5.39.E-06	2.32.E-05	**1.04**	6.00.E-01	7.59.E-01
FAAP20	**1.40**	2.20.E-04	9.60.E-04	**0.92**	4.57.E-01	5.80.E-01	**1.07**	5.56.E-01	7.26.E-01
COL12A1	**1.39**	2.67.E-10	2.74.E-09	**0.92**	2.04.E-01	3.11.E-01	**0.85**	8.04.E-03	2.79.E-02
FMNL3	**1.39**	4.19.E-08	3.35.E-07	**1.52**	6.26.E-12	5.21.E-11	**0.81**	1.05.E-04	6.14.E-04
HCG11	**1.39**	9.55.E-03	2.73.E-02	**2.60**	1.16.E-16	1.41.E-15	**1.24**	1.94.E-02	5.79.E-02
DOCK6	**1.38**	6.31.E-05	3.07.E-04	**2.02**	1.61.E-19	2.41.E-18	**0.54**	6.39.E-15	1.79.E-13
LIMK2	**1.37**	2.78.E-06	1.72.E-05	**1.11**	1.31.E-01	2.17.E-01	**1.03**	7.21.E-01	8.43.E-01
EPB41	**1.36**	2.16.E-07	1.58.E-06	**0.96**	5.60.E-01	6.73.E-01	**1.06**	3.87.E-01	5.76.E-01
LINC01322	**1.36**	1.86.E-01	3.15.E-01	**0.30**	5.28.E-05	1.97.E-04	**1.36**	7.60.E-02	1.76.E-01
SLC9A1	**1.36**	2.83.E-02	6.86.E-02	**1.16**	3.32.E-01	4.56.E-01	**0.91**	3.64.E-01	5.54.E-01
ADGRF3	**1.35**	1.53.E-01	2.71.E-01	**1.59**	3.30.E-02	6.79.E-02	**1.04**	8.38.E-01	9.17.E-01
MIR6079	**1.35**	1.46.E-01	NA	**1.17**	4.37.E-01	NA	**1.08**	5.98.E-01	NA
MORC2-AS1	**1.34**	7.62.E-02	1.55.E-01	**1.50**	1.51.E-02	3.41.E-02	**1.22**	1.52.E-01	2.99.E-01
IRF2BP1	**1.33**	4.06.E-04	1.67.E-03	**0.98**	8.48.E-01	8.97.E-01	**0.97**	7.35.E-01	8.52.E-01
P2RX2	**1.32**	2.89.E-01	4.37.E-01	**1.21**	5.27.E-01	6.44.E-01	**0.95**	7.96.E-01	8.90.E-01
PARM1	**1.32**	1.37.E-03	4.98.E-03	**0.72**	1.06.E-03	3.11.E-03	**1.34**	3.27.E-03	1.28.E-02
SF3A3	**1.32**	1.21.E-09	1.16.E-08	**1.24**	1.47.E-05	5.96.E-05	**0.87**	1.08.E-02	3.56.E-02
MAML2	**1.31**	4.74.E-05	2.36.E-04	**0.58**	1.71.E-13	1.66.E-12	**1.21**	3.23.E-03	1.27.E-02
ZFAND2A	**1.31**	2.17.E-04	9.50.E-04	**0.95**	4.93.E-01	6.13.E-01	**0.86**	3.86.E-02	1.02.E-01
ANXA2P2	**1.31**	4.58.E-03	1.45.E-02	**1.38**	8.77.E-04	2.62.E-03	**0.84**	7.80.E-02	1.79.E-01
ZNF771	**1.31**	3.26.E-02	7.75.E-02	**1.11**	4.65.E-01	5.87.E-01	**0.88**	3.50.E-01	5.39.E-01
LAMB3	**1.31**	6.99.E-05	3.36.E-04	**1.13**	7.92.E-02	1.43.E-01	**0.84**	8.34.E-03	2.88.E-02
TES	**1.29**	9.44.E-06	5.31.E-05	**1.27**	1.10.E-04	3.90.E-04	**0.76**	3.36.E-07	3.32.E-06
UHRF1	**1.29**	1.23.E-04	5.64.E-04	**0.91**	1.89.E-01	2.93.E-01	**1.21**	3.07.E-02	8.48.E-02
ZNF362	**1.29**	3.97.E-03	1.28.E-02	**1.06**	5.57.E-01	6.70.E-01	**0.86**	1.61.E-01	3.12.E-01
LARP7	**1.29**	1.37.E-05	7.50.E-05	**1.09**	1.84.E-01	2.87.E-01	**1.13**	9.09.E-02	2.02.E-01
IFRD1	**1.29**	2.44.E-05	1.28.E-04	**1.24**	1.30.E-03	3.78.E-03	**0.74**	4.69.E-08	5.43.E-07

MIR4435-2HG	**1.29**	7.25.E-06	4.15.E-05	**1.25**	4.57.E-05	1.73.E-04	**0.49**	4.66.E-32	4.48.E-30
LINC00324	**1.28**	1.14.E-02	3.17.E-02	**0.91**	3.86.E-01	5.11.E-01	**1.32**	7.69.E-03	2.69.E-02
CIRBP	**1.28**	3.88.E-07	2.74.E-06	**1.61**	1.66.E-20	2.62.E-19	**0.95**	3.63.E-01	5.53.E-01
MBD1	**1.27**	4.26.E-07	2.99.E-06	**1.14**	8.00.E-03	1.96.E-02	**0.66**	9.48.E-13	2.10.E-11
MYBPC3	**1.26**	2.24.E-01	NA	**1.27**	2.96.E-01	NA	**1.00**	9.97.E-01	NA
CCNI	**1.26**	6.08.E-08	4.77.E-07	**0.84**	5.41.E-04	1.69.E-03	**1.06**	3.01.E-01	4.86.E-01
SH2D3A	**1.26**	3.94.E-02	9.05.E-02	**0.98**	8.58.E-01	9.04.E-01	**0.60**	1.75.E-04	9.76.E-04
RDH10-AS1	**1.26**	3.67.E-01	5.20.E-01	**1.64**	8.38.E-02	1.50.E-01	**0.99**	9.65.E-01	9.85.E-01
DOCK1	**1.26**	7.89.E-07	5.33.E-06	**1.04**	4.05.E-01	5.29.E-01	**1.20**	2.78.E-04	1.48.E-03
C8ORF58	**1.26**	3.12.E-03	1.03.E-02	**0.96**	6.20.E-01	7.24.E-01	**0.96**	6.42.E-01	7.89.E-01
LOC100131496	**1.26**	1.10.E-01	2.07.E-01	**1.64**	5.42.E-04	1.69.E-03	**0.85**	1.77.E-01	3.34.E-01
AKAP12	**1.26**	1.50.E-05	8.17.E-05	**0.75**	6.68.E-05	2.45.E-04	**0.76**	2.66.E-04	1.42.E-03
DMAP1	**1.25**	5.19.E-03	1.61.E-02	**0.82**	3.00.E-02	6.25.E-02	**1.01**	8.69.E-01	9.34.E-01
PISD	**1.25**	1.08.E-04	5.03.E-04	**1.12**	5.97.E-02	1.13.E-01	**1.05**	4.76.E-01	6.60.E-01
ABR	**1.25**	3.49.E-03	1.14.E-02	**1.32**	2.29.E-04	7.64.E-04	**0.78**	5.74.E-06	4.54.E-05
PFN1	**1.25**	9.67.E-07	6.41.E-06	**1.01**	7.78.E-01	8.49.E-01	**0.94**	2.35.E-01	4.11.E-01
MTERF1	**1.25**	1.92.E-02	4.96.E-02	**1.62**	4.41.E-07	2.19.E-06	**0.86**	9.80.E-02	2.13.E-01
POLR2J4	**1.24**	2.31.E-02	5.77.E-02	**1.47**	1.01.E-04	3.60.E-04	**0.70**	2.64.E-04	1.41.E-03
TCEAL1	**1.24**	5.38.E-05	2.65.E-04	**0.52**	4.40.E-24	8.58.E-23	**1.36**	4.60.E-05	2.96.E-04
MIR619	**1.24**	3.82.E-01	5.34.E-01	**1.13**	6.63.E-01	7.61.E-01	**1.24**	2.32.E-01	4.08.E-01
PEAR1	**1.24**	1.43.E-02	3.85.E-02	**2.28**	9.52.E-23	1.72.E-21	**0.74**	1.88.E-04	1.04.E-03
LINC00243	**1.24**	3.09.E-01	4.58.E-01	**0.82**	4.03.E-01	5.28.E-01	**1.10**	6.31.E-01	7.82.E-01
LOC101927027	**1.24**	5.00.E-02	1.10.E-01	**1.52**	1.37.E-04	4.77.E-04	**1.09**	3.97.E-01	5.86.E-01
PLAC8	**1.23**	1.91.E-05	1.02.E-04	**0.71**	1.81.E-10	1.31.E-09	**0.67**	2.66.E-11	4.98.E-10
DAAM1	**1.23**	1.23.E-03	4.54.E-03	**1.29**	5.75.E-05	2.13.E-04	**0.43**	8.46.E-28	6.57.E-26
ITPRIP	**1.22**	2.36.E-01	3.77.E-01	**1.14**	2.31.E-01	3.44.E-01	**1.11**	1.97.E-01	3.62.E-01
BMP1	**1.22**	7.72.E-04	2.98.E-03	**0.62**	1.32.E-08	7.95.E-08	**0.61**	9.59.E-08	1.05.E-06
KCNMA1-AS3	**1.22**	3.70.E-01	5.22.E-01	**1.53**	1.36.E-01	2.25.E-01	**0.90**	5.42.E-01	7.13.E-01
ZBTB39	**1.22**	1.20.E-02	3.31.E-02	**1.56**	1.52.E-09	1.01.E-08	**0.76**	1.61.E-04	9.03.E-04
DEK	**1.22**	1.39.E-06	8.99.E-06	**1.02**	6.73.E-01	7.69.E-01	**1.22**	9.62.E-04	4.42.E-03
MAST2	**1.22**	3.58.E-03	1.16.E-02	**0.91**	2.24.E-01	3.36.E-01	**0.80**	4.02.E-04	2.06.E-03
RSPH6A	**1.21**	3.67.E-01	5.19.E-01	**1.36**	2.56.E-01	3.72.E-01	**1.13**	4.94.E-01	6.76.E-01
VWA5A	**1.21**	4.65.E-01	6.14.E-01	**0.79**	4.29.E-01	5.52.E-01	**1.83**	2.90.E-03	1.15.E-02
CPED1	**1.20**	3.26.E-02	7.74.E-02	**5.07**	3.63.E-114	7.80.E-112	**0.23**	6.73.E-93	3.49.E-90
ISG20L2	**1.20**	1.04.E-03	3.87.E-03	**0.98**	7.31.E-01	8.12.E-01	**0.78**	2.25.E-04	1.22.E-03
PTP4A2	**1.20**	7.79.E-06	4.43.E-05	**1.13**	1.10.E-02	2.60.E-02	**0.90**	5.73.E-02	1.40.E-01
PRPF18	**1.20**	5.06.E-03	1.57.E-02	**0.93**	3.16.E-01	4.39.E-01	**1.27**	9.75.E-04	4.47.E-03
MIR6871	**1.20**	3.76.E-01	NA	**1.32**	2.85.E-01	4.05.E-01	**0.99**	9.52.E-01	9.78.E-01
HOXC5	**1.20**	3.90.E-01	5.42.E-01	**1.82**	3.20.E-03	8.51.E-03	**0.99**	9.54.E-01	9.78.E-01
ZNF250	**1.19**	7.77.E-03	2.28.E-02	**0.86**	3.55.E-02	7.20.E-02	**0.91**	1.86.E-01	3.47.E-01
ADNP-AS1	**1.19**	3.33.E-01	4.84.E-01	**1.41**	5.05.E-02	9.77.E-02	**0.96**	7.77.E-01	8.78.E-01
C11ORF96	**1.18**	5.30.E-01	6.70.E-01	**0.92**	7.80.E-01	8.50.E-01	**1.05**	7.69.E-01	8.73.E-01
COL16A1	**1.18**	5.07.E-02	1.11.E-01	**0.48**	2.10.E-11	1.67.E-10	**0.69**	3.45.E-03	1.34.E-02
LOC101928191	**1.18**	5.12.E-01	6.55.E-01	**1.25**	4.58.E-01	5.80.E-01	**1.20**	3.34.E-01	5.22.E-01
SSRP1	**1.17**	3.21.E-04	1.35.E-03	**1.32**	6.67.E-08	3.68.E-07	**0.89**	1.88.E-02	5.63.E-02
HIP1R	**1.17**	4.33.E-03	1.38.E-02	**0.77**	7.25.E-04	2.20.E-03	**1.10**	2.70.E-01	4.52.E-01
SEC14L1	**1.17**	1.66.E-02	4.39.E-02	**0.81**	1.70.E-03	4.82.E-03	**0.69**	1.30.E-10	2.25.E-09
STX1A	**1.16**	1.28.E-02	3.50.E-02	**1.13**	1.10.E-01	1.88.E-01	**1.11**	1.81.E-01	3.39.E-01
FAM86DP	**1.16**	9.01.E-02	1.78.E-01	**0.87**	1.47.E-01	2.39.E-01	**1.39**	6.10.E-04	2.97.E-03
LINC01655	**1.16**	5.09.E-01	6.52.E-01	**1.10**	7.11.E-01	7.98.E-01	**0.97**	8.44.E-01	NA
AXL	**1.16**	4.68.E-04	1.90.E-03	**1.33**	1.04.E-10	7.70.E-10	**0.63**	1.38.E-22	7.62.E-21

LOC400706	**1.16**	4.00.E-01	NA	**1.12**	5.48.E-01	NA	**1.24**	1.59.E-01	3.10.E-01
MIR6732	**1.15**	6.05.E-01	7.32.E-01	**0.94**	8.28.E-01	8.84.E-01	**1.31**	1.72.E-01	3.26.E-01
CAPNS1	**1.14**	2.25.E-03	7.72.E-03	**1.23**	6.34.E-06	2.70.E-05	**0.83**	1.95.E-04	1.08.E-03
NFIA	**1.14**	5.30.E-02	1.15.E-01	**0.94**	3.56.E-01	4.80.E-01	**0.95**	5.12.E-01	6.91.E-01
RBM17	**1.14**	2.55.E-02	6.29.E-02	**0.94**	2.05.E-01	3.12.E-01	**1.10**	7.77.E-02	1.79.E-01
VGF	**1.14**	5.38.E-01	6.77.E-01	**1.42**	1.14.E-01	1.94.E-01	**0.95**	7.72.E-01	8.75.E-01
LINC00968	**1.13**	4.45.E-01	NA	**1.00**	9.88.E-01	NA	**0.98**	7.72.E-01	NA
R3HCC1	**1.13**	6.53.E-02	1.37.E-01	**1.34**	4.99.E-05	1.87.E-04	**0.81**	1.47.E-03	6.42.E-03
ANKRD52	**1.13**	5.86.E-02	1.25.E-01	**1.05**	4.68.E-01	5.91.E-01	**0.77**	2.85.E-05	1.93.E-04
PPP1R15A	**1.13**	7.22.E-03	2.14.E-02	**1.66**	6.89.E-26	1.50.E-24	**1.06**	3.11.E-01	4.97.E-01
FPR3	**1.12**	5.33.E-01	NA	**0.94**	7.26.E-01	NA	**1.28**	8.14.E-02	1.85.E-01
ADORA3	**1.12**	3.73.E-01	NA	**NA**	NA	NA	**1.03**	6.68.E-01	NA
THAP4	**1.12**	4.29.E-02	9.72.E-02	**0.98**	7.88.E-01	8.56.E-01	**0.91**	1.98.E-01	3.62.E-01
IFT46	**1.12**	7.02.E-02	1.45.E-01	**0.91**	1.48.E-01	2.40.E-01	**1.21**	2.78.E-03	1.11.E-02
MIR5191	**1.12**	4.86.E-01	NA	**1.33**	2.38.E-01	NA	**0.98**	9.06.E-01	9.53.E-01
COPS4	**1.10**	4.58.E-02	1.02.E-01	**1.04**	4.33.E-01	5.57.E-01	**0.83**	2.88.E-03	1.15.E-02
TBC1D1	**1.10**	3.51.E-02	8.23.E-02	**1.06**	2.43.E-01	3.57.E-01	**0.85**	2.23.E-03	9.16.E-03
CMTM3	**1.10**	1.76.E-01	3.03.E-01	**1.29**	8.71.E-04	2.61.E-03	**1.00**	9.92.E-01	9.97.E-01
RAP2C	**1.10**	1.01.E-01	1.94.E-01	**0.71**	4.51.E-07	2.23.E-06	**1.14**	8.76.E-02	1.96.E-01
FAM189B	**1.10**	6.44.E-01	7.62.E-01	**0.68**	7.19.E-03	1.78.E-02	**1.13**	3.11.E-01	4.97.E-01
SERHL2	**1.10**	5.43.E-01	6.81.E-01	**1.10**	5.77.E-01	6.88.E-01	**1.09**	5.70.E-01	7.36.E-01
TTC5	**1.09**	2.51.E-01	3.94.E-01	**1.32**	7.82.E-05	2.83.E-04	**1.16**	3.69.E-02	9.80.E-02
DACT3-AS1	**1.09**	6.85.E-01	7.93.E-01	**1.03**	8.99.E-01	9.33.E-01	**1.13**	4.43.E-01	6.30.E-01
CDH12	**1.09**	7.45.E-01	8.37.E-01	**0.73**	2.94.E-01	4.15.E-01	**7.08**	8.86.E-26	6.10.E-24
KCNC4-AS1	**1.09**	7.38.E-01	8.33.E-01	**0.91**	7.46.E-01	8.24.E-01	**0.90**	4.63.E-01	NA
ZNF385A	**1.09**	6.47.E-01	7.64.E-01	**1.04**	8.24.E-01	8.81.E-01	**0.83**	3.10.E-01	4.96.E-01
MIPEPP3	**1.09**	6.80.E-01	7.89.E-01	**1.46**	7.07.E-02	1.30.E-01	**0.87**	4.36.E-01	6.23.E-01
ADGRE5	**1.09**	6.82.E-01	7.90.E-01	**0.88**	5.20.E-01	6.37.E-01	**1.33**	8.93.E-05	5.34.E-04
BRF2	**1.08**	2.85.E-01	4.33.E-01	**1.18**	3.10.E-02	6.42.E-02	**0.93**	3.53.E-01	5.43.E-01
TFAP2A	**1.08**	6.09.E-01	7.36.E-01	**1.12**	4.90.E-01	6.11.E-01	**1.31**	6.03.E-02	1.46.E-01
LINC00673	**1.08**	3.40.E-01	4.92.E-01	**0.97**	6.90.E-01	7.82.E-01	**1.06**	5.34.E-01	7.09.E-01
LAMTOR3	**1.08**	2.25.E-01	3.64.E-01	**1.09**	2.16.E-01	3.26.E-01	**0.83**	9.62.E-03	3.24.E-02
LPIN1	**1.08**	8.97.E-02	1.77.E-01	**1.23**	3.98.E-06	1.74.E-05	**1.74**	2.65.E-29	2.22.E-27
WRAP53	**1.08**	2.08.E-01	3.43.E-01	**1.17**	5.88.E-03	1.48.E-02	**0.92**	1.63.E-01	3.15.E-01
ENO1	**1.08**	1.10.E-01	2.08.E-01	**1.48**	1.47.E-17	1.91.E-16	**0.90**	2.46.E-02	7.05.E-02
SRGAP2D	**1.07**	4.12.E-01	5.65.E-01	**1.32**	1.54.E-03	4.41.E-03	**1.16**	7.00.E-02	1.65.E-01
ZNF165	**1.07**	5.72.E-01	7.06.E-01	**0.79**	9.02.E-02	1.59.E-01	**1.45**	3.71.E-03	1.43.E-02
LINC00696	**1.07**	7.80.E-01	8.63.E-01	**1.63**	1.06.E-01	1.83.E-01	**0.99**	9.61.E-01	9.83.E-01
SLC7A2	**1.07**	2.18.E-01	3.55.E-01	**1.59**	6.33.E-16	7.31.E-15	**1.02**	7.59.E-01	8.67.E-01
MIR6835	**1.07**	7.86.E-01	8.67.E-01	**1.48**	1.59.E-01	2.55.E-01	**0.84**	3.99.E-01	5.88.E-01
RSAD1	**1.07**	3.55.E-01	5.07.E-01	**1.13**	1.24.E-01	2.08.E-01	**0.96**	5.28.E-01	7.04.E-01
HES5	**1.07**	7.61.E-01	NA	**1.11**	7.02.E-01	7.91.E-01	**1.07**	6.77.E-01	8.14.E-01
DYNC1H1	**1.07**	6.57.E-01	7.73.E-01	**1.92**	2.45.E-05	9.64.E-05	**1.13**	3.79.E-02	1.00.E-01
PAFAH2	**1.07**	5.23.E-01	6.65.E-01	**0.78**	2.41.E-02	5.16.E-02	**1.12**	2.75.E-01	4.57.E-01
KRT8	**1.06**	2.21.E-01	3.58.E-01	**0.64**	1.68.E-15	1.90.E-14	**0.78**	7.92.E-05	4.81.E-04
RPL23AP87	**1.06**	7.80.E-01	NA	**0.99**	9.54.E-01	9.72.E-01	**0.99**	9.47.E-01	NA
HOXB8	**1.06**	8.26.E-01	8.94.E-01	**1.03**	9.29.E-01	9.54.E-01	**0.88**	4.65.E-01	6.50.E-01
LOC100132356	**1.06**	6.52.E-01	7.69.E-01	**1.42**	6.76.E-03	1.68.E-02	**0.98**	8.84.E-01	9.42.E-01
PMP22	**1.06**	2.29.E-01	3.69.E-01	**0.92**	9.29.E-02	1.64.E-01	**1.36**	3.41.E-07	3.37.E-06
ARTN	**1.06**	6.58.E-01	7.74.E-01	**0.34**	1.37.E-10	1.00.E-09	**1.53**	1.48.E-02	4.61.E-02
CHRM3-AS1	**1.06**	6.13.E-01	NA	**1.03**	8.23.E-01	NA	**1.06**	5.36.E-01	NA

FAM83A	**1.06**	4.19.E-01	5.71.E-01	**0.12**	1.16.E-92	1.65.E-90	**2.22**	9.95.E-11	1.76.E-09
RGS3	**1.05**	3.34.E-01	4.85.E-01	**0.95**	4.44.E-01	5.67.E-01	**0.90**	1.44.E-01	2.88.E-01
PITPNM2-AS1	**1.05**	8.37.E-01	9.01.E-01	**0.59**	8.54.E-02	1.52.E-01	**1.36**	1.20.E-01	2.49.E-01
MIR3691	**1.05**	6.26.E-01	NA	**1.15**	3.73.E-01	NA	**1.02**	8.30.E-01	NA
PIGV	**1.05**	4.15.E-01	5.67.E-01	**1.54**	9.29.E-13	8.46.E-12	**0.87**	3.44.E-02	9.30.E-02
ARHGAP23	**1.05**	4.31.E-01	5.82.E-01	**1.04**	4.95.E-01	6.16.E-01	**1.05**	4.94.E-01	6.75.E-01
IL17REL	**1.05**	7.79.E-01	NA	**1.32**	2.90.E-01	4.12.E-01	**1.49**	3.54.E-02	9.49.E-02
PCDH12	**1.05**	7.86.E-01	8.67.E-01	**1.31**	1.41.E-01	2.31.E-01	**0.84**	2.72.E-01	4.55.E-01
POP5	**1.05**	4.72.E-01	6.20.E-01	**1.14**	4.34.E-02	8.58.E-02	**0.94**	3.07.E-01	4.93.E-01
FUT10	**1.05**	5.32.E-01	6.72.E-01	**1.20**	1.02.E-02	2.43.E-02	**0.92**	2.80.E-01	4.63.E-01
MAPK9	**1.05**	3.51.E-01	5.04.E-01	**0.92**	1.19.E-01	2.01.E-01	**1.09**	1.48.E-01	2.94.E-01
PROX2	**1.05**	7.86.E-01	8.67.E-01	**2.27**	8.21.E-08	4.48.E-07	**0.62**	3.24.E-04	1.70.E-03
LOC101929719	**1.05**	7.95.E-01	NA	**1.84**	3.66.E-02	7.40.E-02	**0.91**	6.13.E-01	7.69.E-01
APOC1	**1.04**	7.57.E-01	8.47.E-01	**2.25**	5.91.E-11	4.49.E-10	**0.69**	8.28.E-04	3.88.E-03
CARD8	**1.04**	5.03.E-01	6.47.E-01	**1.33**	6.23.E-06	2.66.E-05	**1.17**	2.31.E-02	6.70.E-02
TOX4	**1.04**	4.45.E-01	5.95.E-01	**0.84**	6.56.E-03	1.64.E-02	**1.27**	7.18.E-05	4.40.E-04
POLD4	**1.04**	5.22.E-01	6.63.E-01	**0.77**	1.65.E-03	4.70.E-03	**0.77**	2.75.E-03	1.10.E-02
LOC101928909	**1.04**	8.85.E-01	9.33.E-01	**1.78**	3.76.E-02	7.57.E-02	**0.82**	3.36.E-01	5.25.E-01
FAM214B	**1.04**	4.62.E-01	6.11.E-01	**0.34**	2.74.E-70	2.49.E-68	**1.43**	9.84.E-06	7.44.E-05
MIR6797	**1.04**	8.85.E-01	9.33.E-01	**1.28**	3.77.E-01	5.02.E-01	**0.85**	4.23.E-01	6.12.E-01
SLC25A21-AS1	**1.03**	8.67.E-01	9.22.E-01	**1.64**	1.12.E-02	2.63.E-02	**1.21**	2.30.E-01	4.05.E-01
KDELC2	**1.03**	4.79.E-01	6.26.E-01	**0.50**	6.01.E-37	2.09.E-35	**1.87**	1.35.E-22	7.46.E-21
KCTD20	**1.03**	4.51.E-01	6.01.E-01	**0.98**	5.90.E-01	6.99.E-01	**1.06**	2.46.E-01	4.24.E-01
LRCH1	**1.03**	7.31.E-01	8.28.E-01	**1.06**	4.97.E-01	6.17.E-01	**0.96**	5.23.E-01	7.00.E-01
KANK2	**1.03**	6.20.E-01	7.44.E-01	**0.94**	2.52.E-01	3.68.E-01	**1.00**	9.79.E-01	9.93.E-01
GRPEL1	**1.03**	6.03.E-01	7.31.E-01	**0.97**	5.76.E-01	6.87.E-01	**1.01**	8.34.E-01	9.14.E-01
RBBP5	**1.03**	5.93.E-01	7.22.E-01	**0.87**	1.18.E-02	2.76.E-02	**0.90**	9.65.E-02	2.11.E-01
MALAT1	**1.02**	8.98.E-01	9.41.E-01	**0.98**	9.16.E-01	9.44.E-01	**0.97**	6.57.E-01	8.00.E-01
RUNX3	**1.02**	9.16.E-01	NA	**0.78**	1.97.E-01	NA	**1.12**	2.19.E-01	NA
GPR37L1	**1.02**	9.25.E-01	9.57.E-01	**0.99**	9.64.E-01	9.78.E-01	**0.91**	4.13.E-01	NA
MIR1236	**1.02**	8.96.E-01	NA	**0.99**	9.63.E-01	NA	**1.02**	8.60.E-01	NA
NEU2	**1.02**	9.24.E-01	9.57.E-01	**0.85**	4.79.E-01	NA	**1.06**	6.10.E-01	NA
PCDH9-AS4	**1.02**	8.34.E-01	NA	**NA**	NA	NA	**NA**	NA	NA
MIR6838	**1.02**	8.34.E-01	NA	**NA**	NA	NA	**NA**	NA	NA
MIR6799	**1.02**	8.34.E-01	NA	**NA**	NA	NA	**1.05**	4.50.E-01	NA
CXCL17	**1.02**	8.34.E-01	NA	**1.08**	5.91.E-01	NA	**1.14**	3.19.E-01	NA
CRCT1	**1.02**	8.34.E-01	NA	**NA**	NA	NA	**NA**	NA	NA
CELA1	**1.02**	8.34.E-01	NA	**1.19**	3.22.E-01	NA	**0.94**	4.97.E-01	NA
KRR1	**1.02**	7.11.E-01	8.13.E-01	**1.44**	4.91.E-11	3.76.E-10	**1.08**	2.75.E-01	4.57.E-01
CRK	**1.02**	6.95.E-01	8.00.E-01	**1.12**	2.08.E-02	4.53.E-02	**0.90**	3.82.E-02	1.01.E-01
USB1	**1.02**	8.01.E-01	8.77.E-01	**0.77**	3.28.E-04	1.07.E-03	**1.08**	3.26.E-01	5.13.E-01
LOC388282	**1.01**	9.56.E-01	9.74.E-01	**1.08**	7.80.E-01	8.49.E-01	**0.74**	1.24.E-01	2.56.E-01
ANKRD2	**1.01**	9.56.E-01	9.74.E-01	**0.53**	3.52.E-02	7.15.E-02	**1.17**	3.47.E-01	5.37.E-01
LOC729609	**1.01**	9.59.E-01	9.76.E-01	**0.94**	8.33.E-01	8.89.E-01	**0.97**	8.44.E-01	9.20.E-01
ATMIN	**1.01**	8.40.E-01	9.03.E-01	**1.67**	1.60.E-21	2.70.E-20	**0.81**	3.44.E-04	1.79.E-03
RANGAP1	**1.01**	8.26.E-01	8.94.E-01	**0.99**	7.78.E-01	8.49.E-01	**1.03**	6.05.E-01	7.63.E-01
NEDD4L	**1.01**	8.57.E-01	9.16.E-01	**1.54**	4.49.E-17	5.62.E-16	**0.56**	1.62.E-32	1.61.E-30
SLC1A7	**1.01**	9.80.E-01	9.89.E-01	**0.67**	1.42.E-01	2.32.E-01	**1.00**	9.90.E-01	9.96.E-01
STK40	**1.00**	9.60.E-01	9.77.E-01	**0.78**	1.89.E-06	8.66.E-06	**0.90**	1.27.E-01	2.60.E-01
ABCD4	**1.00**	9.96.E-01	9.97.E-01	**1.38**	1.07.E-04	3.79.E-04	**0.83**	3.51.E-03	1.36.E-02
CCDC51	**1.00**	9.95.E-01	9.97.E-01	**0.97**	6.15.E-01	7.20.E-01	**1.25**	9.03.E-04	4.19.E-03

HOPX	**1.00**	9.75.E-01	NA	**1.14**	4.75.E-01	NA	**0.99**	9.03.E-01	NA
FYB2	**1.00**	9.74.E-01	NA	**1.17**	4.37.E-01	NA	**0.99**	9.04.E-01	NA
DUOXA2	**1.00**	9.74.E-01	NA	**1.06**	7.48.E-01	NA	**0.97**	6.77.E-01	NA
PSMD1	**1.00**	9.24.E-01	9.57.E-01	**1.15**	1.77.E-03	4.99.E-03	**0.97**	6.07.E-01	7.64.E-01
IL4	**1.00**	9.74.E-01	NA	**1.06**	7.39.E-01	NA	**1.08**	5.20.E-01	NA
LINC01260	**1.00**	9.74.E-01	NA	**1.06**	7.55.E-01	NA	**0.96**	5.38.E-01	NA
PRND	**1.00**	9.74.E-01	NA	**0.97**	8.04.E-01	NA	**NA**	NA	NA
LINC00682	**1.00**	9.73.E-01	NA	**1.00**	9.88.E-01	NA	**1.06**	5.18.E-01	NA
GSN-AS1	**1.00**	9.83.E-01	9.91.E-01	**0.95**	7.85.E-01	8.54.E-01	**1.18**	3.33.E-01	5.22.E-01
MIR4645	**1.00**	9.78.E-01	NA	**1.13**	5.64.E-01	NA	**0.97**	7.83.E-01	NA
ZNF7	**1.00**	9.32.E-01	9.61.E-01	**1.32**	2.75.E-05	1.07.E-04	**0.90**	1.21.E-01	2.52.E-01
APOB	**0.99**	9.59.E-01	NA	**0.94**	6.26.E-01	NA	**1.03**	6.68.E-01	NA
ATP5MC2	**0.99**	8.71.E-01	9.25.E-01	**1.32**	2.36.E-08	1.37.E-07	**0.84**	6.02.E-04	2.94.E-03
MED23	**0.99**	8.40.E-01	9.03.E-01	**1.18**	2.39.E-03	6.54.E-03	**0.96**	5.34.E-01	7.09.E-01
STX1B	**0.99**	9.64.E-01	9.79.E-01	**1.09**	7.47.E-01	8.25.E-01	**1.08**	7.18.E-01	8.42.E-01
KDM3B	**0.99**	7.93.E-01	8.71.E-01	**1.34**	1.12.E-10	8.26.E-10	**0.94**	1.93.E-01	3.55.E-01
LINC02449	**0.98**	9.43.E-01	9.67.E-01	**1.32**	2.63.E-01	3.80.E-01	**0.72**	1.06.E-01	2.27.E-01
MRPL30	**0.98**	7.58.E-01	8.47.E-01	**1.34**	1.54.E-07	8.14.E-07	**0.77**	2.29.E-05	1.59.E-04
ADM	**0.98**	7.45.E-01	8.38.E-01	**0.84**	1.18.E-02	2.75.E-02	**0.76**	1.49.E-04	8.42.E-04
SLC29A3	**0.98**	8.27.E-01	8.94.E-01	**0.61**	2.05.E-05	8.15.E-05	**1.41**	3.50.E-03	1.36.E-02
MRGBP	**0.98**	7.15.E-01	8.15.E-01	**1.09**	1.65.E-01	2.62.E-01	**0.89**	3.63.E-02	9.67.E-02
DNAJB5	**0.98**	7.69.E-01	8.56.E-01	**0.63**	4.81.E-08	2.69.E-07	**1.08**	3.82.E-01	5.72.E-01
OR7E47P	**0.98**	9.15.E-01	9.52.E-01	**0.99**	9.54.E-01	9.72.E-01	**1.06**	6.79.E-01	8.15.E-01
UBL4B	**0.98**	7.93.E-01	NA	**0.97**	8.04.E-01	NA	**1.01**	8.55.E-01	NA
SRARP	**0.98**	7.93.E-01	NA	**0.97**	8.04.E-01	NA	**NA**	NA	NA
SPACA4	**0.98**	7.93.E-01	NA	**1.06**	7.48.E-01	NA	**1.02**	8.57.E-01	NA
NPAS4	**0.98**	7.93.E-01	NA	**1.05**	7.69.E-01	NA	**0.97**	7.17.E-01	NA
MRO	**0.98**	7.93.E-01	NA	**0.97**	8.04.E-01	NA	**NA**	NA	NA
MIR145	**0.98**	7.93.E-01	NA	**1.05**	7.68.E-01	NA	**0.96**	5.67.E-01	NA
MEPE	**0.98**	7.93.E-01	NA	**0.97**	8.04.E-01	NA	**NA**	NA	NA
LINC02265	**0.98**	7.93.E-01	NA	**0.97**	8.04.E-01	NA	**NA**	NA	NA
LINC01819	**0.98**	7.93.E-01	NA	**0.97**	8.04.E-01	NA	**1.03**	6.50.E-01	NA
LINC01485	**0.98**	7.93.E-01	NA	**0.97**	8.04.E-01	NA	**NA**	NA	NA
LINC01391	**0.98**	7.93.E-01	NA	**0.97**	8.04.E-01	NA	**NA**	NA	NA
KCNA2	**0.98**	7.93.E-01	NA	**0.97**	8.04.E-01	NA	**NA**	NA	NA
FAM92B	**0.98**	7.93.E-01	NA	**1.12**	5.55.E-01	NA	**0.95**	5.46.E-01	NA
CEACAM5	**0.98**	7.93.E-01	NA	**1.00**	9.89.E-01	NA	**0.98**	7.72.E-01	NA
CCDC177	**0.98**	7.93.E-01	NA	**1.00**	9.88.E-01	NA	**0.98**	7.72.E-01	NA
C10ORF120	**0.98**	7.93.E-01	NA	**0.97**	8.04.E-01	NA	**NA**	NA	NA
GSK3A	**0.97**	5.72.E-01	7.06.E-01	**1.06**	2.47.E-01	3.63.E-01	**0.76**	2.69.E-06	2.26.E-05
PPP1R1B	**0.97**	8.93.E-01	9.38.E-01	**0.90**	7.08.E-01	7.97.E-01	**1.20**	3.64.E-01	5.53.E-01
ISCU	**0.96**	5.03.E-01	6.47.E-01	**1.10**	6.09.E-02	1.15.E-01	**0.98**	6.95.E-01	8.26.E-01
RHBDF1	**0.96**	5.71.E-01	7.04.E-01	**0.84**	6.15.E-02	1.15.E-01	**1.03**	7.95.E-01	8.89.E-01
AHSG	**0.96**	8.30.E-01	NA	**1.05**	8.38.E-01	8.92.E-01	**1.01**	9.72.E-01	NA
SHC1	**0.96**	3.26.E-01	4.77.E-01	**0.74**	1.37.E-11	1.10.E-10	**0.94**	2.79.E-01	4.61.E-01
MIR4641	**0.96**	7.48.E-01	NA	**0.94**	6.26.E-01	NA	**NA**	NA	NA
LINC00336	**0.96**	7.29.E-01	NA	**0.94**	6.26.E-01	NA	**1.07**	3.83.E-01	NA
MIR7974	**0.96**	7.78.E-01	NA	**0.94**	7.92.E-01	NA	**1.09**	4.77.E-01	NA
ROBO4	**0.95**	4.16.E-01	5.68.E-01	**0.72**	3.23.E-07	1.63.E-06	**1.31**	8.65.E-05	5.20.E-04
GET4	**0.95**	4.34.E-01	5.85.E-01	**1.04**	6.23.E-01	7.27.E-01	**0.97**	7.08.E-01	8.35.E-01
ORAI1	**0.95**	4.00.E-01	5.52.E-01	**0.93**	4.35.E-01	5.58.E-01	**1.05**	7.64.E-01	8.70.E-01

KCNC1	**0.95**	8.15.E-01	8.86.E-01	**0.83**	4.17.E-01	5.41.E-01	**1.11**	3.95.E-01	NA
UBXN11	**0.95**	5.23.E-01	6.65.E-01	**0.60**	4.64.E-07	2.29.E-06	**1.16**	1.64.E-01	3.16.E-01
B3GALT4	**0.95**	7.59.E-01	8.48.E-01	**0.94**	7.45.E-01	8.23.E-01	**1.71**	6.67.E-04	3.22.E-03
KCNJ5	**0.95**	7.38.E-01	NA	**0.94**	7.85.E-01	NA	**1.02**	8.72.E-01	NA
EPS15	**0.95**	2.40.E-01	3.81.E-01	**0.85**	6.17.E-04	1.90.E-03	**1.02**	7.83.E-01	8.82.E-01
GALP	**0.95**	5.90.E-01	NA	**0.95**	7.67.E-01	NA	**0.98**	7.72.E-01	NA
MIR3934	**0.94**	7.90.E-01	8.69.E-01	**1.04**	8.55.E-01	9.02.E-01	**1.10**	5.94.E-01	7.54.E-01
AJUBA	**0.94**	2.89.E-01	4.37.E-01	**0.58**	1.43.E-22	2.57.E-21	**1.07**	1.80.E-01	3.39.E-01
ZNF491	**0.94**	6.09.E-01	7.35.E-01	**0.45**	1.52.E-08	9.06.E-08	**1.07**	6.37.E-01	7.86.E-01
MIR548XHG	**0.94**	5.72.E-01	NA	**0.95**	7.33.E-01	NA	**1.02**	8.24.E-01	NA
ERCC1	**0.94**	2.59.E-01	4.03.E-01	**1.59**	7.72.E-18	1.02.E-16	**0.67**	7.43.E-13	1.66.E-11
DLX2-AS1	**0.94**	7.67.E-01	8.55.E-01	**0.78**	3.41.E-01	4.65.E-01	**1.23**	1.62.E-01	3.13.E-01
LTBP3	**0.93**	5.93.E-01	7.22.E-01	**0.67**	2.14.E-03	5.93.E-03	**0.65**	5.38.E-03	1.97.E-02
ENTPD8	**0.93**	7.88.E-01	8.68.E-01	**0.69**	2.00.E-01	3.06.E-01	**1.34**	1.52.E-01	2.99.E-01
PRKCE	**0.93**	2.28.E-01	3.68.E-01	**1.05**	3.98.E-01	5.22.E-01	**1.01**	9.02.E-01	9.51.E-01
LMNA	**0.93**	1.27.E-01	2.33.E-01	**0.54**	7.38.E-21	1.19.E-19	**1.51**	3.67.E-07	3.60.E-06
SPI1	**0.93**	5.36.E-01	NA	**1.00**	9.96.E-01	NA	**0.97**	7.28.E-01	NA
FBXO34	**0.93**	1.12.E-01	2.11.E-01	**1.22**	1.50.E-04	5.17.E-04	**0.75**	1.04.E-06	9.38.E-06
WDR87	**0.93**	7.73.E-01	8.58.E-01	**0.64**	1.07.E-01	1.83.E-01	**0.97**	5.75.E-01	NA
SEPT9	**0.93**	7.49.E-02	1.53.E-01	**0.83**	3.51.E-04	1.13.E-03	**1.20**	7.10.E-03	2.51.E-02
HAP1	**0.93**	5.28.E-01	NA	**1.34**	2.59.E-01	3.76.E-01	**0.85**	2.07.E-01	NA
C11ORF45	**0.92**	3.98.E-01	5.49.E-01	**1.29**	3.19.E-03	8.50.E-03	**0.86**	8.85.E-02	1.98.E-01
VSTM2L	**0.92**	2.49.E-01	3.91.E-01	**0.45**	2.39.E-21	4.00.E-20	**1.06**	5.91.E-01	7.51.E-01
NME4	**0.92**	1.94.E-01	3.26.E-01	**0.59**	9.25.E-12	7.59.E-11	**0.94**	4.89.E-01	6.71.E-01
MPV17	**0.92**	2.68.E-01	4.14.E-01	**0.83**	4.73.E-03	1.22.E-02	**0.99**	8.91.E-01	9.45.E-01
EVA1B	**0.92**	6.56.E-01	7.72.E-01	**0.37**	1.15.E-04	4.04.E-04	**1.97**	6.88.E-04	3.31.E-03
MIR5188	**0.92**	7.38.E-01	8.33.E-01	**1.24**	4.76.E-01	5.98.E-01	**1.18**	4.28.E-01	6.16.E-01
COMMD2	**0.91**	1.43.E-01	2.56.E-01	**1.50**	1.32.E-11	1.07.E-10	**0.78**	1.48.E-04	8.39.E-04
GMDS-AS1	**0.91**	4.64.E-01	6.13.E-01	**1.35**	1.16.E-02	2.72.E-02	**0.73**	7.28.E-03	2.56.E-02
DHX8	**0.91**	5.42.E-02	1.17.E-01	**1.01**	8.03.E-01	8.66.E-01	**0.96**	4.04.E-01	5.92.E-01
MCHR1	**0.91**	5.11.E-01	NA	**0.87**	3.72.E-01	NA	**1.01**	8.55.E-01	NA
STK17A	**0.91**	4.39.E-02	9.88.E-02	**1.16**	6.25.E-03	1.57.E-02	**1.05**	4.70.E-01	6.54.E-01
ELF5	**0.91**	5.29.E-01	NA	**0.86**	3.58.E-01	NA	**1.01**	8.55.E-01	NA
PFKP	**0.90**	1.06.E-02	2.97.E-02	**0.58**	2.23.E-31	6.46.E-30	**1.35**	1.81.E-06	1.57.E-05
PSG10P	**0.90**	6.63.E-01	7.77.E-01	**0.79**	3.91.E-01	5.15.E-01	**1.12**	4.35.E-01	NA
CAPN2	**0.90**	1.03.E-02	2.90.E-02	**1.22**	2.43.E-06	1.10.E-05	**1.10**	3.60.E-02	9.63.E-02
MIR4685	**0.90**	6.77.E-01	7.87.E-01	**0.78**	3.98.E-01	5.22.E-01	**1.08**	5.90.E-01	7.51.E-01
SMARCD2	**0.90**	2.52.E-02	6.22.E-02	**1.14**	5.86.E-03	1.48.E-02	**0.87**	8.85.E-03	3.02.E-02
MIR5708	**0.90**	6.09.E-01	NA	**0.95**	8.39.E-01	8.92.E-01	**1.00**	9.81.E-01	NA
S100A10	**0.90**	9.71.E-02	1.89.E-01	**0.65**	3.59.E-09	2.31.E-08	**0.88**	3.94.E-02	1.03.E-01
PDLIM4	**0.90**	1.44.E-01	2.58.E-01	**0.59**	6.72.E-09	4.17.E-08	**0.95**	6.31.E-01	7.81.E-01
CDH24	**0.90**	1.57.E-01	2.76.E-01	**0.59**	8.65.E-10	5.90.E-09	**1.15**	1.15.E-01	2.41.E-01
TRNP1	**0.89**	2.91.E-01	4.40.E-01	**1.17**	1.34.E-01	2.21.E-01	**0.89**	2.47.E-01	4.25.E-01
RAPGEF1	**0.89**	4.04.E-02	9.23.E-02	**0.77**	4.20.E-05	1.59.E-04	**0.86**	2.57.E-02	7.30.E-02
FAM46B	**0.89**	1.65.E-01	2.87.E-01	**0.61**	9.43.E-09	5.77.E-08	**0.95**	6.11.E-01	7.68.E-01
DST	**0.89**	3.47.E-02	8.15.E-02	**1.19**	1.47.E-03	4.22.E-03	**1.52**	1.45.E-16	4.76.E-15
DDX18	**0.89**	8.08.E-03	2.36.E-02	**1.20**	2.32.E-04	7.75.E-04	**0.91**	9.74.E-02	2.12.E-01
CALM1	**0.88**	1.64.E-03	5.85.E-03	**1.15**	9.28.E-04	2.76.E-03	**0.75**	7.12.E-08	8.01.E-07
DKFZP434K028	**0.88**	6.31.E-01	7.52.E-01	**0.84**	5.61.E-01	6.74.E-01	**1.15**	4.96.E-01	6.77.E-01
ANKRD40	**0.88**	6.62.E-03	1.99.E-02	**0.99**	8.08.E-01	8.70.E-01	**0.94**	2.10.E-01	3.80.E-01
OC90	**0.88**	3.30.E-01	NA	**0.86**	3.60.E-01	NA	**1.01**	8.55.E-01	NA

S100A16	**0.87**	9.88.E-03	2.80.E-02	**0.75**	4.04.E-09	2.58.E-08	**0.72**	8.85.E-10	1.35.E-08
ST8SIA1	**0.87**	5.95.E-01	7.24.E-01	**2.07**	1.28.E-02	2.96.E-02	**0.80**	2.81.E-01	4.63.E-01
MIR5700	**0.87**	3.00.E-01	NA	**0.94**	7.70.E-01	NA	**0.97**	7.18.E-01	NA
EFNA5	**0.87**	1.26.E-01	2.32.E-01	**1.14**	1.59.E-01	2.55.E-01	**0.78**	8.04.E-04	3.78.E-03
PVRIG	**0.87**	5.05.E-01	6.48.E-01	**0.63**	3.09.E-02	6.41.E-02	**0.99**	9.46.E-01	9.74.E-01
WNT2B	**0.87**	3.85.E-01	5.37.E-01	**1.32**	7.09.E-02	1.30.E-01	**0.93**	5.77.E-01	7.40.E-01
ZNF20	**0.87**	4.90.E-01	NA	**0.86**	5.42.E-01	6.58.E-01	**0.96**	6.97.E-01	NA
FAM222A-AS1	**0.87**	5.96.E-01	7.25.E-01	**1.19**	5.66.E-01	6.79.E-01	**0.86**	4.38.E-01	6.25.E-01
PLIN3	**0.87**	8.25.E-03	2.41.E-02	**0.62**	1.02.E-12	9.25.E-12	**1.06**	4.34.E-01	6.21.E-01
PDGFRA	**0.87**	4.71.E-01	NA	**1.27**	4.19.E-01	5.43.E-01	**1.10**	6.03.E-01	7.61.E-01
SLC2A9	**0.87**	3.98.E-01	NA	**0.91**	6.47.E-01	NA	**0.96**	5.67.E-01	NA
CASQ1	**0.87**	5.18.E-01	6.60.E-01	**0.71**	1.67.E-01	2.65.E-01	**1.08**	4.21.E-01	NA
TCTN3	**0.87**	5.33.E-03	1.64.E-02	**0.84**	2.44.E-03	6.68.E-03	**1.02**	7.88.E-01	8.85.E-01
OPN5	**0.87**	3.82.E-01	NA	**0.85**	4.19.E-01	NA	**0.98**	7.72.E-01	NA
LINGO1	**0.86**	2.73.E-01	NA	**0.85**	3.07.E-01	NA	**NA**	NA	NA
NEK6	**0.86**	2.91.E-03	9.70.E-03	**0.82**	1.27.E-04	4.44.E-04	**0.69**	3.07.E-10	5.01.E-09
VTRNA1-1	**0.86**	4.87.E-01	6.32.E-01	**1.03**	8.92.E-01	9.28.E-01	**0.74**	1.28.E-01	2.63.E-01
LINC01356	**0.86**	9.13.E-02	1.80.E-01	**1.24**	2.13.E-02	4.64.E-02	**0.68**	1.91.E-05	1.35.E-04
LTF	**0.86**	5.62.E-01	6.97.E-01	**0.92**	7.92.E-01	8.58.E-01	**0.90**	5.80.E-01	7.43.E-01
BCL11B	**0.86**	3.59.E-01	NA	**2.46**	3.08.E-03	8.23.E-03	**0.71**	7.46.E-02	1.73.E-01
S100A14	**0.86**	5.33.E-01	6.73.E-01	**0.90**	7.40.E-01	8.19.E-01	**1.03**	8.86.E-01	9.43.E-01
MAVS	**0.86**	6.26.E-03	1.90.E-02	**0.71**	6.86.E-09	4.26.E-08	**0.98**	7.26.E-01	8.46.E-01
ERMN	**0.85**	4.57.E-01	NA	**0.89**	6.62.E-01	7.60.E-01	**0.91**	3.56.E-01	NA
BCAR3	**0.85**	2.25.E-04	9.78.E-04	**0.89**	1.39.E-02	3.19.E-02	**1.09**	1.08.E-01	2.30.E-01
SPA17	**0.85**	5.12.E-02	1.12.E-01	**0.57**	2.08.E-08	1.22.E-07	**1.55**	7.97.E-06	6.14.E-05
TTLL2	**0.85**	3.50.E-01	NA	**0.83**	3.81.E-01	NA	**1.02**	7.86.E-01	NA
MIR4653	**0.85**	5.36.E-01	6.76.E-01	**0.93**	8.07.E-01	8.70.E-01	**0.85**	3.54.E-01	5.44.E-01
SOX15	**0.85**	3.51.E-01	5.03.E-01	**1.19**	3.04.E-01	4.27.E-01	**0.88**	4.03.E-01	5.92.E-01
MIR3654	**0.85**	4.05.E-01	5.57.E-01	**1.44**	3.32.E-02	6.82.E-02	**0.79**	1.31.E-01	2.67.E-01
IP6K3	**0.85**	3.42.E-01	NA	**0.82**	3.72.E-01	NA	**1.02**	8.15.E-01	NA
GFM1	**0.85**	7.54.E-04	2.92.E-03	**1.13**	1.54.E-02	3.48.E-02	**0.94**	2.83.E-01	4.65.E-01
C8ORF59	**0.85**	6.57.E-03	1.98.E-02	**0.80**	1.16.E-03	3.39.E-03	**1.00**	9.70.E-01	9.87.E-01
DNAJC5B	**0.84**	2.38.E-01	NA	**0.85**	4.39.E-01	NA	**1.00**	9.52.E-01	NA
NCF4	**0.84**	4.73.E-01	6.21.E-01	**0.57**	3.03.E-02	6.31.E-02	**1.07**	3.83.E-01	NA
LBR	**0.84**	1.38.E-04	6.26.E-04	**0.91**	6.01.E-02	1.13.E-01	**1.13**	4.16.E-02	1.08.E-01
FIBP	**0.84**	2.73.E-03	9.19.E-03	**0.94**	3.18.E-01	4.41.E-01	**0.81**	1.78.E-04	9.90.E-04
C8ORF86	**0.84**	2.25.E-01	NA	**1.00**	9.88.E-01	9.92.E-01	**0.92**	4.03.E-01	NA
GRK2	**0.84**	2.40.E-03	8.16.E-03	**0.90**	1.04.E-01	1.80.E-01	**0.97**	6.93.E-01	8.25.E-01
TMIGD3	**0.83**	4.95.E-01	6.40.E-01	**1.04**	9.03.E-01	9.35.E-01	**0.95**	7.85.E-01	8.84.E-01
FGF1	**0.83**	4.61.E-02	1.03.E-01	**1.18**	8.01.E-02	1.44.E-01	**0.62**	7.62.E-07	7.06.E-06
CHPF	**0.83**	1.30.E-02	3.56.E-02	**0.48**	8.97.E-12	7.37.E-11	**1.26**	1.81.E-01	3.39.E-01
TMEM205	**0.83**	5.31.E-03	1.64.E-02	**0.69**	1.30.E-06	6.08.E-06	**0.83**	1.04.E-02	3.45.E-02
PDLIM2	**0.83**	2.62.E-02	6.42.E-02	**1.21**	6.39.E-02	1.19.E-01	**0.97**	7.92.E-01	8.88.E-01
UPP1	**0.83**	2.10.E-03	7.24.E-03	**1.13**	7.32.E-02	1.34.E-01	**0.67**	2.14.E-08	2.64.E-07
PALD1	**0.83**	3.83.E-01	NA	**0.68**	9.04.E-02	NA	**1.10**	2.64.E-01	NA
SH3GL1	**0.83**	3.45.E-03	1.13.E-02	**0.87**	7.17.E-02	1.31.E-01	**0.87**	8.26.E-02	1.88.E-01
CEBPE	**0.82**	3.13.E-01	NA	**0.78**	3.35.E-01	4.59.E-01	**1.04**	6.96.E-01	NA
RALGDS	**0.82**	1.06.E-03	3.97.E-03	**0.60**	2.43.E-13	2.33.E-12	**1.76**	4.35.E-14	1.12.E-12
TRAF1	**0.81**	2.66.E-04	1.14.E-03	**0.60**	4.54.E-18	6.14.E-17	**1.35**	1.69.E-06	1.47.E-05
TMEM141	**0.81**	1.80.E-03	6.35.E-03	**0.56**	5.20.E-16	6.05.E-15	**1.11**	1.95.E-01	3.59.E-01
ZBTB20	**0.81**	1.74.E-02	4.55.E-02	**1.28**	1.87.E-03	5.25.E-03	**1.05**	5.00.E-01	6.81.E-01

ANKRD26P1	**0.81**	1.86.E-01	NA	**1.10**	7.20.E-01	8.04.E-01	**0.93**	5.94.E-01	NA
GPR39	**0.81**	2.67.E-03	9.00.E-03	**1.37**	1.47.E-06	6.84.E-06	**0.80**	1.11.E-03	5.02.E-03
SIGLEC1	**0.81**	2.54.E-01	NA	**0.78**	2.80.E-01	NA	**0.98**	7.72.E-01	NA
ODF3L1	**0.79**	2.60.E-01	NA	**0.71**	1.74.E-01	2.74.E-01	**1.06**	5.28.E-01	NA
CRY2	**0.79**	4.44.E-03	1.41.E-02	**0.90**	2.13.E-01	3.23.E-01	**0.96**	6.34.E-01	7.84.E-01
GSN	**0.79**	2.28.E-05	1.21.E-04	**0.49**	2.09.E-26	4.68.E-25	**1.19**	3.55.E-02	9.51.E-02
CLU	**0.79**	1.02.E-03	3.84.E-03	**0.76**	3.32.E-04	1.08.E-03	**1.92**	8.40.E-18	3.10.E-16
EMP3	**0.79**	1.79.E-05	9.65.E-05	**1.28**	1.66.E-06	7.68.E-06	**0.72**	3.34.E-10	5.40.E-09
LINC01714	**0.79**	3.61.E-01	5.14.E-01	**0.45**	8.08.E-03	1.97.E-02	**1.53**	2.31.E-02	6.69.E-02
METTL5	**0.79**	8.94.E-06	5.04.E-05	**1.08**	1.85.E-01	2.87.E-01	**0.91**	1.23.E-01	2.54.E-01
PSG2	**0.78**	2.51.E-01	NA	**0.80**	4.05.E-01	5.30.E-01	**0.97**	7.62.E-01	NA
ACE	**0.78**	1.43.E-01	NA	**0.75**	1.62.E-01	NA	**1.41**	2.07.E-02	6.14.E-02
DECR1	**0.78**	2.47.E-05	1.30.E-04	**1.06**	2.94.E-01	4.16.E-01	**0.86**	1.31.E-02	4.17.E-02
C1ORF216	**0.78**	1.57.E-04	7.07.E-04	**1.03**	7.09.E-01	7.97.E-01	**0.87**	3.15.E-02	8.66.E-02
SLC14A1	**0.78**	2.41.E-01	3.82.E-01	**0.69**	9.11.E-02	1.61.E-01	**1.01**	9.73.E-01	9.89.E-01
LINC01600	**0.78**	2.05.E-01	NA	**1.24**	4.61.E-01	5.84.E-01	**1.35**	1.28.E-01	2.62.E-01
LINC00592	**0.78**	3.46.E-01	4.99.E-01	**0.83**	5.52.E-01	6.66.E-01	**0.83**	2.61.E-01	4.42.E-01
TMTC2	**0.78**	1.29.E-02	3.53.E-02	**0.98**	8.50.E-01	8.99.E-01	**1.21**	4.03.E-02	1.05.E-01
TNXB	**0.78**	1.19.E-02	3.30.E-02	**0.78**	3.40.E-02	6.95.E-02	**0.72**	6.63.E-03	2.37.E-02
SCRN2	**0.77**	4.00.E-04	1.64.E-03	**0.80**	1.27.E-02	2.94.E-02	**1.11**	2.19.E-01	3.91.E-01
LOC100507600	**0.77**	8.87.E-02	1.76.E-01	**0.71**	4.14.E-02	8.23.E-02	**1.11**	5.22.E-01	7.00.E-01
GSG1	**0.76**	2.91.E-01	4.40.E-01	**2.15**	5.99.E-03	1.51.E-02	**1.05**	8.02.E-01	8.93.E-01
LYRM9	**0.76**	2.91.E-01	4.39.E-01	**0.66**	1.67.E-01	2.65.E-01	**0.94**	6.99.E-01	8.28.E-01
DAGLA	**0.76**	1.90.E-03	6.64.E-03	**1.13**	1.98.E-01	3.04.E-01	**1.09**	3.64.E-01	5.54.E-01
UTAT33	**0.75**	2.79.E-01	4.26.E-01	**1.25**	4.61.E-01	5.83.E-01	**0.85**	3.96.E-01	5.85.E-01
MUC4	**0.75**	1.51.E-01	NA	**0.68**	9.11.E-02	NA	**1.01**	8.55.E-01	NA
KCTD14	**0.75**	6.69.E-02	1.39.E-01	**0.64**	1.68.E-02	3.76.E-02	**0.86**	3.88.E-01	5.77.E-01
MIR29B2	**0.75**	1.48.E-01	NA	**1.07**	8.13.E-01	8.74.E-01	**1.00**	9.99.E-01	1.00.E+00
TDRD7	**0.74**	8.82.E-08	6.77.E-07	**0.62**	1.35.E-15	1.53.E-14	**1.10**	1.78.E-01	3.36.E-01
FAM107B	**0.74**	3.71.E-10	3.75.E-09	**0.48**	5.04.E-43	2.24.E-41	**2.03**	3.28.E-33	3.49.E-31
SVILP1	**0.74**	1.85.E-01	3.14.E-01	**0.64**	1.06.E-01	1.83.E-01	**1.06**	6.20.E-01	NA
IRF6	**0.74**	2.30.E-01	3.70.E-01	**0.64**	1.12.E-01	1.91.E-01	**0.91**	6.25.E-01	7.78.E-01
SARDH	**0.73**	2.69.E-04	1.15.E-03	**0.44**	9.42.E-13	8.56.E-12	**1.15**	2.65.E-01	4.47.E-01
TMEM40	**0.73**	2.33.E-01	3.73.E-01	**0.86**	6.30.E-01	7.33.E-01	**1.11**	5.88.E-01	7.50.E-01
MVP	**0.73**	1.58.E-10	1.66.E-09	**0.53**	9.88.E-27	2.25.E-25	**1.49**	4.19.E-08	4.90.E-07
LAPTM5	**0.72**	3.14.E-10	3.20.E-09	**0.35**	8.36.E-71	7.67.E-69	**1.09**	1.84.E-01	3.44.E-01
LOC285847	**0.72**	1.63.E-01	2.84.E-01	**1.21**	4.03.E-01	5.28.E-01	**1.04**	8.33.E-01	9.14.E-01
FLJ42351	**0.72**	1.42.E-01	2.55.E-01	**1.05**	8.44.E-01	8.95.E-01	**1.35**	9.51.E-02	2.09.E-01
LIMK1	**0.72**	2.43.E-10	2.50.E-09	**0.46**	6.96.E-30	1.85.E-28	**0.93**	3.70.E-01	5.60.E-01
STX3	**0.72**	4.37.E-13	5.85.E-12	**0.90**	3.04.E-02	6.33.E-02	**1.32**	5.32.E-08	6.12.E-07
CCDC144B	**0.71**	9.78.E-05	4.57.E-04	**0.49**	1.26.E-13	1.23.E-12	**2.40**	1.62.E-20	7.46.E-19
SHC3	**0.71**	4.39.E-09	3.94.E-08	**1.48**	6.82.E-12	5.66.E-11	**0.86**	3.83.E-03	1.47.E-02
MIR5010	**0.71**	1.96.E-01	3.28.E-01	**0.91**	7.52.E-01	8.28.E-01	**1.07**	7.56.E-01	8.65.E-01
PIK3R3	**0.71**	7.33.E-08	5.70.E-07	**0.44**	1.46.E-31	4.28.E-30	**1.27**	3.02.E-03	1.19.E-02
MYO7A	**0.70**	9.05.E-02	1.78.E-01	**1.43**	6.73.E-02	1.24.E-01	**0.85**	3.24.E-01	5.12.E-01
SGPP1	**0.70**	9.02.E-07	6.02.E-06	**1.01**	9.10.E-01	9.41.E-01	**0.75**	4.46.E-05	2.88.E-04
ST6GALNAC4	**0.70**	4.49.E-07	3.15.E-06	**0.49**	1.53.E-14	1.61.E-13	**1.06**	5.86.E-01	7.48.E-01
LNX1-AS2	**0.70**	1.77.E-01	3.04.E-01	**0.69**	2.11.E-01	3.20.E-01	**1.06**	7.53.E-01	8.63.E-01
BRI3	**0.69**	6.11.E-09	5.40.E-08	**0.99**	9.36.E-01	9.59.E-01	**0.78**	6.84.E-05	4.24.E-04
PRDM12	**0.69**	1.63.E-01	2.85.E-01	**0.76**	3.63.E-01	4.88.E-01	**1.36**	1.19.E-01	2.48.E-01
FAM131C	**0.69**	5.80.E-02	NA	**1.11**	7.25.E-01	8.08.E-01	**0.96**	8.21.E-01	9.06.E-01

SPAG9	**0.69**	4.30.E-20	9.18.E-19	**0.75**	4.62.E-12	3.89.E-11	**1.30**	1.65.E-07	1.74.E-06
ZNF702P	**0.67**	3.72.E-08	2.98.E-07	**0.11**	3.27.E-100	5.33.E-98	**3.34**	1.34.E-24	8.59.E-23
CCDC197	**0.67**	9.37.E-02	1.83.E-01	**0.72**	2.57.E-01	3.73.E-01	**0.90**	3.10.E-01	NA
NECTIN4	**0.66**	1.16.E-01	2.16.E-01	**0.32**	1.51.E-04	5.21.E-04	**1.03**	6.42.E-01	NA
EDN2	**0.66**	9.75.E-02	1.89.E-01	**0.24**	2.32.E-06	1.05.E-05	**1.23**	1.28.E-01	NA
EFCAB7	**0.65**	3.46.E-05	1.77.E-04	**0.70**	8.48.E-04	2.54.E-03	**1.18**	1.58.E-01	3.08.E-01
LINC00853	**0.65**	1.01.E-01	1.94.E-01	**0.63**	1.26.E-01	2.11.E-01	**1.16**	4.51.E-01	6.37.E-01
GINM1	**0.65**	9.85.E-13	1.29.E-11	**0.60**	5.15.E-15	5.59.E-14	**1.16**	3.61.E-02	9.63.E-02
PLA2G4C	**0.65**	6.50.E-03	1.96.E-02	**0.66**	1.17.E-02	2.73.E-02	**0.83**	2.42.E-01	4.20.E-01
TTC39A	**0.64**	2.11.E-02	5.36.E-02	**1.21**	2.87.E-01	4.08.E-01	**0.90**	5.41.E-01	7.13.E-01
NQO2	**0.64**	1.79.E-15	2.86.E-14	**0.75**	8.55.E-07	4.10.E-06	**1.08**	1.63.E-01	3.16.E-01
SOCS2	**0.64**	6.09.E-10	6.05.E-09	**1.31**	2.41.E-05	9.49.E-05	**0.80**	5.81.E-04	2.86.E-03
GPC1	**0.64**	3.30.E-05	1.70.E-04	**0.31**	1.26.E-17	1.64.E-16	**1.45**	1.44.E-02	4.53.E-02
ACBD4	**0.64**	1.79.E-06	1.14.E-05	**0.64**	7.18.E-06	3.04.E-05	**1.15**	2.16.E-01	3.87.E-01
CARD19	**0.63**	9.85.E-09	8.47.E-08	**0.44**	6.46.E-15	6.98.E-14	**1.57**	1.34.E-06	1.18.E-05
CCND3	**0.63**	5.09.E-17	8.91.E-16	**0.42**	2.66.E-49	1.48.E-47	**1.06**	3.46.E-01	5.35.E-01
LEXM	**0.62**	4.85.E-02	1.07.E-01	**0.68**	1.77.E-01	2.78.E-01	**1.03**	8.19.E-01	NA
CSMD3	**0.62**	6.22.E-02	1.31.E-01	**0.51**	2.36.E-02	5.07.E-02	**1.34**	1.43.E-01	2.86.E-01
RAB13	**0.61**	2.45.E-03	8.31.E-03	**0.68**	1.55.E-04	5.31.E-04	**0.88**	5.66.E-02	1.39.E-01
PSCA	**0.61**	4.79.E-02	1.06.E-01	**0.87**	5.69.E-01	6.81.E-01	**2.43**	1.13.E-06	1.01.E-05
GSTA4	**0.61**	3.60.E-07	2.56.E-06	**1.53**	3.44.E-07	1.74.E-06	**0.77**	2.95.E-03	1.17.E-02
MEST	**0.60**	5.71.E-09	5.06.E-08	**0.79**	6.48.E-03	1.62.E-02	**0.44**	1.10.E-17	4.00.E-16
MIR4506	**0.60**	1.98.E-02	5.09.E-02	**0.58**	4.80.E-02	9.36.E-02	**1.00**	9.51.E-01	NA
PAK1	**0.60**	2.89.E-21	6.57.E-20	**0.84**	1.72.E-03	4.87.E-03	**0.79**	1.77.E-04	9.86.E-04
PSG4	**0.60**	1.64.E-09	1.55.E-08	**0.52**	9.29.E-14	9.24.E-13	**0.36**	1.38.E-17	4.96.E-16
MAPK13	**0.60**	2.15.E-11	2.45.E-10	**0.23**	3.23.E-62	2.48.E-60	**2.04**	1.17.E-18	4.63.E-17
POU2F3	**0.60**	5.12.E-02	1.12.E-01	**0.68**	1.99.E-01	3.05.E-01	**1.00**	9.85.E-01	9.94.E-01
ASIC1	**0.59**	4.76.E-03	1.49.E-02	**0.88**	4.57.E-01	5.80.E-01	**1.10**	5.56.E-01	7.26.E-01
MYO1F	**0.59**	1.44.E-10	1.53.E-09	**0.19**	9.64.E-39	3.65.E-37	**1.92**	3.42.E-06	2.83.E-05
REN	**0.59**	4.33.E-02	9.78.E-02	**0.54**	4.37.E-02	8.62.E-02	**1.18**	3.50.E-01	5.40.E-01
PRNP	**0.58**	9.30.E-40	4.33.E-38	**0.66**	1.34.E-21	2.27.E-20	**0.88**	1.16.E-02	3.77.E-02
RAET1G	**0.58**	7.06.E-06	4.05.E-05	**0.35**	1.89.E-15	2.13.E-14	**1.34**	4.72.E-02	1.20.E-01
PPP1R26-AS1	**0.57**	5.99.E-05	2.93.E-04	**0.59**	2.99.E-04	9.76.E-04	**1.42**	1.71.E-02	5.21.E-02
SLC22A18	**0.56**	2.63.E-04	1.13.E-03	**0.55**	1.95.E-03	5.45.E-03	**1.32**	1.29.E-01	2.64.E-01
TNIP1	**0.56**	4.20.E-43	2.13.E-41	**0.75**	1.30.E-10	9.52.E-10	**1.11**	4.53.E-02	1.16.E-01
CRABP2	**0.56**	1.72.E-03	6.10.E-03	**2.00**	3.08.E-07	1.56.E-06	**0.75**	1.30.E-02	4.15.E-02
OAF	**0.55**	2.39.E-32	8.76.E-31	**0.46**	3.17.E-37	1.13.E-35	**1.22**	4.57.E-03	1.72.E-02
PPM1J	**0.55**	3.01.E-03	1.00.E-02	**0.64**	3.29.E-02	6.76.E-02	**0.98**	9.09.E-01	9.54.E-01
CMBL	**0.54**	2.86.E-16	4.79.E-15	**1.04**	5.98.E-01	7.06.E-01	**0.99**	8.81.E-01	9.40.E-01
PROM2	**0.54**	2.52.E-03	8.55.E-03	**0.17**	1.22.E-11	9.87.E-11	**1.30**	1.67.E-01	3.21.E-01
SOX2	**0.54**	2.08.E-02	5.30.E-02	**0.98**	9.42.E-01	9.63.E-01	**1.04**	8.46.E-01	9.21.E-01
SLC43A3	**0.54**	3.47.E-35	1.39.E-33	**0.77**	1.23.E-06	5.79.E-06	**1.13**	1.82.E-02	5.50.E-02
SYTL2	**0.54**	2.52.E-19	5.14.E-18	**0.31**	5.42.E-50	3.08.E-48	**2.23**	1.29.E-20	5.98.E-19
FLVCR2	**0.54**	6.05.E-04	2.39.E-03	**0.61**	7.43.E-03	1.83.E-02	**1.49**	1.83.E-02	5.51.E-02
LINC01605	**0.53**	6.20.E-19	1.22.E-17	**1.22**	1.96.E-03	5.47.E-03	**0.42**	2.21.E-34	2.48.E-32
VTRNA2-1	**0.53**	1.37.E-02	3.71.E-02	**0.47**	8.66.E-03	2.10.E-02	**1.02**	9.25.E-01	9.62.E-01
CD9	**0.52**	1.65.E-41	8.06.E-40	**0.83**	2.68.E-04	8.83.E-04	**1.41**	3.35.E-10	5.42.E-09
LINC01556	**0.52**	1.10.E-02	3.08.E-02	**0.57**	6.38.E-02	1.19.E-01	**1.00**	9.95.E-01	9.98.E-01
ANXA9	**0.51**	3.29.E-06	2.01.E-05	**0.53**	3.22.E-05	1.24.E-04	**1.01**	9.24.E-01	9.62.E-01
SLC2A5	**0.51**	4.54.E-03	1.43.E-02	**0.17**	1.35.E-09	9.07.E-09	**1.02**	8.60.E-01	NA
CCDC88B	**0.50**	2.39.E-04	1.04.E-03	**0.70**	5.75.E-02	1.09.E-01	**1.01**	9.37.E-01	9.68.E-01

NR6A1	**0.50**	4.34.E-09	3.90.E-08	**0.90**	3.71.E-01	4.96.E-01	**1.18**	1.25.E-01	2.57.E-01
CD96	**0.50**	8.52.E-03	2.47.E-02	**6.97**	6.75.E-21	1.10.E-19	**1.30**	3.88.E-02	1.02.E-01
KCNN4	**0.49**	4.53.E-38	2.00.E-36	**0.76**	4.48.E-05	1.69.E-04	**1.06**	4.96.E-01	6.77.E-01
NES	**0.48**	1.14.E-19	2.35.E-18	**0.45**	1.43.E-22	2.57.E-21	**2.75**	4.57.E-42	7.67.E-40
CHI3L2	**0.48**	4.57.E-03	1.44.E-02	**0.33**	1.77.E-04	6.01.E-04	**1.25**	7.61.E-02	NA
LHX6	**0.47**	9.47.E-05	4.44.E-04	**0.67**	3.17.E-02	6.56.E-02	**0.93**	6.93.E-01	8.25.E-01
TNFAIP3	**0.47**	1.97.E-22	4.87.E-21	**1.09**	2.63.E-01	3.80.E-01	**1.55**	1.88.E-11	3.59.E-10
CST4	**0.45**	6.61.E-42	3.27.E-40	**0.43**	2.10.E-35	6.92.E-34	**0.79**	6.22.E-04	3.03.E-03
LINC01843	**0.44**	3.28.E-04	1.38.E-03	**0.32**	1.12.E-05	4.60.E-05	**1.33**	1.60.E-01	3.11.E-01
SERPINB9P1	**0.43**	4.93.E-04	1.99.E-03	**0.49**	6.28.E-03	1.57.E-02	**1.05**	8.10.E-01	8.98.E-01
ARL4D	**0.42**	4.01.E-28	1.30.E-26	**0.34**	3.32.E-38	1.24.E-36	**1.09**	3.72.E-01	5.62.E-01
RARG	**0.42**	1.58.E-39	7.31.E-38	**0.49**	1.02.E-23	1.96.E-22	**1.34**	1.33.E-04	7.63.E-04
GPRC5B	**0.41**	1.17.E-13	1.65.E-12	**1.20**	9.15.E-02	1.61.E-01	**0.47**	1.01.E-12	2.21.E-11
PLAT	**0.41**	4.45.E-78	5.73.E-76	**0.50**	2.10.E-38	7.86.E-37	**0.87**	1.18.E-02	3.83.E-02
LINC00346	**0.41**	2.08.E-05	1.10.E-04	**0.76**	1.60.E-01	2.56.E-01	**2.08**	1.69.E-06	1.47.E-05
LOC101928994	**0.39**	1.37.E-04	6.21.E-04	**0.49**	6.19.E-03	1.55.E-02	**0.89**	5.61.E-01	7.29.E-01
LOC100507002	**0.39**	6.09.E-16	1.00.E-14	**0.96**	6.86.E-01	7.79.E-01	**1.17**	1.18.E-01	2.46.E-01
GRAMD1C	**0.39**	2.22.E-16	3.72.E-15	**0.88**	2.08.E-01	3.16.E-01	**1.14**	1.97.E-01	3.62.E-01
TGM2	**0.37**	7.94.E-151	2.63.E-148	**0.44**	7.44.E-100	1.20.E-97	**0.57**	5.69.E-27	4.18.E-25
TMCC3	**0.35**	2.58.E-51	1.68.E-49	**0.89**	5.68.E-02	1.08.E-01	**1.39**	2.80.E-08	3.37.E-07
NEURL3	**0.33**	1.48.E-05	8.05.E-05	**0.34**	1.54.E-04	5.29.E-04	**1.53**	3.40.E-02	9.21.E-02
GPR68	**0.33**	7.58.E-66	6.93.E-64	**0.43**	7.04.E-34	2.21.E-32	**1.04**	6.26.E-01	7.78.E-01
OTUB2	**0.31**	6.83.E-67	6.44.E-65	**0.39**	1.80.E-57	1.23.E-55	**1.40**	6.14.E-08	7.00.E-07
PARP14	**0.31**	3.89.E-115	9.40.E-113	**0.48**	7.17.E-45	3.40.E-43	**0.90**	5.55.E-02	1.37.E-01
AQP3	**0.30**	1.33.E-32	4.99.E-31	**0.20**	4.24.E-35	1.38.E-33	**1.11**	5.21.E-01	6.99.E-01
S100A2	**0.28**	6.88.E-69	7.07.E-67	**0.35**	1.16.E-48	6.32.E-47	**0.44**	1.77.E-25	1.19.E-23
LINC01693	**0.28**	1.04.E-07	7.89.E-07	**0.21**	4.62.E-09	2.93.E-08	**1.13**	5.12.E-01	6.92.E-01
RARB	**0.25**	4.22.E-65	3.81.E-63	**0.03**	3.19.E-147	1.08.E-144	**2.08**	2.02.E-05	1.42.E-04
GIMAP8	**0.24**	9.09.E-08	6.97.E-07	**0.20**	1.67.E-07	8.75.E-07	**1.14**	1.94.E-01	NA
SPOCD1	**0.24**	1.40.E-55	9.99.E-54	**0.32**	3.55.E-36	1.21.E-34	**1.33**	7.19.E-03	2.54.E-02
IGFBP6	**0.24**	3.37.E-98	6.49.E-96	**0.20**	3.68.E-115	8.10.E-113	**1.50**	5.97.E-07	5.65.E-06
C15ORF48	**0.20**	2.26.E-267	2.70.E-264	**0.09**	0.00.E+00	0.00.E+00	**0.86**	4.28.E-02	1.11.E-01
SOST	**0.18**	2.01.E-13	2.77.E-12	**0.09**	1.48.E-18	2.07.E-17	**1.70**	3.59.E-03	1.39.E-02
SPNS2	**0.18**	3.10.E-69	3.21.E-67	**2.49**	4.19.E-25	8.70.E-24	**0.87**	9.67.E-02	2.11.E-01
IL1R1	**0.16**	2.54.E-77	3.20.E-75	**0.10**	5.69.E-90	7.70.E-88	**1.96**	1.54.E-06	1.35.E-05
TRPV2	**0.15**	1.12.E-41	5.51.E-40	**0.29**	4.06.E-22	7.12.E-21	**2.61**	6.50.E-14	1.63.E-12
PLB1	**0.12**	3.68.E-66	3.38.E-64	**0.13**	8.16.E-59	5.78.E-57	**2.89**	3.62.E-14	9.44.E-13
DHRS3	**0.07**	2.35.E-51	1.54.E-49	**0.06**	2.14.E-47	1.11.E-45	**0.91**	6.47.E-01	7.93.E-01
ZNRD1ASP	**NA**	NA	NA	**NA**	NA	NA	**NA**	NA	NA
ZNF433-AS1	**NA**	NA	NA	**NA**	NA	NA	**NA**	NA	NA
TEKT4	**NA**	NA	NA	**NA**	NA	NA	**1.01**	8.55.E-01	NA
TAS2R38	**NA**	NA	NA	**NA**	NA	NA	**1.03**	6.42.E-01	NA
SCNN1G	**NA**	NA	NA	**NA**	NA	NA	**NA**	NA	NA
OR2V2	**NA**	NA	NA	**NA**	NA	NA	**NA**	NA	NA
OR2A14	**NA**	NA	NA	**NA**	NA	NA	**1.01**	8.55.E-01	NA
MIR8079	**NA**	NA	NA	**NA**	NA	NA	**NA**	NA	NA
MIR6088	**NA**	NA	NA	**1.06**	6.33.E-01	NA	**0.97**	7.17.E-01	NA
MIR5703	**NA**	NA	NA	**NA**	NA	NA	**1.02**	6.76.E-01	NA
MIR548D2	**NA**	NA	NA	**NA**	NA	NA	**NA**	NA	NA
MIR4751	**NA**	NA	NA	**NA**	NA	NA	**NA**	NA	NA
MIR4478	**NA**	NA	NA	**NA**	NA	NA	**NA**	NA	NA

MIR4472-2	**NA**	NA	NA	**NA**	NA	NA	**NA**	NA	NA
MIR4267	**NA**	NA	NA	**NA**	NA	NA	**NA**	NA	NA
MIR3972	**NA**	NA	NA	**1.03**	8.23.E-01	NA	**0.98**	7.72.E-01	NA
MIR373	**NA**	NA	NA	**NA**	NA	NA	**NA**	NA	NA
MIR129-1	**NA**	NA	NA	**NA**	NA	NA	**NA**	NA	NA
LOC392364	**NA**	NA	NA	**NA**	NA	NA	**NA**	NA	NA
LOC102724357	**NA**	NA	NA	**NA**	NA	NA	**NA**	NA	NA
LOC101929488	**NA**	NA	NA	**NA**	NA	NA	**NA**	NA	NA
LOC101929163	**NA**	NA	NA	**NA**	NA	NA	**NA**	NA	NA
LOC101928398	**NA**	NA	NA	**NA**	NA	NA	**NA**	NA	NA
LINC02274	**NA**	NA	NA	**NA**	NA	NA	**NA**	NA	NA
LINC02197	**NA**	NA	NA	**NA**	NA	NA	**NA**	NA	NA
LINC01983	**NA**	NA	NA	**NA**	NA	NA	**NA**	NA	NA
LINC01460	**NA**	NA	NA	**NA**	NA	NA	**NA**	NA	NA
LINC01405	**NA**	NA	NA	**NA**	NA	NA	**NA**	NA	NA
LINC01101	**NA**	NA	NA	**NA**	NA	NA	**NA**	NA	NA
KRT28	**NA**	NA	NA	**NA**	NA	NA	**NA**	NA	NA
KCNJ18	**NA**	NA	NA	**NA**	NA	NA	**1.03**	6.68.E-01	NA
CTD-3080P12.3	**NA**	NA	NA	**NA**	NA	NA	**NA**	NA	NA
CMTM5	**NA**	NA	NA	**NA**	NA	NA	**NA**	NA	NA
CCL1	**NA**	NA	NA	**NA**	NA	NA	**NA**	NA	NA
C19ORF33	**NA**	NA	NA	**NA**	NA	NA	**NA**	NA	NA
BSND	**NA**	NA	NA	**NA**	NA	NA	**1.01**	8.55.E-01	NA
ADAM6	**NA**	NA	NA	**NA**	NA	NA	**NA**	NA	NA
LOC107001062	**NA**	NA	NA	**NA**	NA	NA	**NA**	NA	NA
SNORD141B	**NA**	NA	NA	**NA**	NA	NA	**NA**	NA	NA
LINC01173	**NA**	NA	NA	**NA**	NA	NA	**NA**	NA	NA
LOC105379194	**NA**	NA	NA	**NA**	NA	NA	**NA**	NA	NA
LOC105375843	**NA**	NA	NA	**NA**	NA	NA	**NA**	NA	NA
LOC105375304	**NA**	NA	NA	**NA**	NA	NA	**NA**	NA	NA
HCG20	**NA**	NA	NA	**NA**	NA	NA	**NA**	NA	NA
LINC02029	**NA**	NA	NA	**NA**	NA	NA	**NA**	NA	NA
LOC105370526	**NA**	NA	NA	**NA**	NA	NA	**NA**	NA	NA
GTF2IP7	**NA**	NA	NA	**NA**	NA	NA	**NA**	NA	NA

Supplemental Table S5. Novel "oncogenes" bound by p27-cJun and upregulated only in 231 p27CK-DD and 1833 (See Figure 7D).

	231DD vs. 231	231DD vs. 231	231DD vs. 231	1833 vs. 231	1833 vs. 231	1833 vs. 231		231DD vs. 231	231DD vs. 231	231DD vs. 231	1833 vs. 231	1833 vs. 231	1833 vs. 231
Gene ID (61 genes)	Fold Change	p value	q value	Fold Change	p value	q value	Gene ID (43 genes)	Fold Change	p value	q value	Fold Change	p value	q value
AMTN	22.35	3.E-72	4.E-70	2.03	9.E-03	2.E-02	SERPINE1	9.84	0.E+00	0.E+00	4.77	2.E-107	3.E-105
CGB8	13.25	4.E-42	2.E-40	3.69	5.E-07	2.E-06	FLRT2	6.50	5.E-143	2.E-140	7.01	1.E-143	3.E-141
COL1A1	9.10	4.E-68	4.E-66	3.27	2.E-14	2.E-13	ADAMTS1	4.43	5.E-172	2.E-169	6.50	0.E+00	0.E+00
LOC100507487	7.83	9.E-61	7.E-59	2.86	1.E-10	9.E-10	PIK3IP1	4.04	4.E-52	3.E-50	1.77	8.E-07	4.E-06
ANGPTL4	6.22	4.E-142	1.E-139	2.28	6.E-22	1.E-20	SPSB1	3.15	1.E-78	2.E-76	2.51	5.E-44	2.E-42
THBS1	5.87	8.E-259	9.E-256	1.80	2.E-16	3.E-15	ADAM19	3.14	6.E-64	5.E-62	1.60	4.E-09	2.E-08
CGB5	5.59	3.E-12	3.E-11	2.08	2.E-02	4.E-02	SNAI1	2.99	2.E-09	2.E-08	1.63	3.E-02	5.E-02
EDN1	5.56	2.E-231	2.E-228	4.12	6.E-109	1.E-106	JAG1	2.73	1.E-75	2.E-73	1.77	3.E-23	5.E-22
DPYSL3	4.48	2.E-22	5.E-21	4.91	7.E-25	1.E-23	STARD13	2.54	7.E-61	6.E-59	1.90	6.E-23	1.E-21
GADD45B	4.29	2.E-114	4.E-112	1.90	6.E-21	1.E-19	TRIML2	2.53	5.E-39	3.E-37	2.11	4.E-23	8.E-22
MYH16	4.05	3.E-27	1.E-25	3.39	4.E-18	6.E-17	PRKCQ	2.51	3.E-10	3.E-09	2.26	2.E-07	1.E-06
KCNA7	4.04	7.E-08	6.E-07	2.39	4.E-03	1.E-02	LINC01117	2.49	2.E-06	2.E-05	2.93	6.E-08	3.E-07
LINC00452	3.97	4.E-44	2.E-42	3.49	8.E-31	2.E-29	GALNT16	2.45	2.E-09	2.E-08	2.28	3.E-07	2.E-06
MXRA8	3.40	1.E-47	7.E-46	1.73	2.E-07	1.E-06	ARHGEF18	2.41	9.E-105	2.E-102	1.60	9.E-23	2.E-21
ADAMTS7	3.33	2.E-11	2.E-10	1.69	2.E-02	3.E-02	PAWR	2.29	8.E-72	9.E-70	1.54	3.E-18	4.E-17
FAT1	3.25	1.E-73	2.E-71	1.69	6.E-15	7.E-14	SCD	2.17	6.E-33	2.E-31	1.61	1.E-12	9.E-12
INPP4B	3.21	1.E-120	3.E-118	2.05	5.E-37	2.E-35	ERC2	2.17	1.E-07	1.E-06	1.53	1.E-02	3.E-02
HMOX1	3.00	5.E-60	4.E-58	2.52	4.E-28	1.E-26	MIR137HG	2.05	3.E-07	2.E-06	2.58	1.E-11	1.E-10
NUAK1	2.98	3.E-135	1.E-132	1.74	2.E-30	7.E-29	MOB3B	2.02	2.E-06	1.E-05	2.31	5.E-09	3.E-08
MYO10	2.72	1.E-32	5.E-31	2.07	2.E-17	2.E-16	LOC339059	2.00	1.E-03	5.E-03	2.01	3.E-03	7.E-03
DDB2	2.60	4.E-68	4.E-66	1.58	9.E-14	9.E-13	LOC100270746	1.97	9.E-05	4.E-04	1.62	1.E-02	3.E-02
PDGFC	2.59	2.E-97	5.E-95	2.47	1.E-78	1.E-76	ATXN7L2	1.91	3.E-09	3.E-08	1.99	7.E-12	6.E-11
PLEK2	2.51	1.E-57	8.E-56	3.24	5.E-108	1.E-105	CYP51A1	1.90	2.E-49	1.E-47	1.95	9.E-42	4.E-40
DTX4	2.48	7.E-06	4.E-05	2.18	6.E-04	2.E-03	PGRMC2	1.89	1.E-22	3.E-21	1.66	2.E-13	2.E-12
ZFP69B	2.43	7.E-20	2.E-18	1.86	6.E-09	4.E-08	FOSB	1.81	2.E-03	6.E-03	2.61	7.E-07	3.E-06
LTBP4	2.31	9.E-35	4.E-33	1.52	6.E-04	2.E-03	ARAP3	1.76	3.E-12	4.E-11	1.55	2.E-07	9.E-07
MYOM3	2.22	6.E-05	3.E-04	2.01	8.E-04	2.E-03	IGF1R	1.75	8.E-03	2.E-02	1.60	2.E-02	5.E-02
MIR100HG	2.19	4.E-51	3.E-49	1.56	3.E-16	3.E-15	NOCT	1.74	1.E-18	2.E-17	1.86	4.E-21	6.E-20
LRFN5	2.19	2.E-03	7.E-03	3.77	1.E-05	5.E-05	KLHL32	1.73	4.E-02	9.E-02	2.18	8.E-03	2.E-02
ADGRL1	2.11	9.E-23	2.E-21	1.73	9.E-11	7.E-10	DDI2	1.71	7.E-09	6.E-08	1.63	3.E-07	2.E-06
HLX	2.09	2.E-08	2.E-07	1.55	3.E-03	8.E-03	LMCD1-AS1	1.70	4.E-02	1.E-01	1.85	4.E-02	8.E-02
LOC101928279	2.03	7.E-04	3.E-03	5.04	4.E-18	5.E-17	PPRC1	1.65	5.E-11	6.E-10	1.53	8.E-08	4.E-07
LY6G5C	2.03	2.E-03	8.E-03	2.78	1.E-05	6.E-05	SETD7	1.61	4.E-24	1.E-22	1.91	3.E-44	1.E-42
HIVEP1	2.00	3.E-20	6.E-19	1.75	4.E-13	4.E-12	SETD1A	1.60	3.E-05	1.E-04	1.75	3.E-07	2.E-06
ZFP36L1	1.98	9.E-23	2.E-21	2.07	9.E-26	2.E-24	NHEJ1	1.59	4.E-13	5.E-12	1.55	1.E-10	8.E-10
COL27A1	1.96	8.E-25	2.E-23	2.05	4.E-17	4.E-16	FADS2	1.58	2.E-22	6.E-21	1.55	9.E-18	1.E-16

TNFRSF10D	**1.92**	5.E-38	2.E-36	**2.53**	1.E-72	1.E-70	**ADGRV1**	**1.55**	7.E-10	7.E-09	**1.83**	1.E-17	1.E-16
C11orf91	**1.89**	3.E-08	3.E-07	**1.58**	4.E-04	1.E-03	**JADE1**	**1.53**	7.E-16	1.E-14	**2.12**	2.E-48	9.E-47
LINC00513	**1.88**	4.E-03	1.E-02	**2.20**	1.E-03	3.E-03	**PSTK**	**1.53**	3.E-06	2.E-05	**1.54**	3.E-06	1.E-05
EGFR-AS1	**1.88**	2.E-06	2.E-05	**2.63**	2.E-13	2.E-12	**AGAP4**	**1.52**	5.E-04	2.E-03	**1.50**	1.E-03	3.E-03
MICALCL	**1.85**	4.E-04	2.E-03	**1.59**	1.E-02	3.E-02	**SLFN12**	**1.52**	2.E-11	2.E-10	**1.55**	1.E-10	9.E-10
MIR23A	**1.85**	3.E-04	1.E-03	**1.59**	2.E-02	4.E-02	**HNRNPD**	**1.52**	3.E-06	2.E-05	**1.62**	7.E-09	4.E-08
MKRN3	**1.84**	5.E-06	3.E-05	**1.79**	5.E-05	2.E-04	**SORBS1**	**1.50**	2.E-02	4.E-02	**3.24**	6.E-15	6.E-14
FSCN1	**1.79**	4.E-20	8.E-19	**2.12**	5.E-19	8.E-18							
CMIP	**1.73**	2.E-09	2.E-08	**2.07**	5.E-15	6.E-14							
CPNE4	**1.66**	5.E-02	1.E-01	**4.53**	3.E-07	2.E-06							
FAM43A	**1.64**	6.E-08	5.E-07	**2.25**	7.E-17	9.E-16							
OLFM2	**1.64**	5.E-02	1.E-01	**1.74**	4.E-02	8.E-02							
SCN5A	**1.63**	2.E-14	2.E-13	**1.74**	4.E-17	4.E-16							
MIR17HG	**1.62**	5.E-08	4.E-07	**1.83**	6.E-13	6.E-12							
ADRA1B	**1.60**	5.E-05	2.E-04	**1.59**	9.E-05	3.E-04							
WDR38	**1.59**	3.E-02	7.E-02	**1.81**	8.E-03	2.E-02							
LOC100287036	**1.58**	2.E-04	7.E-04	**4.35**	4.E-43	2.E-41							
ELK3	**1.58**	3.E-17	5.E-16	**1.79**	8.E-28	2.E-26							
UBE4B	**1.58**	3.E-12	4.E-11	**1.79**	4.E-19	5.E-18							
MAP2	**1.56**	2.E-02	5.E-02	**1.75**	6.E-03	2.E-02							
KLHL21	**1.56**	7.E-17	1.E-15	**1.74**	2.E-19	3.E-18							
NXPH4	**1.56**	4.E-02	1.E-01	**3.51**	4.E-10	3.E-09							
BEST3	**1.55**	3.E-02	6.E-02	**1.76**	5.E-03	1.E-02							
PTPN21	**1.54**	3.E-14	4.E-13	**1.75**	2.E-21	3.E-20							
LOC440028	**1.51**	8.E-03	2.E-02	**2.53**	8.E-10	6.E-09							

Supplemental Table S6. Reagents and		
REAGENT or RESOURCE	**SOURCE**	**IDENTIFIER**
Antibodies		
p27 Kip1 (Mouse IgG1)	BD Transduction	610241
p27 (D69C12, Rabbit mAB)	Cell Signaling	3686S
Phospho-p27/Kip1 (T198, Polyclonal Rabbit IgG)	R&D Systems	AF3994
E-cadherin (Mouse IgG2a)	BD Transduction	610182
N-cadherin (Mouse IgG1)	BD Transduction	610920
Vimentin (5G3F10, Mouse mAB)	Cell Signaling	3390S
TGF beta2 (Mouse monoclonal)	abcam	ab36495
Phospho-c-Jun (Ser63, Rabbit IgG)	Cell Signaling	2361S
c-Jun (60A8, Rabbit mAB)	Cell Signaling	9165S
Phospho-Akt (Ser473, Rabbit IgG)	Cell Signaling	9271S
Akt (Rabbit IgG)	Cell Signaling	9272S
JNK (D-2, Mouse IgG1)	Santa Cruz	sc-7435
Beta-tubulin (9F3, Rabbit mAB)	Cell Signaling	2128S
Lamin B2 (D8P3U, Rabbit mAB)	Cell Signaling	12255S
Beta-actin (AC-15, Mouse monoclonal)	Sigma-Aldrich	A1978
H3K27AC (Mouse mAB)	Active Motif	39685
Acetyl-CBP (Lys1535)/p300 (Lys1499, Rabbit IgG)	Cell Signaling	4771S
Pol II (C-21, Rabbit polyclonal IgG)	Santa Cruz	sc-900
Normal mouse IgG	Santa Cruz	sc-2025
Normal rabbit IgG	Santa Cruz	sc-2027
Anti-Mouse IgG (H+L), HRP Conjugate	Promega	W402B
Anti-Rabbit IgG (H+L), HRP Conjugate	Promega	W401B
p27 Kip1 (Mouse IgG1)	BD Transduction	610241
Bacterial and Virus Strains		
N/A		
Biological Samples		
N/A		
Chemicals, Peptides, and Recombinant Proteins		
PF-04691502	Sigma-Aldrich	PZ0235
Lipofectamine 3000 Reagent	Invitrogen	L3000015
High Sensitivity D1000 Reagent	Agilent Technologies	5067-5585
iQ™ SYBR® Green Supermix	BIO-RAD	1708884
TGFB2	Thermo Fisher	PHG9114
Critical Commercial Assays		
Proteome Profiler Human Phospho-Kinase Array	R&D Systems	ARY003
Duolink proximity ligation assay (PLA) kit	Sigma-Aldrich	DUO92101
IRDye 700 AP-1 consensus oligonucleotide	LI-COR	P/N 829-07925
Odyssey EMSA Buffer Kit	LI-COR	P/N 829-07910
NE-PER™ Nuclear and Cytoplasmic Extraction Reagents	Thermo Fisher	78833
NEBNext® Ultra™ DNA Library Prep Kit	NEB	E7370L
High Sensitivity D1000 Screen Tape	Agilent Technologies	5067-5584
TGF beta-2 Human ELISA Kit	Thermo Fisher	EHTGFB2

High Sensitivity Chromatin Preparation	Active Motif	53046
ImmPRESS™ HRP REAGENT KIT	VECTOR	MP-7402
DAB Peroxidase Substractrate Kit	VECTOR	SK-4100
ChIP-IT High Sensitivity	Active Motif	53040
Deposited Data		
Mendeley Data	This paper	http://dx.doi.org/10.17632/bk69wrp755.1
Kaplan-Meier (KM) Plotter	KM Plotter	https://kmplot.com
Encyclopedia of DNA Elements (ENCODE)	ENCODE	https://encodeproject.org
Experimental Models: Cell Lines		
MDA-MB-231, Luciferase conjugate	J. Massague (Minn AJ. et al., 2005)	N/A
MDA-MB-231-p27CK-DD, Luciferase conjugate	J.M. Slingerland (Zhao D. et al., 2015)	N/A
MDA-MB-231-1833, Luciferase conjugate	J. Massague (Minn AJ. et al., 2005)	N/A
UMUC3, Luciferase conjugate	(Nitz MD. et al., 2008)	N/A
UMUC3-p27CK-DD, Luciferase conjugate	J.M. Slingerland (Zhao D. et al., 2015)	N/A
UMUC3-LuL2, Luciferase conjugate	(Nitz MD. et al., 2008)	N/A
MCF-12A	ATCC	CRL-10782
Experimental Models: Organisms/Strains		
NOD *scid* gamma, NSG	The Jackson Laboratory	005557
Oligonucleotides		
QPCR Primer CDKN1B-Forward: TAGCGGAGCAATGCGCAGGA	J.M. Slingerland (Zhao D. et al., 2015)	N/A
QPCR Primer CDKN1B-Reverse: AACCGGCATTTGGGGAACCGT	J.M. Slingerland (Zhao D. et al., 2015)	N/A
QPCR Primer CDH1-Forward: AATTCCTGCCATTCTGGGGA	J.M. Slingerland (Zhao D. et al., 2015)	N/A
QPCR Primer CDH1-Reverse: TCTTCTCCGCCTCCTTCTTC	J.M. Slingerland (Zhao D. et al., 2015)	N/A
QPCR Primer SNAI1-Forward: ACCCCACATCCTTCTCACTG	J.M. Slingerland (Zhao D. et al., 2015)	N/A
QPCR Primer SNAI1-Reverse: TACAAAAACCCACGCAGACA	J.M. Slingerland (Zhao D. et al., 2015)	N/A

QPCR Primer SNAI2-Forward: TGCGATGCCCAGTCTAGAAA	J.M. Slingerland (Zhao D. et al., 2015)	N/A
QPCR Primer SNAI2-Reverse: TTCTCCCCCGTGTGAGTTC	J.M. Slingerland (Zhao D. et al., 2015)	N/A
QPCR Primer ZEB2-Forward: AGGGACAGATCAGCACCAAA	J.M. Slingerland (Zhao D. et al., 2015)	N/A
QPCR Primer ZEB2-Reverse: GTGCGAACTGTAGGAACCAG	J.M. Slingerland (Zhao D. et al., 2015)	N/A
QPCR Primer TWIST1-Forward: GTCCGCAGTCTTACGAGGAG	J.M. Slingerland (Zhao D. et al., 2015)	N/A
QPCR Primer TWIST1-Reverse: GCTTGAGGGTCTGAATCTTGCT	J.M. Slingerland (Zhao D. et al., 2015)	N/A
QPCR Primer TGFB2-Forward: CCATCCCGCCCACTTTCTAC	This paper	N/A
QPCR Primer TGFB2-Reverse: AGCTCAATCCGTTGTTCAGGC	This paper	N/A
QPCR Primer MYO10-Forward: AGGAGGAAGTTCGGGAAGTG	This paper	N/A
QPCR Primer MYO10-Reverse: CATCTGTGAGCTGTGTTGGG	This paper	N/A
QPCR Primer SERPINE1-Forward: TCTGCCCTCACCAACATTCT	This paper	N/A
QPCR Primer SERPINE1-Reverse: CGGTCATTCCCAGGTTCTCT	This paper	N/A
QPCR Primer KLF8-Forward: TGGAACCAGTTGACCTCTCC	This paper	N/A
QPCR Primer KLF8-Reverse: TGAGAGGAGGTCAGGACAGA	This paper	N/A
QPCR Primer GAPDH-Forward: ACCCAGAAGACTGTGGATGG	J.M. Slingerland (Zhao D. et al., 2015)	N/A
QPCR Primer GAPDH-Reverse: TCTAGACGGCAGGTCAGGTC	J.M. Slingerland (Zhao D. et al., 2015)	N/A
ChIP Primer TGFB2-Forward: CCACAAGGTGGTACTGTTGTAC	This paper	N/A
ChIP Primer TGFB2-Reverse: GCTCACTGCCTGACCCAATC	This paper	N/A
ChIP Primer MYO10-Forward: AGGCTACAGGAGGAGTGAGA	This paper	N/A
ChIP Primer MYO10-Reverse: TGTAAGAAAACGGAGGCCCT	This paper	N/A
ChIP Primer SERPINE1-Forward: GGGAGCTGAGCATTTGACTG	This paper	N/A

ChIP Primer SERPINE1-Reverse: GCTCCCTTCTCTCTGACCTC	This paper	N/A
ChIP Primer KLF8-Forward: GCAGCCCAGTATTCAAGCTC	This paper	N/A
ChIP Primer KLF8-Reverse: GCTGGCGGACATAATCTTGG	This paper	N/A
ChIP Primer Negative1-Forward: CCTGGGAACTGGTGCCTACT	This paper	N/A
ChIP Primer Negative1-Reverse: CCATGGCCTCAACCTCACTG	This paper	N/A
ChIP Primer Negative2-Forward: GAGACGGGGTTTCACCATGT	This paper	N/A
ChIP Primer Negative2-Reverse: AAGTTGAAATCTGGGCCGGG	This paper	N/A
p27 siRNA (h2)	Santa Cruz	sc-44215
Recombinant DNA		
pLVX-EF1α-AcGFP	S. Dowdy	N/A
pLVX-EF1α-AcGFP-p27CK-DD (p27CK-DD)	J.M. Slingerland (Zhao D. et al., 2015)	N/A
pGIPZ-IRES-tGFP (shp27)	Dharmacon	RHS4531
psi-LVRU6MH-mCherry (shTGFB2)	GeneCopoeia	HSH054070
psi-LVRU6MH-mCherry (shJUN)	GeneCopoeia	HSH009853
Software and Algorithms		
xCELLigence RTCA Systems	ACEA Biosciences	https://aceabio.com
Duolink ImageTool	Sigma-Aldrich	DUO90806
ImageJ	NIH	https://imagej.nih.gov/ij
Other		
Sequencing data (ChIP seq and RNA seq)	This paper	GSE112446

Supplemental Materials and Methods

p27 phosphomimetic mutant expressing cells. Generation and growth of vector controls and MDA-MB-231, UMUC3, and MCF12A expressing phosphomimetic EGFP-p27CK-T157D/T198D was described (1). Cell were treated with 250nM PI3K/mTOR kinase inhibitor, PF04691502 (PF1502) for 48 hrs, a dose shown to inhibit PI3K without affecting cell cycle progression in these lines (2).

Lentivirus production and infection. Lentivirus vectors encoding 3 different clones of each of sh*JUN* and sh*TGFB2* (from Dharmacon or GeneCopoeia) and were co-transfected with DeltaVPR and CMVVSVG

plasmids (Addgene) into asynchronous 293T with Lipofectamine 3000 Reagent. Viral supernatants were collected after 48 h, concentrated at 22,000 RPM at 4°C and resuspended overnight at 4°C. 231p27CK-DD cells were infected twice with polybrene (10 mg/ml), and analyzed 3-5 days post infection by direct immunofluorescence and western. Stable p27shRNA depleted variants of 1833 and UMUC3-LuL2 were previously described (1, 2).

siRNA mediated knockdown of p27. 3-5 oligonucleotide siRNAs to p27 and scrambled controls were purchased from Santa Cruz Biotechnology and transfected per manufacturer. The oligonucleotides sequences are not provided by the manufacturer.

Quantitative real-time PCR (qPCR). qPCR analysis in biologic and technical triplicate repeats were as described (3) using primers indicated in the Supplementary Table S6. *GAPDH* were used as an internal control. Mean C_t values were normalized to *GAPDH*.

Western blotting. Westerns were performed in at least 3 different biologic repeats and representative data shown as described (4). Where needed, densitometric analysis was used to quantitate data. Antibodies for p27 (D69C12), cJun (60A8), and cJunpS63, Vimentin, TGF-β2, AKT, AKTpS473, and beta-tubulin were from Cell Signaling (Boston, MA, USA); for JNK, β-actin from Santa Cruz Biotechnology (Dallas, TX, USA); for E-Cadherin, N-Cadherin, and p27 from Transduction Labs (San. Jose, CA, USA); for p27pT198 from R&D Systems (Minneapolis, MN, USA). For details on reagents, see Supplemental table S6.

Immunoprecipitation. UMUC3-LuL2 and MDA-MB-231-1833 were treated +/- PI3K inhibitor, 250nM PF-04691502 for 48h, lysed and 500-1000µg lysate incubated with 1 µg of either p27mAb (BD Transduction) or p27mAb (D69C12), or control IgG as in (4). Complexes were resolved, transferred to

PVDF and blotted for associated JNK (Santa Cruz, sc-7435) and cJUN (Cell Signaling, 9165s). All data shown are representative of over 3 biologic repeat assays.

Nuclear and cytoplasmic fractionation. Nuclear-cytoplasmic fractionation used NE-PER™ Nuclear and Cytoplasmic Extraction Reagents from Thermo-Scientific. Equal nuclear and cytoplasmic lysate protein concentrations were blotted for indicated proteins. Lamin B2 served as nuclear and β-tubulin as cytoplasmic controls.

Transwell invasion assays. For transwell invasion assays, 10^5 cells were seeded in the upper chamber of a matrigel (5 mg/ml media) coated transwell membrane (Corning) and invasion quantitated as described (5). Cells adherent to membrane under-surface were visualized, photographed, counted and relative invasion was plotted (5).

Automated transwell invasion assays used the Real-Time Cell Analysis (RTCA) system from Xcelligence as described (1) and invasion was plotted as cell index +/- SEM for at least three wells per group.

Chromatin immunoprecipitation assay. For ChIP assays were as described (6). Briefly, soluble chromatin was prepared from 2×10^7 cells, pre-cleared and precipitated with anti-p27 (Cell Signaling, D69C12), anti-cJun (Cell Signaling, 60A8), anti-CBP/p300 (Cell Signaling, 4771s), anti-Pol II (Santa Cruz, sc-900) or an anti-IgG (Santa Cruz, sc-2025) antibody. For Re-ChIP assays, anti-cJun precipitates were incubated in 10 mM DTT for 30 min, 37°C, and diluted 40X and then incubated with anti-p27 mAb, collected on protein A/G sepharose beads and eluted in 1% SDS, 0.1 m $NaHCO_3$ at room temperature for 20 min. After cross-link reversal at 67°C, digestion with 10 µg proteinase K and 10 µg RNase A at 42 °C for 3 h, DNA was amplified by qPCR with primers specific for the cJun binding sites (-16 kb) upstream of the transcriptional start site in the TGFB2 promoter (See Supplementary Table S6).

Orthotopic xenograft assay. For orthotopic xenograft assays, 5×10^5 cells were suspended in 100 µl Matrigel and injected into the 4th mammary fat-pad of NOD SCID gamma (NOD.Cg-Prkdcscid Il2rgtm1Wjl/SzJ) (NSG) mice (9/group) as described (2). Tumor growth was monitored by weekly IVIS, measured twice-weekly and volumes calculated as (long-side x short-side^2)/2. Orthotopic 5-7 mm tumors were removed and mice were monitored weekly by IVIS for metastasis. Primary tumors in the inguinal mammary fat pads were removed at 100-300 mm^3, but these nearly always recur. The IVIS quantification of metastasis excludes the inguinal region to exclude recurrent primary tumor. Mean normalized photon flux is plotted/time +/- SEM. Animal work was compliant with University of Miami Institutional Animal Care and Use Committee.

Immunohistochemistry. Tumors were fixed and paraffin embedded and immunohistochemistry performed as in (2). Slides were microwaved 45 min in sodium citrate (10 mM, pH 6.0) and TGF-β2 was detected (TGF-β2 antibody, Abcam; 1:50, ab36495) overnight at 4°C and detected as in (2) and photomicrographed.

Proximity ligation assay (PLA). PLA used Duolink® In Situ Kit Mouse/Rabbit (Sigma-Aldrich) per manufacturer. Briefly, 5×10^4 cells were seeded on coverslips, and fixed (4% paraformaldehyde for 10 min), blocked for 1 h, permeabilized with 0.1% tritonX-100 for 10 min and then incubated with cJun (rabbit PAb, Cell Signaling, 9165S) and p27 (mouse, Transduction Labs) antibodies overnight at 4°C, followed by incubation with PLA plus and minus probes for 1h at 37°C. After ligation, polymerase amplifications were performed over 2 h at 37°C. Nuclei were stained with DAPI and red fluorescent PLA ligation signals quantitated by direct confocal microscopy from at least 3 high power fields.

Electrophoretic mobility shift assay (EMSA). EMSA used IRDye 700 AP-1 consensus oligonucleotide (LI-COR) per manufacturer (LI-COR, P/N 829-07925). Nuclear extract (5 μg) was added to AP-1 consensus oligonucleotide conjugated with IRDye (LI-COR; 829-07925), p27 or cJun antibodies (p27; Cell Signaling, cJun; Cell Signaling) and incubated for 1 h. Complexes were resolved and p27 and/or cJun-bound DNA visualized by Oddsey Imaging system.

Microarray data acquisition and analysis. RNA was quantified by Nanodrop 8000 Spectrophotometer (Thermo Scientific, Wilmington) and quality verified by RNA 6000 Nano kit (Agilent, Santa Clara, CA) on a Bioanalyzer 2100. Biotinylated cRNA was prepared per Illumina TotalPrep RNA Amplification Kit (Ambion, Inc., Austin, TX) from 400ng RNA. Samples were added to the Beadchip after randomization using a randomized block design to reduce batch effects. Hybridization to the Sentrix Human-HT12 Expression BeadChip (Illumina, Inc., San Diego, CA), washing and scanning were per Illumina BeadStation 500 manual (revision C). Microarray data analysis used Illumina GenomeStudio software.

Preliminary expression data was filtered used the R/Bioconductor package. Expression data from 47,231 probes was log transformed and Quantile normalized. 23,485 probes having Std. Dev. ≥ 0.1 across all arrays were used for further analysis. Probes significantly differentially expressed ($P < 0.0001$; Bonferroni-Hochberg corrected) with fold change > 1.0 were identified by Student's T-test. Genes commonly expressed in parental MDA-MB-231, 1833 scramble and 1833shp27 were removed from the data set before differences in gene expression between 1833 and 1833shp27 were evaluated by Student's T-test. All gene expression analysis followed MAIME standards.

RNA sequencing (RNA-Seq). Total RNA quality was measured using Bioanalyzer RNA Nano 6000 (Agilent Technologies, Santa Clara, CA, USA). Library preparation was performed by TruSeq Standed Total RNA Library Prep (Illumina, San Diego, USA), and quality confirmed using KAPA qPCR Library

Quantification (Kapa Biosystems, Wilmington, MA, USA). Paired end sequencing was performed on Illumina NextSeq platform using 150 cycles 400M kit.

RNA-Seq bioinformatic analysis. Raw sequence read quality was assessed using FastQC. Quality and adapter trimming was performed by Trimmomatic (7). Genome alignment was performed using STAR (version 2.5.0b) (8) against human genome (hg19). After read alignment, raw counts were calculated with featureCounts (subread v1.5.0) (9), and differentially expressed genes were identified by DESeq2 (version 1.14.1) (10). Pathway and gene set enrichment analysis used Gene Set Enrichment Analysis (GSEA) (11).

ChIP sequencing (ChIP-Seq). DNA quality was measured using Bioanalyzer DNA HS (Agilent Technologies). Libraries were prepared using NEBNext® Ultra™ DNA Library Prep Kit (NEB), and their quality was measured by High Sensitivity D1000 Screen Tape (Agilent Technologies). ChIP sequencing was performed on Illumina 75 cycles 400M reads. Quality control was performed on short read files from sequencing, and short read files were aligned on human reference genome.

ChIP-Seq bioinformatic analysis. Quality of raw sequence reads was assessed using FastQC, while quality and adapter trimming was performed by Trim Galore (version 0.4.4, www.bioinformatics.babraham.ac.uk/projects/trim_galore/). After trimming reads were aligned to the hg19 genome using bowtie2 (version 2.3.3.1) (12), and the PCR duplicates were then marked and removed by Picard (https://broadinstitute.github.io/picard/). Peak calling used MACS2 (version 2.1.1) (12) without building the shifting model and with extension size computed by phantom peakqual tools (13, 14). Peaks overlapping blacklisted genomic regions were removed, and remaining peaks were further filtered with the thresholds q-values < e-10 and fold-change > 6. Peaks were obtained from the 2 ChIPseq biological replicates separately. For each replicate, heatmaps showing signal distribution in peak regions

were generated with deepTools (version 2.5.3, https://github.com/deeptools/deepTools). Subsequently, peaks common to the 2 replicates were selected with bed tools (version 2.26.0, http://bedtools.readthedocs.io/en/latest/content/bedtools-suite.html) for further analysis.

The overlapped peaks were annotated to regions in the hg19 genome with homer (version 4.9.1) (15), and assigned to the nearest gene within 5 kb of the transcription start site (TSS). The binding motifs were identified by Homer de novo motif discovery with whole genome hg19 as background. Binding motifs in proximal regions (<5 kb TSS) were identified using the whole genome TSS +/-5 kb regions as background. Moreover, genes with interesting expression patterns based on RNAseq data were selected, and for each of these genes, the normalized signal intensity of p27 and cJun within +/- 2 kb window of its TSS were plotted with ngs.plot program (the normalized signal intensity was defined as log2 fold-change of sample vs input) (16). For each cell line, an average signal intensity was calculated for each gene within +/-400 bp of its TSS region. The difference of signal intensity in terms of all the selected genes between different cell lines (1833 vs. 231 and 231-DD vs. 231) was evaluated with paired t-test and p values were subsequently adjusted with BH method.

Analysis of p27 regulated gene expression in primary human breast cancers from TCGA/TCPA. Primary human breast cancers (n=830) with both gene expression data and p27pT157 levels reported from Reverse Phase Protein Assays (RPPA) were analyzed from The Cancer Genome Atlas (TCGA)/The Cancer Proteome Atlas as of 8-16-18. A p27pT157 level was determined that distinguished overall survival differences on Kaplan Meyer analysis. A subset of 392 genes differentially expressed in both 1833 and 231p27CK-DD vs 231 and 1833sh from RNA Seq analysis ($q<0.1$) was identified that were coordinately differentially expressed in the breast cancers with high p27pT157 vs all others by RPPA. TCGA cases with gene expression were then divided into training and validation sets of 702 and 168 tumors, respectively. Univariate Cox regression for each of the 392 genes was undertaken to determine contribution to risk. Candidate genes were evaluated one by one to determine individual contributions to

survival p <0.01, followed by two-sided multivariate Cox regression to evaluate risk attributable to the gene cohort. This yielded a 30 gene signature of differentially expressed genes. Principle component analysis of this gene set segregated patients into two groups that were then assayed for differences in overall survival. Receiver operating characteristic curve analysis using this 30 gene profile in an independent breast cancer validation cohort of (n=162) showed sensitivity and specificity of the 30 gene signature for prediction of OS.

Statistical Analysis. All graphed data present mean ± SEM from at least 3 biologic experiments with at least 3 different technical repeats. Comparisons of two groups used the two-tailed Student's t tests for two group. Analysis of variance (ANOVA) was used for comparisons of >2 groups. Following ANOVA, post-hoc analysis used t-tests to define differences between groups. Tests were two-sided unless otherwise specified. Statistical differences between matrigel invasion rates and in vivo tumor growth curves were calculated using "compareGrowthCurves" of statmod software (http://bioinf.wehi.edu.au/software/compareCurves).

1. Zhao D*, et al.* (2015) Cytoplasmic p27 promotes epithelial-mesenchymal transition and tumor metastasis via STAT3-mediated Twist1 upregulation *Oncogene* 34:5447-5459.
2. Wander S*, et al.* (2013) PI3K/mTOR inhibition can impair tumor invasion and metastasis in vivo despite a lack of antiproliferative action in vitro: implications for targeted therapy. *Breast Cancer Res Treat* 138(2):369-381.
3. Lindley LE & Briegel KJ (2010) Molecular characterization of TGFbeta-induced epithelial-mesenchymal transition in normal finite lifespan human mammary epithelial cells. *Biochem.Biophys.Res.Commun.* 399(4):659-664.
4. Sandhu C*, et al.* (1997) Transforming growth factor á stabilizes p15 INK4B protein, increases p15 INK4B -cdk4 complexes and inhibits cyclin D1/cdk4 association in human mammary epithelial cells. *Mol Cell Biol* 17(5):2458-2467.

5. Larrea MD*, et al.* (2009) RSK1 drives p27Kip1 phosphorylation at T198 to promote RhoA inhibition and increase cell motility. *Proc Natl Acad Sci USA* 106(23):9268-9273.
6. Assou S*, et al.* (2007) A meta-analysis of human embryonic stem cells transcriptome integrated into a web-based expression atlas. *Stem Cells* 25(4):961-973.
7. Bolger AM, Lohse M, & Usadel B (2014) Trimmomatic: a flexible trimmer for Illumina sequence data. *Bioinformatics.* 30(15):2114-2120.
8. Dobin A*, et al.* (2013) STAR: ultrafast universal RNA-seq aligner. *Bioinformatics.* 29(1):15-21.
9. Liao Y, Smyth GK, & Shi W (2014) featureCounts: an efficient general purpose program for assigning sequence reads to genomic features. *Bioinformatics.* 30(7):923-930.
10. Love MI, Huber W, & Anders S (2014) Moderated estimation of fold change and dispersion for RNA-seq data with DESeq2. *Genome Biol.* 15(12):550.
11. Subramaniam D, Thombre R, Dhar A, & Anant S (2014) DNA methyltransferases: a novel target for prevention and therapy. *Front Oncol.* 4:80.
12. Langmead B & Salzberg SL (2012) Fast gapped-read alignment with Bowtie 2. *Nat.Methods* 9(4):357-359.
13. Kharchenko PV, Tolstorukov MY, & Park PJ (2008) Design and analysis of ChIP-seq experiments for DNA-binding proteins. *Nat.Biotechnol.* 26(12):1351-1359.
14. Landt SG*, et al.* (2012) ChIP-seq guidelines and practices of the ENCODE and modENCODE consortia. *Genome Res.* 22(9):1813-1831.
15. Heinz S*, et al.* (2010) Simple combinations of lineage-determining transcription factors prime cis-regulatory elements required for macrophage and B cell identities. *Mol.Cell* 38(4):576-589.
16. Shen L, Shao N, Liu X, & Nestler E (2014) ngs.plot: Quick mining and visualization of next-generation sequencing data by integrating genomic databases. *BMC.Genomics* 15:284.

APPENDIX 2

p27 binds cJun, YY1 and HDAC1 to co-repress *PTPN12* and increase tumor-initiating stem cells

Hyunho Yoon[1], Kibeom Jang[1,2], Miyoung Shin[1], Minsoon Kim[1,2], Dekuang Zhao[1,3], Xue Xiao[4], Lluis Morey[5], and Joyce M. Slingerland[1,2,3,6,7]*

[1]Braman Family Breast Cancer Institute at Sylvester Comprehensive Cancer Center
[2]Department of Biochemistry& Molecular Biology
[3]Sheila and David Fuente Graduate Program in Cancer Biology
[4]Bioinformatics Core, Sylvester Comprehensive Cancer Center
[5]Cancer Epigenetics Program of SCCC and Department of Human Genetics
[6]Department of Medicine
University of Miami Miller School of Medicine, Miami, FL, 33136, USA
[7]Lead Contact

*Correspondence: Dr. J Slingerland, Braman Family Breast Cancer Institute at Sylvester Comprehensive Cancer Center, University of Miami Miller School of Medicine, BRB708, 1501 NW 10th Avenue, Miami, FL 33136, USA. Email: jslingerland@med.miami.edu

Abstract

The CDK inhibitor, p27, acquires pro-oncogenic actions in cancer. We showed p27pT157pT198 is broadly recruited to chromatin with cJun to activate gene drivers of EMT and metastasis. Here, we show p27 also interacts with cJun to corepress pro-differentiation genes and increase cancer-initiating stem cells. In breast and bladder cancer cells expressing high endogenous p27pT157pT198 or phosphomimetic cyclin- and CDK-binding-defective p27CK-DD, nearly half of p27/cJun co-targets are repressed and these govern adipogenesis, cardiac and hematopoietic differentiation. The gene encoding phosphatase *PTPN12* was strongly downregulated in p27-activated cells. p27 and cJun recruit SIN3A, YY1, and HDAC1 to corepress this tumor suppressor gene, leading to increased sphere formation and tumor initiating cells. Upon PTPN12 loss, its substrate, PYK2, mediates STAT3 activation, increases spheres and ALDH1 activity *in vitro* and tumor initiating cells *in vivo*. Thus, p27-bound cJun represses differentiation genes and via *PTPN12* repression, activates gene programs that upregulate cancer initiating cells.

Keywords: p27, cJun, PTPN12, cancer stem cell, tumor initiation, transcriptional repressor

INTRODUCTION

$p27^{Kip1}$ (p27), encoded by *CDKN1B*, is a ubiquitously expressed CDK inhibitor that normally restrains cell cycle progression [1-4]. In cancers, phospho-inositol 3' kinase (PI3K) activates AKT, SGK1 and RSK1, all of which can phosphorylate p27 at T157 and T198 to impair CDK inhibition [5-10]. C-terminally phosphorylated p27 acquires pro-oncogenic actions. It binds novel partners including RhoA to increase cell motility [11], it assembles and activates D type cyclin-CDKs [12], and mediates STAT3 activation to promote EMT and breast cancer metastasis [13].

p27 affects development and plays CDK-independent roles in myogenesis, cardiac, neuronal and bone differentiation [14-17]. Knock-in of p27CK- into p27 null mice led to expansion of stem cell compartments in various tissues [18], but the mechanisms whereby p27 modulates developmental programs to date are not known. Recent evidence suggests that p27 might interact with transcriptional regulatory complexes. Interestingly, a ChIP-on-Chip survey in NIH3T3 cells revealed p27 forms a complex with E2F4, SIN3A, and p130 at gene promoters [19]. This p27/p130/E2F4 complex recruits SIN3A/HDAC1 to repress *SOX2* when pluripotent cells differentiate [20]. The accompanying paper describes p27 as a novel cJun binding partner and characterizes genome wide p27 and cJun association chromatin of this complex. cJun binding to p27 and recruitment to chromatin is increased with C-terminal p27 phosphorylation and we identify p27/cJun target genes, including *TGFB2*, whose upregulation drive metastasis[21]. Here, we evaluate the potential for cJun and p27 to co-repress target gene expression and how p27/cJun repressed genes relate to tumor progression.

The protein tyrosine phosphatase non-receptor type 12 (PTPN12) dephosphorylates and inactivates protein tyrosine kinases (PTKs) that drive mitogenic signaling [22]. PTPN12 dephosphorylates Pyk2, paxillin, and $p130^{CAS}$ in various cell types [23]. PTPN12 is a tumor suppressor whose loss promotes cancer cell proliferation and metastasis [22, 24, 25]. Here, we show that C-terminally phosphorylated p27 partners with cJun not only to activate target genes (companion paper)[21], but p27/cJun also interacts with YY1/SIN3A to recruit HDAC1 and repress genes associated with differentiation, activate gene programs associated with stem cell self-renewal, and increase tumor-initiating stem cell abundance. *PTPN12* is identified as a direct p27/cJun-repressed target whose downregulation is required to maintain tumor initiating cell abundance. Thus, p27 appears to play a dual role with cJun: it can co-activate genes like *TGFB2* to promote metastasis, but also bind cJun to repress tumor suppressors like *PTPN12* that restrain tumor progression.

RESULTS

C-terminally phosphorylated p27 downregulates genes associated with differentiation and tumor suppressor genes

Despite its identification over a decade ago as a mediator of cell motility [26] and metastasis [27-29], the mechanisms governing the broad pro-oncogenic p27 actions in cancers have not been fully characterized. Here, we investigated the potential for p27/cJun to repress target genes. We evaluated p27-regulated genes whose expression is decreased in highly metastatic breast cancer cells with high endogenous p27pT157pT198 or in cells transduced with Cyclin-CDK binding defective, phosphomimetic p27 (p27CK-DD). RNA sequencing analysis (RNA-Seq) was performed in the parental MDA-MB-231 (hereafter 231) breast cancer line, p27CK-DD transfected 231, MDA-MB-231-1833 (hereafter 1833) and in 1833shp27 with stable depletion of p27 [29]. 1833 is a highly metastatic derivative isolated from xenografted 231 bone metastases [30] that expresses high levels of p27pT157pT198 due to PI3K activation [29]. To identify putative tumor suppressors repressed by p27, we looked for genes downregulated in 231p27CK-DD cells versus parental. p27CK-DD expression in 231 downregulated 2,566 genes (fold-change < 0.75, $p < 0.005$, $q < 0.1$). We then asked which of these were also upregulated upon p27 depletion in 1833. Expression of 1,433 genes increased (fold-change > 1.5, $p < 0.005$, $q < 0.1$) in 1833shp27compared to 1833. Of these, 536 genes upregulated upon p27 knockdown in 1833 were also downregulated by p27CK-DD (Fig. 1a; Supplementary Table 1a). Gene set enrichment analysis showed these 536 p27-downregulated genes are associated with hematopoietic stem cell and ectoderm differentiation, and cancer pathways (Fig. 1b and Supplementary Fig. 1a). Thus, C-terminal phosphorylation of p27 mediates downregulation of gene profiles associated with differentiation.

We next looked for genes directly repressed by p27-bound cJun. The companion paper shows C-terminally phosphorylated p27 promotes cJun activation, and cJun/p27 complexes localize to the nucleus to transcriptionally co-regulate target genes [21]. ChIP sequencing analysis (ChIP-Seq) revealed 590 target genes were bound by both p27 and cJun within +/-5Kb of their transcriptional start sites in 231, 231p27CK-DD and 1833 [21]. While nearly half of these cJun/p27 target genes were upregulated in highly metastatic lines and may serve as oncogenes, many were repressed. Of 590 p27/cJun target genes, the expression of 233 of these genes was significantly repressed in 231p27CK-DD and 1833 compared to 231 (fold-change > 1.5, $p < 0.005$, $q < 0.1$; Fig. 1c; Supplementary Table 1b). Notably, more cJun and p27 bound to these 233 repressed target genes in 231p27CK-DD and 1833 than in 231 (Fig. 1d). Gene ontology (GO) showed these commonly repressed genes are associated with developmental and cancer related signaling including the Notch3 and MAPK pathways, but notably also with differentiation of cardiac and fat tissue (Fig. 1e and Supplementary Fig. 1b).

Genomic analysis also identified a discrete set of cJun/p27 target genes bound in 231p27CK-DD and 1833, but not in parental 231. cJun/p27 targets genes bound and downregulated uniquely in 1833 and 231p27CK-DD cells but not in 231 might represent novel targets whose stable binding and repression requires a higher threshold of p27 phosphorylation. Of the 252 cJun/p27 target genes bound only in the p27 activated lines, 146 genes were strongly downregulated in the p27-activated lines compared to 231 (Fig. 1F and Supplementary Fig. 1c; Supplementary Table 1c). GO analysis revealed that these cJun/p27-repressed genes also associated strongly with differentiation including hematopoietic stem cell differentiation, and with cancer pathways (Fig. 1g). Thus, in cells with activated, C-terminally phosphorylated p27, cJun and p27 corepress genes strongly associated with cancer pathways and with cardiac, myogenic and hematopoietic stem cell differentiation.

C-terminally phosphorylated p27 downregulates tumor suppressor genes

A series of transcriptionally repressed cJun/p27 co-target genes were selected for validation. *MYO1F* is a cJun and p27 target identified in all of 231, 231p27CK-DD and 1833 (Fig. 2a). p27 and cJun recruitment to *TMEM71* may require higher p27 phosphorylation since binding to this target was detected only in 1833 and 231CK-DD but not in 231(Fig. 2b). The cJun/p27 binding sites on *MYO1F* (-8 kb) and *TMEM71* (-1 kb) both contain AP1 consensus motifs. cJun and p27 binding observed by ChIP-Seq at these targets was confirmed by ChIP-qPCR, with greater binding in 231p27CK-DD and 1833 cells than in 231. p27 depletion decreased not only p27 recruitment (as expected) but also significantly attenuated cJun recruitment to these promoters (Fig. 2c, f), suggesting p27 facilitates cJun binding or enhances complex stability. Furthermore, expression of both *MYO1F* and *TMEM71* was lower in 231-p27CK-DD and 1833 cells than in 231, and increased in 1833shp27 (Fig. 2d, g). *MYO1F* encodes a form of myosin expressed mainly in mammalian immune cells. MYO1F depletion increased thyroid cancer cell motility, and mutational inactivation of *MYO1F* induced tumor proliferation, suggesting a tumor suppressor role for MYO1F [31, 32]. The biological function of transmembrane protein, TMEM71, has not been characterized. Of note, both of these novel cJun/p27-repressed target genes appear to play tumor suppressor roles in human breast cancer, since high expression of each is associated with improved relapse-free survival on Kaplan Meier (KM) analysis of breast cancer patient data from KM-Plotter™ (Fig. 2e, h).

Two other cJun/p27 co-target genes were validated and may play tumor suppressor roles. cJun and p27 binding to *SH3TC1* (-1 kb) and *RCSD1* (-2 kb) was greater in p27-activated lines and both decreased upon p27 knockdown in ChIP

Seq tracks. This pattern was validated by ChIP-qPCR (Supplementary Fig. 2a, b, e, f, respectively). Both *SH3TC1* and *RCSD1* were significantly repressed in 231p27CK-DD and 1833 compared to 231, while p27 knockdown in 1833 increased expression of both (Supplementary Fig. 2c, g, respectively). The biological function of SH3TC1 is not known. RCSD1 (RCSD Domain Containing 1) is involved in actin filament binding. An *RCSD1-ABL1* translocation is associated with acute lymphoblastic leukemia [33], suggesting that RCSD1 disruption is oncogenic. Interestingly, RCSD1 promotes cardiomyogenic differentiation [34]. KM Plotter data analysis revealed that loss of each of each of *SH3TC1* and *RCSD1* correlates with poor breast cancer patient outcome (Supplementary Fig. 2d, h, i), suggesting the both may be breast cancer tumor suppressors. Thus, cJun and p27 can corepress genes that mediate differentiation and that appear to act as tumor suppressors in breast cancer.

A novel complex of p27, cJun, YY1 and HDAC1 transcriptionally represses *PTPN12*

PTPN12 [22, 25] was one of the most strongly downregulated genes in p27CK-DD compared to 231 (log2 fold change = -2.82, p = 7.05e-293, q = 1.15e-289; Fig. 3a). Loss of PTPN12 was confirmed in p27CK-DD expressing MCF12A and 231, and in two highly metastatic derivatives, 1833 and 4175, compared to 231 (Fig. 3b, c).

Our ChIPSeq identified cJun and p27 binding sites at -1 and at +2 kb on *PTPN12*. Recruitment of each of cJun and p27 to both sites was greater in p27-activated lines than in 231, and both decreased upon p27 depletion in 1833 (Fig. 3d). The +2 kb site bears a cJun consensus motif and publicly available ENCODE ChIPSeq tracks showed cJun bound this site in K562 cells (Supplementary Fig. 3a). ChIP-qPCR confirmed that cJun and p27 are co-recruited the +2 kb *PTPN12* promoter proximal site, with greater binding in 231p27CK-DD and 1833 than 231. Notably, in 1833, both p27 depletion and treatment with a PI3K inhibitor that abolishes p27 T157 and T198 phosphorylation [29], attenuated p27 and cJun recruitment to this site. These data are consistent with the notion that cJun co-recruitment with p27 to chromatin is regulated by p27 phosphorylation (Fig. 3e). ChIP/ re-ChIP assays confirmed that cJun and p27 co-occupy the site +2 kb of *PTPN12*, and that C-terminally phosphorylated p27 regulates this (Fig. 3e and Supplementary Fig. 3b, c).

To further investigate cJun/p27-mediated gene repression, we assayed for the presence of YY1 and SIN3A, which are known to recruit HDAC1 to other developmentally important transcription factors [35]. Analysis of publicly available ENCODE tracks showed these repressive elements can bind this *PTPN12* site (Supplementary Fig. 3a). SIN3A, YY1 and HDAC1 were detected at this +2 kb *PTPN12* site in our breast cancer lines. Their recruitment was enhanced in p27CK-DD

expressing 231, and reduced by p27 depletion and by PI3K inhibition in 1833 (Fig. 3f). Moreover, cJun ChIP-Western also showed SIN3A, YY1, and HDAC1 binding was p27-regulated (Fig. 3g). p27 can form a transcriptional repressive complex with E2F4 [19, 20]. However, ChIP-qPCR with anti-E2F4 showed no E2F4 recruitment to the cJun/p27 binding site at +2 kb on *PTPN12* (Supplementary Fig. 3d). These data suggest a model in which p27 and cJun recruit SIN3A, YY1, and HDAC1 to this AP1 motif to repress *PTPN12* expression (Fig. 3h). PTPN12 is frequently lost in aggressive triple negative breast cancers [22]. The biologic importance of *PTPN12* loss is supported by Kaplan-Meier analysis that shows poor outcome in breast cancer patients whose tumors have reduced *PTPN12* expression ($p = 0.00651$, Fig. 3i).

p27 increases stem-like cells *in vitro* through loss of PTPN12 and activation of PYK2

Since cJun/p27 complexes repress genes associated with differentiation (present data) and activate EMT and metastasis (accompanying paper), both of which are linked to cancer stem cells [36], we assayed effects of p27 on tumor initiating ability. Sphere formation is a stem cell property assayed in vitro [37]. The MCF12A normal human mammary epithelial line is immortal but non-tumorigenic and formed spheres slowly over 4-6 weeks. Transduction of p27CK-DD, but not p27CK-alone, significantly increased mammosphere formation compared to vector control in MCF12A (Fig. 4a). p27CK-DD expression caused a shift from predominantly surface $CD44^{+}/CD24^{+}$ to a population expressing stem cell markers $CD44^{+}CD24^{low/-}$ (Fig. 4b, left), a hall mark of breast cancer initiating cells [38]. CD44 was markedly increased (Fig. 4b, right) and MCF12Ap27CK-DD cells acquired the ability to form soft agar colonies (Supplementary Fig. 4a). Notably, p27CK-DD increased sphere formation and expression of embryonic stem cell transcription factors (ES-TFs) *SOX2*, *NANOG*, and *cMYC* in 231 (Fig. 4c) and increased spheres in MCF7 breast cancer cells and in the UMUC3 bladder cancer line (Supplementary Fig. 4b)

Conversely, p27 depletion in highly metastatic breast cancer (1833) and bladder cancer models (UMUC3-LuL2) (Supplementary Fig. 4c) [13] significantly reduced not only mammospheres, but also ES-TF expression (Fig. 4d and Supplementary Fig. 4d). Soft agar colony formation increased in 231p27CK-DD and decreased with p27 depletion in 1833 (Supplementary Fig. 4e).

To address the role of PTPN12 in p27-regulated tumor initiation, PTPN12 was depleted in 231 and UMUC3, and overexpressed in 1833 (Supplementary Fig. 4f-h). PTPN12 depletion in 231 and UMUC3 (sh*PTPN12*) increased ES-TF expression (Fig. 4e, left and Supplementary Fig. 4h) and *PTPN12* transduction in 1833 decreased *NANOG*, *cMYC*, and

SOX2 expression (Fig. 4e, right). PTPN12 depleted 231 and UMUC3 formed more spheres (Fig. 4f and Supplementary Fig. 4i) and PTPN12 overexpressing 1833 formed fewer (Fig. 4f). Effects on soft agar colony formation were similar: PTPN12 depletion increased and PTPN12 overexpression decreased colony formation (Supplementary Fig. 4j).

PTPN12 dephosphorylates mediators of focal adhesion signaling Paxillin, PYK2, and p130^{Cas} [22]. Transient PTPN12 knockdown activated these substrates in 231 (Fig. 4g). Stable PTPN12 depletion activated pPYK2 in 231, while PTPN12 overexpression decreased pPYK2 in 1833 (Supplementary Fig. 4g). Notably, in 231p27CK-DD, PYK2 depletion reversed the stem cell effects of phosphomimetic p27 expression, decreasing ES-TF expression (Fig. 4h), sphere formation (Fig. 4i) and ALDH1 activity (Fig. 4j). Treatment with PYK2 inhibitor, PF431396, also attenuated sphere formation in 231p27CK-DD cells (Fig. 4k). Notably, PI3K inhibition over 48 hrs decreased AKTpT308, led to loss of p27pT198, and pPYK2, and reduced MYC and SOX2, consistent with the notion that PI3K drives p27 phosphorylation leading to *PTPN12* repression, PYK2 activation and cancer stem cell (CSC) expansion (Fig. 4l).

p27 increases phospho-PYK2 to activate STAT3 and drives a STAT3 gene expression signature

Although FAK is known to regulate CSC [39], the role of PYK2 (also known as FAK2) is less well studied. STAT3 is. PYK2 inhibition by 48 hrs of treatment with PYK2 inhibitor, PF431396, not only decreased activated pPYK2 but significantly downregulated activated STAT3pS63 (pSTAT3), a known regulator of breast CSC expansion [40] (Fig. 5a). Both acute and stable PYK2 depletion also reduced pSTAT3, indicating that PYK2 is required for STAT3 activation in these cells (Fig. 5b, c).

Since phosphorylated p27 represses *PTPN12* and activates PYK2 to drive STAT3 activation, p27 activated lines would have activation of STAT3-dependent genes. We used The Cancer Genome Atlas (TCGA)/The Cancer Proteome Atlas (TCPA) data to identify genes differentially expressed between primary human breast cancers in the top quartiles of pSTAT3 and p27pT157 expression and all others. This pSTAT3/p27pT157 (STAT-3) activated gene expression profile was then compared to the genes differentially expressed in 231, 231p27CK-DD, 1833 versus 1833shp27. p27-activate lines express a subset of STAT3-activated genes identified in human ER negative breast cancers (heatmaps in Fig. 5d). GO analysis of genes coordinately upregulated in both p27-activated breast cancer lines and the STAT-3 activation signature from primary cancers identifies signaling pathways strongly associated with cancer and cancer stem cells (Fig. 5e and Supplementary Fig. 5a).

Since p27 activated lines appear to be enriched for tumor initiating stem cells, we assayed for preferential expression of target genes up and downregulated by NANOG, OCT4 and SOX2 (NOS) in ESC[41]. A subset of NOS signature genes were also coordinately expressed in p27 activated 231p27CK-DD and 1833 compared to 231 and 1833shp27 (Fig. 5f). GO of these shared NOS target signature genes expressed in our p27-activated lines identifies important stem cell and developmental pathways (Fig. 5g, h and Supplementary Fig. 5b).

p27 mediates tumor-initiating stem cell expansion through loss of PTPN12 and activation of PYK2

Tumor-initiating stem cells (T-ISC) abundance was assayed *in vivo* by injecting limiting dilutions of 231, 231-p27CK-DD, 1833, and 1833shp27 (10, 100, or 1000 cells/mouse) orthotopically into Balb/c nude mice. T-ISC frequency was considerably higher and tumor latency shorter for 1833 cells and for 231p27CK-DD and compared to 231, and T-ISC frequency was decreased significantly by p27 depletion in 1833 (Fig. 6a, b) and by cJun depletion in 231p27CK-DD (Supplementary Fig. 6a, b). Thus, C-terminally phosphorylated p27 appears to increase tumor-initiating cell abundance in a cJun-dependent manner *in vivo* in this model.

PTPN12 depletion in 231 significantly increased T-ISC abundance (Fig. 6a), while PTPN12 overexpression in 1833decreased T-ISC (Fig. 6b). PYK2 knockdown in 231p27CK-DD abrogated the gain in T-ISC abundance conferred by phosphomimetic p27CK-DD and prolonged tumor latency (Fig. 6a). T-ISC frequency is calculated in Fig. 6c. Taken together, these data support a model of PI3K-activated cancers, in which p27 appears to activate T-ISC expansion or maintenance though p27/cJun-dependent PTPN12 loss and the resulting activation of PYK2.

DISCUSSION

p27 is an atypical tumor suppressor. In normal cells it restrains proliferation, but in cancers its cell cycle inhibitory action is disrupted and it acquires novel actions that promote tumor progression. Although p27 is decreased in up to 60% of human cancers by excess proteolysis or decreased translation, it is never fully lost, and bi-allelic mutation or deletion of its encoding gene, *CDKN1B,* has not been described [42]. In cancers, cytoplasmic p27 heralds PI3K activation, C-terminal p27 phosphorylation and poor patient outcome [42, 43]. While C-terminal p27 phosphorylation increases cell motility and invasion, known mechanisms of oncogenic gain of function [12, 44] are not sufficient to explain the profound effect of deregulated p27 to drive human tumor metastases. Transduction of cytoplasmic p27 into PTEN deficient melanoma increased metastasis *in*

vivo [27] and p27 depletion dramatically decreased extravasation and metastasis formation [13, 28, 29] and metastasis from primary tumors [21]. In the companion paper, we identify cJun as a novel binding partner and showed p27 can co-activate cJun to upregulated gene programs associated with EMT and metastasis [21]. Here, we identified a novel subset of cJun/p27-repressed genes that also appear to actively govern gene programs.

Here, we show p27 has a dual role as a cJun co-regulator. While p27 is co-recruited to a large number of cJun target genes together with activators such as p300 [21] to activate gene expression, it also recruited to chromatin in a cJun-complex containing YY1, SIN3A and HDAC1 to repress target expression. p27 phosphorylation increases not only the extent of cJun and p27 co-recruitment but also that of YY1, SIN3A and HDAC1 to target genes on chromatin. cJun/p27 repressive complexes are increased in cells with high endogenous p27pT157pT198 or phosphomimetic p27 and decreased by PI3K inactivation. Notably, p27-bound cJun represses target genes associated with pathways governing cardiac, adipocyte and hematopoietic stem cell differentiation.

cJun forms homo- or hetero-dimeric AP1 transcription complexes to drive expression of genes governing cell proliferation, invasion, and apoptosis [45]. While known to play critical roles in oncogenesis, cJun complexes can also play cell type and complex specific tumor suppressor roles [46]. cJun phosphorylation by JNK at S63 and S73 serves as a molecular switch, promoting coactivator binding and prohibiting stable corepressor complex formation [46]. cJun-mediated transactivation is opposed by binding to corepressors, including NCOR1 [47], NCOR2 [48] and mbd bound to the Nucleosome remodeling and histone deacetylation complex (NuRD) [49]. These interactions preferentially occur with inactive cJun and have been shown to extinguish cJun-activated gene expression, but none of these cJun/co-repressor complexes has been shown to regulate a profile of cJun-repressed genes. Here, we present evidence that cJun/p27 co-repress tumor suppressor genes and gene programs associated with differentiation. In cell expressing constitutively phosphorylated p27, cJun is highly activated and yet it can form co-repressive complexes with p27 to downregulate functionally important genes, suggesting a novel mechanism of cJun-mediated transcriptional repression in complex with p27, YY1, HDAC1 and SIN3A.

The differentiation pathways affected by p27/cJun-repressed genes echo p27 effects in development and illuminate a decade of research on genetic loss of p27 and effects of p27CK- knock-in into p27 null mice and frogs. Despite ubiquitous expression of p27, p27 null mice exhibit a discrete profile of hyperproliferation in specific tissues including neuronal, muscle, cardiac, pituitary and germ cells [26, 50]. That the p27 null phenotype is not compensated by CDK2 knock out in mice [51, 52], suggested p27 might play non-CDK-related roles in development. While p27 levels are higher in post-mitotic cells

than in their corresponding differentiating stem/progenitor cells, p27 plays CDK-independent roles in addition to the induction of quiescence in development [26]. Knock-in of p27CK- into p27 null frogs revealed a CDK-independent role for p27 in myogenic lineage commitment with MYOD, at a point in development prior to loss of proliferation [53]. Similarly, p27 binds transcription factor, neurogenin 2, to modulate neuronal differentiation [16]. Moreover p27 and p130 interact genetically in bone development [17]. All of these studies suggested transcriptional regulation by p27, but little data directly supported a transcriptional regulatory role for this CDK inhibitor. p27 was recently shown to bind MYOD [54] and to form a repressive complex with E2F4, p130, and HDAC1 [19, 20] but targets of these complexes have not been fully characterized. Present findings, together with the companion paper, identify the breadth of p27-genome binding and reveal that p27-phosphorylation regulates changes in the profile and extent of p27/cJun recruitment to target genes. We also characterize p27 as a corepressor together with cJun to govern expression of transcriptional targets critical to development and differentiation. While our investigations have been limited to immortal mammary epithelial cells and cancer models, prior work suggests p27 may regulate cJun action in normal cells. p27 was shown to limit clonal expansion of anergic T cells by binding to JAB1 to block cJun-dependent activation of interleukin-2 [55]. Furthermore, in normal mouse embryo fibroblasts, p27 loss increased AP1-mediated *EGFR* transcription [56]. In both of these normal cell populations, p27 opposed AP1 driven gene expression. These observations raise the possibility that in cancer cells, constitutive p27 phosphorylation may subvert normal transcriptional regulatory processes to promote oncogenic cJun action and tumor progression. cJun is broadly expressed during organogenesis in mice [57] and plays critical roles in the development of tissues also regulated by p27, including cardiac, bone, hematopoietic and neuronal development [58-60]. Further investigation is required to clarify the roles of p27/cJun mediated transcriptional regulation in normal differentiation.

Stem cell self-renewal is in many ways the transcriptional converse of differentiation. ESC self-renewal is maintained through repression of differentiation genes [61]. Here, we make the unprecedented observation that C-terminally phosphorylated p27 mediates expansion or maintenance of cancer cells with stem cell features *in vitro* and with tumor initiating stem cell ability *in vivo*. Expression of phosphomimetic p27CK-DD in immortal, non-malignant MCF12A caused them to acquire malignant features, with an increase in sphere formation, accumulation of CSC markers CD44+ $CD24^{low/-}$ and acquisition of soft agar colony formation. p27CK-DD transduction also increased ES-TF expression and sphere formation in both ER+ and ER- breast cancer lines and in the UMUC3 bladder cancer model, supporting the broader

relevance of our findings. Finally, p27 phosphorylation also appears to modulate tumor initiating stem cell abundance *in vivo*.

The first evidence for a stem cell role for p27 came from p27 null mice, which showed an increase in the abundance of committed glial and hematopoietic progenitor cells [62-64]. Knock-in of p27CK- in p27 null mice disrupted the balance of self-renewal and differentiation, leading to expansion of lung bronchoalveolar stem cells and other progenitor cell populations, and late emergence of tumors in the lungs, pituitary, retina, ovary and lymphoid tissues [18]. Here, we show that p27/cJun-downregulated targets include not only genes critical for stem cell differentiation in various tissues, but we also identify the phosphatase, PTPN12 as a critical signaling regulator repressed by cJun/p27. PTPN12 is a tumor suppressor frequently lost in aggressive breast cancers [22]. Its loss increased activation of both HER2 and EGFR to accelerate development and metastasis of HER2-positive breast cancer models [22]. Present work indicates that PTPN12 also restricts CSC abundance. We found *PTPN12* repression is required for PYK2 activation and for maintenance of embryonic stem cell transcription factor expression, sphere formation and p27-mediated increases in tumor initiating stem cells in highly metastatic breast cancer lines. PYK2 not only activates STAT3, a known mediator of ES [61] and cancer stem cell self-renewal [40], but STAT3, once activated would upregulate PYK2 expression [65], providing a feedforward mechanism to maintain stem cell expansion.

The relevance of this p27/PTPN12/PYK2/STAT3 pathway to breast cancer is reflected in the coordinate activation of a subset of p27-regulated genes and a STAT3-activated gene signature derived from primary human breast cancers from the TGCA/TCPA database. A subset of p27-target genes are also coordinately regulated in profiles of genes directly regulated by NANOG, OCT4 and SOX2 [41]. p27 activation may have both direct and indirect effects to drive transcriptional programs of CSC renewal. Constitutive PI3K/AKT-mediated p27 phosphorylation would directly modulate transcription to expand CSC by repressing p27-bound cJun target genes critical for differentiation. In addition, p27/cJun mediated repression of *PTPN12* would lead to PYK2-mediated STAT3 activation and induction of STAT3 transcription programs. Activation of PI3K/AKT, pSTAT3 and C-terminal p27 phosphorylation are strongly correlated in primary human breast cancers [13]. STAT3 activation in 231p27CK-DD leads to activation of AKT [13], thus several mechanisms would feedforward to amplify p27-mediated EMT, metastasis and stem cell expansion. Cancer populations enriched in tumor initiating stem cells show an increased ability to metastasize [36, 66]. The transcriptional actions of p27-bound cJun link cancer stem cells and metastasis. p27 co-regulates cJun to activate gene drivers of EMT and metastasis [21]. cJun also plays an active role with p27 to repress gene programs of differentiation and promote expansion of cells with tumor initiating ability.

METHODS

Cell lines and cell culture

The MCF12A cell line was purchased from ATCC (Manassas, VA, USA) and cultured as described [13]. UMUC3 and UMUC3-LuL2 were grown as described [67]. The 231p27CK-DD was grown as in [13]. Luciferase tagged MDA-MB-231/1833/4175 were from J Massague (MSKCC, New York, NY, USA), and grown in Dulbecco's Modified Eagle Medium (DMEM; Gibco, Grand Island, NY, USA) with 10% fetal bovine serum, 1% glutamine, 1% sodium pyruvate (Invitrogen, Carlsbad, CA, USA), and 50 µg/ml gentamicin (Mediatech, Manassas, VA, USA)[30, 68].

Vectors and transfection

pMD-PTPN12 cDNA clone was obtained from Sino Biological Inc. (Beijing, China). Lentiviral vectors expressing p27 shRNA (Open Biosystems, Lafayette, CO, USA) and PTPN12 shRNA (Applied Biological Materials, Richmond, Canada) were generated, and transfection were performed as described [29].

Western blot analysis

Cells were lysed in RIPA buffer (Sigma-Aldrich, St. Louis, MO, USA) resolved by SDS–PAGE, and transferred to a polyvinylidene difluoride membrane (Bio-Rad, Hercules, CA, USA). The membranes were incubated with the indicated primary antibodies and HRP-conjugated secondary antibodies (Promega, Madison, WI, USA). Primary antibodies for PYK2, pPYK2, STAT3, pSTAT3, p130CAs, p-p130CAS and cJun, and cJunpS63 were obtained from Cell Signaling (Boston, MA, USA); for β-actin from Santa Cruz Biotechnology (Dallas, TX, USA); for p27 from Transduction Labs (San. Jose, CA, USA) and from Cell Signaling (Boston, MA, USA); for PTPN12 from Abcam (Cambridge, MA, USA); and for p27pT198 from R&D Systems (Minneapolis, MN, USA). The immune-reactive bands were visualized using a chemiluminescent substrate (Invitrogen), and were exposed to X-ray film (Denville, Holliston, MA, USA).

Quantitative real-time PCR (Q-PCR)

Total RNA was extracted from cell lines with a TRIzol reagent kit (Invitorogen), according to the manufacturer's instructions. cDNA was synthesized from total RNA (2 µg) using the First Strand cDNA synthesis kit (Invitrogen). qPCR was performed using SYBR green (Bio-Rad) on Light Cycler 480 (Roche). The fold changes were normalized using GAPDH, and each reaction was conducted in triplicated. All qPCR reactions were repeated in at least 3 independent biological assays. The primers were as follows: for *PTPN12*, forward 5' TGGAGAAGTGGCCTTAGGGT 3' and reverse

5’ ATTGAGCCACTGCACTCCAA 3’; for *Sox2*, forward 5’ ACCAGCTCGCAGACCTACAT 3’ and reverse 5’ CTTGACCACCGAACCCATGG 3’; for *Oct4*, forward 5’ TCAGCCAAACGATCTGC 3’ and reverse 5’ TTCGCTTTCTCTTTCGGGCC 3’; for *Nanog*, forward 5’ CAGACCTGGTGCACCCAATC 3’ and reverse 5’ CTTCCAAGGCAGCCTCCAAG 3’; for *c-Myc*, forward 5’ GTGGAAAAGAGGCAGGCTCC 3’ and reverse 5’ CTTGACCCTCTTGGCAGCAG 3’; and for *p27, SNAIL, SLUG, TWIST1, ZEB1, ZEB2,* and *GAPDH* as described [13].

RNA sequencing (RNA-seq) assay

The quality of total RNA isolated from the cell lines was measured using Bioanalyzer RNA Nano 6000 (Agilent Technologies, Santa Clara, CA, USA). Library preparation was performed by TruSeq Standed Total RNA Library Prep (Illumina, San Diego, USA), and the quality was confirmed using KAPA qPCR Library Quantification (Kapa Biosystems, Wilmington, MA, USA). Paired end sequencing was performed on Illumina 150 cycles 400M reads. Quality of raw sequence reads was assessed using FastQC. Trimmomatic [69] was used to trim sequences of bad quality bases, adapter, and primer sequences. Genome alignment was performed using STAR aligner [70], with UCSC human genome (hg38). After the read alignment, raw counts were estimated using featureCounts [71]. DESeq2 [72] was applied to identify differentially expressed genes between groups of samples. Pathway and gene set analysis was performed using Gene Set Enrichment Analysis (GSEA) [73].

Chromatin immunoprecipitation (ChIP) assay

ChIP assay was performed as described [20]. Briefly, after cells were crosslinked with 1% formaldehyde, the cells were lysed and sonicated. For the immunoprecipitation, sonicated samples were incubated with anti-cJun (Cell Signaling; 9165s), p27 (Cell Signaling; 3686), SIN3A (Abcam; ab3479), YY1 (Abcam; ab12132), and HDAC1 (Santa Cruz; sc-7872) antibodies overnight at 4°C. For Re-ChIP assay, sonicated sample with anti-cJun antibody was incubated in 10 mM DTT for 30 min, and then diluted 40 fold for incubation with re-ChIP with anti-p27 antibody. Samples were collected on A/G plus-agarose (Santa Cruz), and DNA was eluted by DNA Purification Kit (Qiagen, Hilden, Germany). Eluted DNA was used for q-PCR. The following primers were used for *PTPN12* promoter: forward 5’ TGAAGATTCACCTCCTCCC 3’ and reverse 5’ CCGCTGGATGATCACATTTC 3’.

Sphere formation assay

The cells (5×10^3 cells/well) were plated in ultra-low attachment 6-well plates (Corning Inc., Corning, NY, USA) with 2 mL of MammoCult™ medium (STEMCELL™, Cambridge, MA, USA), and incubated in culture conditions for 12-21 days. Spheres > 75 µm in size were visualized and counted using a GelCount™ Tumor Colony Counter (Oxford Optronix, Abingdon, UK).

Colony formation assay

The cells (5000 cells/well) were seeded into 6-well plate with 0.5% and 0.35% of agarose for bottom and upper layers. After incubation for 4 weeks, colonies stained with Thiazolyl Blue tetrazolium bromide (Alfa Aesar, Ward Hill, MA, USA) visualized and counted using a GelCount™ Tumor Colony Counter.

Flow cytometry

Cells were incubated with anti-CD44-APC and anti-CD24-PE antibodies (BD Biosciences, franklin Lakes, NJ, USA) for 60 min at 4°C. After washing twice with PBS containing 0.1% bovine serum albumin (BSA), the cells were analyzed using a BD FACSCanto II Flow Cytometer (BD Biosciences).

STAT3/p27pT157 activated gene expression profile

All patient data are derived from The Cancer Genome Atlas breast cancer (TCGA-BRCA) data set, comprising 179 ER negative breast cancers. Clinical and RNA-seq data for these breast cancers were downloaded using R "TCGAbiolinks" package [74]. Reverse phase protein lysate array phosphoprotein data (normalized data: Level 3) for these patient tumors were downloaded from the data portal on TCPA website (http://tcpaportal.org/tcpa/). Breast cancers within the top quartiles of both STAT3_pY705 (pSTAT3-high) and p27pT157 (p27-high) were grouped together versus all other patients. Genes differentially expressed in tumors with p27-high and pSTAT3 high compared to all others were identified with R DESeq2 package [72]. The expression of 851 differentially expressed genes was compared to our RNA-seq data from 231, 231p27CK-DD, 188 and 1833shp27 lines to identify STAT- activated genes whose expression was elevated in p27 activated lines compared to 231 and 1833shp27.

Coordinate expression of NOS signature and p27-regulated genes

The profiles of NOS activated and repressed genes in ESC[41] were compared to our RNA-seq data in all 4 lines. A subset of NOS activated target genes preferentially upregulated in p27 activated lines and a subset of NOS-repressed genes that were

also preferentially repressed in p27-activated lines versus 231 and 1833shp27 were displayed in heatmaps and analyzed by GO.

In vivo limiting dilution T-ISC assay

All animal research was conducted in accordance with the University of Miami Animal Care Committee. For limiting dilution T-ISC assays, 5 week-old female Balb/c nude mice were purchased from Charles River Laboratories (Boston, MA, USA). Limiting dilutions of 10, 100, and 1000 cells were each suspended in 10 mg/ml Matrigel with Hanks' Balanced Salt Solution (HBSS; Lonza, Walkersville, MD, USA), and injected into the 4rth inguinal mammary fat pad (n=12, 10, 8 mice per group). Mice were euthanized per IACUC guidelines. Tumor size was measured twice/week, and tumor volumes were estimated as length × width × width × 0.5. T-ISC frequency was calculated by L-Calc Limiting Dilution Software (STEMCELL™).

Experimental data analysis

Data are presented as the mean ± SEM. Statistical comparisons between two groups were performed by the Student's *t* test. One-way ANOVA, followed by the Student's *t* test, and Tukey's multiple comparison test was used to compare more than two groups. A value of $P < 0.05$ was considered significant.

DATA AND SOFTWARE AVAILABILITY

The accession number for the sequencing data reported in this paper is GSE 112446

ACKNOWLEDGMENTS

Work was supported by 2R01CA105118-05A1 (JMS) and by DOD BCRP W81XWH-17-1-0456 (JMS).

AUTHOR CONTRIBUTIONS

J.M.S. conceived the study, designed experiments and funded the work. H.Y., K.B., M.K., and D.Z. designed and performed in vitro and/or in vivo experiments. K.J. and D.Z. established cell lines. L.M. and J.M.S. directed analysis of ChIP-seq and RNA-seq data. M.S., H.Y., L.M., and X.X. analyzed the sequencing data. J.M.S. and X.X. analyzed the TCGA/TCPA data. H.Y. wrote and all authors contributed to the manuscript.

MATERIALS AND CORRESPONDENCE

Correspondence and material requests should be addressed to J. Slingerland

COMPETING INTERESTS

The authors declare no conflicts of interest.

Reference List

1. Slingerland,J.M. *et al.* A novel inhibitor of cyclin-Cdk activity detected in transforming growth factor beta-arrested epithelial cells. *Mol Cell Biol* **14**, 3683-3694 (1994).

2. Hengst,L., Dulic,V., Slingerland,J.M., Lees,E., & Reed,S.I. A cell cycle-regulated inhibitor of cyclin-dependent kinases. *Proc Natl Acad Sci USA* **91**, 5291-5295 (1994).

3. Polyak,K. *et al.* Cloning of p27KIP1, a cyclin-dependent kinase inhibitor and a potential mediator of extracellular antimitogenic signals. *Cell* **78**, 59-66 (1994).

4. Koff,A., Ohtsuki,M., Polyak,K., Roberts,J.M., & Massague,J. Negative regulation of G1 in mammalian cells: inhibition of cyclin E-dependent kinase by TGF-beta. *Science* **260**, 536-539 (1993).

5. Liang,J. *et al.* PKB/Akt phosphorylates p27, impairs nuclear import of p27 and opposes p27-mediated G1 arrest. *Nat Med* **8**, 1153-1160 (2002).

6. Shin,I. *et al.* PKB/Akt mediates cell-cycle progression by phosphorylation of p27(Kip1) at threonine 157 and modulation of its cellular localization. *Nat Med* **8**, 1145-1152 (2002).

7. Viglietto,G. *et al.* Cytoplasmic relocalization and inhibition of the cyclin-dependent kinase inhibitor p27(Kip1) by PKB/Akt-mediated phosphorylation in breast cancer. *Nat Med* **8**, 1136-1144 (2002).

8. Hong,F. *et al.* mTOR-raptor binds and activates SGK1 to regulate p27 phosphorylation. *Mol Cell* **30**, 701-711 (2008).

9. Fujita,N., Sato,S., & Tsuruo,T. Phosphorylation of p27Kip1 at threonine 198 by p90 ribosomal protein S6 kinases promotes its binding to 14-3-3 and cytoplasmic localization. *J Biol Chem* **278**, 49254-49260 (2003).

10. Larrea,M.D. *et al.* RSK1 drives p27Kip1 phosphorylation at T198 to promote RhoA inhibition and increase cell motility. *Proc Natl Acad Sci USA* **106**, 9268-9273 (2009).

11. Besson,A., Gurian-West,M., Schmidt,A., Hall,A., & Roberts,J.M. p27Kip1 modulates cell migration through the regulation of RhoA activation. *Genes Dev* **18**, 862-876 (2004).

12. Larrea,M.D. *et al.* Phosphorylation of p27Kip1 regulates assembly and activation of cyclin D1-Cdk4. *Mol Cell Biol* **28**, 6462-6472 (2008).

13. Zhao D. *et al.* Cytoplasmic p27 promotes epithelial-mesenchymal transition and tumor metastasis via STAT3-mediated Twist1 upregulation . Oncogene 34, 5447-5459. 2015.

14. Messina,G. *et al.* p27Kip1 acts downstream of N-cadherin-mediated cell adhesion to promote myogenesis beyond cell cycle regulation. *Mol. Biol. Cell* **16**, 1469-1480 (2005).

15. Movassagh,M. & Philpott,A. Cardiac differentiation in Xenopus requires the cyclin-dependent kinase inhibitor, p27Xic1. *Cardiovasc. Res.* **79**, 436-447 (2008).

16. Nguyen,L. *et al.* p27kip1 independently promotes neuronal differentiation and migration in the cerebral cortex. *Genes Dev.* **20**, 1511-1524 (2006).

17. Yeh,N. *et al.* Cooperation between p27 and p107 during endochondral ossification suggests a genetic pathway controlled by p27 and p130. *Mol. Cell Biol.* **27**, 5161-5171 (2007).

18. Besson,A. *et al.* Discovery of an oncogenic activity in p27Kip1 that causes stem cell expansion and a multiple tumor phenotype. *Genes Dev* **21**, 1731-1746 (2007).

19. Pippa,R. *et al.* p27Kip1 represses transcription by direct interaction with p130/E2F4 at the promoters of target genes. *Oncogene* **31**, 4207-4220 (2012).

20. Li,H. *et al.* p27(Kip1) directly represses Sox2 during embryonic stem cell differentiation. *Cell Stem Cell* **11**, 845-852 (2012).

21. Hyunho Yoon *et al.* p27 is a cJun co-regulator broadly recruited to chromatin to drive gene programs of metastasis. *Submitted*(2018).

22. Sun,T. *et al.* Activation of multiple proto-oncogenic tyrosine kinases in breast cancer via loss of the PTPN12 phosphatase. *Cell* **144**, 703-718 (2011).

23. Tonks,N.K. Protein tyrosine phosphatases: from genes, to function, to disease. *Nat. Rev. Mol. Cell Biol.* **7**, 833-846 (2006).

24. Nair,A. *et al.* Combinatorial inhibition of PTPN12-regulated receptors leads to a broadly effective therapeutic strategy in triple-negative breast cancer. *Nat. Med.* **24**, 505-511 (2018).

25. Li,J. *et al.* Loss of PTPN12 Stimulates Progression of ErbB2-Dependent Breast Cancer by Enhancing Cell Survival, Migration, and Epithelial-to-Mesenchymal Transition. *Mol. Cell Biol.* **35**, 4069-4082 (2015).

26. Besson,A., Dowdy,S.F., & Roberts,J.M. CDK inhibitors: cell cycle regulators and beyond. *Dev Cell* **14**, 159-169 (2008).

27. Denicourt,C., Saenz,C.C., Datnow,B., Cui,X.S., & Dowdy,S.F. Relocalized p27(KiP1) tumor suppressor functions as a cytoplasmic metastatic oncogene in melanoma. *Cancer Res* **67**, 9238-9243 (2007).

28. Wu,F.Y. *et al.* Reduction of cytosolic p27(Kip1) inhibits cancer cell motility, survival, and tumorigenicity. *Cancer Res* **66**, 2162-2172 (2006).

29. Wander,S. *et al.* PI3K/mTOR inhibition can impair tumor invasion and metastasis in vivo despite a lack of antiproliferative action in vitro: implications for targeted therapy. *Breast Cancer Res Treat* **138**, 369-381 (2013).

30. Kang,Y. *et al.* A multigenic program mediating breast cancer metastasis to bone. *Cancer Cell* **3**, 537-549 (2003).

31. Kim,S.V. *et al.* Modulation of cell adhesion and motility in the immune system by Myo1f. *Science* **314**, 136-139 (2006).

32. Diquigiovanni,C. *et al.* Mutant MYO1F alters the mitochondrial network and induces tumor proliferation in thyroid cancer. *Int. J. Cancer*(2018).

33. De Braekeleer,E. *et al.* Acute lymphoblastic leukemia associated with RCSD1-ABL1 novel fusion gene has a distinct gene expression profile from BCR-ABL1 fusion. *Leukemia* **27**, 1422-1424 (2013).

34. Hempel,A. *et al.* The CapZ interacting protein Rcsd1 is required for cardiogenesis downstream of Wnt11a in Xenopus laevis. *Dev. Biol.* **424**, 28-39 (2017).

35. Lu,P. *et al.* The developmental regulator protein Gon4l associates with protein YY1, co-repressor Sin3a, and histone deacetylase 1 and mediates transcriptional repression. *J. Biol. Chem.* **286**, 18311-18319 (2011).

36. Ceppi,P. & Peter,M.E. MicroRNAs regulate both epithelial-to-mesenchymal transition and cancer stem cells. *Oncogene* **33**, 269-278 (2014).

37. Visvader,J.E. & Lindeman,G.J. Cancer stem cells in solid tumours: accumulating evidence and unresolved questions. *Nat Rev Cancer* **8**, 755-768 (2008).

38. Al Hajj,M., Wicha,M.S., Benito-Hernandez,A., Morrison,S.J., & Clarke,M.F. Prospective identification of tumorigenic breast cancer cells. *Proc Natl Acad Sci USA* **100**, 3983-3988 (2003).

39. Begum,A. *et al.* The extracellular matrix and focal adhesion kinase signaling regulate cancer stem cell function in pancreatic ductal adenocarcinoma. *PLoS. One.* **12**, e0180181 (2017).

40. Marotta,L.L. *et al.* The JAK2/STAT3 signaling pathway is required for growth of $CD44^{+}CD24^{-}$ stem cell-like breast cancer cells in human tumors. *J Clin Invest* **121**, 2723-2735 (2011).

41. Boyer,L.A. *et al.* Core transcriptional regulatory circuitry in human embryonic stem cells. *Cell* **122**, 947-956 (2005).

42. Chu,I.M., Hengst,L., & Slingerland,J.M. The Cdk inhibitor p27 in human cancer: prognostic potential and relevance to anticancer therapy. *Nat Rev Cancer* **8**, 253-267 (2008).

43. Wander,S.A., Zhao,D., & Slingerland,J.M. p27: a barometer of signaling deregulation and potential predictor of response to targeted therapies. *Clin Cancer Res.* **17**, 12-18 (2011).

44. LaBaer,J. *et al.* New functional activities for the p21 family of CDK inhibitors. *Genes Dev* **11**, 847-862 (1997).

45. Eferl,R. & Wagner,E.F. AP-1: a double-edged sword in tumorigenesis. *Nat. Rev. Cancer* **3**, 859-868 (2003).

46. Shaulian,E. AP-1--The Jun proteins: Oncogenes or tumor suppressors in disguise? *Cell Signal.* **22**, 894-899 (2010).

47. Ogawa,S. *et al.* A nuclear receptor corepressor transcriptional checkpoint controlling activator protein 1-dependent gene networks required for macrophage activation. *Proc. Natl. Acad. Sci. U. S. A* **101**, 14461-14466 (2004).

48. Ghisletti,S. *et al.* Cooperative NCoR/SMRT interactions establish a corepressor-based strategy for integration of inflammatory and anti-inflammatory signaling pathways. *Genes Dev.* **23**, 681-693 (2009).

49. Aguilera,C. *et al.* c-Jun N-terminal phosphorylation antagonises recruitment of the Mbd3/NuRD repressor complex. *Nature* **469**, 231-235 (2011).

50. Sicinski,P., Zacharek,S., & Kim,C. Duality of p27Kip1 function in tumorigenesis. *Genes Dev* **21**, 1703-1706 (2007).

51. Aleem,E., Kiyokawa,H., & Kaldis,P. Cdc2-cyclin E complexes regulate the G1/S phase transition. *Nat Cell Biol* **7**, 831-836 (2005).

52. Martin,A. *et al.* Cdk2 is dispensable for cell cycle inhibition and tumor suppression mediated by p27(Kip1) and p21(Cip1). *Cancer Cell* **7**, 591-598 (2005).

53. Vernon,A.E. & Philpott,A. A single cdk inhibitor, p27Xic1, functions beyond cell cycle regulation to promote muscle differentiation in Xenopus. *Development* **130**, 71-83 (2003).

54. Bicer,A. *et al.* ChIP-Seq analysis identifies p27(Kip1)-target genes involved in cell adhesion and cell signalling in mouse embryonic fibroblasts. *PLoS. One.* **12**, e0187891 (2017).

55. Boussiotis,V.A. *et al.* p27kip1 functions as an anergy factor inhibiting interleukin 2 transcription and clonal expansion of alloreactive human and mouse helper T lymphocytes. *Nat. Med.* **6**, 290-297 (2000).

56. Fang,Y. *et al.* A new tumour suppression mechanism by p27Kip1: EGFR down-regulation mediated by JNK/c-Jun pathway inhibition. *Biochem. J.* **463**, 383-392 (2014).

57. Wilkinson,D.G., Bhatt,S., Ryseck,R.P., & Bravo,R. Tissue-specific expression of c-jun and junB during organogenesis in the mouse. *Development* **106**, 465-471 (1989).

58. Eferl,R. *et al.* Functions of c-Jun in liver and heart development. *J. Cell Biol.* **145**, 1049-1061 (1999).

59. Ikeda,F. *et al.* Critical roles of c-Jun signaling in regulation of NFAT family and RANKL-regulated osteoclast differentiation. *J. Clin. Invest* **114**, 475-484 (2004).

60. Jochum,W., Passegue,E., & Wagner,E.F. AP-1 in mouse development and tumorigenesis. *Oncogene* **20**, 2401-2412 (2001).

61. Li,Y.Q. Master stem cell transcription factors and signaling regulation. *Cell Reprogram.* **12**, 3-13 (2010).

62. Nakayama,K. *et al.* Mice lacking p27(Kip1) display increased body size, multiple organ hyperplasia, retinal dysplasia, and pituitary tumors. *Cell* **85**, 707-720 (1996).

63. Fero,M.L. *et al.* A syndrome of multi-organ hyperplasia with features of gigantism, tumorigenesis and female sterility in p27Kip1-deficient mice. *Cell* **85**, 733-744 (1996).

64. Kiyokawa,H. *et al.* Enhanced growth of mice lacking the cyclin-dependent kinase inhibitor function of p27Kip1. *Cell* **85**, 721-732 (1996).

65. Verma,N. *et al.* PYK2 sustains endosomal-derived receptor signalling and enhances epithelial-to-mesenchymal transition. *Nat. Commun.* **6**, 6064 (2015).

66. Frank,N.Y., Schatton,T., & Frank,M.H. The therapeutic promise of the cancer stem cell concept. *J Clin Invest* **120**, 41-50 (2010).

67. Nitz,M.D., Harding,M.A., & Theodorescu,D. Invasion and metastasis models for studying RhoGDI2 in bladder cancer. *Methods Enzymol.* **439**, 219-233 (2008).

68. Minn,A.J. *et al.* Genes that mediate breast cancer metastasis to lung. *Nature* **436**, 518-524 (2005).

69. Bolger,A.M., Lohse,M., & Usadel,B. Trimmomatic: a flexible trimmer for Illumina sequence data. *Bioinformatics.* **30**, 2114-2120 (2014).

70. Dobin,A. *et al.* STAR: ultrafast universal RNA-seq aligner. *Bioinformatics.* **29**, 15-21 (2013).

71. Liao,Y., Smyth,G.K., & Shi,W. featureCounts: an efficient general purpose program for assigning sequence reads to genomic features. *Bioinformatics.* **30**, 923-930 (2014).

72. Love,M.I., Huber,W., & Anders,S. Moderated estimation of fold change and dispersion for RNA-seq data with DESeq2. *Genome Biol.* **15**, 550 (2014).

73. Subramanian,A. *et al.* Gene set enrichment analysis: a knowledge-based approach for interpreting genome-wide expression profiles. *Proc. Natl. Acad. Sci. U. S. A* **102**, 15545-15550 (2005).

74. Colaprico,A. *et al.* TCGAbiolinks: an R/Bioconductor package for integrative analysis of TCGA data. *Nucleic Acids Res.* **44**, e71 (2016).

FIGURE LEGENDS

Fig. 1. C-terminally phosphorylated 27/cJun target tumor suppressor genes. **a**, Venn diagram comparing genes downregulated in 231p27CK-DD vs. 231 (fold-change < 0.75, p value < 0.005, q value < 0.1) and upregulated in 1833shp27 vs. 1833 (fold change > 1.5, p value < 0.005, q value < 0.1). Gene numbers are indicated. See also Supplementary Table 1a. **b**, ENRICHR analysis from the WikiPathway 2016 database using the 536 p27-downregulated genes from (**a**). See also Supplementary Fig. 1a. **c**, Heat map showing differential expression of 233 cJun/p27 target genes that are commonly bound in all of 231, 231p27CK-DD (231DD), and 1833. See also Supplementary Table 1b. **d**, Graphs shows differential binding of cJun (left) and p27 (right) to 233 target genes commonly bound in 231, 231p27CK-DD (231DD), and 1833. **e**, Pathway analysis (WikiPathway 2016) of 233 cJun/p27 target genes common to all 3 lines whose expression is downregulated in p27 activated lines compared to control 231. See also Supplementary Fig. 1b. **f**, Heat map showing differential expression profile of 233 cJun/p27 target genes that are novel targets bound in, 231p27CK-DD (231DD), and 1833 but not in 231. See also Supplementary Table 1c. WikiPathway database showing the main signaling pathways associated with these 146 unique targets downregulated in p27 activated lines compared to 231. See also Supplementary Fig. 1c.

Fig. 2. Validation of novel cJun/p27 repressed tumor suppressors, *MYO1F* and *TMEM71*. a, ChIP-Seq tracks show cJun and p27 binding at site -8 kb of the *MYO1F* transcription start site (TSS). **b**, ChIP-Seq tracks of cJun and p27 bindings at a site -1 kb of the *TMEM71* TSS. **c**, **d**, **e**, Validation of binding to and expression of *MYO1F*, a cJun/p27 repressed target gene bound in all 3 lines. (**c**) ChIP-qPCR with anti-cJun (left) and anti-p27 (right) antibodies at the -8 kb site of *MYO1F*. (**d**) qPCR expression of *MYO1F* by qPCR in the indicated lines. (**e**) Kaplan-Meier plotter™ data showing relapse free survival curves according to *MYO1F* mRNA expression above or below the median in 3951 primary breast cancers (red

line: high, n = 1971; black line: low, n = 1980). **f**, **g**, **h**, Validation of p27/cJun binding to and expression of *TMEM71*, a cJun/p27 repressed target gene unique to 231p27CK-DD (231DD) and 1833, but not bound in 231. (**f**) ChIP-qPCR with anti-cJun (left) and -p27 (right) antibodies at the site -1kb of the *TMEM71* TSS. (**g**) qPCR expression of *TMEM71* in the indicated lines. (**h**) Kaplan-Meier plotter^{TM} data showing relapse free survival curves according to *TMEM71* expression above or below the median in 1764 primary breast cancers (red line: high, n = 871; black line: low, n = 893). All non-KM graphs show mean ± SEM from at least 3 replicate assays, and p-values were represented by ANOVA analysis (**p < 0.01, ***p < 0.001). See also Supplementary Fig. 2.

Fig. 3. cJun/p27 represses *PTPN12* transcription in complex with YY1, SIN3A and HDAC1. a, A volcano plot of genes differentially expressed in 231-p27CK-DD vs. 231-vector by RNA-Seq. *PTPN12* expression was strongly decreased by p27CK-DD transduction (FDR < 0.01, log2 Fold change = -2.81, p < 0.0001). **b**, qPCR expression of *PTPN12* in MCF12A-vector and MCF12A-p27CK-DD (left); and in 231, 231-p27CK-DD, 1833, and 4175 cells (right). **c**, Lysates from the indicated lines from (**b**) above were analyzed by Western for PTPN12 with β-actin as a loading control. **d**, ChIP-Seq analysis with anti-cJun and -p27 antibodies. Schematic representation for cJun and p27 bindings at the +2 kb site of *PTPN12* TSS. See also Supplementary Fig. 3a. **e**, ChIP-qPCR analysis for cJun and p27 binding and for ChIP cJun; Re-ChIP p27 at the +2 kb site of *PTPN12* TSS in 231, 231p27CK-DD (231-DD), 1833, 1833shp27, and 1833 treated with PI3K inhibitor (1833+PI3Ki). IgG; negative control (see also controls for ChIP Re-ChIP Supplementary Fig. 3b, c). **f**, ChIP analysis using anti-SIN3A, anti-YY1, and anti-HDAC1 antibodies show binding at the +2 kb site of *PTPN12* TSS. See also Supplementary Fig. 3d. **g**, ChIP-Western blot. After ChIP with cJun antibody, cJun-bound chromatin immunoprecipitates (IP cJun) were resolved and associated p27, SIN3A, YY1, and HDAC1 detected by Western in 231 and 231p27CK-DD (right). Input protein levels are shown (left). **h**, Proposed model of cJun/p27 complex in the transcriptional regulation of *PTPN12*. **i**, Kaplan-Meier analysis using distant metastasis free survival (DMFS) from Gene Expression-Based Outcome for Breast Cancer Online (GOBO; www.co.bmc.lu.se/gobo). n = 821 patients, p = 0.00651. All non-KM graphs show mean ± SEM, and p-values were represented by Student's T Test or ANOVA analysis (**p < 0.01, ***p < 0.001).

Fig. 4. Activated p27 increases CSC properties *in vitro* via loss of PTPN12 and activation of pPYK2. a, Sphere forming assays in MCF12A-vector, MCF12A-p27CK-, and MCF12A-p27CK-DD lines. Left: representative images in vector only

(top), p27CK- (middle), and p27CK-DD (bottom) of MCF12A. Scale bars, 100 μm. Right: Mean spheres/2000 cells plated graphed +/-SEM. **b**, Surface expression of CD44 and CD24 in MCF12A-vector and MCF12A-p27CK-DD assayed by Flow cytometry (left). Western shows CD44 with β-actin controls in the same cells. **c**, Sphere forming assays and qPCR for *SOX2*, *MYC* and *NANOG* expression in 231-vector and 231-p27CK-DD. See also Supplementary Fig. 4a. **d**, Effects of stable *p27* knockdown (shp27) on sphere formation and *SOX2*, *MYC* and *NANOG* expression in 1833-scramble (Scr), and 1833shp27. See also Supplementary Fig. 4b-d. **e**, Effects of stable PTPN12 knockdown on qPCR expression CSC-TFs in 231 cells. The cells were infected with shPTPN12 lentiviruses. The expression and CSC-TFs (SOX2, NANOG and OCT4) was analyzed by qPCR (left). Overexpression of PTPN12 in 1833 on qPCR expression (NANOG, cMYC, and SOX2; right). See also Supplementary Fig. 4e, f. **f**, Sphere forming assay in 231, 231shPTPN12, 1833, and 1833PTPN12. See also Supplementary Fig. 4g-j. **g**, Effects of transient PTPN12 knockdown on protein tyrosine activation. 231 cells were transfected with control siRNA, PTPN12 siRNA #1 and #2, and subjected to Western blot for protein kinases. **h**, Effects of stable PYK2 knockdown on qPCR expression (left) and Western blot (right) of CSC-TFs in 231-p27CK-DD. **i**, Sphere forming assay in 231 and 231-p27CK-DD with transient PYK2 knockdown (top) confirmed by Western blot (bottom). **j**, Effects of stable PYK2 knockdown on ALDH1+ expression analyzed by flow cytometry. **k**, Sphere forming assay in 231 and 231 with PYK2 kinase inhibitor (PF431396) treatment (right). The cells were subjected to Western blot for PYK2 phosphorylation (left). **l**, PI3K inhibition reverses p27-mediated SOX2 and cMYC expression. 231, 1833, and 1833+PF1502 (PI3Ki) cells were subjected to Western blot for the indicated proteins. All graphs show mean ± SEM from at least 3 replicate assays, and p-values were represented by Student's T Test or ANOVA analysis (*$p < 0.05$, **$p < 0.01$, ***$p < 0.001$).

Fig. 5. p27 activated lines show PYK2-dependent STAT3 activation and show preferential downregulation of genes repressed in ESC, NOS and STAT3 gene signatures. a, Western blots show total and phosphorylated PYK2 and STAT3 levels in the indicated lines and effects of 48 hrs of PF431396. **b**, Effects of transient siPYK2-mediated PYK2 loss on total and phosphorylated PYK2 and STAT3. Levels of p27 and p27pT198 are shown. **c**, Effects of stable shPYK2 expression on total and phosphorylated PYK2 and STAT3. **d,** Gene expression heatmaps show changes in expression of STAT3 target signatures in 231, 231p27CK-DD, 1833 and 1833shp27. **e**, Gene ontogeny in NCI-Nature and KEGG 2016 database of STAT3 activated target genes. See also Supplementary Fig. 5a. **f**, Gene expression heatmaps of NOS target gene signatures

genes in the indicated cell lines. **g**, **h**, Gene ontogeny of NOS target genes that are regulated by p27. See also Supplementary Fig. 5b.

Fig. 6. p27 is required for tumor-initiating ability *in vivo* via loss of PTPN12 and activation of pPYK2. a, **b**, Graphs showing tumor free mice (%). The cells were injected in the mammary fat pads of Balb/c nude mice at limiting dilution (n = 8, 10, 12 mice per group) of 231 vector controls, 231p27CK-DD, 231p27CK-DD + shPYK2 and 231shPTPN12 (**a**); 1833, 1833PTPN12 and 1833shp27 (**b**). **c**, Tumor-initiating stem cell (T-ISC) frequencies (top) were calculated by L-Calc Limiting Dilution Software in the indicated cell lines. Pairwise comparisons of T-ISC frequencies are shown (bottom). See also Supplementary Fig. 6

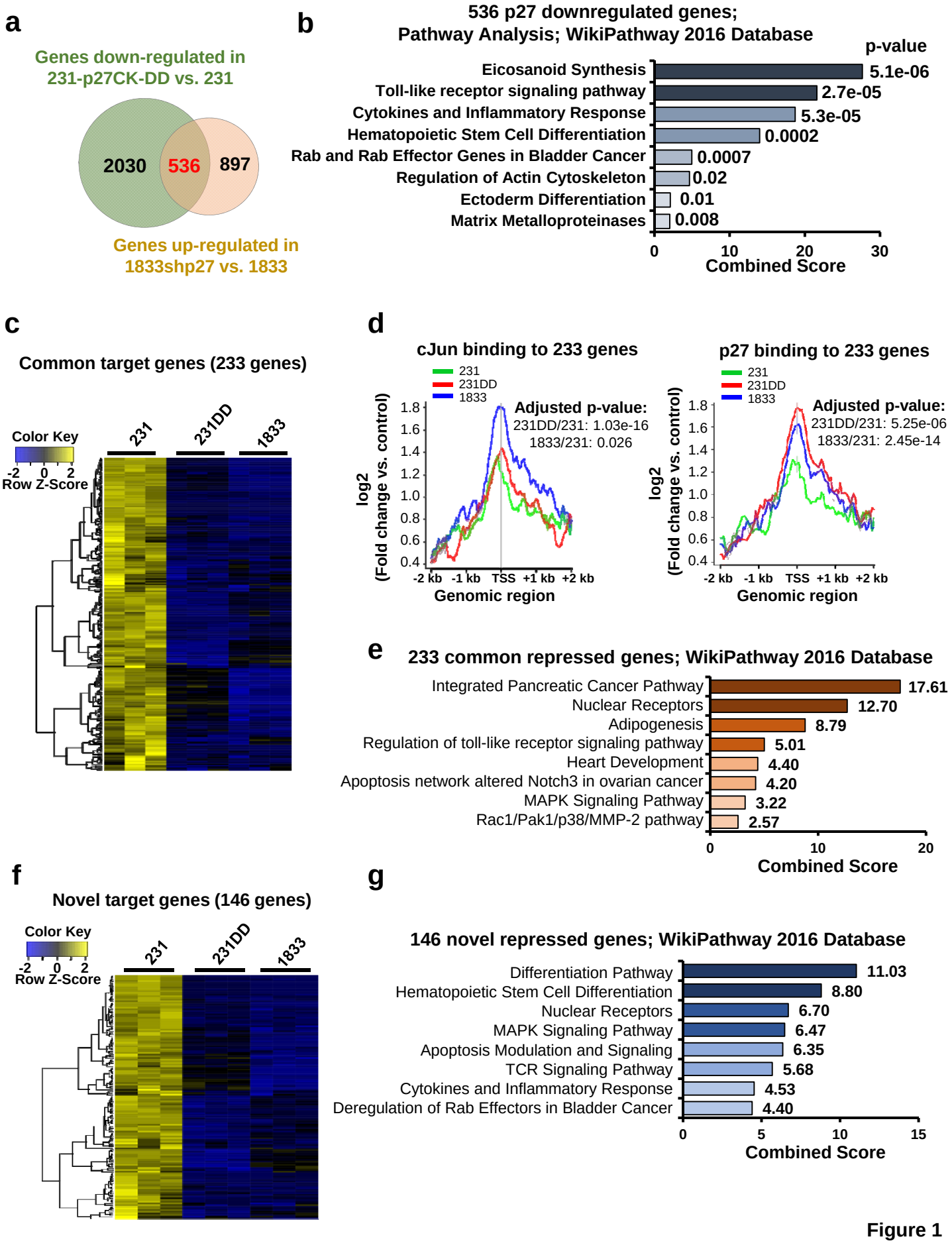
a
Genes down-regulated in
231-p27CK-DD vs. 231
2030
536
897
Genes up-regulated in
1833shp27 vs. 1833
b
536 p27 downregulated genes;
Pathway Analysis; WikiPathway 2016 Database
p-value
Eicosanoid Synthesis
5.1e-06
Toll-like receptor signaling pathway
2.7e-05
Cytokines and Inflammatory Response
5.3e-05
Hematopoietic Stem Cell Differentiation
0.0002
Rab and Rab Effector Genes in Bladder Cancer
0.0007
Regulation of Actin Cytoskeleton
0.02
Ectoderm Differentiation
0.01
Matrix Metalloproteinases
0.008
0
10
20
30
Combined Score
c
Common target genes (233 genes)
Color Key
-2 0 2
Row Z-Score
231
231DD
1833
d
cJun binding to 233 genes
231
231DD
1833
Adjusted p-value:
231DD/231: 1.03e-16
1833/231: 0.026
log2
(Fold change vs. control)
1.8
1.6
1.4
1.2
1.0
0.8
0.6
0.4
-2 kb
-1 kb
TSS
+1 kb
+2 kb
Genomic region
p27 binding to 233 genes
231
231DD
1833
Adjusted p-value:
231DD/231: 5.25e-06
1833/231: 2.45e-14
log2
(Fold change vs. control)
1.8
1.6
1.4
1.2
1.0
0.8
0.6
0.4
-2 kb
-1 kb
TSS
+1 kb
+2 kb
Genomic region
e
233 common repressed genes; WikiPathway 2016 Database
Integrated Pancreatic Cancer Pathway
17.61
Nuclear Receptors
12.70
Adipogenesis
8.79
Regulation of toll-like receptor signaling pathway
5.01
Heart Development
4.40
Apoptosis network altered Notch3 in ovarian cancer
4.20
MAPK Signaling Pathway
3.22
Rac1/Pak1/p38/MMP-2 pathway
2.57
0
10
20
Combined Score
f
Novel target genes (146 genes)
Color Key
-2 0 2
Row Z-Score
231
231DD
1833
g
146 novel repressed genes; WikiPathway 2016 Database
Differentiation Pathway
11.03
Hematopoietic Stem Cell Differentiation
8.80
Nuclear Receptors
6.70
MAPK Signaling Pathway
6.47
Apoptosis Modulation and Signaling
6.35
TCR Signaling Pathway
5.68
Cytokines and Inflammatory Response
4.53
Deregulation of Rab Effectors in Bladder Cancer
4.40
0
5
10
15
Combined Score

Figure 1

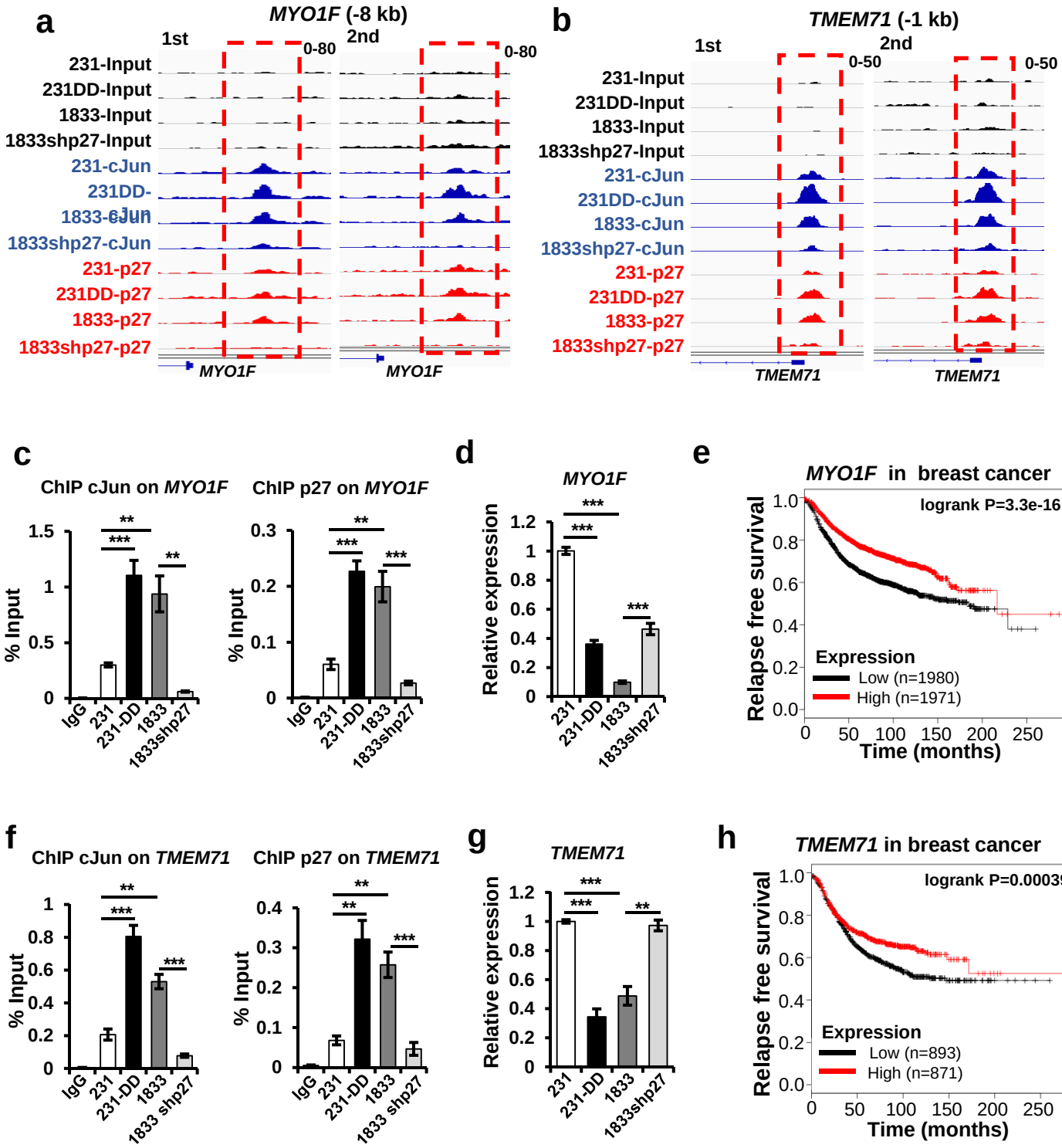
a
MYO1F (-8 kb)
1st
2nd
0-80
0-80
231-Input
231DD-Input
1833-Input
1833shp27-Input
231-cJun
231DD-cJun
1833-cJun
1833shp27-cJun
231-p27
231DD-p27
1833-p27
1833shp27-p27
MYO1F
MYO1F
b
TMEM71 (-1 kb)
1st
2nd
0-50
0-50
231-Input
231DD-Input
1833-Input
1833shp27-Input
231-cJun
231DD-cJun
1833-cJun
1833shp27-cJun
231-p27
231DD-p27
1833-p27
1833shp27-p27
TMEM71
TMEM71
c
ChIP cJun on MYO1F
% Input
IgG
231
231-DD
1833
1833shp27
ChIP p27 on MYO1F
% Input
IgG
231
231-DD
1833
1833shp27
d
MYO1F
Relative expression
231
231-DD
1833
1833shp27
e
MYO1F in breast cancer
logrank P=3.3e-16
Relapse free survival
Expression
Low (n=1980)
High (n=1971)
Time (months)
f
ChIP cJun on TMEM71
% Input
IgG
231
231-DD
1833
1833 shp27
ChIP p27 on TMEM71
% Input
IgG
231
231-DD
1833
1833 shp27
g
TMEM71
Relative expression
231
231-DD
1833
1833shp27
h
TMEM71 in breast cancer
logrank P=0.00039
Relapse free survival
Expression
Low (n=893)
High (n=871)
Time (months)

Figure 2

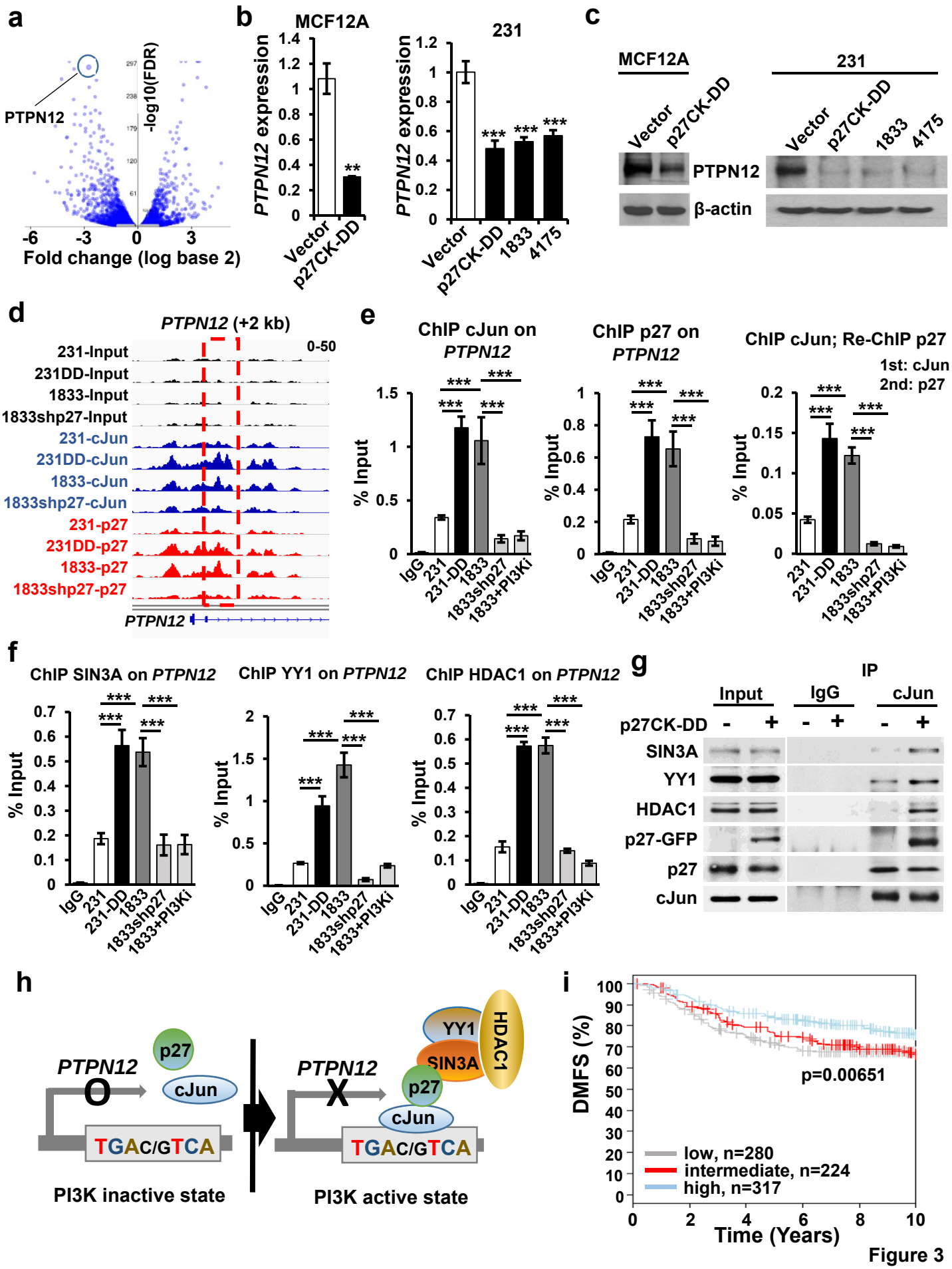
a
PTPN12
-log10(FDR)
Fold change (log base 2)
b
MCF12A
231
PTPN12 expression
Vector
p27CK-DD
1833
4175
c
MCF12A
231
Vector
p27CK-DD
1833
4175
PTPN12
β-actin
d
PTPN12 (+2 kb)
0-50
231-Input
231DD-Input
1833-Input
1833shp27-Input
231-cJun
231DD-cJun
1833-cJun
1833shp27-cJun
231-p27
231DD-p27
1833-p27
1833shp27-p27
PTPN12
e
ChIP cJun on PTPN12
ChIP p27 on PTPN12
ChIP cJun; Re-ChIP p27
1st: cJun
2nd: p27
% Input
IgG
231
231-DD
1833
1833shp27
1833+PI3Ki
f
ChIP SIN3A on PTPN12
ChIP YY1 on PTPN12
ChIP HDAC1 on PTPN12
g
IP
Input
IgG
cJun
p27CK-DD
SIN3A
YY1
HDAC1
p27-GFP
p27
cJun
h
PTPN12
p27
cJun
TGAC/GTCA
PI3K inactive state
PI3K active state
YY1
SIN3A
HDAC1
i
DMFS (%)
p=0.00651
low, n=280
intermediate, n=224
high, n=317
Time (Years)

Figure 3

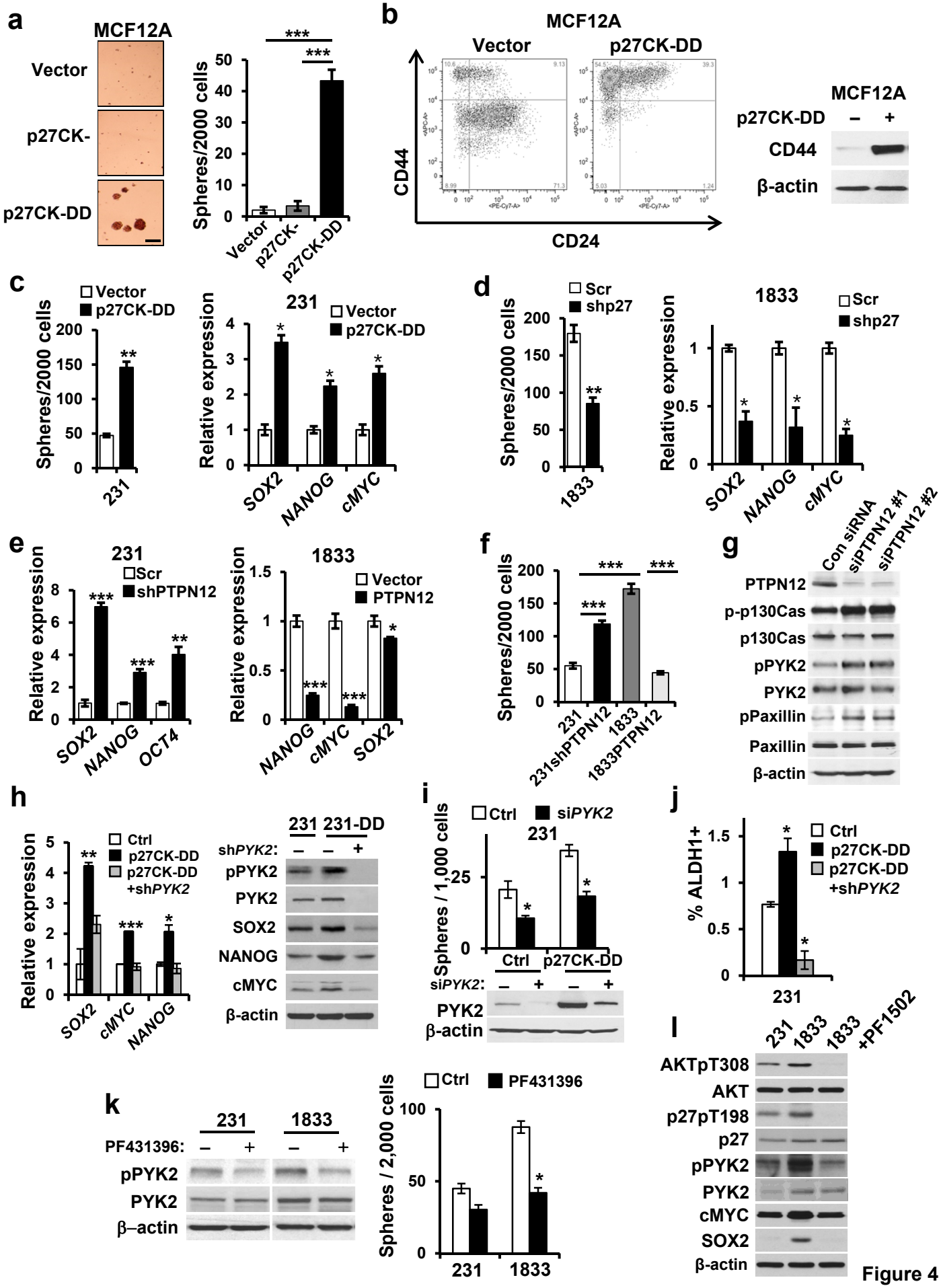
a
MCF12A
Vector
p27CK-
p27CK-DD
Spheres/2000 cells
***
***
Vector
p27CK-
p27CK-DD
b
MCF12A
Vector
p27CK-DD
CD44
CD24
MCF12A
p27CK-DD – +
CD44
β-actin
c
Vector
p27CK-DD
Spheres/2000 cells
231
Relative expression
231
Vector
p27CK-DD
SOX2
NANOG
cMYC
d
Scr
shp27
Spheres/2000 cells
1833
Relative expression
1833
Scr
shp27
SOX2
NANOG
cMYC
e
Relative expression
231
Scr
shPTPN12
SOX2
NANOG
OCT4
Relative expression
1833
Vector
PTPN12
NANOG
cMYC
SOX2
f
Spheres/2000 cells
231
231shPTPN12
1833
1833PTPN12
g
Con siRNA
siPTPN12 #1
siPTPN12 #2
PTPN12
p-p130Cas
p130Cas
pPYK2
PYK2
pPaxillin
Paxillin
β-actin
h
Relative expression
Ctrl
p27CK-DD
p27CK-DD +shPYK2
SOX2
cMYC
NANOG
231
231-DD
shPYK2: – – +
pPYK2
PYK2
SOX2
NANOG
cMYC
β-actin
i
Ctrl
siPYK2
231
Spheres / 1,000 cells
Ctrl
p27CK-DD
siPYK2: – + – +
PYK2
β-actin
j
% ALDH1+
Ctrl
p27CK-DD
p27CK-DD +shPYK2
231
k
231
1833
PF431396: – + – +
pPYK2
PYK2
β–actin
Ctrl
PF431396
Spheres / 2,000 cells
231
1833
l
231
1833
1833
+PF1502
AKTpT308
AKT
p27pT198
p27
pPYK2
PYK2
cMYC
SOX2
β-actin

Figure 4

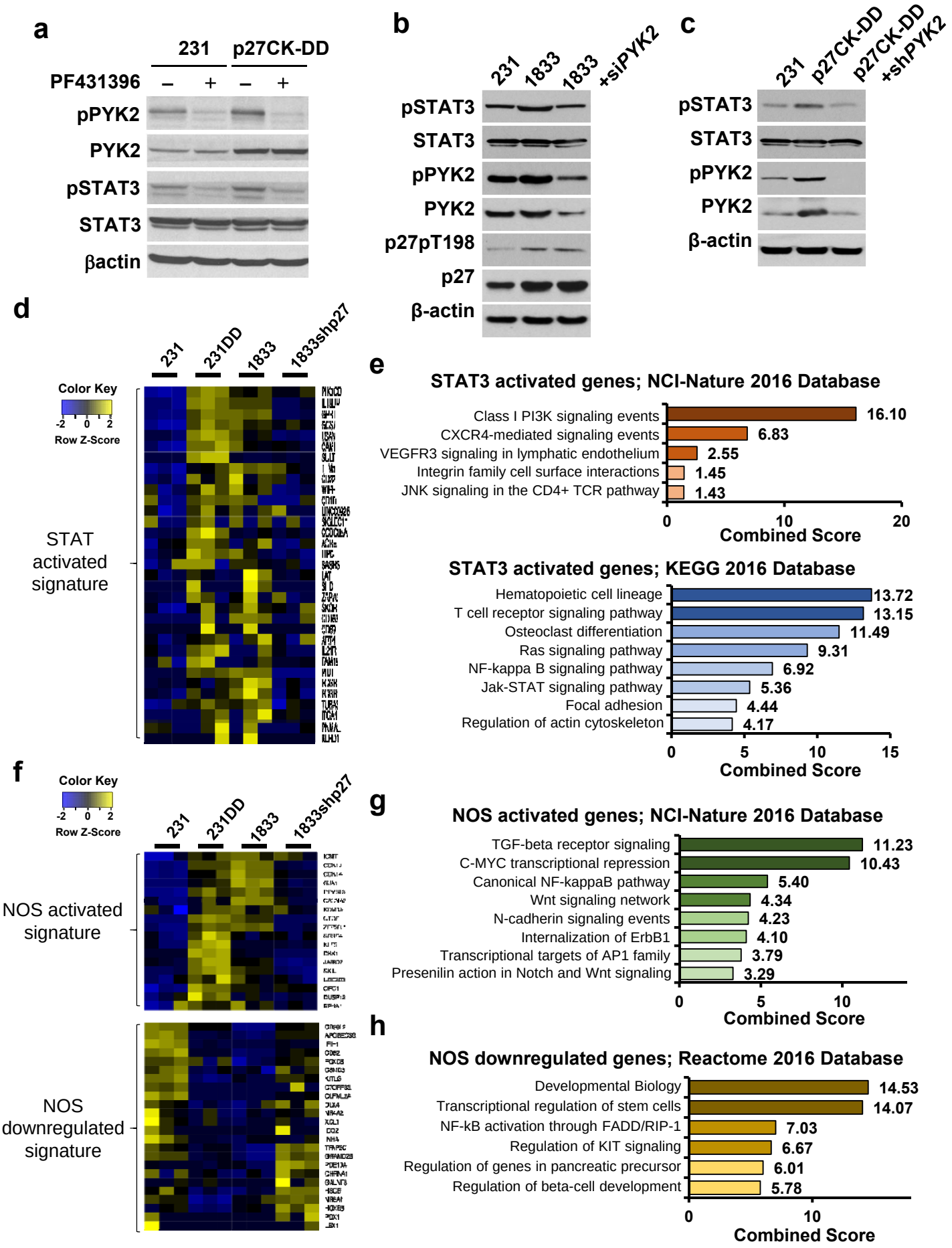
a
231
p27CK-DD
PF431396
–
+
–
+
pPYK2
PYK2
pSTAT3
STAT3
βactin
b
231
1833
1833
+siPYK2
pSTAT3
STAT3
pPYK2
PYK2
p27pT198
p27
β-actin
c
231
p27CK-DD
p27CK-DD
+shPYK2
pSTAT3
STAT3
pPYK2
PYK2
β-actin
d
231
231DD
1833
1833shp27
Color Key
-2
0
2
Row Z-Score
STAT activated signature
e
STAT3 activated genes; NCI-Nature 2016 Database
Class I PI3K signaling events
16.10
CXCR4-mediated signaling events
6.83
VEGFR3 signaling in lymphatic endothelium
2.55
Integrin family cell surface interactions
1.45
JNK signaling in the CD4+ TCR pathway
1.43
0
10
20
Combined Score
STAT3 activated genes; KEGG 2016 Database
Hematopoietic cell lineage
13.72
T cell receptor signaling pathway
13.15
Osteoclast differentiation
11.49
Ras signaling pathway
9.31
NF-kappa B signaling pathway
6.92
Jak-STAT signaling pathway
5.36
Focal adhesion
4.44
Regulation of actin cytoskeleton
4.17
0
5
10
15
Combined Score
f
Color Key
-2
0
2
Row Z-Score
231
231DD
1833
1833shp27
NOS activated signature
NOS downregulated signature
g
NOS activated genes; NCI-Nature 2016 Database
TGF-beta receptor signaling
11.23
C-MYC transcriptional repression
10.43
Canonical NF-kappaB pathway
5.40
Wnt signaling network
4.34
N-cadherin signaling events
4.23
Internalization of ErbB1
4.10
Transcriptional targets of AP1 family
3.79
Presenilin action in Notch and Wnt signaling
3.29
0
5
10
Combined Score
h
NOS downregulated genes; Reactome 2016 Database
Developmental Biology
14.53
Transcriptional regulation of stem cells
14.07
NF-kB activation through FADD/RIP-1
7.03
Regulation of KIT signaling
6.67
Regulation of genes in pancreatic precursor
6.01
Regulation of beta-cell development
5.78
0
10
Combined Score

Figure 5

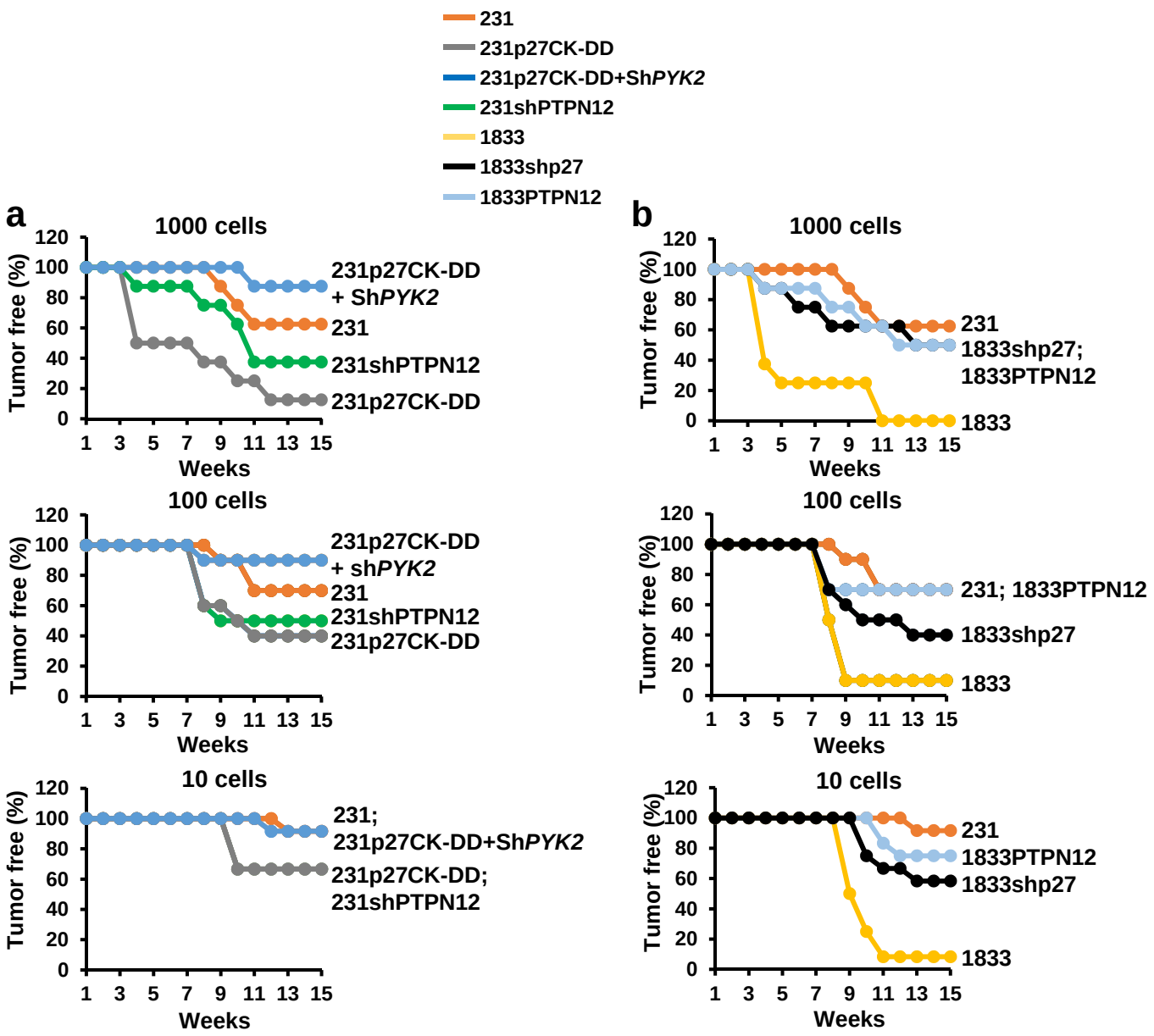

c

T-ISC frequency

Group	Limiting dilution (Tumors/Implantation)			Frequency
	1000 cell	100 cell	10 cell	
231	3/8	3/10	1/12	1/1,032
231p27CK-DD	7/8	6/10	4/12	1/175
231p27CK-DDsh*PYK2*	1/8	1/10	1/12	1/2,845
231sh*PTPN12*	6/8	6/10	5/12	1/402
1833	8/8	9/10	11/12	1/14
1833shp27	4/8	6/10	5/12	1/402
1833-PTPN12	4/8	3/10	3/12	1/645

Pairwise Differences		p-value
231	231p27CK-DD↑	0.0028
231	1833↑	<0.0001
231	231sh*PTPN12*↑	0.0437
231p27CK-DD	231p27CK-DD + sh*PYK2*↓	0.0002
1833	1833sh*p27*↓	<0.0001
1833	1833-PTPN12↓	<0.0001

Figure 6

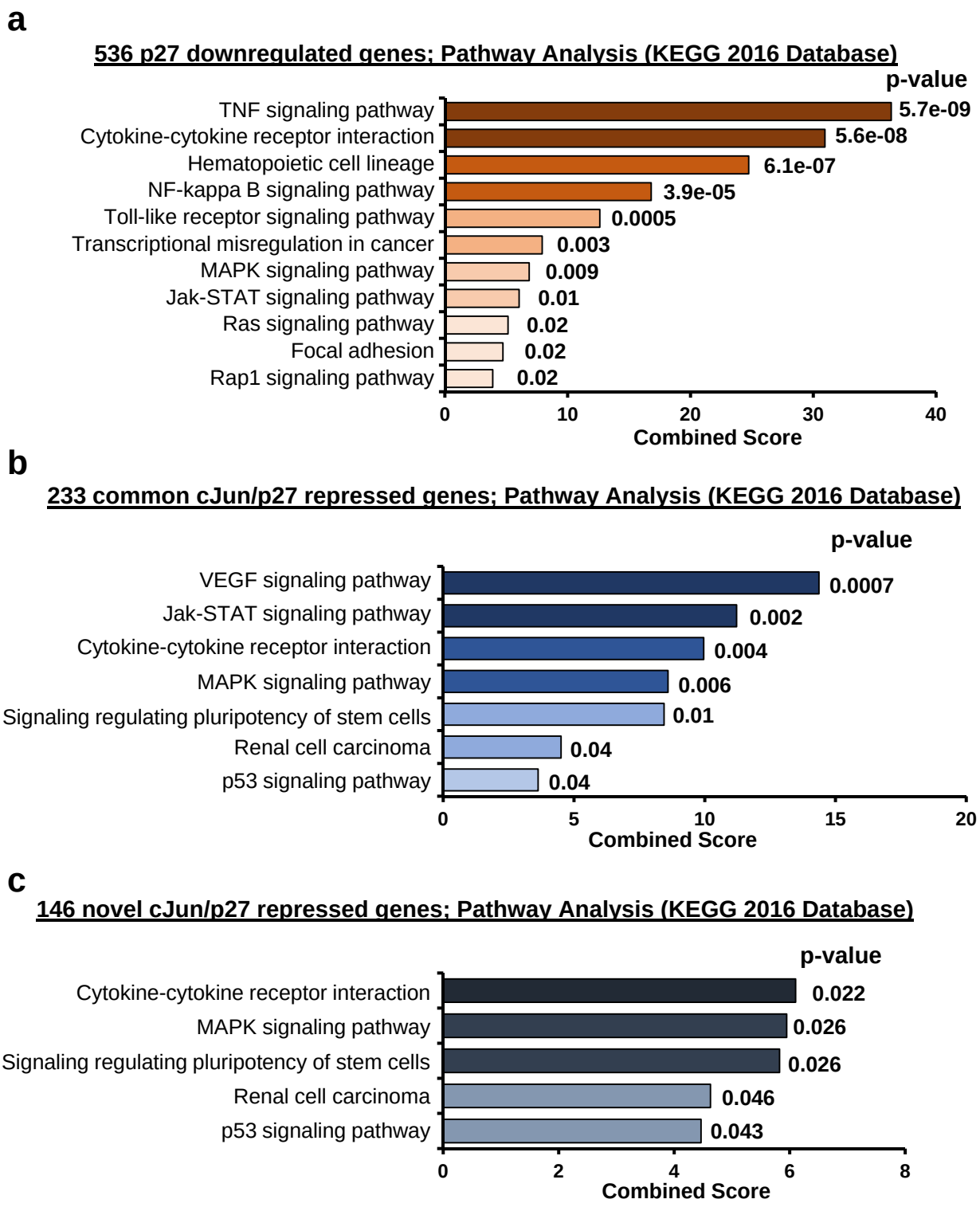

Supplementary Figure 1. p27-mediated signaling pathways

a, ENRICHR analysis from KEGG 2016 database using the 536 genes that are regulated by p27. **b**, **c**, KEGG database showing the main signaling pathways associated with 233 cJun/p27 common target genes (**b**) and 146 unique target genes (**c**).

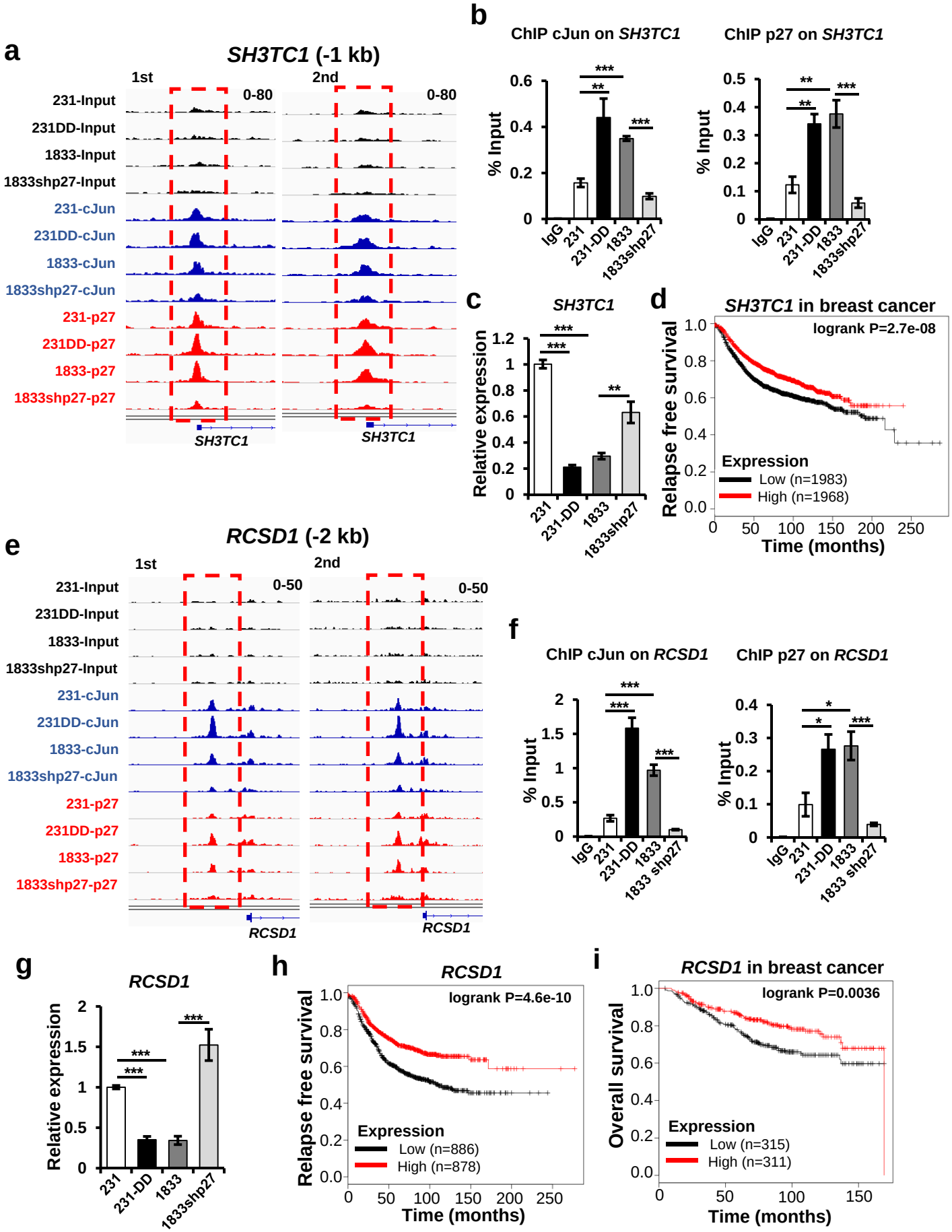
a
SH3TC1 (-1 kb)
1st
2nd
0-80
0-80
231-Input
231DD-Input
1833-Input
1833shp27-Input
231-cJun
231DD-cJun
1833-cJun
1833shp27-cJun
231-p27
231DD-p27
1833-p27
1833shp27-p27
SH3TC1
SH3TC1
b
ChIP cJun on SH3TC1
ChIP p27 on SH3TC1
% Input
IgG
231
231-DD
1833
1833shp27
c
SH3TC1
Relative expression
d
SH3TC1 in breast cancer
logrank P=2.7e-08
Relapse free survival
Expression
Low (n=1983)
High (n=1968)
Time (months)
e
RCSD1 (-2 kb)
1st
2nd
0-50
0-50
231-Input
231DD-Input
1833-Input
1833shp27-Input
231-cJun
231DD-cJun
1833-cJun
1833shp27-cJun
231-p27
231DD-p27
1833-p27
1833shp27-p27
RCSD1
RCSD1
f
ChIP cJun on RCSD1
ChIP p27 on RCSD1
% Input
IgG
231
231-DD
1833
1833 shp27
g
RCSD1
Relative expression
231
231-DD
1833
1833shp27
h
RCSD1
logrank P=4.6e-10
Relapse free survival
Expression
Low (n=886)
High (n=878)
Time (months)
i
RCSD1 in breast cancer
logrank P=0.0036
Overall survival
Expression
Low (n=315)
High (n=311)
Time (months)

Supplementary Figure 2. SH3TC1 and RSCD1 are novel cJun/p27 repressed target genes.

a, The IGV genome browser tracks showing binding of p27 and cJun to p27/cJun-repressed target gene, *SH3TC1* from two independent ChIP Seq experiments in the indicated lines. **b**, **c**, Validation for cJun/p27 binding and expression profiles of *SH3TC1*. (**b**) ChIP-qPCR with cJun (left) and p27 antibodies (right) at -1 kb of the *SH3TC1* transcription start site (TSS). (**c**) The expression level of *SH3TC1* by qPCR in the indicated cell lines. **d**, Kaplan-Meier curves for relapse free survival according to *SH3TC1* expression for breast cancers from the KM Plotter™ database (red: above median, n=1968; blue: below median, n=1983). **e**, The 1st and 2nd ChIP-Seq tracks of *RCSD1* from 2 independent experiments. **f**, Validation of p27 and cJun binding to *RCSD1* by ChIP-qPCR the indicated cell lines. **g**, Validation p27 mediated *RCSD1* from RNA Seq by qPCR in the indicated cell lines. **h**, **i**, Kaplan-Meier curves for relapse free (**h**) and overall survival (**i**) curves according to *RCSD1* expression from the KM Plotter™ breast cancer dataset (red line: high, blue line: low). Patient numbers (n) are indicated. All graphs show mean +/- SEM from at least 3 replicate assays, and p-values were represented by ANOVA analysis (*$p < 0.05$, **$p < 0.01$, ***$p < 0.001$).

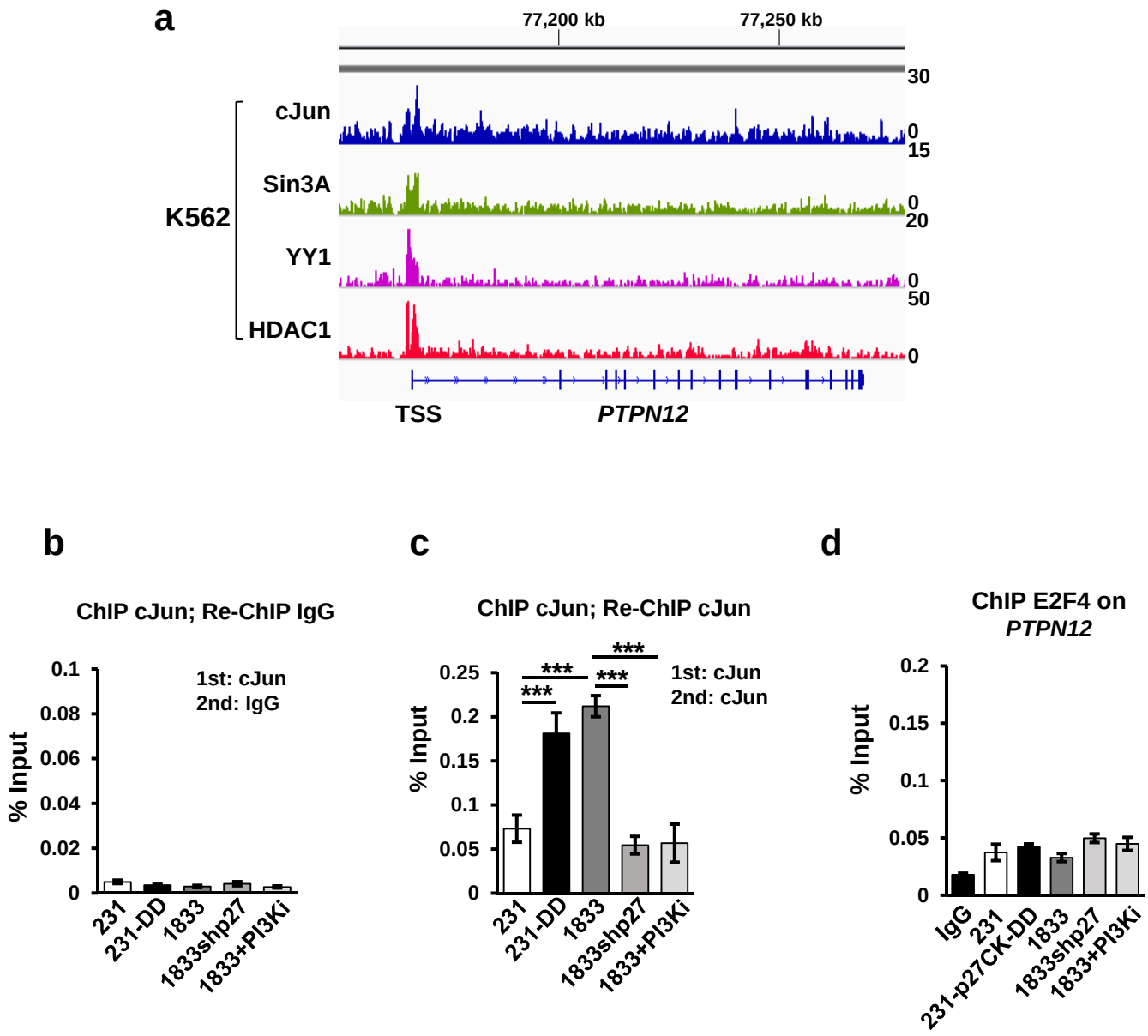

Supplementary Figure 3. cJun/p27 regulates PTPN12 expression transcriptionally.

a, cJun, Sin3A, YY1, and HDAC1 ChIPSeq tracks in K562 cell lines from the ENCODE database. The track shows consensus binding motif of each transcription factor at +2 kb of the *PTPN12* transcriptional start site. **b**, **c**, Re-ChIP analysis. After dissociation of 1st cJun ChIPs, 2nd ChIPs with IgG (negative control; **b**) and anti-cJun antibody (positive control; **c**) were performed in the indicated cell lines. **d**, ChIP-qPCR analysis for E2F4 bindings at the +2kb site of *PTPN12* TSS in 231, 231p27CK-DD, 1833, 1833shp27, and 1833 treated with PI3K inhibitor (1833+PI3Ki). IgG; negative control. All graphs show mean ± SEM from at least 3 replicate assays, and p-values were represented by Student's T Test or ANOVA analysis (*$p < 0.05$, **$p < 0.01$).

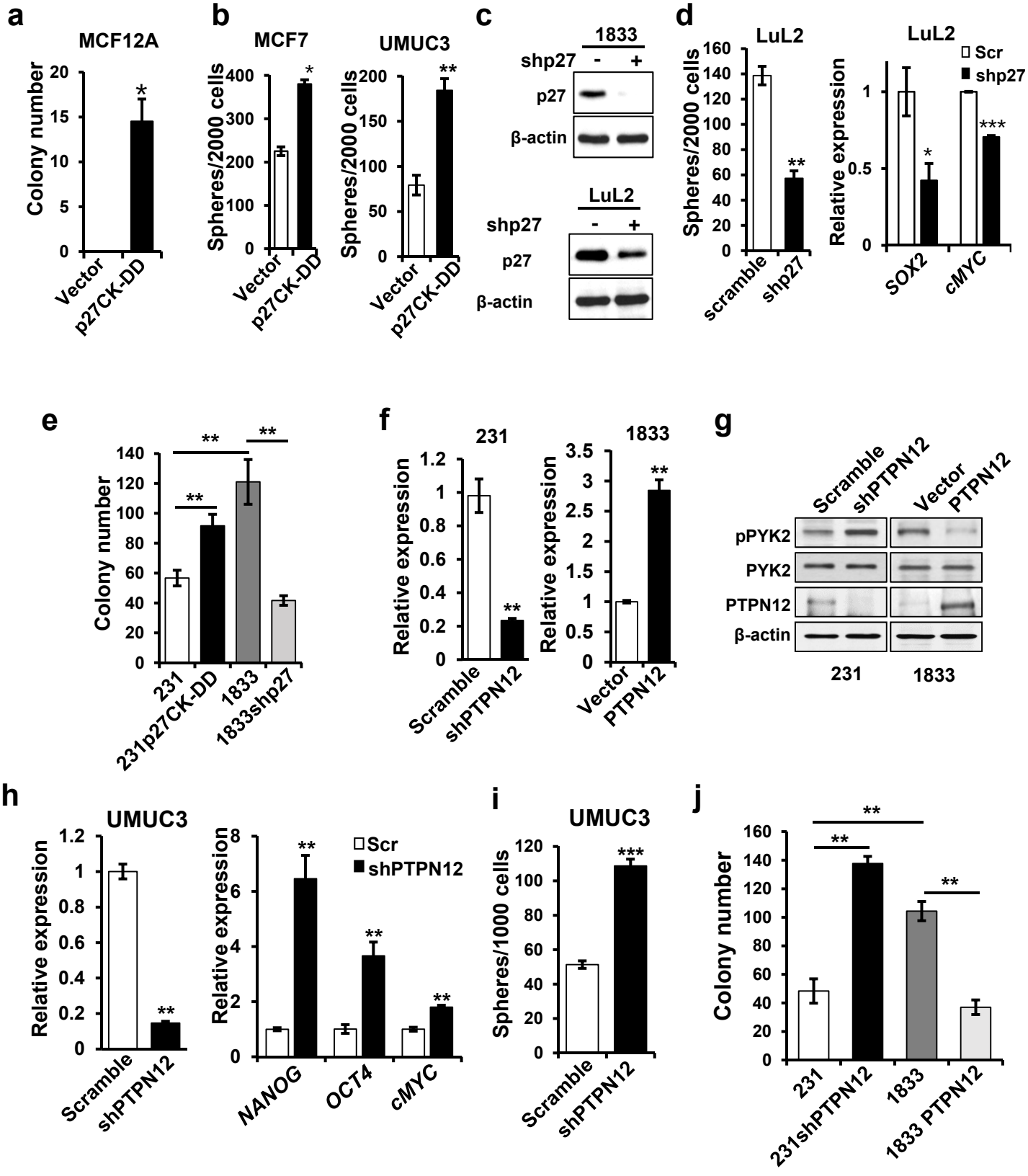
a
MCF12A
Colony number
Vector
p27CK-DD
b
MCF7
UMUC3
Spheres/2000 cells
c
1833
shp27
p27
β-actin
LuL2
d
LuL2
Scr
shp27
Relative expression
scramble
SOX2
cMYC
e
Colony number
231
231p27CK-DD
1833
1833shp27
f
231
1833
Relative expression
Scramble
shPTPN12
Vector
PTPN12
g
Scramble
shPTPN12
Vector
PTPN12
pPYK2
PYK2
PTPN12
β-actin
231
1833
h
UMUC3
Relative expression
Scramble
shPTPN12
Scr
NANOG
OCT4
cMYC
i
UMUC3
Spheres/1000 cells
j
Colony number
231
231shPTPN12
1833
1833 PTPN12

Supplementary Figure 4. C-terminally phosphorylated p27 and PTPN12 loss enhance self-renewal ability.

a, Colony forming assays in MCF12A-vector and MCF12A-p27CK-DD. Colonies were counted by GelCount™ Tumor Colony Counter. **b**, Sphere forming assays in MCF7-vector and MCF7-p27CK-DD; UMUC3-vector and UMUC3-p27CK-DD. **c**, Knockdown of p27 was confirmed by Western in 1833 and LuL2. β-actin as a loading control. **d**, Sphere forming assays in 4175-scramble and 4175shp27 (left). The effects of p27 knockdown on CSC-TFs including *Sox2* and *cMyc* in LuL2. **e**, 231-vector, 231-p27CK-DD, 1833-scramble, and 1833shp27 cells were subjected to soft agar colony-forming assays . Colonies were counted by GelCount™ Tumor Colony Counter. **f**, Knockdown and overexpression of PTPN12 was confirmed by qPCR in 231 (left) and 1833 (right). **g**, Effects of stable PTPN12 knockdown and overexpression on PYK2 activation by Western blot. **h**, Effects of stable *PTPN12* knockdown on expression of PTPN12 (left) and CSC-TFs (middle) and sphere forming assay (right) in UMUC3 cells. The cells were infected with shPTPN12 lentiviruses. The expression of *PTPN12* and CSC-TFs (*NANOG*, *OCT4,* and *cMYC*) was analyzed by qPCR. **i**, Colony forming assays in 231, 231shPTPN12, 1833, and 1833-PTPN12 cells. All graphs show mean ± SEM from at least 3 replicate assays, and p-values were represented by Student's T Test or ANOVA analysis (*$p < 0.05$, **$p < 0.01$).

a

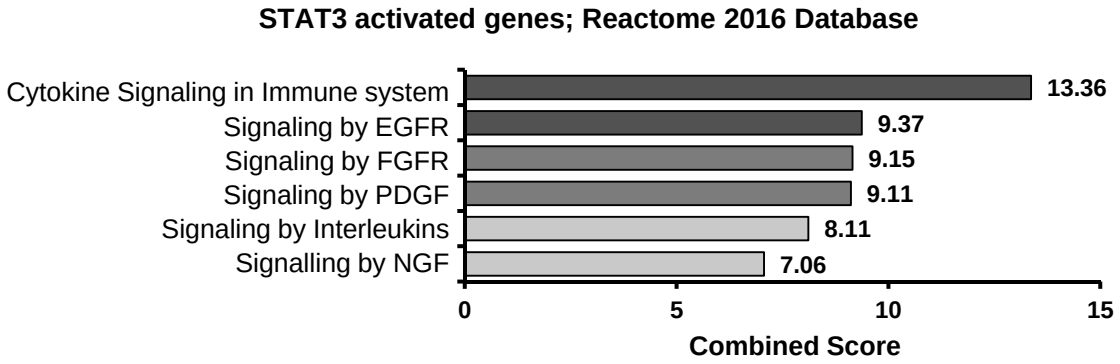

b

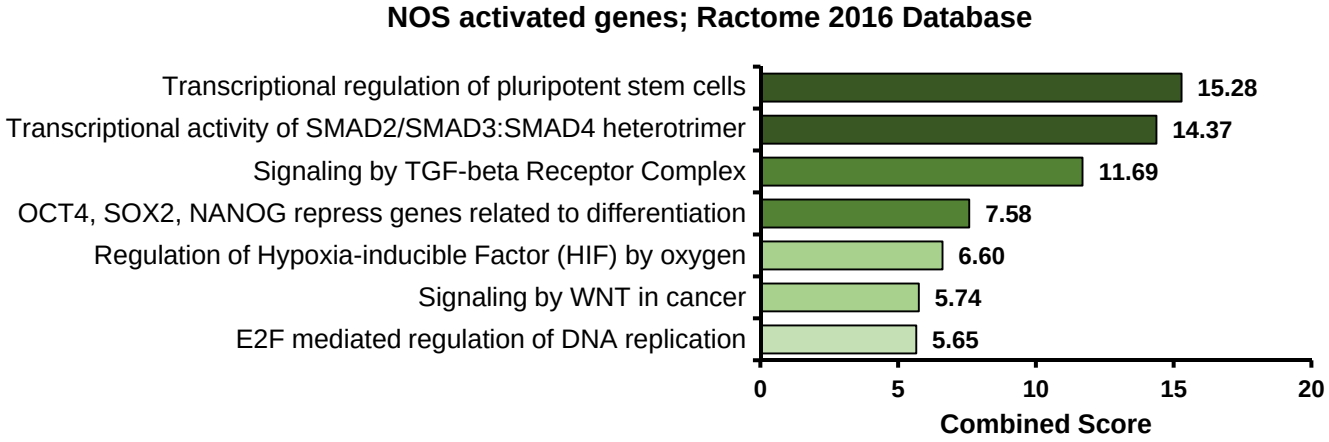

Supplementary Figure 5. p27 is associated with STAT3 and NOS activated genes.

a, **b**, ENRICHR analysis from Reactome 2016 database using the STAT3 activated genes (**a**) and NOS activated genes (**b**) that are regulated by p27.

a

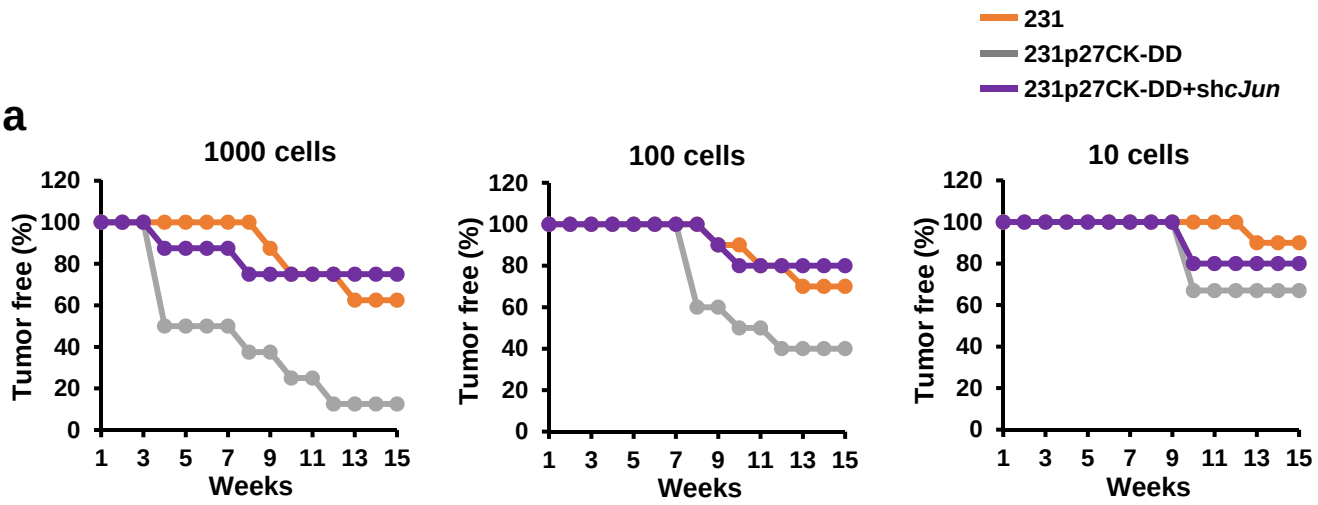

b

T-ISC frequency

Group	Limiting dilution (Tumors/Implantation)			Frequency
	1000 cell	100 cell	10 cell	
231	**3/8**	**3/10**	**1/12**	**1/1,032**
231p27CK-DD	**7/8**	**6/10**	**4/12**	**1/175**
231p27CK-DDsh*cJun*	**2/8**	**2/10**	**3/12**	**1/1,122**

c

Pairwise Differences		p-value
231	**231p27CK-DD ↑**	**0.0028**
231p27CK-DD	**231p27CK-DD + sh*cJun* ↓**	**<0.0001**

Supplementary Figure 6. cJun is required for p27-mediated tumor initiation.

a, Graphs showing tumor free mice (%). The cells were injected in the mammary fat pads of Balb/c nude mice at limiting dilution (n = 8, 10, 12 mice per group) of 231, 231p27CK-DD, and 231p27CK-DD + sh*cJun*. **b**, **c**, Tumor-initiating stem cell (T-ISC) frequencies were calculated by L-Calc Limiting Dilution Software in the indicated cell lines (**b**). Pairwise comparisons of T-ISC frequencies are shown (**c**).

Supplementary Table 1a. The 536 genes that are regulated by p27.

	231DD vs. 231	231DD vs. 231	231DD vs. 231	1833shp27 vs. 1833	1833shp27 vs. 1833	1833shp27 vs. 1833
Gene ID	**Fold Change**	**p value**	**q value**	**Fold Change**	**p value**	**q value**
A4GALT	**0.55**	1.10.E-08	9.39.E-08	**1.65**	7.44.E-04	3.54.E-03
ABCG2	**0.50**	2.60.E-12	3.26.E-11	**2.34**	1.71.E-14	4.65.E-13
ABI3BP	**0.56**	2.05.E-05	1.09.E-04	**1.52**	5.85.E-06	4.61.E-05
ACOT4	**0.53**	8.17.E-04	3.14.E-03	**2.76**	1.67.E-08	2.09.E-07
ACOT6	**0.43**	2.59.E-04	1.11.E-03	**1.61**	1.72.E-02	5.24.E-02
ACOX2	**0.19**	6.95.E-37	2.97.E-35	**1.99**	8.19.E-13	1.83.E-11
ACOXL	**0.29**	8.98.E-07	6.00.E-06	**4.27**	2.09.E-14	5.60.E-13
ACSL5	**0.43**	4.69.E-86	7.11.E-84	**1.97**	3.33.E-35	3.94.E-33
ADAM8	**0.33**	2.52.E-81	3.52.E-79	**1.66**	9.02.E-04	4.18.E-03
ADAMTS15	**0.71**	2.71.E-07	1.95.E-06	**2.05**	1.00.E-13	2.48.E-12
ADAMTS9	**0.29**	1.14.E-51	7.53.E-50	**2.91**	2.73.E-31	2.52.E-29
ADAMTS9-AS1	**0.60**	4.77.E-02	1.06.E-01	**1.61**	1.02.E-02	3.42.E-02
ADAP1	**0.41**	1.52.E-10	1.61.E-09	**1.76**	6.98.E-05	4.30.E-04
ADGRF1	**0.05**	1.42.E-62	1.21.E-60	**1.56**	1.13.E-02	3.70.E-02
ADGRF5	**0.36**	3.58.E-122	9.42.E-120	**6.20**	2.92.E-187	7.36.E-184
ADIRF	**0.30**	5.10.E-31	1.80.E-29	**2.66**	4.48.E-18	1.69.E-16
ADORA2B	**0.37**	2.61.E-58	1.98.E-56	**1.71**	1.54.E-19	6.53.E-18
AGAP2	**0.53**	1.27.E-03	4.65.E-03	**1.90**	1.73.E-05	1.24.E-04
AIM2	**0.29**	1.10.E-24	3.09.E-23	**1.54**	7.72.E-03	2.69.E-02
AK5	**0.51**	4.39.E-10	4.41.E-09	**1.51**	2.01.E-03	8.39.E-03
ALDH1A3	**0.35**	7.55.E-36	3.13.E-34	**2.80**	3.15.E-26	2.22.E-24
ALDH3A1	**0.32**	7.24.E-06	4.14.E-05	**4.03**	4.60.E-13	1.06.E-11
ALS2CR11	**0.70**	9.74.E-03	2.77.E-02	**5.08**	5.05.E-17	1.74.E-15
AMDHD1	**0.59**	9.15.E-05	4.30.E-04	**2.00**	3.29.E-08	3.91.E-07
ANGPTL2	**0.46**	7.48.E-22	1.77.E-20	**2.25**	3.29.E-09	4.59.E-08
ANKRD20A5P	**0.58**	2.08.E-02	5.29.E-02	**1.74**	2.53.E-03	1.02.E-02
ANKRD22	**0.22**	5.56.E-09	4.93.E-08	**1.63**	1.08.E-02	3.56.E-02
ANXA10	**0.38**	8.07.E-05	3.83.E-04	**1.69**	8.12.E-03	2.81.E-02
ANXA11	**0.66**	3.77.E-22	9.14.E-21	**1.63**	2.51.E-18	9.74.E-17
APBA2	**0.71**	5.07.E-07	3.50.E-06	**1.63**	3.10.E-07	3.10.E-06
APH1B	**0.70**	1.39.E-05	7.61.E-05	**1.86**	9.44.E-13	2.09.E-11
APLN	**0.39**	1.10.E-14	1.69.E-13	**2.58**	1.60.E-14	4.35.E-13
APOBEC3C	**0.52**	2.86.E-10	2.92.E-09	**2.04**	5.10.E-16	1.60.E-14
APOBEC3D	**0.49**	2.05.E-11	2.34.E-10	**1.65**	7.43.E-07	6.90.E-06
APOBEC3F	**0.43**	1.88.E-07	1.38.E-06	**2.34**	7.13.E-11	1.28.E-09
APOBEC3G	**0.26**	2.08.E-58	1.61.E-56	**5.69**	3.16.E-54	7.42.E-52
APOBEC3H	**0.49**	4.91.E-03	1.54.E-02	**1.68**	3.08.E-03	1.21.E-02
ARHGEF10L	**0.37**	1.26.E-25	3.72.E-24	**2.99**	2.22.E-12	4.67.E-11
ARHGEF3	**0.52**	1.13.E-22	2.86.E-21	**1.64**	5.39.E-10	8.46.E-09
ARHGEF4	**0.25**	5.00.E-46	2.83.E-44	**2.29**	1.41.E-11	2.73.E-10
ARHGEF6	**0.63**	1.64.E-03	5.85.E-03	**1.66**	1.44.E-03	6.30.E-03
ARMCX1	**0.68**	1.41.E-12	1.83.E-11	**1.51**	5.49.E-12	1.11.E-10
ARRB1	**0.63**	1.48.E-16	2.51.E-15	**1.81**	4.79.E-19	1.96.E-17
ARSE	**0.46**	6.65.E-09	5.84.E-08	**1.57**	4.27.E-03	1.61.E-02
ASB2	**0.02**	6.57.E-99	1.29.E-96	**1.57**	2.25.E-03	9.20.E-03
ASB9	**0.65**	1.21.E-06	7.89.E-06	**1.57**	5.50.E-06	4.36.E-05
ASS1	**0.38**	4.61.E-46	2.62.E-44	**2.39**	1.94.E-22	1.06.E-20
ATOH8	**0.12**	1.43.E-53	9.98.E-52	**2.78**	2.21.E-10	3.71.E-09
ATP2B4	**0.52**	1.10.E-29	3.76.E-28	**2.51**	1.05.E-45	2.02.E-43
AVPI1	**0.33**	2.70.E-44	1.46.E-42	**1.61**	9.12.E-07	8.31.E-06
B3GALT5	**0.18**	4.66.E-19	9.29.E-18	**1.97**	8.08.E-07	7.43.E-06
B3GNT3	**0.47**	4.59.E-09	4.11.E-08	**1.64**	2.53.E-06	2.13.E-05
B3GNT5	**0.43**	1.32.E-23	3.53.E-22	**1.67**	4.28.E-10	6.82.E-09
B3GNT7	**0.50**	2.13.E-09	1.99.E-08	**3.59**	1.31.E-28	1.08.E-26
BACH2	**0.68**	1.05.E-02	2.95.E-02	**1.52**	9.77.E-04	4.48.E-03
BATF	**0.15**	1.69.E-17	3.04.E-16	**3.76**	6.90.E-11	1.24.E-09
BCKDHA	**0.67**	4.03.E-06	2.43.E-05	**1.57**	2.75.E-05	1.87.E-04
BCL2A1	**0.07**	1.71.E-108	3.68.E-106	**9.43**	2.98.E-100	1.94.E-97
BCL3	**0.32**	8.17.E-15	1.26.E-13	**1.53**	4.12.E-03	1.56.E-02
BDKRB1	**0.27**	9.32.E-07	6.19.E-06	**1.83**	2.37.E-03	9.66.E-03
BDKRB2	**0.32**	1.80.E-05	9.66.E-05	**2.47**	8.51.E-06	6.52.E-05
BEND3	**0.54**	4.16.E-20	8.89.E-19	**2.94**	2.82.E-57	7.01.E-55
BIRC3	**0.46**	3.37.E-57	2.46.E-55	**1.90**	1.62.E-23	9.59.E-22
BOLA1	**0.33**	3.81.E-08	3.05.E-07	**3.30**	4.14.E-09	5.67.E-08
C10orf54	**0.33**	8.92.E-36	3.69.E-34	**3.33**	2.18.E-12	4.59.E-11
C10orf90	**0.34**	1.37.E-05	7.51.E-05	**1.57**	1.76.E-02	5.33.E-02
C14orf132	**0.43**	1.36.E-03	4.95.E-03	**2.71**	9.78.E-07	8.82.E-06
C1QTNF1	**0.09**	1.92.E-26	5.91.E-25	**1.85**	2.13.E-03	8.82.E-03
C20orf96	**0.68**	4.18.E-03	1.33.E-02	**1.72**	1.36.E-05	9.97.E-05
C3	**0.05**	2.79.E-269	3.57.E-266	**1.57**	5.28.E-13	1.21.E-11
C3orf18	**0.56**	1.15.E-14	1.75.E-13	**1.67**	1.93.E-10	3.28.E-09
C5orf63	**0.62**	8.06.E-05	3.83.E-04	**1.84**	1.21.E-06	1.08.E-05
C6orf203	**0.59**	1.70.E-08	1.42.E-07	**1.59**	2.59.E-07	2.62.E-06
C9orf64	**0.74**	1.12.E-05	6.23.E-05	**2.04**	1.82.E-20	8.35.E-19
C9orf89	**0.63**	9.85.E-09	8.47.E-08	**1.57**	1.34.E-06	1.18.E-05

CACNA1S	**0.50**	6.86.E-03	2.05.E-02	**1.50**	9.50.E-03	3.20.E-02
CACNB4	**0.45**	3.30.E-08	2.67.E-07	**1.67**	9.49.E-06	7.20.E-05
CACNG7	**0.58**	2.18.E-02	5.50.E-02	**1.75**	1.74.E-03	7.41.E-03
CCDC144B	**0.71**	9.78.E-05	4.57.E-04	**2.40**	1.62.E-20	7.46.E-19
CCDC153	**0.56**	1.19.E-03	4.40.E-03	**1.66**	5.22.E-03	1.93.E-02
CCDC3	**0.49**	1.56.E-11	1.80.E-10	**2.89**	3.52.E-08	4.17.E-07
CCDC71	**0.71**	4.61.E-05	2.31.E-04	**1.65**	7.98.E-09	1.05.E-07
CCR7	**0.42**	1.63.E-04	7.30.E-04	**1.60**	1.83.E-02	5.51.E-02
CCRL2	**0.27**	1.65.E-59	1.31.E-57	**1.60**	4.83.E-08	5.60.E-07
CD14	**0.20**	3.46.E-20	7.42.E-19	**1.68**	8.98.E-03	3.05.E-02
CD22	**0.12**	1.32.E-68	1.34.E-66	**1.56**	5.12.E-07	4.91.E-06
CD24	**0.52**	2.20.E-19	4.49.E-18	**1.84**	4.29.E-12	8.78.E-11
CD34	**0.43**	4.11.E-07	2.90.E-06	**1.54**	2.68.E-02	7.57.E-02
CD55	**0.48**	7.47.E-50	4.74.E-48	**1.53**	9.21.E-13	2.04.E-11
CD82	**0.39**	1.33.E-39	6.18.E-38	**2.43**	1.27.E-24	8.12.E-23
CD99L2	**0.71**	2.03.E-15	3.22.E-14	**1.86**	1.70.E-28	1.38.E-26
CDC42BPG	**0.41**	6.24.E-06	3.61.E-05	**1.69**	4.30.E-03	1.62.E-02
CDCP1	**0.38**	2.65.E-47	1.55.E-45	**2.64**	3.61.E-90	1.77.E-87
CDK15	**0.33**	9.26.E-09	7.99.E-08	**1.64**	1.02.E-02	3.41.E-02
CEMIP	**0.11**	2.00.E-96	3.72.E-94	**2.75**	1.94.E-23	1.14.E-21
CEP19	**0.70**	4.83.E-04	1.95.E-03	**1.86**	6.40.E-09	8.52.E-08
CFB	**0.18**	8.09.E-172	3.53.E-169	**1.64**	3.72.E-08	4.39.E-07
CFP	**0.43**	3.89.E-14	5.65.E-13	**2.71**	8.01.E-07	7.37.E-06
CHST4	**0.52**	5.85.E-03	1.79.E-02	**2.16**	1.29.E-04	7.43.E-04
CLDN7	**0.31**	1.19.E-74	1.42.E-72	**2.15**	1.23.E-18	4.86.E-17
CLIP2	**0.46**	2.89.E-37	1.24.E-35	**1.76**	6.75.E-10	1.04.E-08
CLMP	**0.42**	5.75.E-52	3.83.E-50	**6.37**	7.94.E-127	9.33.E-124
CMKLR1	**0.57**	1.73.E-09	1.64.E-08	**7.93**	1.40.E-40	2.19.E-38
COL15A1	**0.21**	4.13.E-23	1.07.E-21	**1.57**	1.68.E-02	5.13.E-02
COL17A1	**0.28**	5.21.E-70	5.65.E-68	**3.07**	2.40.E-62	6.81.E-60
COL6A1	**0.61**	1.25.E-11	1.46.E-10	**1.79**	2.15.E-04	1.17.E-03
COL6A2	**0.43**	5.23.E-22	1.26.E-20	**2.20**	5.20.E-07	4.98.E-06
COL9A2	**0.41**	4.84.E-21	1.08.E-19	**3.01**	6.22.E-14	1.57.E-12
CPNE5	**0.36**	2.40.E-10	2.47.E-09	**2.23**	4.43.E-09	6.06.E-08
CRISPLD2	**0.27**	4.14.E-48	2.46.E-46	**2.09**	1.19.E-10	2.07.E-09
CRLF2	**0.08**	5.39.E-138	1.64.E-135	**5.05**	2.11.E-16	6.76.E-15
CRTAP	**0.69**	2.71.E-19	5.53.E-18	**1.51**	1.36.E-17	4.92.E-16
CRYZL1	**0.73**	1.07.E-04	4.99.E-04	**1.53**	2.67.E-07	2.70.E-06
CSF1	**0.13**	1.13.E-218	9.23.E-216	**1.74**	8.53.E-16	2.61.E-14
CSF2	**0.24**	7.69.E-102	1.55.E-99	**1.54**	3.16.E-07	3.15.E-06
CSF2RA	**0.21**	4.33.E-115	1.03.E-112	**2.87**	1.68.E-17	6.03.E-16
CSF3	**0.09**	3.06.E-94	5.41.E-92	**3.26**	7.40.E-26	5.13.E-24
CST2	**0.32**	8.65.E-37	3.68.E-35	**2.67**	4.11.E-15	1.17.E-13
CST7	**0.13**	3.12.E-59	2.47.E-57	**2.39**	8.32.E-06	6.38.E-05
CTSD	**0.63**	2.73.E-28	8.88.E-27	**1.83**	4.32.E-06	3.49.E-05
CTSL	**0.69**	2.47.E-11	2.79.E-10	**1.61**	6.26.E-16	1.94.E-14
CTSS	**0.23**	5.85.E-138	1.75.E-135	**2.35**	1.10.E-16	3.67.E-15
CTSW	**0.13**	1.89.E-69	1.98.E-67	**3.72**	1.66.E-18	6.55.E-17
CX3CL1	**0.08**	3.06.E-24	8.45.E-23	**2.22**	2.61.E-05	1.79.E-04
CXCL10	**0.19**	9.62.E-13	1.26.E-11	**2.43**	1.30.E-05	9.56.E-05
CXCL11	**0.07**	4.25.E-61	3.55.E-59	**2.34**	1.61.E-05	1.16.E-04
CXCL2	**0.47**	1.56.E-12	2.01.E-11	**1.67**	5.93.E-09	8.00.E-08
CXCL3	**0.50**	1.01.E-07	7.70.E-07	**2.56**	1.94.E-16	6.27.E-15
CXCL8	**0.27**	8.10.E-166	3.45.E-163	**2.15**	2.06.E-35	2.49.E-33
CYP1A1	**0.31**	1.40.E-21	3.25.E-20	**2.16**	1.02.E-07	1.11.E-06
CYP1B1	**0.06**	7.03.E-163	2.73.E-160	**6.09**	1.70.E-99	1.07.E-96
CYP27A1	**0.42**	4.24.E-13	5.68.E-12	**1.63**	6.71.E-05	4.16.E-04
CYTH4	**0.06**	1.84.E-67	1.75.E-65	**2.79**	2.30.E-17	8.17.E-16
DENND2A	**0.62**	1.53.E-10	1.61.E-09	**1.53**	2.11.E-07	2.18.E-06
DGAT2	**0.27**	7.86.E-68	7.69.E-66	**2.33**	3.22.E-19	1.34.E-17
DHH	**0.51**	5.78.E-03	1.77.E-02	**1.76**	4.71.E-03	1.76.E-02
DMD	**0.58**	1.66.E-03	5.91.E-03	**1.64**	7.50.E-03	2.63.E-02
DMKN	**0.40**	2.81.E-04	1.20.E-03	**1.91**	3.86.E-04	1.98.E-03
DMTN	**0.23**	5.44.E-15	8.47.E-14	**1.61**	1.53.E-02	4.74.E-02
DNAH2	**0.15**	1.43.E-135	4.14.E-133	**2.47**	3.29.E-42	5.58.E-40
DUSP5	**0.39**	2.30.E-84	3.34.E-82	**1.92**	7.95.E-38	1.12.E-35
DZIP1	**0.66**	8.74.E-05	4.12.E-04	**1.67**	4.99.E-07	4.79.E-06
EDARADD	**0.26**	4.92.E-10	4.92.E-09	**4.41**	3.94.E-16	1.24.E-14
EFEMP2	**0.41**	8.96.E-11	9.71.E-10	**1.53**	5.26.E-03	1.94.E-02
EGFLAM	**0.58**	1.34.E-02	3.64.E-02	**1.50**	1.02.E-02	3.41.E-02
EGLN3	**0.66**	4.93.E-04	1.99.E-03	**1.75**	3.53.E-05	2.33.E-04
EHF	**0.19**	5.02.E-237	4.73.E-234	**27.42**	0.00.E+00	0.00.E+00
ENO2	**0.52**	6.48.E-25	1.85.E-23	**1.80**	1.03.E-16	3.45.E-15
ENPP4	**0.59**	9.77.E-18	1.78.E-16	**1.69**	5.83.E-11	1.06.E-09
ENTPD3	**0.19**	3.09.E-76	3.81.E-74	**1.57**	1.17.E-04	6.79.E-04
EPAS1	**0.71**	1.66.E-02	4.37.E-02	**1.59**	1.91.E-10	3.25.E-09
ETFB	**0.67**	9.66.E-09	8.32.E-08	**2.75**	4.27.E-26	3.00.E-24
EVI2B	**0.25**	1.14.E-52	7.79.E-51	**1.83**	3.35.E-14	8.77.E-13

EYA4	**0.71**	3.34.E-04	1.40.E-03	**1.76**	4.02.E-10	6.43.E-09
F8	**0.70**	5.98.E-04	2.36.E-03	**1.63**	9.48.E-06	7.19.E-05
FAM105A	**0.58**	1.36.E-14	2.07.E-13	**2.15**	8.66.E-28	6.69.E-26
FAM107B	**0.74**	3.71.E-10	3.75.E-09	**2.03**	3.28.E-33	3.49.E-31
FAM109B	**0.49**	1.64.E-06	1.05.E-05	**1.60**	1.14.E-03	5.13.E-03
FAM179A	**0.55**	1.23.E-03	4.52.E-03	**1.61**	3.60.E-03	1.39.E-02
FAM20C	**0.28**	4.64.E-95	8.40.E-93	**2.19**	3.58.E-18	1.36.E-16
FAM45B	**0.63**	9.71.E-03	2.76.E-02	**1.52**	2.25.E-02	6.56.E-02
FAM49A	**0.46**	3.82.E-04	1.58.E-03	**4.95**	1.06.E-41	1.75.E-39
FAM83H	**0.43**	2.20.E-04	9.58.E-04	**2.26**	2.39.E-05	1.65.E-04
FAM9B	**0.60**	4.32.E-02	9.77.E-02	**1.64**	5.84.E-03	2.12.E-02
FBXO6	**0.61**	7.69.E-04	2.97.E-03	**1.62**	2.31.E-03	9.42.E-03
FCMR	**0.41**	9.83.E-06	5.51.E-05	**1.89**	6.08.E-04	2.97.E-03
FERMT3	**0.72**	4.02.E-02	9.19.E-02	**1.58**	3.75.E-03	1.44.E-02
FFAR4	**0.44**	1.40.E-03	5.05.E-03	**1.75**	2.24.E-03	9.19.E-03
FHDC1	**0.32**	1.15.E-15	1.87.E-14	**1.86**	2.46.E-04	1.32.E-03
FLJ41200	**0.49**	6.41.E-03	1.93.E-02	**1.70**	8.04.E-03	2.79.E-02
FMO3	**0.54**	2.00.E-02	5.12.E-02	**1.97**	8.54.E-04	3.99.E-03
FOSL2	**0.40**	6.79.E-79	8.94.E-77	**1.59**	4.16.E-13	9.65.E-12
FOXD3-AS1	**0.63**	5.94.E-04	2.35.E-03	**1.83**	2.92.E-05	1.97.E-04
FOXQ1	**0.46**	9.98.E-22	2.34.E-20	**2.10**	7.27.E-23	4.08.E-21
FPR1	**0.09**	6.15.E-24	1.67.E-22	**1.82**	9.53.E-04	4.39.E-03
FSIP2	**0.45**	1.81.E-07	1.34.E-06	**3.32**	1.12.E-34	1.29.E-32
FUCA1	**0.45**	2.19.E-38	9.83.E-37	**1.51**	3.68.E-08	4.35.E-07
FUT1	**0.63**	1.81.E-03	6.36.E-03	**1.69**	7.65.E-05	4.66.E-04
FUZ	**0.67**	2.86.E-03	9.56.E-03	**2.30**	1.17.E-08	1.50.E-07
FZD4	**0.69**	1.17.E-08	9.99.E-08	**3.43**	5.08.E-78	1.87.E-75
GABBR2	**0.54**	2.12.E-02	5.36.E-02	**6.76**	2.33.E-22	1.27.E-20
GALNT12	**0.10**	1.01.E-59	8.07.E-58	**1.97**	2.22.E-04	1.21.E-03
GAS7	**0.43**	1.35.E-03	4.91.E-03	**1.56**	6.21.E-03	2.23.E-02
GBP5	**0.07**	1.07.E-81	1.51.E-79	**2.79**	3.04.E-07	3.04.E-06
GCKR	**0.62**	3.15.E-03	1.04.E-02	**4.79**	1.68.E-20	7.71.E-19
GCNT4	**0.40**	7.63.E-05	3.65.E-04	**1.63**	1.54.E-02	4.78.E-02
GGT1	**0.12**	1.19.E-85	1.78.E-83	**1.87**	1.42.E-03	6.22.E-03
GGT5	**0.40**	5.67.E-20	1.20.E-18	**1.86**	9.42.E-10	1.43.E-08
GMPR	**0.47**	2.92.E-15	4.60.E-14	**1.69**	2.82.E-09	3.97.E-08
GOLGA7B	**0.51**	9.62.E-04	3.62.E-03	**3.21**	8.47.E-16	2.60.E-14
GPCPD1	**0.48**	1.35.E-25	3.96.E-24	**1.71**	1.98.E-11	3.76.E-10
GPR162	**0.34**	2.01.E-09	1.89.E-08	**2.33**	3.76.E-09	5.18.E-08
GPRC5A	**0.73**	2.82.E-07	2.03.E-06	**1.65**	6.75.E-18	2.51.E-16
GPRC5C	**0.09**	2.53.E-38	1.13.E-36	**14.13**	1.13.E-55	2.74.E-53
GPX7	**0.41**	7.52.E-04	2.91.E-03	**2.16**	9.07.E-05	5.41.E-04
GRAMD1B	**0.33**	1.60.E-05	8.69.E-05	**26.25**	1.68.E-101	1.18.E-98
GRHL1	**0.47**	4.06.E-04	1.67.E-03	**1.61**	3.81.E-03	1.46.E-02
GRIK4	**0.43**	1.21.E-09	1.17.E-08	**1.76**	1.91.E-03	8.06.E-03
GRIN2A	**0.24**	4.02.E-09	3.63.E-08	**1.52**	3.80.E-02	1.00.E-01
GSAP	**0.35**	1.03.E-21	2.42.E-20	**1.97**	7.63.E-16	2.35.E-14
GSTM1	**0.54**	1.74.E-13	2.40.E-12	**8.01**	6.73.E-46	1.30.E-43
HDAC11	**0.61**	9.53.E-12	1.13.E-10	**3.01**	2.16.E-35	2.59.E-33
HIP1	**0.61**	1.23.E-13	1.72.E-12	**2.11**	2.95.E-18	1.14.E-16
HIST1H2AA	**0.51**	8.87.E-03	2.56.E-02	**11.07**	2.65.E-45	4.97.E-43
HIST1H2BA	**0.45**	1.47.E-06	9.46.E-06	**34.92**	2.70.E-168	4.76.E-165
HLA-F	**0.51**	6.02.E-10	5.98.E-09	**2.04**	2.54.E-06	2.15.E-05
HMMR	**0.69**	7.14.E-06	4.09.E-05	**1.55**	5.18.E-06	4.13.E-05
HOXB3	**0.61**	7.14.E-03	2.12.E-02	**1.56**	2.51.E-03	1.02.E-02
HPCAL1	**0.47**	7.06.E-63	6.11.E-61	**1.65**	2.23.E-09	3.18.E-08
HS6ST3	**0.40**	4.78.E-19	9.50.E-18	**2.00**	1.45.E-12	3.12.E-11
HSBP1L1	**0.66**	4.39.E-06	2.63.E-05	**2.01**	2.37.E-11	4.46.E-10
HSD3B7	**0.44**	1.53.E-20	3.35.E-19	**1.85**	9.05.E-11	1.61.E-09
ICAM1	**0.65**	5.55.E-19	1.10.E-17	**2.31**	2.10.E-38	3.06.E-36
ICOSLG	**0.39**	1.57.E-04	7.06.E-04	**2.17**	1.09.E-04	6.37.E-04
ID1	**0.29**	1.14.E-44	6.20.E-43	**4.40**	5.89.E-64	1.82.E-61
ID3	**0.25**	1.92.E-44	1.04.E-42	**3.20**	1.42.E-34	1.60.E-32
IFIT1	**0.22**	5.34.E-185	2.99.E-182	**1.85**	7.07.E-15	1.97.E-13
IFIT2	**0.11**	0.00.E+00	0.00.E+00	**2.05**	1.99.E-26	1.42.E-24
IFIT3	**0.14**	0.00.E+00	0.00.E+00	**1.61**	1.74.E-16	5.68.E-15
IFITM1	**0.38**	3.12.E-41	1.51.E-39	**2.01**	1.11.E-16	3.70.E-15
IFNLR1	**0.35**	2.82.E-17	5.00.E-16	**1.55**	8.96.E-04	4.16.E-03
IGFBP6	**0.24**	3.37.E-98	6.49.E-96	**1.50**	5.97.E-07	5.65.E-06
IKBKE	**0.40**	1.01.E-67	9.84.E-66	**1.51**	3.09.E-08	3.71.E-07
IL17RE	**0.64**	2.78.E-04	1.19.E-03	**3.42**	1.39.E-18	5.50.E-17
IL1B	**0.11**	1.04.E-185	5.99.E-183	**2.12**	2.46.E-22	1.33.E-20
IL1R1	**0.16**	2.54.E-77	3.20.E-75	**1.96**	1.54.E-06	1.35.E-05
IL23A	**0.57**	3.80.E-03	1.23.E-02	**1.83**	2.03.E-03	8.45.E-03
IL24	**0.15**	4.64.E-49	2.82.E-47	**4.14**	4.29.E-19	1.77.E-17
IL6	**0.16**	9.75.E-166	4.06.E-163	**1.54**	6.66.E-07	6.25.E-06
IL7R	**0.24**	2.96.E-155	1.06.E-152	**1.86**	2.20.E-18	8.57.E-17
INHBB	**0.54**	9.77.E-20	2.02.E-18	**3.69**	2.17.E-41	3.48.E-39

IQCD	**0.27**	8.75.E-16	1.43.E-14	**2.45**	9.06.E-10	1.37.E-08
IRAK2	**0.58**	4.82.E-23	1.24.E-21	**2.16**	1.43.E-36	1.85.E-34
ISG20	**0.15**	4.01.E-122	1.04.E-119	**3.18**	3.80.E-24	2.38.E-22
ITGB2-AS1	**0.61**	2.55.E-06	1.59.E-05	**1.86**	1.51.E-09	2.22.E-08
JAK3	**0.59**	4.46.E-02	1.00.E-01	**1.86**	1.93.E-03	8.10.E-03
KBTBD3	**0.68**	1.23.E-03	4.53.E-03	**1.60**	5.42.E-04	2.68.E-03
KCCAT198	**0.53**	1.53.E-03	5.50.E-03	**1.73**	2.97.E-03	1.18.E-02
KCCAT211	**0.18**	5.11.E-12	6.19.E-11	**1.70**	7.16.E-03	2.53.E-02
KCNK2	**0.55**	9.36.E-04	3.54.E-03	**1.50**	4.37.E-02	1.13.E-01
KCNN3	**0.15**	3.57.E-21	8.08.E-20	**6.65**	3.98.E-27	2.95.E-25
KIAA1217	**0.40**	3.51.E-19	7.07.E-18	**1.79**	4.93.E-13	1.13.E-11
KIAA1462	**0.38**	2.28.E-18	4.35.E-17	**1.84**	3.44.E-04	1.79.E-03
KIF13B	**0.74**	3.71.E-06	2.24.E-05	**1.50**	2.89.E-11	5.38.E-10
KIF21B	**0.41**	2.89.E-08	2.35.E-07	**4.37**	5.24.E-18	1.97.E-16
KIF7	**0.59**	1.75.E-11	2.01.E-10	**1.76**	2.16.E-08	2.66.E-07
KRBOX1	**0.64**	1.03.E-06	6.79.E-06	**20.38**	1.67.E-93	8.90.E-91
KRT19	**0.51**	2.31.E-44	1.25.E-42	**1.68**	1.04.E-15	3.14.E-14
KRT32	**0.47**	3.83.E-03	1.24.E-02	**2.61**	2.32.E-06	1.97.E-05
KYNU	**0.08**	1.34.E-287	2.00.E-284	**1.91**	6.83.E-23	3.85.E-21
LAMA5	**0.44**	2.12.E-38	9.51.E-37	**1.61**	1.18.E-02	3.83.E-02
LAMP3	**0.33**	7.41.E-07	5.02.E-06	**3.39**	1.86.E-11	3.55.E-10
LAT2	**0.56**	1.18.E-06	7.73.E-06	**2.84**	3.30.E-23	1.90.E-21
LHX4	**0.50**	4.02.E-07	2.84.E-06	**1.59**	3.84.E-03	1.47.E-02
LIMD2	**0.72**	4.74.E-04	1.92.E-03	**1.65**	4.84.E-09	6.59.E-08
LINC00261	**0.65**	1.29.E-07	9.65.E-07	**1.93**	5.12.E-20	2.24.E-18
LINC00326	**0.54**	1.37.E-02	3.71.E-02	**1.59**	2.25.E-02	6.55.E-02
LINC00346	**0.41**	2.08.E-05	1.10.E-04	**2.08**	1.69.E-06	1.47.E-05
LINC00473	**0.53**	5.88.E-03	1.79.E-02	**1.72**	2.34.E-03	9.55.E-03
LINC00589	**0.25**	4.68.E-08	3.71.E-07	**1.69**	3.95.E-03	1.51.E-02
LINC00654	**0.42**	1.25.E-08	1.06.E-07	**2.12**	3.67.E-06	3.01.E-05
LINC00857	**0.67**	3.37.E-06	2.06.E-05	**1.51**	3.18.E-06	2.64.E-05
LINC00910	**0.68**	4.19.E-02	9.51.E-02	**1.66**	2.15.E-03	8.87.E-03
LINC00989	**0.57**	3.56.E-02	8.33.E-02	**4.03**	4.71.E-12	9.59.E-11
LINC00996	**0.06**	3.71.E-31	1.32.E-29	**1.53**	1.99.E-02	5.94.E-02
LINC01518	**0.47**	1.43.E-03	5.17.E-03	**1.71**	3.48.E-03	1.35.E-02
LINC01537	**0.30**	4.61.E-06	2.74.E-05	**1.93**	7.18.E-04	3.44.E-03
LINC01547	**0.74**	1.03.E-03	3.84.E-03	**1.60**	1.32.E-06	1.17.E-05
LIPH	**0.46**	4.21.E-11	4.70.E-10	**1.66**	1.08.E-06	9.67.E-06
LMO2	**0.75**	8.23.E-03	2.40.E-02	**1.81**	9.67.E-08	1.06.E-06
LMTK3	**0.49**	1.24.E-03	4.55.E-03	**1.59**	2.29.E-02	6.66.E-02
LOC100130298	**0.38**	1.63.E-04	7.30.E-04	**1.66**	9.41.E-03	3.18.E-02
LOC100507642	**0.39**	1.41.E-08	1.19.E-07	**1.52**	3.68.E-02	9.79.E-02
LOC102724297	**0.32**	4.48.E-12	5.46.E-11	**1.51**	9.51.E-03	3.21.E-02
LOC148696	**0.49**	6.69.E-04	2.62.E-03	**1.72**	2.32.E-03	9.48.E-03
LOXL4	**0.12**	0.00.E+00	0.00.E+00	**1.66**	3.64.E-12	7.49.E-11
LPL	**0.45**	3.90.E-09	3.52.E-08	**3.34**	2.79.E-14	7.34.E-13
LRP5L	**0.60**	2.72.E-05	1.42.E-04	**1.78**	1.49.E-06	1.31.E-05
LRRC34	**0.54**	6.67.E-04	2.61.E-03	**2.83**	6.79.E-11	1.22.E-09
LRRC61	**0.35**	4.68.E-25	1.34.E-23	**8.03**	1.48.E-30	1.32.E-28
LY6E	**0.48**	1.94.E-34	7.60.E-33	**2.80**	2.48.E-37	3.39.E-35
LY6K	**0.43**	4.24.E-06	2.54.E-05	**3.34**	1.02.E-18	4.07.E-17
LZTS1	**0.16**	1.90.E-12	2.42.E-11	**1.61**	8.44.E-03	2.90.E-02
MAGI2-AS3	**0.68**	1.11.E-02	3.10.E-02	**2.48**	2.22.E-07	2.29.E-06
MAMLD1	**0.73**	9.64.E-04	3.63.E-03	**1.60**	2.02.E-07	2.10.E-06
MANSC1	**0.66**	4.80.E-05	2.39.E-04	**2.70**	2.72.E-24	1.71.E-22
MAP1LC3A	**0.35**	2.28.E-07	1.66.E-06	**2.25**	5.60.E-05	3.54.E-04
MAP3K8	**0.43**	4.61.E-30	1.58.E-28	**1.54**	2.11.E-05	1.48.E-04
MAPK13	**0.60**	2.15.E-11	2.45.E-10	**2.04**	1.17.E-18	4.63.E-17
MBP	**0.35**	5.46.E-92	9.39.E-90	**1.58**	2.93.E-18	1.13.E-16
MCF2L2	**0.42**	2.28.E-04	9.93.E-04	**2.13**	5.68.E-05	3.58.E-04
MEI1	**0.66**	2.80.E-02	6.79.E-02	**2.72**	2.80.E-11	5.22.E-10
MEIS3P1	**0.46**	3.30.E-16	5.49.E-15	**4.69**	1.12.E-24	7.19.E-23
METTL7A	**0.34**	2.17.E-23	5.72.E-22	**1.67**	3.31.E-03	1.30.E-02
MFI2	**0.46**	1.17.E-38	5.29.E-37	**1.82**	6.90.E-10	1.06.E-08
MMP1	**0.07**	0.00.E+00	0.00.E+00	**31.10**	0.00.E+00	0.00.E+00
MMP11	**0.74**	1.99.E-02	5.11.E-02	**1.74**	2.93.E-04	1.56.E-03
MMP16	**0.72**	3.76.E-02	8.68.E-02	**1.90**	3.07.E-09	4.30.E-08
MMP3	**0.04**	6.46.E-184	3.50.E-181	**12.99**	1.52.E-116	1.49.E-113
MNX1-AS1	**0.71**	1.73.E-02	4.54.E-02	**1.93**	7.08.E-05	4.36.E-04
MORC4	**0.56**	2.73.E-34	1.06.E-32	**1.52**	1.85.E-12	3.93.E-11
MST1R	**0.47**	4.54.E-14	6.56.E-13	**2.93**	2.28.E-23	1.33.E-21
MTSS1	**0.56**	4.26.E-04	1.74.E-03	**1.53**	5.21.E-04	2.59.E-03
MUC5AC	**0.44**	1.57.E-03	5.61.E-03	**1.76**	2.01.E-03	8.40.E-03
MUC5B	**0.58**	3.68.E-02	8.55.E-02	**4.25**	3.44.E-13	8.06.E-12
MX1	**0.26**	5.57.E-79	7.39.E-77	**2.57**	2.37.E-28	1.90.E-26
MX2	**0.26**	1.17.E-17	2.13.E-16	**1.99**	2.19.E-04	1.20.E-03
MYEF2	**0.62**	1.81.E-07	1.34.E-06	**1.80**	1.38.E-15	4.12.E-14
MYLK	**0.39**	2.78.E-49	1.71.E-47	**2.28**	8.91.E-40	1.34.E-37

MYO18A	**0.45**	6.02.E-28	1.93.E-26	**1.58**	1.01.E-10	1.79.E-09
MYO1F	**0.59**	1.44.E-10	1.53.E-09	**1.92**	3.42.E-06	2.83.E-05
MYO5C	**0.71**	3.12.E-02	7.46.E-02	**2.31**	8.69.E-33	8.80.E-31
NCKAP1L	**0.06**	4.31.E-44	2.28.E-42	**3.15**	4.54.E-20	1.98.E-18
NDP	**0.31**	6.28.E-10	6.22.E-09	**2.90**	4.93.E-10	7.78.E-09
NDRG2	**0.41**	2.36.E-04	1.03.E-03	**1.98**	2.61.E-06	2.19.E-05
NES	**0.48**	1.14.E-19	2.35.E-18	**2.75**	4.57.E-42	7.67.E-40
NEURL3	**0.33**	1.48.E-05	8.05.E-05	**1.53**	3.40.E-02	9.21.E-02
NGEF	**0.52**	8.65.E-12	1.03.E-10	**2.31**	6.12.E-13	1.39.E-11
NGFR	**0.06**	3.65.E-164	1.48.E-161	**2.57**	7.25.E-07	6.75.E-06
NLRX1	**0.74**	2.71.E-04	1.16.E-03	**1.53**	4.52.E-04	2.28.E-03
NMB	**0.27**	1.27.E-10	1.35.E-09	**2.90**	1.28.E-12	2.78.E-11
NMNAT2	**0.58**	8.21.E-08	6.33.E-07	**1.82**	6.06.E-15	1.70.E-13
NOP14-AS1	**0.73**	3.11.E-04	1.31.E-03	**1.83**	9.02.E-12	1.78.E-10
NOX5	**0.14**	1.34.E-52	9.14.E-51	**6.09**	1.43.E-29	1.21.E-27
NOXA1	**0.62**	2.35.E-03	8.01.E-03	**1.85**	7.32.E-05	4.48.E-04
NR1H3	**0.73**	8.27.E-06	4.69.E-05	**1.58**	2.66.E-07	2.69.E-06
NRG2	**0.35**	3.20.E-07	2.29.E-06	**1.72**	9.07.E-05	5.41.E-04
NRIP1	**0.69**	1.78.E-12	2.28.E-11	**1.66**	1.73.E-15	5.09.E-14
NRROS	**0.49**	3.15.E-06	1.93.E-05	**2.05**	1.34.E-07	1.43.E-06
NTNG2	**0.45**	3.29.E-12	4.08.E-11	**1.52**	8.36.E-03	2.88.E-02
NTRK2	**0.43**	1.26.E-03	4.60.E-03	**5.77**	1.28.E-19	5.45.E-18
NUP210	**0.25**	4.02.E-37	1.73.E-35	**3.32**	1.57.E-42	2.72.E-40
NUP62CL	**0.68**	8.27.E-03	2.41.E-02	**1.55**	1.14.E-02	3.74.E-02
OAS3	**0.48**	1.34.E-27	4.25.E-26	**1.84**	3.37.E-23	1.93.E-21
OASL	**0.16**	3.96.E-207	2.84.E-204	**1.71**	1.98.E-11	3.76.E-10
OBFC1	**0.73**	2.86.E-08	2.32.E-07	**1.57**	3.68.E-15	1.06.E-13
OLFML2A	**0.17**	4.52.E-78	5.78.E-76	**1.79**	6.67.E-07	6.26.E-06
OLFML3	**0.63**	1.14.E-04	5.26.E-04	**2.67**	1.76.E-18	6.93.E-17
OSBP2	**0.42**	1.90.E-10	1.98.E-09	**1.58**	2.56.E-05	1.76.E-04
P2RX6	**0.16**	5.71.E-16	9.43.E-15	**1.69**	9.77.E-03	3.28.E-02
PAK6	**0.14**	2.91.E-44	1.56.E-42	**3.46**	1.09.E-10	1.91.E-09
PAPL	**0.38**	3.35.E-06	2.05.E-05	**1.91**	1.39.E-04	7.93.E-04
PARD6B	**0.25**	1.03.E-76	1.29.E-74	**1.87**	2.86.E-20	1.27.E-18
PCBP3	**0.59**	1.76.E-02	4.61.E-02	**1.74**	1.67.E-05	1.20.E-04
PDE4B	**0.15**	5.54.E-68	5.47.E-66	**2.17**	1.12.E-07	1.21.E-06
PDE7B	**0.29**	3.86.E-43	1.97.E-41	**1.53**	1.87.E-05	1.33.E-04
PDK4	**0.28**	5.96.E-09	5.27.E-08	**1.63**	7.71.E-03	2.69.E-02
PDZK1IP1	**0.09**	3.13.E-151	1.06.E-148	**1.92**	7.83.E-04	3.69.E-03
PGF	**0.48**	2.21.E-37	9.59.E-36	**2.06**	2.28.E-13	5.44.E-12
PHYH	**0.57**	2.54.E-15	4.02.E-14	**1.65**	9.48.E-10	1.43.E-08
PIEZO2	**0.35**	2.63.E-09	2.42.E-08	**1.78**	1.61.E-04	9.05.E-04
PIGX	**0.60**	5.41.E-14	7.77.E-13	**1.59**	1.42.E-09	2.09.E-08
PIK3AP1	**0.54**	1.65.E-07	1.23.E-06	**3.52**	2.18.E-25	1.44.E-23
PIK3C2B	**0.30**	2.52.E-25	7.30.E-24	**1.54**	6.24.E-04	3.04.E-03
PIM3	**0.53**	3.16.E-16	5.27.E-15	**1.85**	1.50.E-09	2.20.E-08
PKHD1	**0.48**	1.69.E-05	9.12.E-05	**1.90**	1.51.E-03	6.56.E-03
PLA2G4D	**0.25**	1.02.E-07	7.78.E-07	**1.74**	1.95.E-03	8.19.E-03
PLA2G6	**0.48**	1.65.E-07	1.23.E-06	**2.53**	1.06.E-11	2.08.E-10
PLB1	**0.12**	3.68.E-66	3.38.E-64	**2.89**	3.62.E-14	9.44.E-13
PLCL2	**0.47**	4.29.E-27	1.34.E-25	**1.65**	3.79.E-15	1.09.E-13
PLCXD3	**0.60**	2.52.E-02	6.21.E-02	**4.50**	1.37.E-13	3.36.E-12
PLD1	**0.49**	1.12.E-24	3.15.E-23	**1.67**	3.25.E-12	6.75.E-11
PLEKHS1	**0.28**	7.96.E-08	6.17.E-07	**1.64**	6.84.E-03	2.43.E-02
PLLP	**0.29**	2.51.E-21	5.75.E-20	**2.13**	9.03.E-17	3.03.E-15
PPAP2B	**0.33**	8.92.E-59	6.97.E-57	**1.85**	8.46.E-19	3.40.E-17
PPFIA4	**0.53**	7.42.E-09	6.47.E-08	**1.57**	5.34.E-03	1.96.E-02
PPFIBP2	**0.50**	3.17.E-13	4.30.E-12	**1.88**	3.23.E-08	3.85.E-07
PPL	**0.24**	1.62.E-21	3.74.E-20	**2.18**	4.19.E-10	6.68.E-09
PPP1R3C	**0.19**	1.81.E-37	7.88.E-36	**1.53**	2.14.E-05	1.50.E-04
PPP2R2C	**0.37**	1.99.E-25	5.79.E-24	**2.25**	1.07.E-26	7.74.E-25
PREX1	**0.34**	4.70.E-05	2.34.E-04	**1.82**	2.12.E-03	8.78.E-03
PROS1	**0.57**	1.57.E-19	3.22.E-18	**1.58**	3.29.E-11	6.09.E-10
PSCA	**0.61**	4.79.E-02	1.06.E-01	**2.43**	1.13.E-06	1.01.E-05
PTGES	**0.22**	1.83.E-179	9.09.E-177	**4.79**	7.56.E-78	2.72.E-75
PTGS1	**0.46**	5.27.E-07	3.63.E-06	**3.01**	4.62.E-08	5.36.E-07
PTGS2	**0.23**	4.20.E-104	8.65.E-102	**1.69**	1.98.E-09	2.85.E-08
PTH1R	**0.52**	9.69.E-03	2.76.E-02	**1.52**	4.02.E-02	1.05.E-01
PTK2B	**0.31**	1.07.E-20	2.35.E-19	**1.57**	1.03.E-03	4.70.E-03
PTPRH	**0.19**	1.22.E-26	3.78.E-25	**1.78**	3.79.E-05	2.48.E-04
PTPRJ	**0.43**	1.04.E-69	1.11.E-67	**1.80**	1.23.E-27	9.39.E-26
PXMP4	**0.35**	3.32.E-43	1.70.E-41	**1.68**	3.15.E-07	3.14.E-06
PXYLP1	**0.58**	9.41.E-08	7.19.E-07	**1.96**	1.26.E-12	2.74.E-11
RAB31	**0.45**	9.54.E-58	7.14.E-56	**1.54**	1.73.E-13	4.19.E-12
RAB36	**0.67**	4.44.E-04	1.81.E-03	**2.84**	9.59.E-08	1.05.E-06
RAB37	**0.50**	1.80.E-06	1.14.E-05	**4.82**	2.40.E-57	6.04.E-55
RAB38	**0.53**	8.21.E-21	1.82.E-19	**1.54**	7.91.E-08	8.84.E-07
RAB3D	**0.43**	4.43.E-17	7.77.E-16	**1.78**	6.04.E-11	1.09.E-09

RAC2	**0.45**	1.26.E-51	8.30.E-50	**1.60**	5.15.E-12	1.04.E-10
RARB	**0.25**	4.22.E-65	3.81.E-63	**2.08**	2.02.E-05	1.42.E-04
RASD1	**0.21**	1.53.E-52	1.04.E-50	**2.60**	3.19.E-11	5.93.E-10
RASGRF1	**0.56**	1.40.E-08	1.18.E-07	**2.01**	1.07.E-11	2.11.E-10
RASL11A	**0.28**	1.19.E-16	2.03.E-15	**2.95**	1.41.E-19	6.00.E-18
RASSF2	**0.72**	9.83.E-04	3.69.E-03	**2.27**	2.50.E-20	1.12.E-18
RBKS	**0.58**	2.46.E-06	1.54.E-05	**2.34**	2.41.E-11	4.52.E-10
RBM47	**0.10**	2.09.E-58	1.61.E-56	**2.27**	1.84.E-07	1.93.E-06
RCSD1	**0.70**	3.07.E-09	2.81.E-08	**1.78**	1.77.E-11	3.40.E-10
REEP2	**0.42**	1.56.E-23	4.15.E-22	**1.55**	1.13.E-06	1.01.E-05
RGS14	**0.60**	7.22.E-04	2.81.E-03	**1.88**	6.79.E-06	5.27.E-05
RHEBL1	**0.58**	2.57.E-06	1.60.E-05	**1.52**	1.15.E-03	5.16.E-03
RIBC2	**0.65**	7.48.E-03	2.21.E-02	**1.88**	6.86.E-04	3.30.E-03
RIN1	**0.45**	2.09.E-24	5.84.E-23	**1.70**	5.90.E-07	5.59.E-06
RNF144A	**0.19**	3.69.E-10	3.73.E-09	**1.63**	9.91.E-03	3.32.E-02
RPL13AP20	**0.73**	1.92.E-02	4.95.E-02	**1.68**	1.73.E-03	7.37.E-03
RSAD2	**0.14**	1.38.E-56	1.00.E-54	**1.88**	1.48.E-03	6.45.E-03
RSPH3	**0.68**	4.23.E-04	1.73.E-03	**1.54**	5.94.E-04	2.91.E-03
RTN4RL2	**0.56**	6.29.E-03	1.90.E-02	**1.53**	2.50.E-02	7.14.E-02
S100A3	**0.29**	1.75.E-70	1.92.E-68	**1.65**	9.76.E-07	8.81.E-06
S100P	**0.35**	5.71.E-18	1.06.E-16	**2.91**	1.51.E-09	2.22.E-08
SAA1	**0.14**	1.26.E-34	4.99.E-33	**12.74**	1.88.E-50	4.08.E-48
SAA2	**0.09**	1.21.E-205	8.36.E-203	**3.90**	2.04.E-11	3.87.E-10
SASH1	**0.50**	9.45.E-14	1.34.E-12	**1.56**	1.52.E-12	3.26.E-11
SBSN	**0.32**	1.68.E-05	9.07.E-05	**1.79**	3.39.E-03	1.32.E-02
SCARA3	**0.68**	9.45.E-06	5.31.E-05	**3.02**	3.59.E-33	3.79.E-31
SCNN1A	**0.20**	8.80.E-19	1.72.E-17	**1.66**	1.29.E-02	4.13.E-02
SDPR	**0.33**	9.90.E-67	9.28.E-65	**4.42**	1.97.E-82	8.09.E-80
SEC14L4	**0.26**	3.37.E-07	2.40.E-06	**3.00**	5.65.E-08	6.49.E-07
SECTM1	**0.19**	6.27.E-74	7.33.E-72	**1.61**	3.72.E-05	2.44.E-04
SELENBP1	**0.43**	2.43.E-15	3.84.E-14	**2.83**	1.55.E-07	1.64.E-06
SEMA3B	**0.27**	5.28.E-40	2.47.E-38	**2.18**	5.92.E-10	9.24.E-09
SEMA3F	**0.30**	4.42.E-21	9.95.E-20	**2.09**	3.71.E-07	3.64.E-06
SEMA6B	**0.35**	2.02.E-28	6.62.E-27	**1.64**	2.37.E-06	2.01.E-05
SERPINA1	**0.16**	4.41.E-73	5.06.E-71	**10.83**	2.13.E-55	5.08.E-53
SERPINB9	**0.31**	1.28.E-60	1.04.E-58	**1.89**	3.56.E-12	7.35.E-11
SERPIND1	**0.26**	7.76.E-14	1.10.E-12	**3.60**	1.35.E-16	4.45.E-15
SETBP1	**0.51**	1.07.E-05	5.96.E-05	**2.46**	1.60.E-08	2.01.E-07
SFR1	**0.47**	1.89.E-19	3.87.E-18	**2.26**	8.44.E-22	4.34.E-20
SH3PXD2A-AS1	**0.52**	9.45.E-03	2.70.E-02	**2.16**	1.37.E-05	9.99.E-05
SH3TC1	**0.66**	2.93.E-03	9.76.E-03	**1.64**	2.21.E-03	9.08.E-03
SHC4	**0.23**	4.37.E-14	6.34.E-13	**1.56**	1.76.E-02	5.34.E-02
SHH	**0.35**	1.44.E-09	1.37.E-08	**9.17**	2.46.E-37	3.39.E-35
SHISA2	**0.51**	4.16.E-29	1.40.E-27	**1.52**	4.45.E-12	9.08.E-11
SIAE	**0.69**	7.94.E-07	5.36.E-06	**1.57**	3.76.E-06	3.08.E-05
SIGIRR	**0.55**	7.62.E-07	5.16.E-06	**2.93**	8.13.E-14	2.02.E-12
SIRPB1	**0.45**	2.49.E-03	8.43.E-03	**7.03**	2.43.E-23	1.41.E-21
SLC12A8	**0.18**	2.71.E-28	8.84.E-27	**1.58**	1.69.E-02	5.15.E-02
SLC16A14	**0.44**	2.19.E-04	9.55.E-04	**1.70**	7.55.E-03	2.64.E-02
SLC16A6	**0.42**	5.51.E-06	3.22.E-05	**1.79**	9.86.E-05	5.84.E-04
SLC22A18AS	**0.49**	1.50.E-03	5.41.E-03	**2.17**	5.01.E-05	3.21.E-04
SLC37A1	**0.36**	1.65.E-23	4.38.E-22	**4.12**	4.32.E-23	2.46.E-21
SLC45A1	**0.33**	8.71.E-06	4.91.E-05	**2.05**	3.99.E-04	2.05.E-03
SLC47A1	**0.16**	1.18.E-23	3.16.E-22	**2.63**	3.16.E-10	5.16.E-09
SLCO3A1	**0.45**	4.53.E-11	5.04.E-10	**5.35**	3.12.E-18	1.19.E-16
SLCO4A1	**0.42**	7.61.E-51	4.88.E-49	**2.17**	2.11.E-20	9.53.E-19
SLCO4A1-AS1	**0.19**	1.00.E-107	2.13.E-105	**2.30**	4.45.E-26	3.11.E-24
SLK	**0.64**	2.59.E-22	6.31.E-21	**1.59**	8.62.E-17	2.91.E-15
SLPI	**0.47**	1.58.E-03	5.64.E-03	**1.85**	1.84.E-03	7.79.E-03
SMAD6	**0.63**	1.10.E-06	7.23.E-06	**2.30**	2.70.E-09	3.82.E-08
SMC2-AS1	**0.22**	1.02.E-16	1.75.E-15	**2.35**	1.94.E-05	1.38.E-04
SNAP91	**0.73**	2.25.E-02	5.65.E-02	**2.03**	8.99.E-08	9.94.E-07
SORCS2	**0.34**	1.33.E-18	2.58.E-17	**1.57**	2.04.E-02	6.06.E-02
SORL1	**0.27**	8.28.E-22	1.96.E-20	**6.95**	3.61.E-25	2.36.E-23
SOST	**0.18**	2.01.E-13	2.77.E-12	**1.70**	3.59.E-03	1.39.E-02
SOX21-AS1	**0.57**	3.04.E-02	7.29.E-02	**2.39**	1.02.E-05	7.65.E-05
SP140	**0.36**	7.62.E-34	2.93.E-32	**1.56**	2.48.E-10	4.12.E-09
SP6	**0.53**	5.02.E-04	2.02.E-03	**1.82**	2.21.E-04	1.20.E-03
SPNS3	**0.28**	8.57.E-07	5.75.E-06	**1.84**	2.38.E-03	9.67.E-03
SPTLC3	**0.41**	1.01.E-52	6.94.E-51	**1.67**	3.43.E-15	9.91.E-14
SPTSSB	**0.52**	1.03.E-02	2.91.E-02	**2.43**	1.24.E-05	9.12.E-05
SRPX2	**0.55**	2.68.E-13	3.65.E-12	**1.66**	9.28.E-06	7.05.E-05
SRRM3	**0.41**	1.11.E-04	5.16.E-04	**1.74**	2.60.E-03	1.05.E-02
SSTR2	**0.51**	1.15.E-07	8.71.E-07	**1.73**	8.53.E-05	5.14.E-04
ST3GAL4	**0.61**	2.95.E-17	5.22.E-16	**1.75**	2.49.E-14	6.60.E-13
ST3GAL4-AS1	**0.62**	8.06.E-03	2.36.E-02	**1.52**	2.41.E-02	6.92.E-02
ST3GAL5	**0.34**	1.26.E-38	5.72.E-37	**1.50**	3.62.E-05	2.38.E-04
ST3GAL6	**0.73**	5.07.E-06	2.99.E-05	**1.81**	1.12.E-17	4.09.E-16

STC1	**0.24**	7.37.E-164	2.93.E-161	**2.15**	3.47.E-35	4.08.E-33
SULT1A1	**0.39**	3.41.E-04	1.42.E-03	**2.16**	5.76.E-05	3.63.E-04
SVIL	**0.51**	1.01.E-45	5.64.E-44	**1.62**	1.22.E-21	6.12.E-20
SYT9	**0.50**	2.86.E-03	9.56.E-03	**3.32**	1.01.E-09	1.52.E-08
SYTL2	**0.54**	2.52.E-19	5.14.E-18	**2.23**	1.29.E-20	5.98.E-19
SYTL3	**0.42**	4.49.E-13	6.01.E-12	**3.20**	7.70.E-22	3.98.E-20
SYTL4	**0.69**	2.53.E-10	2.60.E-09	**2.09**	1.30.E-26	9.41.E-25
TBC1D10A	**0.63**	3.30.E-08	2.67.E-07	**1.59**	9.76.E-07	8.81.E-06
TBC1D8	**0.55**	1.74.E-23	4.62.E-22	**1.77**	4.26.E-24	2.63.E-22
TBXAS1	**0.54**	1.03.E-06	6.78.E-06	**1.67**	6.94.E-04	3.34.E-03
TCEA3	**0.72**	1.43.E-05	7.84.E-05	**1.58**	1.10.E-09	1.65.E-08
TCN2	**0.31**	4.95.E-22	1.19.E-20	**2.07**	3.43.E-09	4.76.E-08
TDRP	**0.65**	7.56.E-03	2.23.E-02	**3.16**	1.44.E-08	1.82.E-07
TEC	**0.69**	7.57.E-06	4.32.E-05	**1.50**	1.48.E-05	1.07.E-04
TFF2	**0.53**	1.56.E-03	5.58.E-03	**3.37**	1.83.E-09	2.65.E-08
TGFA	**0.42**	1.50.E-71	1.67.E-69	**3.12**	7.37.E-53	1.69.E-50
TGFBR3	**0.47**	4.51.E-35	1.79.E-33	**1.78**	1.42.E-24	9.04.E-23
TGM5	**0.28**	4.53.E-07	3.17.E-06	**2.34**	2.86.E-05	1.93.E-04
THBD	**0.46**	3.81.E-26	1.15.E-24	**1.83**	1.93.E-13	4.64.E-12
TIRAP	**0.75**	1.80.E-03	6.33.E-03	**1.62**	1.82.E-05	1.30.E-04
TJP3	**0.50**	9.40.E-03	2.69.E-02	**1.53**	3.51.E-02	9.44.E-02
TM4SF19	**0.51**	1.07.E-02	3.00.E-02	**2.28**	4.48.E-05	2.90.E-04
TMC5	**0.56**	3.04.E-05	1.57.E-04	**3.77**	1.20.E-17	4.34.E-16
TMC6	**0.66**	3.84.E-06	2.31.E-05	**1.83**	4.29.E-04	2.18.E-03
TMC8	**0.33**	1.43.E-12	1.85.E-11	**2.16**	1.05.E-06	9.46.E-06
TMEM135	**0.63**	3.28.E-14	4.80.E-13	**2.62**	6.32.E-36	7.85.E-34
TMEM163	**0.31**	1.19.E-10	1.28.E-09	**2.74**	6.18.E-19	2.52.E-17
TMEM218	**0.70**	4.86.E-07	3.38.E-06	**1.64**	1.90.E-09	2.74.E-08
TMEM71	**0.62**	2.50.E-13	3.41.E-12	**1.72**	5.39.E-14	1.37.E-12
TMPRSS2	**0.15**	1.56.E-14	2.35.E-13	**1.56**	1.21.E-02	3.91.E-02
TNFAIP3	**0.47**	1.97.E-22	4.87.E-21	**1.55**	1.88.E-11	3.59.E-10
TNFRSF10C	**0.18**	5.55.E-15	8.62.E-14	**2.95**	1.19.E-10	2.08.E-09
TNFRSF1B	**0.10**	1.16.E-66	1.08.E-64	**1.97**	2.12.E-09	3.05.E-08
TNFRSF21	**0.55**	3.60.E-30	1.24.E-28	**1.78**	1.34.E-23	7.99.E-22
TNFRSF9	**0.38**	1.63.E-10	1.71.E-09	**1.65**	2.17.E-03	8.94.E-03
TNRC6C-AS1	**0.62**	1.33.E-06	8.66.E-06	**1.82**	2.09.E-07	2.16.E-06
TOX2	**0.59**	3.80.E-03	1.23.E-02	**1.77**	3.62.E-05	2.38.E-04
TPCN1	**0.51**	8.81.E-16	1.44.E-14	**1.58**	3.67.E-11	6.77.E-10
TPP1	**0.66**	7.57.E-06	4.32.E-05	**1.71**	1.63.E-10	2.80.E-09
TRIM7	**0.69**	3.30.E-02	7.82.E-02	**1.51**	6.38.E-03	2.29.E-02
TRPM4	**0.71**	8.63.E-03	2.50.E-02	**2.45**	1.83.E-08	2.28.E-07
TRPV2	**0.15**	1.12.E-41	5.51.E-40	**2.61**	6.50.E-14	1.63.E-12
TSPAN1	**0.52**	2.77.E-14	4.08.E-13	**1.87**	5.34.E-09	7.22.E-08
TTC12	**0.73**	9.99.E-07	6.62.E-06	**1.77**	5.42.E-14	1.37.E-12
TTC39B	**0.66**	4.48.E-04	1.82.E-03	**1.53**	1.97.E-04	1.08.E-03
TUBB2B	**0.70**	3.71.E-02	8.60.E-02	**1.52**	1.60.E-02	4.92.E-02
TWSG1	**0.75**	8.49.E-07	5.69.E-06	**1.56**	4.13.E-14	1.07.E-12
UNC13A	**0.53**	6.90.E-07	4.70.E-06	**2.67**	3.00.E-09	4.21.E-08
USP18	**0.55**	1.49.E-05	8.13.E-05	**1.57**	2.64.E-03	1.06.E-02
VIPR1	**0.43**	7.68.E-09	6.69.E-08	**2.43**	1.05.E-08	1.35.E-07
VNN1	**0.17**	3.97.E-52	2.68.E-50	**1.94**	1.02.E-07	1.11.E-06
VNN2	**0.11**	6.58.E-20	1.38.E-18	**1.53**	3.60.E-02	9.62.E-02
VNN3	**0.13**	1.11.E-16	1.90.E-15	**1.79**	3.46.E-03	1.35.E-02
VSIG1	**0.55**	1.68.E-02	4.43.E-02	**1.99**	6.95.E-04	3.34.E-03
WFDC13	**0.49**	1.43.E-03	5.16.E-03	**1.54**	3.24.E-02	8.86.E-02
WT1	**0.29**	1.11.E-21	2.60.E-20	**2.45**	1.24.E-06	1.10.E-05
WTAPP1	**0.29**	5.86.E-08	4.61.E-07	**11.59**	3.24.E-39	4.80.E-37
ZBED6CL	**0.18**	1.14.E-51	7.54.E-50	**4.27**	3.61.E-13	8.42.E-12
ZBTB7C	**0.16**	2.74.E-12	3.43.E-11	**1.79**	9.51.E-04	4.38.E-03
ZC3H12C	**0.55**	4.62.E-25	1.33.E-23	**2.34**	3.39.E-50	7.28.E-48
ZC3H12D	**0.49**	3.47.E-03	1.13.E-02	**1.53**	3.35.E-02	9.10.E-02
ZDHHC11	**0.60**	3.02.E-02	7.26.E-02	**1.76**	4.36.E-03	1.64.E-02
ZKSCAN7	**0.41**	2.11.E-04	9.25.E-04	**2.61**	2.98.E-07	2.99.E-06
ZNF138	**0.74**	4.16.E-02	9.47.E-02	**1.75**	2.60.E-05	1.78.E-04
ZNF257	**0.52**	3.50.E-07	2.49.E-06	**7.68**	2.33.E-31	2.17.E-29
ZNF287	**0.68**	1.18.E-02	3.26.E-02	**2.23**	2.83.E-05	1.92.E-04
ZNF558	**0.71**	2.03.E-08	1.68.E-07	**5.24**	2.40.E-69	7.96.E-67
ZNF611	**0.69**	1.69.E-08	1.41.E-07	**1.51**	4.66.E-07	4.49.E-06
ZNF660	**0.57**	2.98.E-02	7.17.E-02	**1.63**	1.53.E-02	4.75.E-02
ZNF702P	**0.67**	3.72.E-08	2.98.E-07	**3.34**	1.34.E-24	8.59.E-23

Supplementary Table 1b. The p27/cJun common target genes (233 genes).

	231DD vs. 231	231DD vs. 231	231DD vs. 231	1833shp27 vs. 1833	1833shp27 vs. 1833	1833shp27 vs. 1833
Gene ID	**Fold Change**	**p value**	**q value**	**Fold Change**	**p value**	**q value**
ABCC3	**0.18**	1.12.E-60	9.13.E-59	**0.37**	3.26.E-27	7.60.E-26
ACBD4	**0.64**	1.79.E-06	1.14.E-05	**0.64**	7.18.E-06	3.04.E-05
ACOX2	**0.19**	6.95.E-37	2.97.E-35	**0.69**	2.87.E-04	9.41.E-04
ACVR1C	**0.48**	3.56.E-03	1.16.E-02	**0.56**	3.08.E-02	6.39.E-02
ADAM12	**0.50**	1.11.E-05	6.16.E-05	**0.57**	4.26.E-04	1.35.E-03
ADORA2B	**0.37**	2.61.E-58	1.98.E-56	**0.40**	3.52.E-45	1.69.E-43
ADPRHL1	**0.71**	2.51.E-04	1.08.E-03	**0.58**	9.72.E-08	5.25.E-07
ALDH1L1	**0.59**	5.42.E-07	3.73.E-06	**0.46**	1.67.E-11	1.34.E-10
ALDH3A1	**0.32**	7.24.E-06	4.14.E-05	**0.47**	7.03.E-03	1.74.E-02
ANKRD6	**0.51**	2.32.E-13	3.17.E-12	**0.66**	4.52.E-06	1.96.E-05
ANXA9	**0.51**	3.29.E-06	2.01.E-05	**0.53**	3.22.E-05	1.24.E-04
APOE	**0.45**	8.63.E-05	4.07.E-04	**0.40**	3.21.E-05	1.24.E-04
AQP3	**0.30**	1.33.E-32	4.99.E-31	**0.20**	4.24.E-35	1.38.E-33
ARHGEF16	**0.63**	2.32.E-02	5.79.E-02	**0.31**	2.31.E-06	1.05.E-05
ARL4D	**0.42**	4.01.E-28	1.30.E-26	**0.34**	3.32.E-38	1.24.E-36
ASB2	**0.02**	6.57.E-99	1.29.E-96	**0.11**	4.95.E-71	4.59.E-69
ASMTL	**0.65**	2.41.E-07	1.75.E-06	**0.76**	2.63.E-03	7.15.E-03
ATOH8	**0.12**	1.43.E-53	9.98.E-52	**0.10**	1.62.E-53	1.01.E-51
B3GALT5	**0.18**	4.66.E-19	9.29.E-18	**0.57**	3.72.E-04	1.20.E-03
B4GALT5	**0.62**	6.20.E-26	1.87.E-24	**0.64**	4.71.E-21	7.74.E-20
BDNF	**0.62**	4.22.E-15	6.59.E-14	**0.53**	2.22.E-22	3.94.E-21
BID	**0.53**	4.05.E-23	1.05.E-21	**0.66**	9.81.E-11	7.31.E-10
BMF	**0.69**	1.84.E-04	8.13.E-04	**0.60**	1.69.E-06	7.81.E-06
BUB1	**0.65**	2.87.E-25	8.28.E-24	**0.72**	3.94.E-12	3.36.E-11
C10orf10	**0.58**	1.01.E-09	9.78.E-09	**0.42**	7.32.E-18	9.73.E-17
C10orf54	**0.33**	8.92.E-36	3.69.E-34	**0.05**	2.18.E-93	3.16.E-91
C15orf48	**0.20**	2.26.E-267	2.70.E-264	**0.09**	0.00.E+00	0.00.E+00
C19orf12	**0.69**	5.07.E-11	5.60.E-10	**0.65**	2.03.E-12	1.79.E-11
C9orf89	**0.63**	9.85.E-09	8.47.E-08	**0.44**	6.46.E-15	6.98.E-14
CA13	**0.69**	4.69.E-06	2.78.E-05	**0.68**	5.01.E-05	1.88.E-04
CCDC144B	**0.71**	9.78.E-05	4.57.E-04	**0.49**	1.26.E-13	1.23.E-12
CCDC153	**0.56**	1.19.E-03	4.40.E-03	**0.41**	1.23.E-05	5.05.E-05
CCDC3	**0.49**	1.56.E-11	1.80.E-10	**0.06**	1.76.E-53	1.09.E-51
CCND3	**0.63**	5.09.E-17	8.91.E-16	**0.42**	2.66.E-49	1.48.E-47
CCR7	**0.42**	1.63.E-04	7.30.E-04	**0.44**	7.63.E-04	2.31.E-03
CD63	**0.71**	9.77.E-15	1.50.E-13	**0.69**	5.35.E-16	6.21.E-15
CD82	**0.39**	1.33.E-39	6.18.E-38	**0.21**	3.49.E-72	3.31.E-70
CDC42BPG	**0.41**	6.24.E-06	3.61.E-05	**0.46**	1.39.E-04	4.83.E-04
CETP	**0.55**	7.49.E-03	2.21.E-02	**0.46**	1.23.E-03	3.59.E-03
CFAP54	**0.42**	4.40.E-10	4.42.E-09	**0.52**	1.06.E-04	3.75.E-04
CHI3L2	**0.48**	4.57.E-03	1.44.E-02	**0.33**	1.77.E-04	6.01.E-04
COMTD1	**0.74**	1.27.E-02	3.49.E-02	**0.56**	7.87.E-05	2.85.E-04
CORO2B	**0.72**	5.64.E-06	3.29.E-05	**0.54**	1.15.E-14	1.21.E-13
CPNE5	**0.36**	2.40.E-10	2.47.E-09	**0.57**	2.68.E-04	8.84.E-04
CPNE7	**0.29**	2.39.E-08	1.96.E-07	**0.17**	2.75.E-12	2.39.E-11
CSF3	**0.09**	3.06.E-94	5.41.E-92	**0.27**	2.10.E-27	4.96.E-26
CST4	**0.45**	6.61.E-42	3.27.E-40	**0.43**	2.10.E-35	6.92.E-34
CST6	**0.22**	5.97.E-22	1.43.E-20	**0.13**	1.34.E-29	3.54.E-28
CYB561	**0.61**	5.95.E-20	1.26.E-18	**0.62**	9.82.E-16	1.12.E-14
DHRS3	**0.07**	2.35.E-51	1.54.E-49	**0.06**	2.14.E-47	1.11.E-45
DLG3	**0.68**	1.21.E-10	1.29.E-09	**0.54**	2.63.E-21	4.37.E-20
DUSP13	**0.42**	1.08.E-03	4.02.E-03	**0.43**	5.94.E-03	1.50.E-02
EFCAB7	**0.65**	3.46.E-05	1.77.E-04	**0.70**	8.48.E-04	2.54.E-03
EFNB2	**0.39**	1.43.E-38	6.45.E-37	**0.47**	3.61.E-25	7.53.E-24
ELFN2	**0.43**	1.25.E-13	1.75.E-12	**0.30**	6.03.E-21	9.80.E-20
ELMSAN1	**0.54**	2.59.E-16	4.35.E-15	**0.75**	7.12.E-05	2.60.E-04
EPB41L4B	**0.59**	2.97.E-19	6.04.E-18	**0.68**	3.81.E-11	2.95.E-10
EPN2	**0.73**	1.32.E-07	9.87.E-07	**0.67**	9.97.E-12	8.14.E-11
EPOR	**0.75**	1.97.E-03	6.86.E-03	**0.69**	4.22.E-04	1.34.E-03
ERBB3	**0.60**	1.15.E-06	7.52.E-06	**0.49**	1.59.E-11	1.28.E-10
EZR	**0.73**	7.83.E-14	1.11.E-12	**0.63**	1.67.E-25	3.54.E-24
FAM107B	**0.74**	3.71.E-10	3.75.E-09	**0.48**	5.04.E-43	2.24.E-41
FAM225A	**0.67**	5.29.E-03	1.64.E-02	**0.63**	2.72.E-03	7.37.E-03
FCGRT	**0.58**	2.17.E-19	4.44.E-18	**0.24**	3.70.E-83	4.39.E-81
FES	**0.59**	1.50.E-02	4.02.E-02	**0.44**	1.10.E-03	3.23.E-03
FHOD3	**0.58**	1.43.E-23	3.82.E-22	**0.52**	6.16.E-26	1.34.E-24
FLVCR2	**0.54**	6.05.E-04	2.39.E-03	**0.61**	7.43.E-03	1.83.E-02
FOXQ1	**0.46**	9.98.E-22	2.34.E-20	**0.78**	4.27.E-03	1.11.E-02
FUCA1	**0.45**	2.19.E-38	9.83.E-37	**0.29**	3.53.E-96	5.33.E-94
FZD1	**0.70**	5.43.E-07	3.74.E-06	**0.56**	9.83.E-14	9.75.E-13
GAS7	**0.43**	1.35.E-03	4.91.E-03	**0.29**	4.02.E-05	1.53.E-04
GATA2	**0.53**	8.14.E-10	7.99.E-09	**0.66**	1.24.E-04	4.35.E-04
GDPD5	**0.74**	6.67.E-06	3.84.E-05	**0.72**	1.40.E-04	4.84.E-04
GFAP	**0.30**	2.41.E-31	8.54.E-30	**0.21**	2.17.E-41	9.17.E-40
GIMAP8	**0.24**	9.09.E-08	6.97.E-07	**0.20**	1.67.E-07	8.75.E-07

GINM1	**0.65**	9.85.E-13	1.29.E-11	**0.60**	5.15.E-15	5.59.E-14
GPC1	**0.64**	3.30.E-05	1.70.E-04	**0.31**	1.26.E-17	1.64.E-16
GPR68	**0.33**	7.58.E-66	6.93.E-64	**0.43**	7.04.E-34	2.21.E-32
GRB7	**0.45**	1.16.E-04	5.37.E-04	**0.40**	7.13.E-05	2.60.E-04
GRIK4	**0.43**	1.21.E-09	1.17.E-08	**0.16**	1.62.E-24	3.23.E-23
HS3ST1	**0.49**	1.01.E-12	1.32.E-11	**0.54**	1.48.E-08	8.84.E-08
HSD3B7	**0.44**	1.53.E-20	3.35.E-19	**0.34**	8.19.E-25	1.67.E-23
ICAM1	**0.65**	5.55.E-19	1.10.E-17	**0.36**	1.67.E-65	1.39.E-63
ICOSLG	**0.39**	1.57.E-04	7.06.E-04	**0.43**	1.56.E-03	4.47.E-03
IFI6	**0.50**	2.28.E-17	4.07.E-16	**0.38**	1.86.E-22	3.30.E-21
IGFBP6	**0.24**	3.37.E-98	6.49.E-96	**0.20**	3.68.E-115	8.10.E-113
IL12A	**0.41**	2.18.E-08	1.80.E-07	**0.55**	1.18.E-04	4.15.E-04
IL1R1	**0.16**	2.54.E-77	3.20.E-75	**0.10**	5.69.E-90	7.70.E-88
INHBB	**0.54**	9.77.E-20	2.02.E-18	**0.13**	2.84.E-129	7.53.E-127
IQSEC2	**0.33**	3.33.E-39	1.54.E-37	**0.29**	4.22.E-39	1.62.E-37
ISG20	**0.15**	4.01.E-122	1.04.E-119	**0.10**	2.30.E-119	5.46.E-117
KCNN4	**0.49**	4.53.E-38	2.00.E-36	**0.76**	4.48.E-05	1.69.E-04
KIAA0895	**0.60**	1.07.E-06	7.06.E-06	**0.71**	1.35.E-03	3.90.E-03
KLF10	**0.74**	5.20.E-09	4.63.E-08	**0.76**	1.70.E-06	7.85.E-06
LAPTM5	**0.72**	3.14.E-10	3.20.E-09	**0.35**	8.36.E-71	7.67.E-69
LAT2	**0.56**	1.18.E-06	7.73.E-06	**0.68**	2.31.E-03	6.36.E-03
LHX6	**0.47**	9.47.E-05	4.44.E-04	**0.67**	3.17.E-02	6.56.E-02
LIMK1	**0.72**	2.43.E-10	2.50.E-09	**0.46**	6.96.E-30	1.85.E-28
LINC00857	**0.67**	3.37.E-06	2.06.E-05	**0.54**	7.75.E-11	5.86.E-10
LINC01119	**0.51**	9.31.E-03	2.67.E-02	**0.41**	2.33.E-03	6.39.E-03
LINC01186	**0.66**	3.38.E-02	7.98.E-02	**0.44**	1.52.E-04	5.24.E-04
LINC01411	**0.25**	4.25.E-28	1.37.E-26	**0.02**	1.30.E-55	8.43.E-54
LINC01559	**0.22**	9.16.E-17	1.58.E-15	**0.41**	8.76.E-07	4.20.E-06
LOC100506844	**0.75**	3.95.E-02	9.07.E-02	**0.76**	3.76.E-02	7.58.E-02
LOC101928994	**0.39**	1.37.E-04	6.21.E-04	**0.49**	6.19.E-03	1.55.E-02
LOC101930010	**0.61**	1.74.E-03	6.14.E-03	**0.43**	1.41.E-06	6.58.E-06
LOC148696	**0.49**	6.69.E-04	2.62.E-03	**0.60**	2.10.E-02	4.57.E-02
LRP5L	**0.60**	2.72.E-05	1.42.E-04	**0.60**	4.19.E-05	1.59.E-04
LRRC15	**0.26**	1.54.E-12	1.98.E-11	**0.09**	1.32.E-22	2.38.E-21
LRRK1	**0.59**	2.70.E-09	2.48.E-08	**0.57**	1.69.E-10	1.23.E-09
MAPK13	**0.60**	2.15.E-11	2.45.E-10	**0.23**	3.23.E-62	2.48.E-60
MAPKAPK3	**0.50**	3.31.E-35	1.33.E-33	**0.70**	4.43.E-11	3.40.E-10
MATN2	**0.55**	1.36.E-25	3.98.E-24	**0.16**	1.66.E-108	3.09.E-106
MB	**0.24**	5.47.E-13	7.28.E-12	**0.08**	1.88.E-22	3.34.E-21
MBTPS2	**0.66**	2.85.E-04	1.22.E-03	**0.67**	8.13.E-04	2.45.E-03
MCAM	**0.63**	6.18.E-20	1.30.E-18	**0.22**	2.31.E-161	8.60.E-159
MEST	**0.60**	5.71.E-09	5.06.E-08	**0.79**	6.48.E-03	1.62.E-02
MIR4506	**0.60**	1.98.E-02	5.09.E-02	**0.58**	4.80.E-02	9.36.E-02
MKNK2	**0.60**	3.37.E-23	8.78.E-22	**0.65**	7.78.E-10	5.33.E-09
MMP19	**0.55**	1.01.E-06	6.71.E-06	**0.37**	3.58.E-13	3.37.E-12
MST1R	**0.47**	4.54.E-14	6.56.E-13	**0.38**	2.72.E-19	3.99.E-18
MTUS1	**0.39**	1.27.E-30	4.41.E-29	**0.59**	4.22.E-12	3.58.E-11
MVP	**0.73**	1.58.E-10	1.66.E-09	**0.53**	9.88.E-27	2.25.E-25
MYO18A	**0.45**	6.02.E-28	1.93.E-26	**0.46**	2.29.E-27	5.38.E-26
MYO1F	**0.59**	1.44.E-10	1.53.E-09	**0.19**	9.64.E-39	3.65.E-37
NES	**0.48**	1.14.E-19	2.35.E-18	**0.45**	1.43.E-22	2.57.E-21
NEURL3	**0.33**	1.48.E-05	8.05.E-05	**0.34**	1.54.E-04	5.29.E-04
NOP14-AS1	**0.73**	3.11.E-04	1.31.E-03	**0.50**	2.88.E-14	2.96.E-13
NOXA1	**0.62**	2.35.E-03	8.01.E-03	**0.70**	4.05.E-02	8.07.E-02
NPR1	**0.50**	1.31.E-04	5.99.E-04	**0.48**	1.43.E-04	4.93.E-04
NPTN	**0.69**	2.67.E-15	4.22.E-14	**0.71**	3.81.E-12	3.26.E-11
NQO2	**0.64**	1.79.E-15	2.86.E-14	**0.75**	8.55.E-07	4.10.E-06
NR1H3	**0.73**	8.27.E-06	4.69.E-05	**0.47**	1.05.E-19	1.59.E-18
NR4A1	**0.35**	3.20.E-07	2.29.E-06	**0.52**	1.31.E-03	3.80.E-03
NXN	**0.75**	8.18.E-07	5.50.E-06	**0.23**	2.37.E-103	4.01.E-101
OAF	**0.55**	2.39.E-32	8.76.E-31	**0.46**	3.17.E-37	1.13.E-35
OLFML2A	**0.17**	4.52.E-78	5.78.E-76	**0.17**	1.10.E-68	9.69.E-67
OTUB2	**0.31**	6.83.E-67	6.44.E-65	**0.39**	1.80.E-57	1.23.E-55
PADI3	**0.36**	6.32.E-05	3.08.E-04	**0.31**	3.82.E-05	1.46.E-04
PAK6	**0.14**	2.91.E-44	1.56.E-42	**0.04**	4.38.E-65	3.63.E-63
PARP14	**0.31**	3.89.E-115	9.40.E-113	**0.48**	7.17.E-45	3.40.E-43
PCAT7	**0.58**	2.56.E-02	6.31.E-02	**0.58**	4.03.E-02	8.04.E-02
PCGF5	**0.72**	1.32.E-09	1.27.E-08	**0.76**	3.45.E-07	1.74.E-06
PDE2A	**0.39**	1.53.E-14	2.31.E-13	**0.61**	3.13.E-05	1.21.E-04
PIK3R3	**0.71**	7.33.E-08	5.70.E-07	**0.44**	1.46.E-31	4.28.E-30
PIM2	**0.50**	1.67.E-25	4.87.E-24	**0.36**	1.15.E-44	5.39.E-43
PLA2G4C	**0.65**	6.50.E-03	1.96.E-02	**0.66**	1.17.E-02	2.73.E-02
PLAT	**0.41**	4.45.E-78	5.73.E-76	**0.50**	2.10.E-38	7.86.E-37
PLB1	**0.12**	3.68.E-66	3.38.E-64	**0.13**	8.16.E-59	5.78.E-57
PPARGC1A	**0.16**	3.91.E-40	1.85.E-38	**0.61**	3.89.E-06	1.71.E-05
PPM1J	**0.55**	3.01.E-03	1.00.E-02	**0.64**	3.29.E-02	6.76.E-02
PPP1R26-AS1	**0.57**	5.99.E-05	2.93.E-04	**0.59**	2.99.E-04	9.76.E-04
PRNP	**0.58**	9.30.E-40	4.33.E-38	**0.66**	1.34.E-21	2.27.E-20

PROM2	**0.54**	2.52.E-03	8.55.E-03	**0.17**	1.22.E-11	9.87.E-11
PSG4	**0.60**	1.64.E-09	1.55.E-08	**0.52**	9.29.E-14	9.24.E-13
PSG9	**0.55**	1.08.E-02	3.03.E-02	**0.53**	1.19.E-02	2.78.E-02
PTPRH	**0.19**	1.22.E-26	3.78.E-25	**0.37**	5.78.E-13	5.38.E-12
RAB13	**0.61**	2.45.E-03	8.31.E-03	**0.68**	1.55.E-04	5.31.E-04
RAB38	**0.53**	8.21.E-21	1.82.E-19	**0.45**	3.87.E-28	9.56.E-27
RAET1G	**0.58**	7.06.E-06	4.05.E-05	**0.35**	1.89.E-15	2.13.E-14
RAMP1	**0.49**	7.90.E-14	1.12.E-12	**0.68**	1.60.E-03	4.57.E-03
RARB	**0.25**	4.22.E-65	3.81.E-63	**0.03**	3.19.E-147	1.08.E-144
RARG	**0.42**	1.58.E-39	7.31.E-38	**0.49**	1.02.E-23	1.96.E-22
RASD1	**0.21**	1.53.E-52	1.04.E-50	**0.15**	1.29.E-54	8.22.E-53
RASGRF1	**0.56**	1.40.E-08	1.18.E-07	**0.52**	4.17.E-10	2.91.E-09
RCN1	**0.61**	1.90.E-26	5.84.E-25	**0.60**	1.65.E-25	3.51.E-24
REN	**0.59**	4.33.E-02	9.78.E-02	**0.54**	4.37.E-02	8.62.E-02
RGS9	**0.61**	1.14.E-04	5.26.E-04	**0.58**	4.81.E-05	1.81.E-04
RIMS3	**0.64**	6.15.E-05	3.00.E-04	**0.67**	4.52.E-04	1.43.E-03
RP1L1	**0.35**	1.64.E-05	8.90.E-05	**0.41**	6.39.E-04	1.96.E-03
RTN4RL2	**0.56**	6.29.E-03	1.90.E-02	**0.62**	3.84.E-02	7.71.E-02
S100A2	**0.28**	6.88.E-69	7.07.E-67	**0.35**	1.16.E-48	6.32.E-47
S100A6	**0.58**	2.56.E-28	8.37.E-27	**0.45**	2.40.E-57	1.64.E-55
S100P	**0.35**	5.71.E-18	1.06.E-16	**0.09**	1.08.E-45	5.24.E-44
S1PR1	**0.55**	1.00.E-04	4.67.E-04	**0.70**	1.67.E-02	3.73.E-02
SARDH	**0.73**	2.69.E-04	1.15.E-03	**0.44**	9.42.E-13	8.56.E-12
SBNO2	**0.62**	1.28.E-11	1.49.E-10	**0.67**	2.56.E-05	1.00.E-04
SDSL	**0.52**	1.88.E-09	1.77.E-08	**0.46**	4.63.E-12	3.89.E-11
SEC22B	**0.65**	1.19.E-18	2.30.E-17	**0.79**	1.91.E-06	8.76.E-06
SERPINB9P1	**0.43**	4.93.E-04	1.99.E-03	**0.49**	6.28.E-03	1.57.E-02
SHH	**0.35**	1.44.E-09	1.37.E-08	**0.12**	7.10.E-21	1.15.E-19
SLC16A14	**0.44**	2.19.E-04	9.55.E-04	**0.18**	4.93.E-10	3.42.E-09
SLC22A18	**0.56**	2.63.E-04	1.13.E-03	**0.55**	1.95.E-03	5.45.E-03
SLC2A5	**0.51**	4.54.E-03	1.43.E-02	**0.17**	1.35.E-09	9.07.E-09
SLC43A3	**0.54**	3.47.E-35	1.39.E-33	**0.77**	1.23.E-06	5.79.E-06
SLC45A1	**0.33**	8.71.E-06	4.91.E-05	**0.36**	1.66.E-04	5.66.E-04
SLC9A7	**0.37**	8.24.E-109	1.80.E-106	**0.53**	1.06.E-36	3.68.E-35
SMAD6	**0.63**	1.10.E-06	7.23.E-06	**0.24**	6.41.E-30	1.71.E-28
SNCG	**0.30**	2.04.E-10	2.11.E-09	**0.32**	4.10.E-11	3.16.E-10
SNPH	**0.65**	5.16.E-08	4.08.E-07	**0.44**	8.21.E-16	9.42.E-15
SOCS1	**0.38**	2.31.E-06	1.45.E-05	**0.46**	5.74.E-04	1.78.E-03
SOST	**0.18**	2.01.E-13	2.77.E-12	**0.09**	1.48.E-18	2.07.E-17
SPAG9	**0.69**	4.30.E-20	9.18.E-19	**0.75**	4.62.E-12	3.89.E-11
SPATA20	**0.69**	3.98.E-11	4.45.E-10	**0.76**	7.02.E-05	2.56.E-04
SPEG	**0.65**	2.51.E-06	1.57.E-05	**0.72**	1.62.E-03	4.62.E-03
SPOCD1	**0.24**	1.40.E-55	9.99.E-54	**0.32**	3.55.E-36	1.21.E-34
SPOCK1	**0.17**	1.31.E-119	3.26.E-117	**0.35**	2.84.E-51	1.67.E-49
ST14	**0.44**	2.50.E-04	1.08.E-03	**0.37**	4.55.E-05	1.72.E-04
ST3GAL1	**0.69**	5.97.E-14	8.54.E-13	**0.66**	3.41.E-15	3.77.E-14
ST6GALNAC4	**0.70**	4.49.E-07	3.15.E-06	**0.49**	1.53.E-14	1.61.E-13
STYK1	**0.68**	2.10.E-04	9.20.E-04	**0.61**	1.41.E-05	5.73.E-05
SULT2B1	**0.65**	3.71.E-02	8.59.E-02	**0.60**	4.25.E-02	8.42.E-02
SYT12	**0.47**	5.07.E-07	3.50.E-06	**0.36**	2.87.E-08	1.65.E-07
SYT2	**0.35**	1.03.E-09	1.00.E-08	**0.38**	3.44.E-08	1.96.E-07
SYTL2	**0.54**	2.52.E-19	5.14.E-18	**0.31**	5.42.E-50	3.08.E-48
SYTL3	**0.42**	4.49.E-13	6.01.E-12	**0.30**	1.24.E-19	1.87.E-18
TAF12	**0.73**	6.97.E-03	2.08.E-02	**0.46**	2.18.E-08	1.28.E-07
TBL1X	**0.66**	8.36.E-09	7.25.E-08	**0.75**	8.29.E-05	2.99.E-04
TCEA2	**0.71**	1.12.E-06	7.36.E-06	**0.70**	3.65.E-05	1.40.E-04
TDRD7	**0.74**	8.82.E-08	6.77.E-07	**0.62**	1.35.E-15	1.53.E-14
TGM2	**0.37**	7.94.E-151	2.63.E-148	**0.44**	7.44.E-100	1.20.E-97
TIMP3	**0.43**	8.44.E-61	6.97.E-59	**0.59**	1.70.E-23	3.24.E-22
TNFRSF14	**0.59**	2.29.E-06	1.44.E-05	**0.48**	4.49.E-09	2.85.E-08
TNFRSF21	**0.55**	3.60.E-30	1.24.E-28	**0.25**	1.29.E-133	3.56.E-131
TNIP1	**0.56**	4.20.E-43	2.13.E-41	**0.75**	1.30.E-10	9.52.E-10
TNRC6C-AS1	**0.62**	1.33.E-06	8.66.E-06	**0.32**	2.11.E-24	4.18.E-23
TPCN1	**0.51**	8.81.E-16	1.44.E-14	**0.69**	2.15.E-06	9.79.E-06
TRIM16L	**0.28**	1.11.E-57	8.27.E-56	**0.44**	7.41.E-22	1.28.E-20
TRPV2	**0.15**	1.12.E-41	5.51.E-40	**0.29**	4.06.E-22	7.12.E-21
TSKU	**0.69**	1.25.E-09	1.20.E-08	**0.31**	2.13.E-42	9.26.E-41
TUBGCP2	**0.74**	1.01.E-10	1.09.E-09	**0.73**	4.33.E-08	2.44.E-07
TXNRD1	**0.59**	2.56.E-35	1.04.E-33	**0.73**	2.85.E-12	2.47.E-11
TYSND1	**0.70**	8.27.E-10	8.11.E-09	**0.57**	4.27.E-19	6.19.E-18
UBE2L6	**0.48**	8.65.E-39	3.95.E-37	**0.68**	4.51.E-12	3.80.E-11
ULBP2	**0.65**	1.00.E-08	8.61.E-08	**0.49**	1.31.E-18	1.84.E-17
VEGFA	**0.69**	8.59.E-14	1.21.E-12	**0.58**	1.76.E-25	3.73.E-24
VNN2	**0.11**	6.58.E-20	1.38.E-18	**0.17**	1.24.E-13	1.21.E-12
VTRNA2-1	**0.53**	1.37.E-02	3.71.E-02	**0.47**	8.66.E-03	2.10.E-02
WDR45	**0.73**	3.40.E-08	2.75.E-07	**0.55**	6.37.E-27	1.47.E-25
ZBTB7B	**0.72**	4.55.E-06	2.71.E-05	**0.44**	9.80.E-17	1.20.E-15
ZNF611	**0.69**	1.69.E-08	1.41.E-07	**0.43**	2.12.E-31	6.17.E-30

ZNF702P	**0.67**	3.72.E-08	2.98.E-07	**0.11**	3.27.E-100	5.33.E-98
ZNF703	**0.70**	8.61.E-03	2.50.E-02	**0.38**	2.28.E-10	1.63.E-09

Supplementary Table 1c. The p27/cJun novel target genes (146 genes).

	231DD vs. 231	231DD vs. 231	231DD vs. 231	1833shp27 vs. 1833	1833shp27 vs. 1833	1833shp27 vs. 1833
Gene ID	**Fold Change**	**p value**	**q value**	**Fold Change**	**p value**	**q value**
ABCC1	**0.65**	2.34.E-05	1.24.E-04	**0.79**	1.41.E-02	3.22.E-02
ABHD17C	**0.36**	3.30.E-40	1.57.E-38	**0.54**	8.15.E-17	1.00.E-15
ABHD2	**0.75**	6.68.E-10	6.59.E-09	**0.80**	1.95.E-06	8.93.E-06
ACSF2	**0.50**	7.47.E-32	2.68.E-30	**0.55**	3.75.E-21	6.19.E-20
ACSL5	**0.43**	4.69.E-86	7.11.E-84	**0.56**	2.36.E-34	7.54.E-33
ADAM15	**0.75**	1.60.E-11	1.85.E-10	**0.31**	1.13.E-93	1.65.E-91
ADAMTS14	**0.21**	1.64.E-10	1.72.E-09	**0.13**	6.65.E-13	6.13.E-12
ADAP1	**0.41**	1.52.E-10	1.61.E-09	**0.41**	1.47.E-10	1.07.E-09
ADGRF5	**0.36**	3.58.E-122	9.42.E-120	**0.03**	0.00.E+00	0.00.E+00
AIFM2	**0.58**	5.32.E-19	1.06.E-17	**0.49**	1.12.E-27	2.68.E-26
AIM1L	**0.46**	1.27.E-03	4.65.E-03	**0.15**	1.27.E-10	9.36.E-10
AKR1C2	**0.45**	2.23.E-05	1.18.E-04	**0.42**	2.03.E-05	8.10.E-05
AMOTL1	**0.73**	2.79.E-06	1.73.E-05	**0.50**	2.61.E-23	4.92.E-22
ANXA11	**0.66**	3.77.E-22	9.14.E-21	**0.51**	1.44.E-42	6.27.E-41
APOL3	**0.25**	4.52.E-49	2.76.E-47	**0.38**	3.03.E-27	7.09.E-26
ATP8A1	**0.55**	1.61.E-15	2.58.E-14	**0.73**	5.41.E-06	2.33.E-05
BEND3	**0.54**	4.16.E-20	8.89.E-19	**0.59**	1.09.E-17	1.42.E-16
BLVRB	**0.53**	1.18.E-14	1.80.E-13	**0.52**	1.43.E-10	1.04.E-09
BTN3A3	**0.46**	2.69.E-17	4.77.E-16	**0.57**	7.34.E-09	4.54.E-08
C1RL	**0.52**	7.32.E-08	5.70.E-07	**0.64**	3.27.E-04	1.06.E-03
CA11	**0.57**	2.46.E-04	1.06.E-03	**0.73**	4.31.E-02	8.53.E-02
CASP7	**0.65**	1.42.E-11	1.65.E-10	**0.63**	1.19.E-15	1.36.E-14
CD14	**0.20**	3.46.E-20	7.42.E-19	**0.13**	5.26.E-26	1.16.E-24
CELSR2	**0.63**	8.42.E-06	4.76.E-05	**0.80**	3.08.E-02	6.40.E-02
CFB	**0.18**	8.09.E-172	3.53.E-169	**0.09**	1.13.E-234	8.99.E-232
COL14A1	**0.59**	3.32.E-02	7.86.E-02	**0.51**	1.89.E-02	4.18.E-02
CPA4	**0.57**	5.34.E-19	1.06.E-17	**0.35**	1.35.E-49	7.64.E-48
CSF1	**0.13**	1.13.E-218	9.23.E-216	**0.33**	4.90.E-55	3.14.E-53
CSGALNACT1	**0.44**	8.01.E-08	6.20.E-07	**0.45**	1.19.E-06	5.62.E-06
CUEDC2	**0.69**	5.05.E-12	6.12.E-11	**0.62**	7.83.E-15	8.38.E-14
CXADR	**0.24**	9.13.E-29	3.01.E-27	**0.73**	4.22.E-03	1.10.E-02
DAPK2	**0.26**	2.84.E-23	7.46.E-22	**0.24**	3.38.E-23	6.31.E-22
DBNDD1	**0.54**	2.34.E-12	2.95.E-11	**0.61**	4.82.E-07	2.38.E-06
DHX58	**0.30**	1.90.E-30	6.61.E-29	**0.29**	4.98.E-31	1.42.E-29
DPP7	**0.67**	4.56.E-06	2.72.E-05	**0.61**	7.63.E-03	1.87.E-02
DRAP1	**0.70**	3.00.E-11	3.37.E-10	**0.56**	1.54.E-18	2.14.E-17
DUSP5	**0.39**	2.30.E-84	3.34.E-82	**0.71**	1.99.E-12	1.75.E-11
DUSP6	**0.56**	1.21.E-36	5.14.E-35	**0.80**	2.23.E-06	1.01.E-05
DYNLT1	**0.72**	3.16.E-10	3.21.E-09	**0.68**	3.40.E-10	2.39.E-09
EHF	**0.19**	5.02.E-237	4.73.E-234	**0.01**	0.00.E+00	0.00.E+00
ENDOD1	**0.72**	3.28.E-11	3.68.E-10	**0.50**	2.02.E-38	7.58.E-37
ETFB	**0.67**	9.66.E-09	8.32.E-08	**0.26**	2.08.E-43	9.34.E-42
FAH	**0.41**	3.75.E-46	2.14.E-44	**0.57**	2.01.E-19	2.99.E-18
FAM179A	**0.55**	1.23.E-03	4.52.E-03	**0.66**	2.46.E-02	5.26.E-02
FAM45B	**0.63**	9.71.E-03	2.76.E-02	**0.50**	5.71.E-04	1.77.E-03
FAM46A	**0.31**	5.11.E-46	2.89.E-44	**0.30**	5.62.E-37	1.97.E-35
FAM73A	**0.70**	2.55.E-10	2.62.E-09	**0.57**	4.48.E-21	7.38.E-20
FAM8A1	**0.58**	9.84.E-13	1.29.E-11	**0.72**	3.21.E-05	1.24.E-04
FERMT3	**0.72**	4.02.E-02	9.19.E-02	**0.50**	1.31.E-04	4.57.E-04
FIG4	**0.43**	1.06.E-40	5.09.E-39	**0.75**	4.36.E-06	1.90.E-05
FOSL2	**0.40**	6.79.E-79	8.94.E-77	**0.39**	5.86.E-56	3.84.E-54
GBP4	**0.13**	9.93.E-180	5.08.E-177	**0.08**	5.29.E-215	3.02.E-212
GGT8P	**0.51**	9.96.E-03	2.82.E-02	**0.39**	1.52.E-03	4.35.E-03
GINS4	**0.57**	1.98.E-33	7.55.E-32	**0.63**	5.74.E-21	9.37.E-20
GJD3	**0.71**	1.76.E-03	6.21.E-03	**0.41**	1.73.E-12	1.54.E-11
GPR160	**0.60**	3.48.E-04	1.45.E-03	**0.72**	2.64.E-02	5.59.E-02
GRINA	**0.74**	8.09.E-09	7.03.E-08	**0.58**	6.69.E-18	8.92.E-17
GSTM1	**0.54**	1.74.E-13	2.40.E-12	**0.05**	8.24.E-86	1.02.E-83
HEG1	**0.65**	3.04.E-02	7.29.E-02	**0.45**	6.48.E-05	2.38.E-04

HERC5	**0.52**	2.81.E-37	1.22.E-35	**0.34**	1.04.E-88	1.35.E-86
HKDC1	**0.41**	7.49.E-16	1.23.E-14	**0.31**	2.45.E-19	3.61.E-18
HLA-DMA	**0.25**	6.94.E-80	9.49.E-78	**0.16**	8.73.E-121	2.13.E-118
HMOX2	**0.74**	1.68.E-08	1.40.E-07	**0.64**	4.84.E-17	6.04.E-16
HPCAL1	**0.47**	7.06.E-63	6.11.E-61	**0.53**	5.63.E-19	8.08.E-18
HPS1	**0.70**	2.40.E-09	2.22.E-08	**0.63**	1.55.E-12	1.38.E-11
HSD17B14	**0.39**	4.03.E-04	1.66.E-03	**0.36**	7.37.E-04	2.24.E-03
ICAM2	**0.35**	9.48.E-20	1.97.E-18	**0.52**	5.08.E-09	3.20.E-08
IL4I1	**0.44**	1.59.E-03	5.69.E-03	**0.41**	1.87.E-03	5.26.E-03
IL6	**0.16**	9.75.E-166	4.06.E-163	**0.15**	1.20.E-163	4.55.E-161
INHA	**0.55**	2.37.E-02	5.89.E-02	**0.52**	3.37.E-02	6.91.E-02
ITM2C	**0.60**	3.54.E-19	7.13.E-18	**0.59**	9.33.E-21	1.50.E-19
KIAA1217	**0.40**	3.51.E-19	7.07.E-18	**0.39**	2.62.E-21	4.37.E-20
KLF9	**0.43**	4.39.E-12	5.36.E-11	**0.41**	3.82.E-13	3.60.E-12
KRT80	**0.54**	6.62.E-37	2.83.E-35	**0.43**	9.15.E-63	7.20.E-61
LINC01186	**0.66**	3.38.E-02	7.98.E-02	**0.44**	1.52.E-04	5.24.E-04
LINC01358	**0.43**	3.17.E-05	1.64.E-04	**0.53**	2.01.E-03	5.61.E-03
LINC01537	**0.30**	4.61.E-06	2.74.E-05	**0.22**	1.82.E-07	9.50.E-07
LINC01588	**0.63**	1.03.E-08	8.81.E-08	**0.72**	7.64.E-05	2.77.E-04
LIPH	**0.46**	4.21.E-11	4.70.E-10	**0.36**	8.65.E-17	1.06.E-15
LMBRD1	**0.72**	1.59.E-05	8.64.E-05	**0.61**	2.37.E-11	1.87.E-10
LOC100506178	**0.51**	3.41.E-13	4.61.E-12	**0.60**	2.00.E-08	1.18.E-07
MFI2	**0.46**	1.17.E-38	5.29.E-37	**0.21**	1.34.E-85	1.65.E-83
NAT2	**0.58**	3.71.E-02	8.60.E-02	**0.50**	2.12.E-02	4.61.E-02
NDRG1	**0.31**	1.06.E-124	2.84.E-122	**0.33**	7.87.E-90	1.06.E-87
NFIL3	**0.62**	4.89.E-10	4.89.E-09	**0.77**	3.69.E-04	1.19.E-03
NFKBIZ	**0.62**	7.28.E-17	1.26.E-15	**0.72**	5.33.E-11	4.07.E-10
NMT2	**0.65**	9.25.E-16	1.51.E-14	**0.52**	1.42.E-28	3.60.E-27
NR2F2	**0.69**	1.04.E-09	1.01.E-08	**0.67**	4.78.E-10	3.32.E-09
NUDT14	**0.74**	2.14.E-03	7.39.E-03	**0.64**	4.17.E-05	1.58.E-04
OASL	**0.16**	3.96.E-207	2.84.E-204	**0.06**	0.00.E+00	0.00.E+00
OLFML3	**0.63**	1.14.E-04	5.26.E-04	**0.53**	3.48.E-07	1.75.E-06
OSR1	**0.73**	1.74.E-03	6.15.E-03	**0.65**	1.67.E-04	5.70.E-04
OSTM1	**0.61**	4.22.E-17	7.42.E-16	**0.55**	5.98.E-22	1.04.E-20
PDZK1IP1	**0.09**	3.13.E-151	1.06.E-148	**0.01**	4.06.E-123	1.05.E-120
PECAM1	**0.22**	5.56.E-68	5.47.E-66	**0.54**	1.99.E-14	2.07.E-13
PFKFB4	**0.68**	4.40.E-11	4.89.E-10	**0.50**	5.55.E-29	1.43.E-27
PHF10	**0.73**	1.52.E-06	9.82.E-06	**0.53**	3.50.E-16	4.13.E-15
PHLDB2	**0.64**	1.57.E-22	3.92.E-21	**0.65**	9.22.E-19	1.31.E-17
PI16	**0.31**	6.31.E-09	5.56.E-08	**0.20**	1.29.E-11	1.04.E-10
PON3	**0.41**	2.83.E-06	1.75.E-05	**0.52**	4.14.E-04	1.32.E-03
PPIF	**0.64**	6.95.E-26	2.07.E-24	**0.74**	2.03.E-11	1.61.E-10
PPP4R3CP	**0.59**	4.69.E-05	2.34.E-04	**0.02**	1.03.E-47	5.44.E-46
PREX1	**0.34**	4.70.E-05	2.34.E-04	**0.39**	1.75.E-03	4.96.E-03
PRRG1	**0.60**	2.71.E-12	3.40.E-11	**0.66**	1.14.E-08	6.92.E-08
PRSS23	**0.66**	1.50.E-24	4.21.E-23	**0.30**	7.75.E-181	3.54.E-178
PRSS35	**0.63**	1.22.E-02	3.38.E-02	**0.63**	2.11.E-02	4.61.E-02
PTGES	**0.22**	1.83.E-179	9.09.E-177	**0.04**	0.00.E+00	0.00.E+00
PTK2B	**0.31**	1.07.E-20	2.35.E-19	**0.32**	6.93.E-19	9.87.E-18
RAB27A	**0.57**	4.33.E-11	4.83.E-10	**0.67**	5.55.E-06	2.38.E-05
RAB27B	**0.16**	1.37.E-192	8.73.E-190	**0.48**	1.05.E-46	5.30.E-45
RAVER2	**0.69**	5.80.E-07	3.99.E-06	**0.65**	1.17.E-09	7.91.E-09
RCSD1	**0.70**	3.07.E-09	2.81.E-08	**0.29**	3.25.E-63	2.58.E-61
RNF43	**0.24**	1.07.E-09	1.03.E-08	**0.50**	2.36.E-03	6.48.E-03
RPL13AP20	**0.73**	1.92.E-02	4.95.E-02	**0.36**	1.01.E-09	6.85.E-09
RSPO3	**0.49**	6.55.E-03	1.97.E-02	**0.43**	4.85.E-03	1.25.E-02
SCG2	**0.41**	2.39.E-06	1.50.E-05	**0.35**	1.17.E-07	6.28.E-07
SCN1B	**0.40**	2.19.E-07	1.60.E-06	**0.32**	5.65.E-09	3.54.E-08
SEMA3B	**0.27**	5.28.E-40	2.47.E-38	**0.25**	1.81.E-40	7.30.E-39
SERPINB6	**0.73**	1.44.E-11	1.67.E-10	**0.51**	1.19.E-43	5.37.E-42
SFR1	**0.47**	1.89.E-19	3.87.E-18	**0.54**	9.33.E-15	9.91.E-14

SLCO4A1-AS1	**0.19**	1.00.E-107	2.13.E-105	**0.50**	3.78.E-22	6.64.E-21
SMPDL3B	**0.26**	7.12.E-16	1.17.E-14	**0.22**	9.26.E-16	1.06.E-14
SMTNL1	**0.38**	1.94.E-04	8.56.E-04	**0.56**	4.66.E-02	9.12.E-02
SNX21	**0.74**	1.43.E-06	9.24.E-06	**0.61**	2.91.E-12	2.52.E-11
SNX8	**0.49**	6.11.E-29	2.04.E-27	**0.55**	8.22.E-20	1.25.E-18
SORL1	**0.27**	8.28.E-22	1.96.E-20	**0.04**	7.48.E-47	3.81.E-45
ST3GAL5	**0.34**	1.26.E-38	5.72.E-37	**0.27**	1.17.E-47	6.17.E-46
TCEAL8	**0.71**	9.53.E-10	9.27.E-09	**0.79**	3.38.E-05	1.30.E-04
TGFA	**0.42**	1.50.E-71	1.67.E-69	**0.10**	0.00.E+00	0.00.E+00
TGM5	**0.28**	4.53.E-07	3.17.E-06	**0.24**	4.30.E-07	2.14.E-06
THBD	**0.46**	3.81.E-26	1.15.E-24	**0.70**	2.21.E-06	1.00.E-05
THRA	**0.51**	3.76.E-17	6.63.E-16	**0.73**	2.03.E-05	8.07.E-05
THSD4	**0.34**	1.46.E-46	8.44.E-45	**0.50**	7.98.E-21	1.28.E-19
TMEM132A	**0.52**	3.58.E-35	1.43.E-33	**0.45**	1.41.E-16	1.71.E-15
TMEM171	**0.27**	3.74.E-89	6.14.E-87	**0.57**	2.08.E-19	3.08.E-18
TMEM71	**0.62**	2.50.E-13	3.41.E-12	**0.72**	4.43.E-07	2.20.E-06
TMSB4X	**0.66**	1.55.E-21	3.58.E-20	**0.64**	6.20.E-28	1.51.E-26
TNFAIP8L1	**0.66**	6.35.E-09	5.59.E-08	**0.74**	7.24.E-05	2.64.E-04
TNFRSF9	**0.38**	1.63.E-10	1.71.E-09	**0.36**	1.89.E-10	1.36.E-09
TNFSF10	**0.09**	9.18.E-187	5.48.E-184	**0.03**	2.69.E-196	1.29.E-193
TRABD2A	**0.52**	4.83.E-20	1.03.E-18	**0.61**	3.57.E-11	2.78.E-10
TRAF3IP2	**0.65**	7.17.E-11	7.82.E-10	**0.66**	2.03.E-09	1.34.E-08
TYRO3	**0.74**	7.09.E-07	4.81.E-06	**0.77**	6.33.E-06	2.69.E-05
XKR8	**0.70**	3.50.E-06	2.13.E-05	**0.43**	6.59.E-28	1.60.E-26
ZCCHC24	**0.51**	6.40.E-28	2.04.E-26	**0.54**	7.28.E-21	1.18.E-19
ZP3	**0.52**	1.02.E-02	2.87.E-02	**0.43**	4.32.E-03	1.12.E-02